Electronic Supporting Information

Stereocontrolled Protein Surface Recognition Using Chiral Oligoamide Proteomimetic Foldamers

Valeria Azzarito,[1,2] Jennifer A. Miles,[1,2] Julie Fisher,[1] Thomas A. Edwards,[2,3] Stuart L. Warriner,[1,2] Andrew J. Wilson[1,2]*

[1]School of Chemistry, [2]Astbury Centre for Structural Molecular Biology, [3]School of Molecular and Cellular Biology, University of Leeds, Woodhouse Lane, Leeds LS2 9JT, e-mail: A.J.Wilson@leeds.ac.uk

Contents

General methods

Unless otherwise stated, all the chemicals and reagents were obtained commercially from Sigma-Aldrich, Fisher Scientific, Alfa Aesar or Merck and used without further purification. Amino acid derivatives, coupling reagents and resins were purchased from Merck Millipore. All solvents used were HPLC grade. Analytical Thin Layer Chromatography was performed on precoated silica gel plates (Kieselgel 60F254, Merck). Column chromatographic purifications were performed either with flash silica gel or with aluminium oxide Brockmann I (50, 200 μm) from Acros Organics. NMR spectra were recorded in $CDCl_3$ or DMSO-d_6, unless otherwise stated, either on DPX300, AV 400 MHz or AV 500 MHz Bruker NMR spectrometers. All chemical shifts are reported in δ ppm downfield of TMS and peak multiplicities as singlet (s), doublet (d), quartet (q), quintet (quin), septet (sep), doublet of doublets (dd), broad singlet (bs), and multiplet (m). Signal assignment, where possible/necessary, was made with the help of 2D-NMR techniques (COSY, HMQC, HMBC, and NOESY). High resolution mass spectra (HRMS) were obtained using either a Waters GCT Premier mass spectrometer, using electron impact (EI), a Bruker micrOTOF using electrospray ionisation (ESI), or a Bruker MaXis Impact, using electrospray ionisation (ESI). Liquid chromatography mass spectra (LC-MS) were run on an Agilent 1200 LC system equipped with a Phenomenex Luna C18(2) 50 × 2 mm column, 5 μm particle size, on an acetonitrile/water gradient (5-95% acetonitrile, 0.1% formic acid, over 3 minutes) and a Bruker Daltonics HTCUltra™ system equipped with an Ion trap MS detector. Analytical HPLC experiments were run on an Agilent 1290 Infinity LC series system equipped with an Ascentis® Express Peptide ES-C18 100 × 2.1 mm column, 2.7 μm particle size, on an acetonitrile/water gradient (5-95% acetonitrile, 0.1% TFA, over 5 minutes). Mass-directed HPLC purifications were run on an Agilent 1260 Infinity Preparative HPLC system equipped with a Waters XBridge™ Prep C18 19 × 100 mm column, 5 μm particle size, on an acetonitrile or methanol/water gradient (5-95% acetonitrile or methanol over 8 minutes) and an Agilent 6120 Quadrupole system equipped with a quadrupole MS detector, using electrospray ionisation (ESI). Infra-red (IR) analyses were performed using a Perkin Elmer FT-IR spectrometer or a Bruker Platinum-ATR system equipped with an Alpha FT-IR spectrometer and the samples were analysed as solids. Optical rotations were recorded on a Schmidt Haensch Polatronic H 532 polarimeter using the sodium D line (589 nm). $[\alpha]_D$ are reported in units of 10^{-1} deg dm^2 g^{-1}.

Synthetic schemes

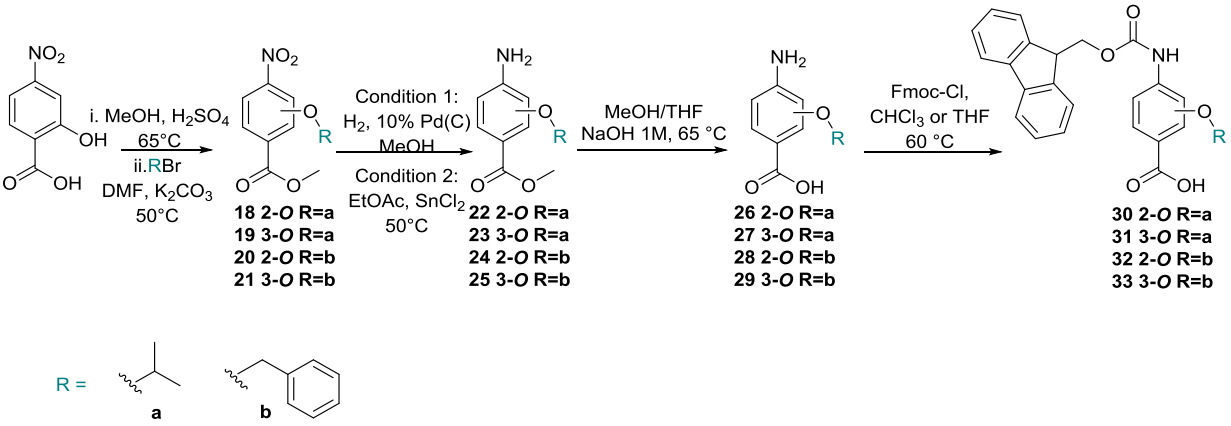

Scheme S 1. Synthetic route to Fmoc-protected building blocks of the 2-*O* and 3-*O*-alkylated *p*-aminobenzoic acid series.

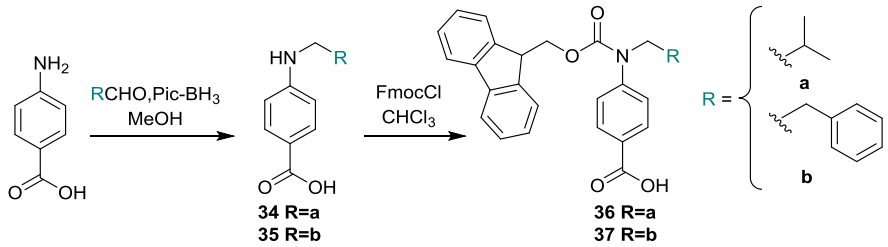

Scheme S 2. Synthetic route to Fmoc-protected building blocks of *N*-alkylated *p*-aminobenzoic acid series.

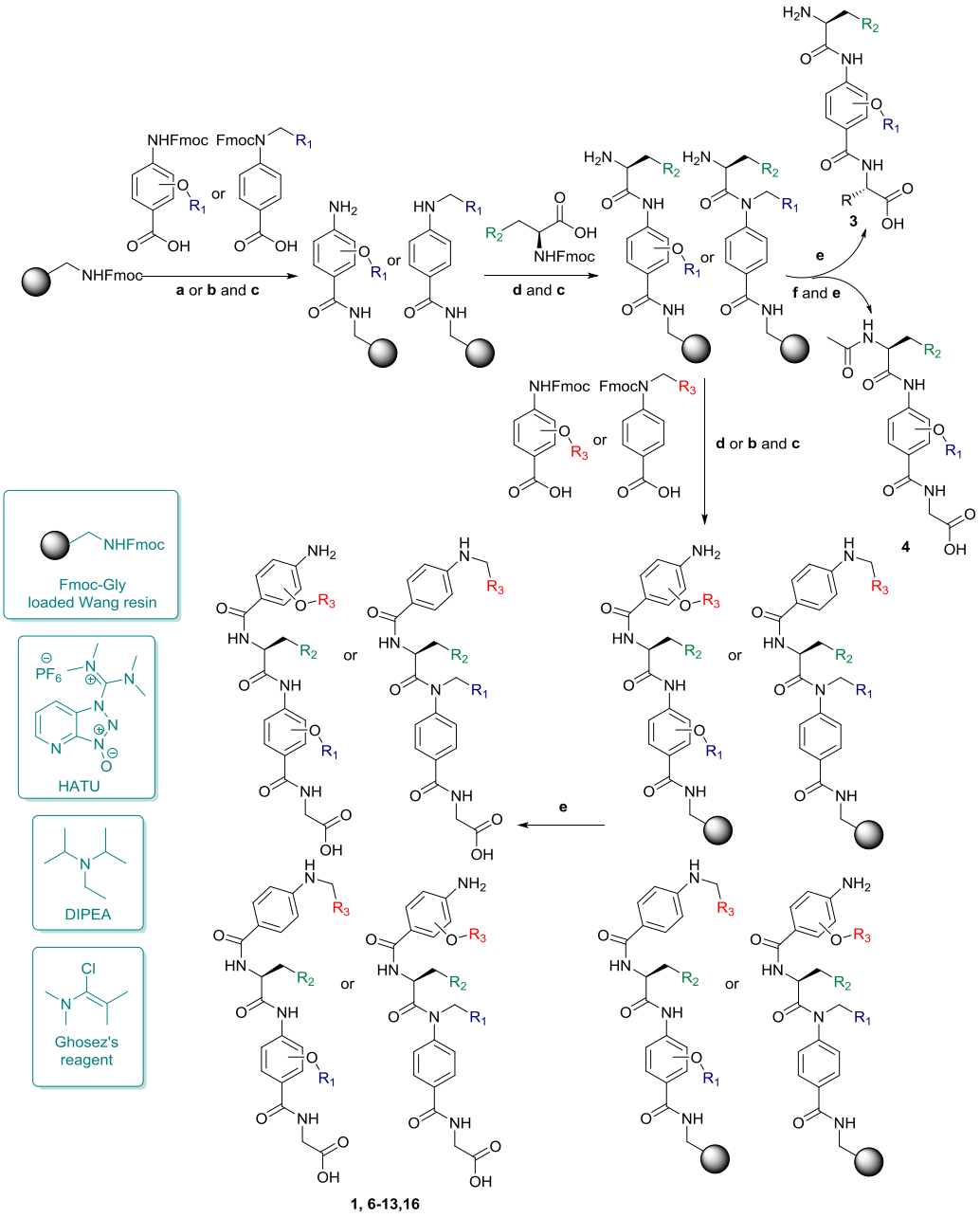

Scheme S 3. Solid phase synthesis of hybrid α-helix mimetics a Loading: resin (1 eq.) swelled in anhydrous DMF and deprotected with 20% (v/v) piperidine/DMF (two cycles of 3 min at 75 °C), 2-*O* or 3-*O*-alkylated monomer (1.5 eq.) in anhydrous DMF pre-activated with HATU (1.9 eq.) and DIPEA (3.8 eq.), single coupling method (30 min at 50 °C); b Coupling of *N*-alkylated building blocks: monomer (3 eq. per coupling) in anhydrous DMF pre-activated for a minimum of 2 hours with Ghosez's reagent (2.7 eq. per coupling), double coupling method (2×20 min at 60 °C); c Deprotection: 20% (v/v) piperidine/DMF (two cycles of 3 min at 75 °C); d Coupling: amino acid (2.5 eq. per coupling) or 2-*O* and 3-*O*-alkylated monomer (1.5 eq. per coupling) in anhydrous DMF pre-activated with HATU (3 eq. per coupling) and DIPEA (5 eq. per coupling), double or triple coupling method (2 or 3×30 min at 60 °C); e Manual cleavage: 50% (v/v) TFA/CH_2Cl_2 (two cycles of 40 min at r.t.); f Manual *N*-acetylation: acetic anhydride (10 eq.) in anhydrous DMF (overnight, r.t.).

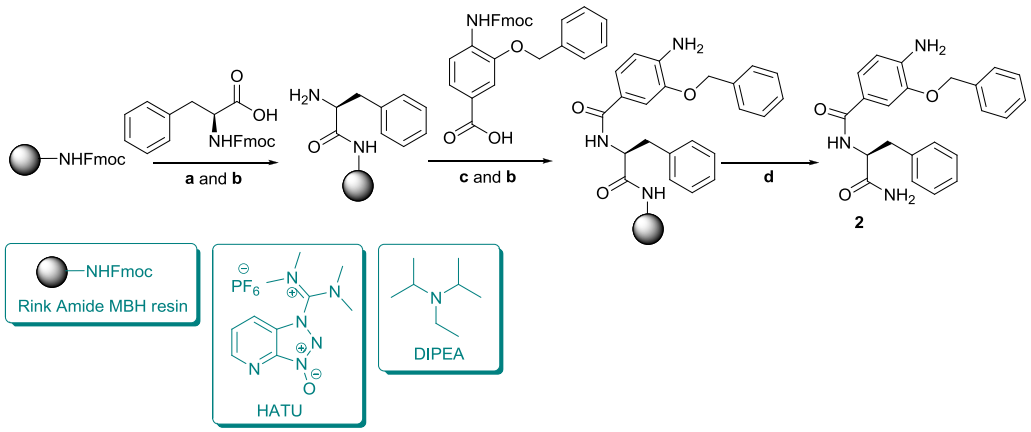

Scheme S 4. Solid phase synthesis of a control hybrid α-helix mimetic a Loading: resin (1 eq.) swelled in anhydrous DMF and deprotected with 20% (v/v) piperidine/DMF (two cycles of 3 min at 75 °C), amino acid (2.5 eq. per coupling) in anhydrous DMF pre-activated with HATU (3 eq. per coupling) and DIPEA (5 eq. per coupling), double coupling method (2×30 min at 60 °C); b Deprotection: 20% (v/v) piperidine/DMF (two cycles of 3 min at 75 °C); c Coupling: *O*-alkylated monomer (1.5 eq. per coupling) in anhydrous DMF pre-activated with HATU (3 eq. per coupling) and DIPEA (5 eq. per coupling), double coupling method (2×30 min at 60 °C); d Manual cleavage: 50% (v/v) TFA/CH_2Cl_2 (two cycles of 40 min at r.t.).

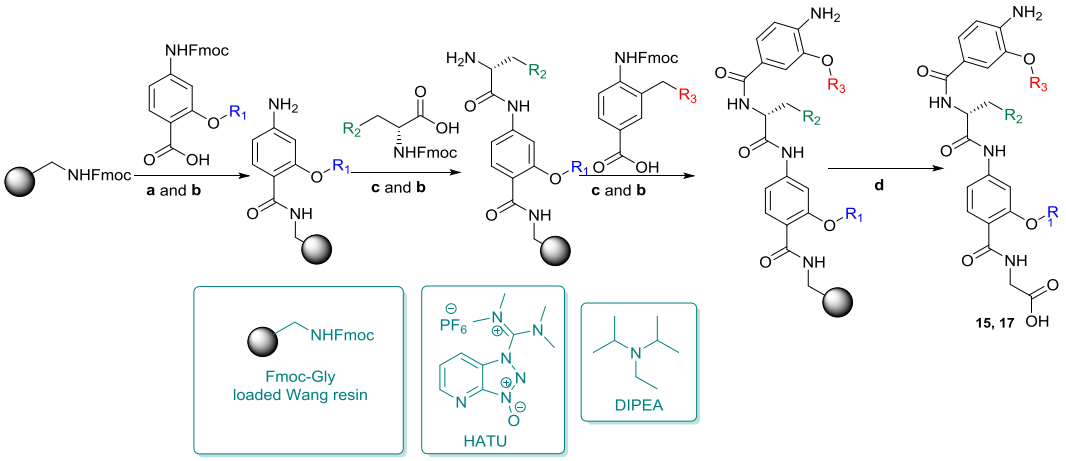

Scheme S 5. Solid phase synthesis of D-amino acid functionalised hybrid α-helix mimetics a Loading: resin (1 eq.) swelled in anhydrous DMF and deprotected with 20% (v/v) piperidine/DMF (two cycles of 3 min at 75 °C), 2-*O*-alkylated monomer (1.5 eq.) in anhydrous DMF pre-activated with HATU (1.9 eq.) and DIPEA (3.8 eq.), single coupling method (30 min at 50 °C); b Deprotection: 20% (v/v) piperidine/DMF (two cycles of 3 min at 75 °C); c Coupling: amino acid (2.5 eq. per coupling) or 2-*O*-alkylated monomer (1.5 eq. per coupling) in anhydrous DMF pre-activated with HATU (3 eq. per coupling) and DIPEA (5 eq. per coupling), double or triple coupling method (2 or 3×30 min at 60 °C); d Manual cleavage: 50% (v/v) TFA/CH_2Cl_2 (two cycles of 40 min at r.t.).

Numbering system for hybrid α-helix mimetics

To simplify the numbering and NMR assignment of the hybrid α-helix mimetics, a sequential nomenclature has been devised, where each of the monomer building blocks is considered separately (Figure S1). The monomers are numbered from 1 to 4 (or 5) starting from the *C*-terminus. *O*-Alkylated monomers are named as [*R*-(*n*-HABA)], where *R* is the alkoxy side-chain, *n*- indicates the position of the alkoxy moiety on the aromatic ring (*e.g.* for a 2-*O*-alkylated monomer *n* = 2) and HABA is the acronym for Hydroxy Amino Benzoic Acid; *N*-alkylated monomers are named as [*R*-(ABA)], where *R* is the *N*-alkyl side-chain, and ABA is the acronym for Amino Benzoic Acid. . Within each alkylated monomer, the numbering is the same: the carbons from the aminobenzoic acid are numbered using the standard system (the aromatic carbon bearing the carboxylic acid is C1, the one bearing the amine is C4). Then, the lateral chain is numbered: the carbon attached to the oxygen is the Cα, and the numbering of the aliphatic part of the side chain continues with Cβ, etc. In the case of aromatic side chains, the aromatic carbons are numbered CAr1, CAr2, etc. Amino acids are numbered using the standard convention.

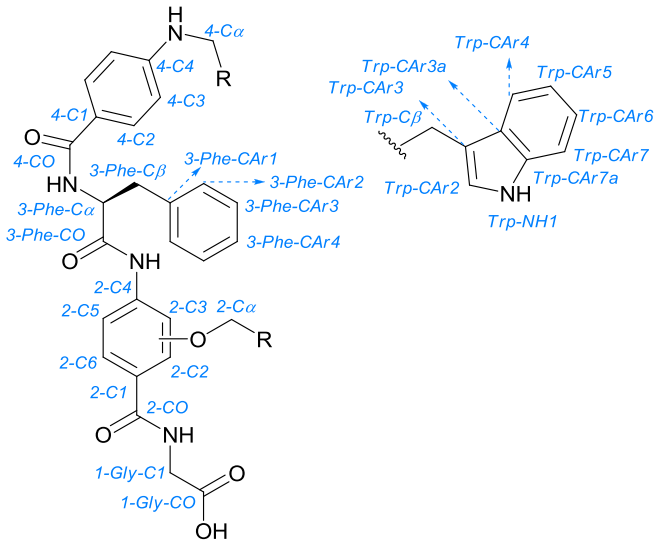

Figure S 1. Numbering of atoms in hybrid α-helix mimetics.

The numbering of the protons is based on the carbon numbering. To differentiate each individual carbon/proton, the monomer number is added as a prefix to the carbon/proton number.

Synthetic Procedures: Monomer building blocks

A generic procedure was followed using minor modifications to the previously reported work for the *O*-alkylation, ester hydrolysis, nitro group reduction and coupling reactions to make novel oligomers. These procedures are described briefly below:

(a) Procedure for *O*-Alkylation

Alkyl halide (1.2 equiv.) was added to a solution of the phenol (1 equiv.) in dry DMF under an argon or nitrogen atmosphere, followed by potassium carbonate (3 equiv.) and the reaction mixture was stirred at 50^{o} C for 12-48 h. After complete consumption of starting material based on TLC, the reaction mixture was diluted with ethyl acetate and acidified with 1N hydrochloric acid solution. The product was extracted into ethyl acetate (3 x 30 mL) and the combined organic layers were washed with water and dried over anhydrous sodium sulfate. The crude product obtained after the removal of solvent was purified either by crystallization or column chromatography.

(b) Procedure for ester hydrolysis

Ester (1 equiv.) in a mixture of tetrahydrofuran-methanol (10 mL) was subjected to hydrolysis using 1 M sodium hydroxide solution. After completion of the reaction (24-36 h), the pale yellow precipitate obtained on acidification was extracted into dichloromethane and the organic layer was washed with water until the pH was neutral. The organic layer was dried over anhydrous sodium sulfate. The product isolated after the removal of the solvent was used for the next step.

(c) Procedure for nitro reduction

Tin (II) chloride dihydrate (5 equiv.) was added to a solution of nitro compound (1 equiv.) in ethyl acetate, and the reaction mixture was stirred at 50^{o} C for 12-48 h. The reaction was diluted with ethyl acetate, basified with 1N sodium hydroxide solution and the product was extracted into ethyl acetate (3 x 30 mL). The organic layer was dried over anhydrous sodium sulfate and the product isolated after the removal of the solvent was used for the next step without further purification.

(d) Procedure for the coupling

Dichloro triphenylphosphorane (4.5 equiv.) was added to a stirred solution of amine (1.2 equiv.) and acid (1 equiv.) in anhydrous chloroform (5 mL per 50 mg of acid) under an argon atmosphere and the solution was heated to reflux (80°C) until TLC analysis showed complete conversion. The crude product obtained after the removal of chloroform was treated with ethyl acetate (20-30 mL), filtered and washed with ethyl acetate (3x10 ml) to obtain a pale yellow coloured solid.

(e) Procedure for Fmoc-protection

To a refluxing solution of amino benzoic acid (1 equiv) in anhydrous chloroform or tetrahydrofuran (10 mL) was added dropwise a solution of Fmoc-Chloride (1.2 equiv.) in chloroform (15 mL) over a period of 30 minutes. The reaction mixture was allowed to stir for 48 h and the solvent was removed under reduced pressure. The resulting oil was crystallized from a mixture of dichloromethane-hexane.

Compounds **18**-**25**, **27**, **29**, **31**, **33**-**37** were synthesized as described previously.[1-6]

H_2N-[*Oi*Pr-(2-HABA)]-CO_2H (26)

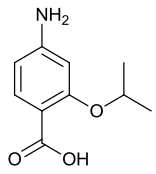

Using general procedure for ester hydrolysis (b) (heated at 65 ºC), H_2N-[*Oi*Pr-(2-HABA)]-CO_2Me **22** (500 mg, 2.4 mmol, 1 eq.); sodium hydroxide 1 M (5 mL); anhydrous methanol (40 mL). On cooling, the reaction mixture was acidified to pH ≈ 1 (ca 5 mL, hydrochloric acid 1 N) and extracted with dichloromethane (3 × 50 mL). The organic was dried (sodium sulphate) and the solvent removed under reduced pressure to leave the pure product as a yellow solid (449 mg, 96%); R_f 0.51 (SiO_2, 40% ethylacetate in dichloromethane); ^{1}H NMR ($CDCl_3$, 500 MHz) δ: 10.83 (s, 1 H, CO_2H), 7.86 (d, J = 8.5 Hz, 1 H, H6), 6.27 (s, 1 H, H3), 6.17 (d, J = 8.5 Hz 1 H, H5), 4.72-4.67 (apparent quin, J = 6 Hz, 1 H, Hα), 4.20 (br, 2 H, NH_2), 1.38 (d, J = 6 Hz, 6H, Hβ) ppm; ^{13}C NMR ($CDCl_3$, 126 MHz) δ: 165.0 (CO), 157.2 (C2), 151.9 (C4), 134.3 (C6), 107.5 (C5), 106.9 (C1), 97.7 (C3), 72.4 (Cα), 21.0 (Cβ) ppm; IR (neat) ν(cm^{-1}): 3437, 3356, 3246, 2978, 1685, 1600, 1507, 1456, 1383, 1270; ESI-MS found: 194 $(M-H)^-$; HRMS m/z calculated for $C_{10}H_{13}NNaO_3$ $(M+Na)^+$: 218.0788; Found: 218.0796.

H_2N-[*O*Bn-(2-HABA)]-CO_2H (28)

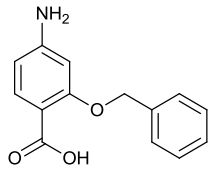

Using general procedure for ester hydrolysis (b) (heated at 65 ºC). H_2N-[*O*Bn-(2-HABA)]-CO_2Me **24** (300.0 mg, 1.2 mmol); sodium hydroxide 1 M (3 mL); anhydrous methanol (15 mL) and anhydrous tetrahydrofuran (15 mL). On cooling, the reaction mixture was acidified to pH ≈ 1 (ca 5 mL, hydrochloric acid 1 N) and extracted with dichloromethane (3 × 150 mL). The organic was dried (sodium sulphate) and the solvent removed under reduced pressure. The product was eventually purified by column chromatography (SiO_2, gradient dichloromethane:ethyl acetate) to leave a grey gel (228.7 mg, 80%); R_f 0.40 (SiO_2, 20% ethylacetate in dichloromethane); ^{1}H NMR ($CDCl_3$, 500 MHz) δ: 10.54 (s, 1 H, CO_2H), 7.96 (d, J = 8 Hz, 1 H, H6), 7.44-7.34 (m, 5 H, HAr2, HAr3, HAr4), 6.36 (d, J = 8 Hz 1 H, H5), 6.30 (s, 1 H, H1), 5.20 (s, 2 H, Hα), 4.25 (br, 2 H, NH_2) ppm; ^{13}C NMR ($CDCl_3$, 126 MHz) δ: 166.0 (CO), 159.3 (C2), 153.5 (C4), 135.4 (C6), 134.5 (CAr1), 129.1 (CAr), 129.0 (CAr4), 127.3 (CAr), 108.6 (C5), 106.9 (C1), 97.9 (C3), 71.9 (Cα) ppm; IR (neat) ν (cm^{-1}): 3470, 3359, 3237, 1704, 1602, 1453; ESI-MS found: 244 $(M+H)^+$, 509 $(2M+Na)^+$; HRMS *m*/*z* calculated for $C_{14}H_{14}NO_3$ $(M+H)^+$: 244.0968; Found: 244.0969.

FmocNH-[*Oi*Pr-(2-HABA)]-CO_2H (30)

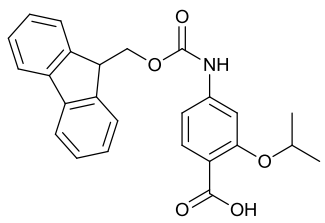

Using general procedure for Fmoc-protection (e). H_2N-[*Oi*Pr-(2-HABA)]-CO_2H **26** (350.0 mg, 1.8 mmol); anhydrous chloroform (12 mL); Fmoc-Chloride (555.0 mg, 2.14 mmol) in chloroform (15 mL). The reaction mixture was allowed to stir for 46 h until TLC analysis showed complete conversion. The solvent was removed under reduced pressure and the resulting oil was crystallized from a mixture of dichloromethane-hexane to leave the pure product as a colourless solid (448 mg, 60%); R_f 0.60 (SiO_2, 30% ethylacetate in dichloromethane); ^{1}H NMR ($CDCl_3$, 500 MHz) δ: 8.11 (d, J = 8.5 Hz, 1 H, H6), 7.82 (d, J = 7.5 Hz, 2 H, Fmoc-HAr5), 7.68 (br, 1 H, NH), 7.64 (d, J = 7.5 Hz, 2 H, Fmoc-HAr2), 7.46 (t, J = 7.5 Hz, 2 H, Fmoc-HAr4), 7.37 (d, J = 7.5 Hz, 2 H, Fmoc-HAr3), 6.98 (s, 1 H, H3), 6.76 (d, J = 8.5 Hz 1 H, H5), 4.94-4.89 (apparent quin, J = 6 Hz, 1 H, Hα), 4.61 (d, J = 6.5 Hz, 2 H, Fmoc-Hα), 4.31 (t, J = 6.5 Hz, 1 H, Fmoc-Hβ), 1.49 (d, J = 6 Hz, 6H, Hβ) ppm; ^{13}C NMR ($CDCl_3$, 126 MHz) δ: 165.2 (CO), 157.6 (C2), 159.2 (Fmoc-CO), 143.8 (C4), 143.4 (Fmoc-CAr1), 141.4 (Fmoc-CAr6), 134.5 (C6), 127.9 (Fmoc-

CAr4), 127.2 (Fmoc-CAr3), 124.8 (Fmoc-CAr2), 120.2 (Fmoc-CAr5), 113.3 (C1), 111.5 (C5), 103.3 (C3), 74.2 (Cα), 67.2 (Fmoc-Cα), 47.0 (Fmoc-Cβ), 22.0 (Cβ) ppm; IR (neat) ν (cm^{-1}): 3282, 2978, 1714, 1593, 1531, 1414, 1217; ESI-MS found: 416 $(M-H)^-$; HRMS *m*/*z* calculated for $C_{25}H_{23}NNaO_5$ $(M+Na)^+$: 440.1468; Found: 440.1478; Elemental analysis calculated: C, 71.93; H, 5.55; N, 3.36; Found: C, 71.90; H, 5.60; N, 3.30.

FmocNH-[*O*Bn-(2-HABA)]-CO_2H (32)

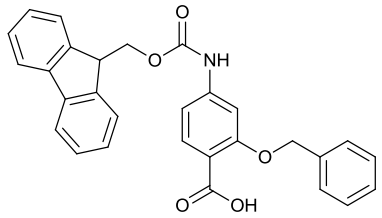

Using general procedure for Fmoc-protection (e). H_2N-[*O*Bn-(2-HABA)]-CO_2H **28** (150.0 mg, 0.62 mmol); anhydrous chloroform (4 mL); Fmoc-Chloride (192.0 mg, 0.74 mmol) in chloroform (3 mL). The reaction mixture was allowed to stir for 50 h until TLC analysis showed complete conversion. The solvent was removed under reduced pressure and the resulting oil was crystallized from a mixture of dichloromethane-hexane to leave the pure product as a colourless solid (205.7 mg, 71%); R_f 0.30 (SiO_2, (SiO_2, 30% ethylacetate in dichloromethane); ^{1}H NMR ($CDCl_3$, 500 MHz) δ: 8.16 (d, *J* = 8.3 Hz, 1 H, H6), 7.86 (d, *J* = 7.5 Hz, 2 H, Fmoc-HAr5), 7.83 (br, 1 H, NH), 7.69 (d, *J* = 7.5 Hz, 2 H, Fmoc-HAr2), 7.47-7.51 (m, 5 H, HAr2, HAr3, HAr4), 7.39 (t, *J* = 7.5 Hz, 4 H, Fmoc-HAr4, Fmoc-HAr3), 7.33 (s, 1 H, H3), 6.88 (d, *J* = 8.3 Hz 1 H, H5), 5.33 (s, 2 H, Hα), 4.65 (d, *J* = 6.5 Hz, 2 H, Fmoc-Hα), 4.34 (t, *J* = 6.5 Hz, 1 H, Fmoc-Hβ) ppm; ^{13}C NMR ($CDCl_3$, 126 MHz) δ: 165.2 (CO), 158.5 (C2), 153.0 (Fmoc-CO), 144.2 (C4), 143.4 (Fmoc-CAr1), 141.4 (Fmoc-CAr6), 134.6 (C6), 134.1 (CAr1), 129.2 (CAr4), 129.1 (CAr), 128.2 (Fmoc-CAr4), 127.9 (Fmoc-CAr3), 127.2 (CAr), 124.9 (Fmoc-CAr2), 120.2 (Fmoc-CAr5), 112.4 (C1), 111.7 (C5), 102.4 (C3), 72.3 (Cα), 67.2 (Fmoc-Cα), 47.0 (Fmoc-Cβ) ppm; IR (neat) ν (cm^{-1}): 3333, 1722, 1702, 1612, 1524, 1411; ESI-MS found: 488 $(M+Na)^+$; HRMS *m*/*z* calculated for $C_{29}H_{24}NO_5$ $(M+H)^+$: 466.1649; Found: 466.1644.

Synthetic procedures: Solid phase synthesis of hybrid α-helix mimetics

A generic procedure was followed by adapting the previously reported solid phase syntheses[6,7] of 3-*O*-alkylated and *N*-alkylated oligobenzamides. The reactions were all carried out on a CEM Liberty® automated microwave assisted peptide synthesiser. The procedure is described briefly below:

Resin preparation

127 mg of Fmoc-Gly-Wang resin (0.79 mmol g^{-1}, 100-200 mesh; carrier: polystyrene, crosslinked with 1% DVB) were used for hybrid mimetics **1**, **3**-**18**; 170 mg of Rink Amide MBH resin (0.59 mmol g^{-1}) were used for hybrid mimetic **2**. The resin was swelled in Corning® tubes in DMF for at least 30 minutes prior to coupling. Standard washing and deprotection cycles were carried out on the synthesiser. A filtered drain took place in between every wash as follows: wash the reaction vessel from the top ('DMF top', 5 mL), then from the bottom ('DMF bottom', 7 mL), then 'DMF top' (5 mL).

Fmoc deprotection

Before coupling of each monomer and after the last coupling reaction, two deprotection cycles were carried out on the CEM synthesiser using 6 mL of a 25% piperidine solution in DMF, under microwave heating at 75 °C. The initial deprotection lasted 30 seconds and was followed by a 'DMF top' wash and filtered drain. After a second addition of deprotection mixture, the deprotection was maintained under microwave heating for 3 minutes, and was again followed by DMF washes.

Coupling of 2-O and 3-O-alkylated monomers to the resin

Prior to the reaction, each fully protected monomer (1.5 eq.) was dissolved in anhydrous DMF (2.5 mL) in a dry 50 mL Corning® tube (stored in an oven at 60 °C for at least 24 hours), and pre-activated with HATU (1.9 eq.) and DIPEA (3.8 eq.) at room temperature. A single coupling method of 30 min was carried out under microwave heating at 50 °C.

Coupling of N-alkylated monomers

Prior to the reaction, each fully protected monomer (3 eq. per coupling) was dissolved in anhydrous chloroform (2.5 mL per coupling, *i.e.* 5 mL for a double coupling) in a dry 50 mL Corning® tube (stored in an oven at 60 °C for at least 24 hours), and pre-activated with Ghosez's reagent (2.7 eq. per coupling) at room temperature for 1-3 hours under a nitrogen atmosphere. For each monomer, a double coupling of 20 minutes was carried out under microwave heating at 60 °C.

Coupling of middle amino acids

Prior to the reaction, each fully protected aminoacid (2.5 eq. per coupling) was dissolved in anhydrous DMF (2.5 mL per coupling) in a dry 50 mL Corning® tube (stored in an oven at

60 °C for at least 24 hours), and pre-activated with HATU (3 eq. per coupling) and DIPEA (5 eq. per coupling) at room temperature for 1-3 hours under a nitrogen atmosphere. For natural amino acid derivatives, a double coupling of 30 minutes was carried out under microwave heating at 60 °C. For non-natural amino acids, a triple coupling of 30 minutes was carried out under microwave heating at 60 °C.

Coupling of 2-O and 3-O-alkylated monomers

Prior to the reaction, each fully protected monomer (1.5 eq. per coupling) was dissolved in anhydrous DMF (2.5 mL per coupling) in a dry 50 mL Corning® tube (stored in an oven at 60 °C for at least 24 hours), and pre-activated with HATU (3 eq. per coupling) and DIPEA (5 eq. per coupling) at room temperature. A double coupling method of 30 min was carried out under microwave heating at 60 °C.

Cleavage

The cleavage step was carried out manually, in 3 mL 'Extract-Clean' polypropylene reservoirs fitted with 20 µm polyethylene frits, both available from Alltech. The resin was transferred to a reservoir then washed with dichloromethane (2 × 3 mL × 2 min) and diethylether (2 × 3 mL × 2 min). 3 mL of a 1:1 mixture of TFA in dichloromethane was added and the mixture was allowed to stir at room temperature for 40 minutes. The content of the reservoir was collected and the procedure was repeated. The combined solution was then concentrated under reduced pressure and the resulting oil was washed with hexane and diethylether to afford a solid.

Purification

The hybrid mimetics were purified using mass-directed preparative HPLC (0.1% formic acid water/methanol or acetonitrile; 5-95% gradient) to afford the desired products with purity higher than 90-95%.

H_2N-[*O*-Bn-(3-HABA)]-Phe-[*O*-*i*Pr-(2-HABA)]-Gly-CO_2H (1)

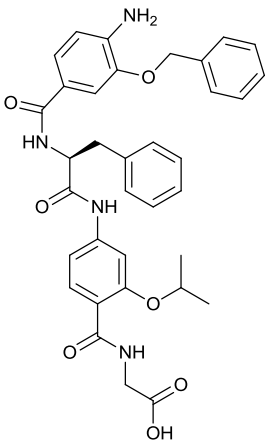

Pale orange solid, > 95% pure by NMR; isolated yield: 11.6 mg, 19%; R_f 0.50 (SiO_2, 20% methanol in acetonitrile); $[\alpha]_D^{27.5}$ = + 22.8° (c 0.008 g mL^{-1}, methanol); ^{1}H NMR (DMSO-d_6, 500 MHz) δ: 10.46 (s, 1H,1-Gly-CO_2H), 8.49 (t, *J* = 5 Hz, 1 H, 1-Gly-NH), 8.36 (d, *J* = 8 Hz, 1 H, 3-Phe-NH), 7.91 (d, *J* = 8.5 Hz, 1 H, 2-H6), 7.64 (s, 1 H, 2-H3), 7.53 (d, *J* = 8.5 Hz, 2 H, 3-Phe-HAr2), 7.45 (s, 1 H, 4-H2), 7.43-7.40 (m, 5 H, 4-HAr2, 4-H-Ar3, 4-HAr4), 7.35 (t, *J* = 8.5 Hz, 2 H, 3-Phe-HAr3), 7.30 (d, *J* = 8.5 Hz, 2 H, 4-H6, 2-H5), 7.28 (br, 1H, 2-NH), 7.20 (t, *J* = 8.5 Hz, 1H, 3-Phe-HAr4), 6.66 (d, *J* = 8.5 Hz, 1 H, 4-H5), 5.34 (br, 2H, 4-NH_2), 5.17 (s, 2 H, 4-Hα), 4.85-4.81 (dd, *J* = 8.5 , 5.5 Hz, 1 H, 3-Phe-Hα), 4.76-4.71 (apparent quin, *J* = 6 Hz, 1 H, 2-Hα), 4.05 (d, *J* = 5 Hz, 2 H, 1-Gly-H1), 3.16-3.12 (dd, *J* = 8.5 , 5.5 Hz, 2 H, 3-Phe-Hβ), 1.45-1.43 (dd, *J* = 8.5, 6 Hz, 6 H, 2-Hβ) ppm; ^{13}C NMR (DMSO-d_6, 126 MHz) δ: 171.5 (1-Gly-CO), 166.4 (4-CO), 163.9 (2-CO), 156.2 (3-Phe-CO), 144.0 (4-C3), 143.1 (2-C2), 141.5 (4-C4), 138.2 (2-C4), 137.2 (2-C6), 131.9 (4-CAr1), 129.2 (3-Phe-CAr3), 128.4 (4-CAr2, 4-CAr3), 128.1 (4-CAr4), 127.7 (4-C2), 127.4 (3-Phe-CAr2, 3-Phe-CAr4), 126.3 (3-Phe-CAr1), 121.8 (4-C6), 120.8 (4-C1), 116.6 (2-C1), 112.3 (4-C5), 111.4 (2-C5), 104.7 (2-C3), 71.9 (2-Cα), 69.4 (4-Cα), 55.9 (3-Phe-Cα), 41.7 (1-Gly-C1), 37.1 (3-Phe-Cβ), 21.6 (2-Cβ) ppm; IR (neat) ν (cm^{-1}): 3344, 2922, 1682, 1594, 1494, 1257, 1208; ESI-MS found: 625 $(M+H)^+$; HRMS *m/z* calculated for $C_{35}H_{37}N_4O_7$ $(M+H)^+$: 625.2657; Found: 625.2666.

H_2N-[O-Bn-(3-HABA)]-Phe-$CONH_2$ (2)

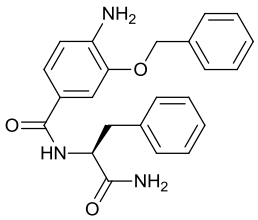

Colourless solid, > 95% pure by NMR; isolated yield: 9.6 mg, 25%; R_f 0.03 (SiO_2, 20% methanol in acetonitrile); $[\alpha]_D^{26.9}$ = - 36.0° (c 0.002 g mL^{-1}, methanol); ^{1}H NMR (DMSO-d_6, 500 MHz) δ: 8.05 (d, *J* = 8.5 Hz, 1 H, 1-Phe-NH), 7.51 (d, *J* = 7.5 Hz, 2 H, 2-HAr2), 7.46 (s, 1 H, 2-H2), 7.41 (t, *J* = 8 Hz, 2 H, 1-Phe-HAr3), 7.35 (d, *J* = 7.5 Hz, 1 H, 2-HAr4), 7.32 (d, *J* = 8 Hz, 2 H, 1-Phe-HAr2), 7.27 (d, *J* = 8.5 Hz, 1 H, 2-H6), 7.24 (t, *J* = 7, 5 Hz, 2 H, 2-HAr3), 7.16 (t, *J* = 8 Hz, 1 H, 1-Phe-HAr4), 7.06 (s, 2H, 1-NH_2), 6.63 (d, *J* = 8.5 Hz, 1 H, 2-H5), 5.29 (s, 2H, 2-NH_2), 5.15 (s, 2H, 2-Hα), 4.63 - 4.58 (apparent quin, *J* = 4.5 Hz, 1 H, 1-Phe-

Hα), 3.11-3.07 (dd, *J* = 13.5, 4.5 Hz, 1 H, 1-Phe-Hβ), 3.0-2.96 (dd, *J* = 13.5, 4.5 Hz, 1 H, 1-Phe-Hβ') ppm; ^{13}C NMR (DMSO-d_6, 126 MHz) δ: 173.7 (1-Phe-CO), 166.0 (2-CO), 144.1 (2-C3), 141.4 (2-C4), 138.7 (2-CAr1), 137.2 (1-Phe-CAr1), 129.1 (1-Phe-CAr2), 129.1 (4-C4), 128.4 (1-Phe-CAr3), 128.0 (2-CAr4), 127.4 (2-CAr2, 2-CAr3), 126.1 (1-Phe-CAr4), 121.5 (2-C6), 121.3 (2-C1), 112.3 (2-C2), 111.3 (2-C5), 69.4 (2-Cα), 54.5 (1-Phe-Cα), 35.1 (1-Phe-Cβ) ppm; IR (neat) ν (cm^{-1}): 3482, 3386, 3303, 2925, 2853, 1682, 1615, 1579, 1499, 1260, 1228; ESI-MS found: 801 $(2M+Na)^+$; HRMS *m/z* calculated for $C_{23}H_{24}N_3O_3$ $(M+H)^+$: 390.1812; Found: 390.1821.

H_2N-Phe-[*O*-*i*Pr-(2-HABA)]-Gly-CO_2H (3)

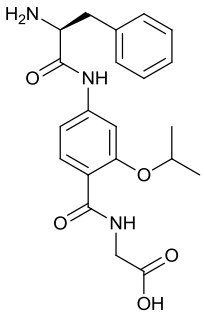

Colourless solid, > 95% pure by NMR; isolated yield: 10 mg, 25%; R_f 0.05 (SiO_2, 20% methanol in acetonitrile); $[\alpha]_D^{26.6}$ = + 37.3° (c 0.003 g mL^{-1}, methanol); ^{1}H NMR (DMSO-d_6, 500MHz) δ: 8.51 (t, *J* = 5 Hz, 1 H, 1-Gly-NH), 8.20 (s, 1 H, 2-NH), 7.90 (d, *J* = 8.5 Hz, 1 H, 2-H6), 7.59 (s, 1 H, 2-H3), 7.29 (d, *J* = 8.5 Hz, 2 H, 3-Phe-HAr), 7.27 (s, 1 H3-Phe-HAr4), 7.26 (d, *J* = 8.5 Hz, 2 H, 3-Phe-HAr), 7.23 (d, *J* = 8.5 Hz, 1 H, 2-H5), 4.66 - 4.76 (apparent quin, *J* = 6 Hz, 1 H, 2-Hα), 3.99 (d, *J* = 5 Hz, 2 H, 1-Gly-H1), 3.78 (t, *J* = 5.5 Hz, 2 H, 3-Phe-Hα), 3.10-3.06 (dd, *J* = 12.8, 5.5 Hz, 1 H, 3-Phe-Hβ), 2.88-2.85 (dd, *J* = 12.8, 5.5 Hz, 1 H, 3-Phe-Hβ'), 1.42 ppm (d, *J* = 6 Hz, 6 H, 2-Hβ); ^{13}C NMR (DMSO-d_6, 126MHz) δ: 171.4 (1-Gly-CO), 164.0 (2-CO), 156.4 (3-Phe-CO), 142.5 (2-C2, 2-C4), 136.8 (3-Phe-CAr1), 132.2 (2-C6), 129.5 (3-Phe-CAr), 128.6 (3-Phe-CAr), 126.9 (3-Phe-CAr4), 117.3 (2-C1), 111.6 (2-C3), 105.1 (2-C5), 72.1 (2-Cα), 56.1 (3-Phe-Cα), 40.4 (1-Gly-C1), 40.1 (3-Phe-Cβ), 21.7 (2-Cβ) ppm; IR (neat) ν (cm^{-1}): 3356, 2979, 2930, 1693, 1629, 1593, 1491, 1258, 1229; ESI-MS found: 400 $(M+H)^+$; HRMS *m/z* calculated for $C_{21}H_{26}N_3O_5$ $(M+H)^+$: 400.1867; Found: 400.1872.

Ac-HN-Phe-[*O*-*i*Pr-(2-HABA)]-Gly-CO_2H (4)

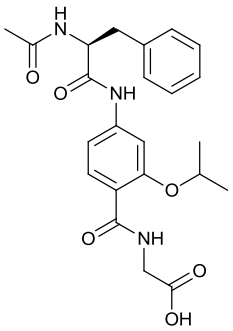

Colourless solid, > 95% pure by NMR; isolated yield: 45.5 mg, quant.; R_f 0.17 (SiO_2, 20% methanol in acetonitrile); $[\alpha]_D^{26.9}$ = + 18.1° (c 0.005 g mL^{-1}, methanol); ^{1}H NMR (DMSO-d_6, 500 MHz) δ: 10.35 (s, 1H, 1-Gly-CO_2H), 8.46 (t, *J* = 5 Hz, 1 H, 1-Gly-NH), 8.32 (d, *J* = 8.5 Hz, 1 H, 3-Phe-NH), 7.89 (d, *J* = 8.5 Hz, 1 H, 2-H6), 7.59 (s, 1 H, 2-H3), 7.30-7.27 (m, 6 H, 3-Phe-HAr and 2-NH), 7.22 (d, *J* = 8.5 Hz, 1 H, 2-H5), 4.68 - 4.73 (apparent quin, *J* = 6 Hz, 1 H, 2-Hα), 4.64-4.67 (m, *J* = 5.5 Hz, 2 H, 3-Phe-Hα), 4.05 (d, *J* = 5 Hz, 2 H, 1-Gly-H1), 3.07-3.03 (dd, *J* = 12.8, 5.5 Hz, 1 H, 3-Phe-Hβ), 2.90-2.85 (dd, *J* = 12.8, 5.5 Hz, 1 H, 3-Phe-Hβ'), 1.82 (s, 1 H, Ac-H1), 1.43-1.41 (dd, *J* = 6, 9.5 Hz, 6 H, 2-Hβ) ppm; ^{13}C NMR (DMSO-d_6, 126 MHz) δ: 171.2 (1-Gly-CO), 169.3 (Ac-CO), 163.9 (2-CO), 156.2 (3-Phe-CO), 142.9 (2-C2), 137.6 (2-C4), 131.9 (2-C6), 129.5 (3-Phe-CAr1), 129.1 (3-Phe-CAr), 128.1 (3-Phe-CAr), 126.4 (3-Phe-CAr4), 116.7 (2-C1), 111.4 (2-C3), 104.7 (2-C5), 71.2 (2-Cα), 55.0 (3-Phe-Cα), 41.6 (1-Gly-C1), 37.5 (3-Phe-Cβ), 22.3 (Ac-C1), 21.6 (2-Cβ) ppm; IR (neat) ν (cm^{-1}): 3285, 3063, 2981, 2931, 1640, 1596, 1495, 1258, 1186; ESI-MS found: 442 $(M+H)^+$; HRMS *m/z* calculated for $C_{23}H_{27}N_3NaO_6$ $(M+Na)^+$: 464.1792; Found: 464.1794.

H_2N-[ABA]-Phe-[*O*-*i*Pr-(2-HABA)]-Gly-CO_2H (5)

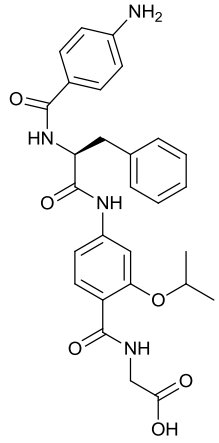

Pale brown solid, > 95% pure by NMR; isolated yield: 15.8 mg, 19%; R_f 0.18 (SiO_2, 20% methanol in acetonitrile); $[\alpha]_D^{27.0}$ = + 26.0° (c 0.005 g mL^{-1}, methanol); ^{1}H NMR (DMSO-d_6, 500 MHz) δ: 10.41 (s, 1H,1-Gly-CO_2H), 8.46 (t, *J* = 5 Hz, 1 H, 1-Gly-NH), 8.25 (d, *J* = 8.5 Hz, 1 H, 3-Phe-NH), 7.90 (d, *J* = 8.5 Hz, 1 H, 2-H6), 7.60 (s, 1 H, 2-H3), 7.59 (d, *J* = 8.5 Hz, 2 H, 4-H2), 7.40 (d, *J* = 7.5 Hz, 2 H, 3-Phe-HAr2), 7.32 (d, *J* = 7.5 Hz, 1 H, 3-Phe-HAr2'), 7.29 (s, 1H, 2-NH), 7.25 (d, *J* = 8.5 Hz, 1 H, 2-H5), 7.20-7.18 (dd, *J* = 7, 5 Hz, 1 H, 3-Phe-HAr4), 7.13 (d, *J* = 7.5 Hz, 1 H, 3-Phe-HAr3), 6.54 (d, *J* = 8.5 Hz, 2 H, 4-H3), 4.82 - 4.79 (m, *J* = 5.5 Hz, 1 H, 3-Phe-Hα), 4.75-4.70 (apparent quin, *J* = 6 Hz, 1 H, 2-Hα), 4.06 (d, *J* = 5 Hz, 2 H, 1-Gly-H1), 3.14-3.07 (dd, *J* = 12.8, 5.5 Hz, 2 H, 3-Phe-Hβ), 1.43-1.41 (dd, *J* = 6, 9.5 Hz, 6 H, 2-Hβ) ppm; ^{13}C NMR (DMSO-d_6, 126 MHz) δ: 171.2 (1-Gly-CO), 166.5 (4-CO), 163.9

(2-CO), 156.2 (3-Phe-CO), 151.6 (2-C2), 143.8 (2-C4), 138.2 (3-Phe-CAr4), 131.9 (2-C6), 129.2 (3-Phe-CAr2), 129.1 (4-C4), 129.0 (4-C2), 128.3 (3-Phe-CAr3), 128.0 (3-Phe-CAr3'), 126.3 (3-Phe-CAr4), 116.6 (2-C1), 112.6 (4-C3), 112.6 (2-C5), 111.3 (2-C3), 71.9 (2-Cα), 55.8 (3-Phe-Cα), 41.6 (1-Gly-C1), 37.0 (3-Phe-Cβ), 21.6 (2-Cβ) ppm; IR (neat) ν (cm^{-1}): 3359, 3023, 2980, 2931, 1721, 1630, 1596, 1494, 1259, 1184; ESI-MS found: 519 $(M+H)^+$; HRMS *m/z* calculated for $C_{28}H_{30}N_4NaO_6$ $(M+Na)^+$: 541.2057; Found: 541.2063.

H_2N-[*O*-Bn-(3-HABA)]-His-[*O*-*i*Pr-(2-HABA)]-Gly-CO_2H (6)

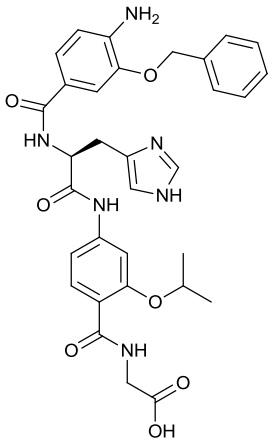

Colourless solid, > 95% pure by NMR; isolated yield: 2.6 mg, 4%; R_f 0.01 (SiO_2, 20% methanol in acetonitrile); $[\alpha]_D^{27.0}$ = + 32.5° (c 0.002 g mL^{-1}, methanol); ^{1}H NMR DMSO-d_6, 500 MHz) δ: 10.36 (s, 1H,1-Gly-CO_2H), 8.47 (t, *J* = 5 Hz, 1 H, 1-Gly-NH), 8.40 (d, *J* = 8 Hz, 1 H, 3-His-NH), 7.89 (d, *J* = 8.5 Hz, 1 H, 2-H6), 7.86 (s, 1 H, 3-His-HAr5), 7.63 (s, 1 H, 2-H3), 7.52 (d, *J* = 7.5 Hz, 2 H, 4-HAr2), 7.46 (s, 1 H, 4-H2), 7.41 (t, *J* = 7.5 Hz, 3 H, 4-HAr3, 4-HAr4), 7.35 (s, 1H, 2-NH), 7.34 (d, *J* = 8 Hz, 1 H, 4-H6), 7.25 (d, *J* = 8.5 Hz, 1 H, 2-H5), 6.99 (s, 1 H, 3-His-HAr2), 6.67 (d, *J* = 8 Hz, 1 H, 4-H5), 5.34 (br, 2H, 4-NH_2), 5.16 (s, 2 H, 4-Hα), 4.80-4.76 (dd, *J* = 8, 6 Hz, 1 H, 3-His-Hα), 4.73-4.68 (apparent quin, *J* = 5.5 Hz, 1 H, 2-Hα), 4.5 (d, *J* = 5 Hz, 2 H, 1-Gly-H1), 3.14-3.07 (dd, *J* = 9, 6 Hz, 2 H, 3-His-Hβ), 1.42-1.40 (dd, *J* = 10.5, 5.5 Hz, 6 H, 2-Hβ) ppm; ^{13}C NMR (DMSO-d_6, 126 MHz) δ: 171.2 (1-Gly-CO), 166.2 (4-CO), 163.9 (2-CO), 156.2 (3-His-CO), 144.2 (4-C3), 143.1 (2-C2), 141.6 (4-C4), 137.2 (2-C4), 134.5 (4-CAr4), 131.8 (2-C6), 129.6 (3-HisCAr4), 128.4 (4-CAr2), 128.1 (4-CAr1, 4-CAr3), 127.7 (4-C2), 127.4 (3-His-CAr2), 121.6 (4-C6), 120.8 (4-C1), 116.5 (2-C1), 115.3 (3-His-CAr5), 112.4 (4-C5), 111.4 (2-C5), 104.7 (2-C3), 71.9 (2-Cα), 69.5 (4-Cα), 54.3 (3-His-Cα), 41.6 (1-Gly-C1), 28.8 (3-His-Cβ), 21.6 (2-Cβ) ppm; IR (neat) ν (cm^{-1}): 3456, 3356, 2980, 2931, 1728, 1688, 1614, 1493, 1259, 1213; ESI-MS found: 615 $(M+H)^+$; HRMS *m/z* calculated for $C_{32}H_{35}N_6O_7$ $(M+H)^+$: 615.72; Found: 615.2573.

H_2N-[O-Bn-(2-HABA)]-Phe-[O-iPr-(2-HABA)]-Gly-CO_2H (7)

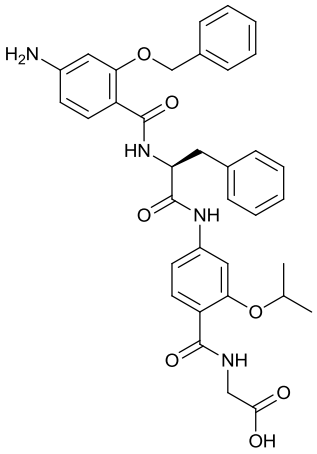

Yellow solid, > 95% pure by NMR; isolated yield: 10 mg, 16%; R_f 0.63 (SiO_2, 20% methanol in acetonitrile); $[\alpha]_D^{26.2}$ = + 38.3° (c 0.002 g mL^{-1}, methanol);^{1}H NMR (DMSO-d_6, 500 MHz) δ: 10.40 (s, 1H,1-Gly-CO_2H), 8.46 (t, *J* = 4.5 Hz, 1 H, 1-Gly-NH), 8.11 (d, *J* = 7.5 Hz, 1 H, 3-Phe-NH), 7.87 (d, *J* = 8.5 Hz, 1 H, 2-H6), 7.59 (d, *J* = 8.5 Hz, 1 H, 4-H6), 7.58 (s, 1 H, 2-H3), 7.50 (d, *J* = 7 Hz, 2 H, 4-HAr2), 7.42 (t, *J* = 7 Hz 3 H, 3-Phe-HAr4, 4-HAr3), 7.36 (t, *J* = 7 Hz, 1 H, 4-HAr4), 7.18 (s, 1H, 2-NH), 7.17 (t, *J* = 7 Hz, 2 H, 3-Phe-HAr3), 7.12 (d, *J* = 8.5 Hz, 1 H, 2-H5), 6.93 (d, *J* = 7 Hz, 2H, 3-Phe-HAr2), 6.31 (s, 1H, 4-H3), 6.17 (d, *J* = 8.5 Hz, 1 H, 4-H5), 5.77 (s, 2H, 4-NH_2), 5.20-5.12 (dd, *J* = 31.5, 11.5 Hz, 2 H, 4-Hα), 4.82-4.78 (dd, *J* = 9.5 , 4.5 Hz, 1 H, 3-Phe-Hα), 4.71-4.66 (apparent quin, *J* = 6 Hz, 1 H, 2-Hα), 3.99 (d, *J* = 4.5 Hz, 2 H, 1-Gly-H1), 3.03-2.99 (dd, *J* = 9.5 , 4.5 Hz, 1 H, 3-Phe-Hβ), 2.65-2.61 (dd, *J* = 9.5 , 4.5 Hz, 1 H, 3-Phe-Hβ'), 1.41-1.38 (dd, *J* = 8.5, 6 Hz, 6 H, 2-Hβ) ppm; ^{13}C NMR (DMSO-d_6, 126 MHz) δ: 171.0 (1-Gly-CO), 164.6 (2-CO), 163.9 (4-CO), 158.3(4-C2), 156.2 (3-Phe-CO), 153.6 (4-C4), 142.9 (2-C2), 137.1 (2-C4), 136.2 (4-CAr1), 132.7 (4-C6), 131.9 (2-C6), 128.9 (4-CAr4), 128.6 (4-CAr2, 4-CAr3), 128.1 (3-Phe-CAr2, 3-Phe-CAr3, 3-Phe-CAr4), 126.4 (3-Phe-CAr1), 116.6 (2-C1), 111.3 (2-C5), 108.0 (4-C5), 106.5 (4-C1), 104.7 (2-C3), 97.1 (4-C3), 71.9 (2-Cα), 69.9 (4-Cα), 55.2 (3-Phe-Cα), 41.7 (1-Gly-C1), 37.8 (3-Phe-Cβ), 21.6 (2-Cβ) ppm; IR (neat) ν (cm^{-1}): 3357, 2980, 2932, 1690, 1596, 1494, 1259, 1208; ESI-MS found: 625 $(M+H)^+$; HRMS *m/z* calculated for $C_{35}H_{37}N_4O_7$ $(M+H)^+$: 625.2657; Found: 625.2660.

H_2N-[N-Bn-(ABA)]-Phe-[O-iPr-(2-HABA)]-Gly-CO_2H (8)

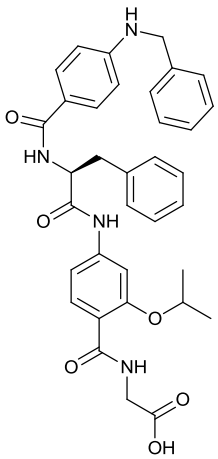

Pale yellow solid, > 95% pure by NMR; isolated yield: 9 mg, 15%; R_f 0.49 (SiO_2, 20% methanol in acetonitrile);); $[\alpha]_D^{26.1}$ = + 44.7° (c 0.004 g mL^{-1}, methanol); ^{1}H NMR (DMSO-d_6, 500 MHz) δ: 10.37 (s, 1H,1-Gly-CO_2H), 8.44 (t, *J* = 5 Hz, 1 H, 1-Gly-NH), 8.22 (d, *J* = 8 Hz, 1 H, 3-Phe-NH), 7.87 (d, *J* = 8.5 Hz, 1 H, 2-H6), 7.59 (s, 1 H, 2-H3), 7.58 (d, *J* = 8.5 Hz, 2 H, 4-H2), 7.36 (d, *J* = 8 Hz, 2 H, 4-HAr2), 7.24-7.29 (m, 5 H, 3-Phe-HAr2, 3-Phe-HAr3, 3-Phe-HAr4), 7.26 (d, *J* = 8.5 Hz, 1 H, 2-H5),

7.25 (s, 1H, 2-NH), 7.24-7.21 (dd, *J* = 8, 5 Hz, 2H, 4-HAr3), 7.15 (t, *J* = 8 Hz, 1 H, 4-HAr4), 6.80 (t, *J* = 6 Hz, 1 H, 4-NH), 6.55 (d, *J* = 8 Hz, 2 H, 4-H3), 4.78-4.74 (dd, *J* = 8.5 , 5.5 Hz, 1 H, 3-Phe-Hα), 4.71-4.67 (apparent quin, *J* = 6 Hz, 1 H, 2-Hα), 4.31 (d, *J* = 6 Hz, 2 H, 4-Hα), 4.01 (d, *J* = 5 Hz, 2 H, 1-Gly-H1), 3.11-3.60 (dd, *J* = 8.5 , 5.5 Hz, 2 H, 3-Phe-Hβ), 1.40-1.38 (dd, *J* = 8.5, 6 Hz, 6 H, 2-Hβ) ppm; ^{13}C NMR (DMSO-d_6, 126 MHz) δ: 171.2 (1-Gly-CO), 166.5 (4-CO), 164.0 (2-CO), 156.2 (3-Phe-CO), 151.8 (4-C4), 143.1 (2-C2), 138.2 (2-C4), 134.6 (2-C6), 131.9 (4-CAr1), 129.5 (4-CAr2, 4-CAr3), 129.1(3-Phe-CAr2, 3-Phe-CAr4), 128.3 (4-C2), 128.1 (3-Phe-CAr3), 127.1 (4-CAr4), 126.3 (3-Phe-CAr1), 120.3 (4-C1), 116.5 (2-C1), 112.4 (4-C3), 111.3 (2-C5), 104.7 (2-C3), 71.9 (2-Cα), 55.8 (3-Phe-Cα), 45.9(4-Cα), 41.6 (1-Gly-C1), 37.0 (3-Phe-Cβ), 21.6 (2-Cβ) ppm; IR (neat) ν (cm^{-1}): 3336, 3029, 2925, 1680, 1605, 1494, 1256, 1222;ESI-MS found: 609 $(M+H)^+$; HRMS *m/z* calculated for $C_{35}H_{37}N_4O_6$ $(M+H)^+$: 609.2708; Found: 609.2716.

H_2N-[O-Bn-(3-HABA)]-Phe-[O-iPr-(3-HABA)]-Gly-CO_2H (9)

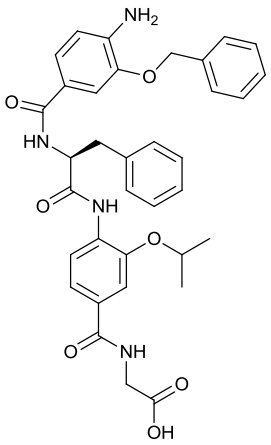

Yellow solid, > 95% pure by NMR; isolated yield: 10 mg, 16%; R_f 0.13 (SiO_2, 20% methanol in acetonitrile); $[\alpha]_D^{26.4}$ = - 31.7° (c 0.003 g mL^{-1}, methanol);^{1}H NMR (DMSO-d_6, 500 MHz) δ: 9.28 (s, 1H,1-Gly-CO_2H), 8.69 (t, *J* = 5.5 Hz, 1 H, 1-Gly-NH), 8.56 (d, *J* = 8 Hz, 1 H, 3-Phe-NH), 7.29 (d, *J* = 8.5 Hz, 1 H, 2-H6), 7.51 (s, 1 H, 2-H2), 7.48 (d, *J* = 8.5 Hz, 1 H, 2-H5), 7.46 (d, *J* = 7 Hz, 2 H, 4-HAr2), 7.41 (s, 1 H, 4-H2), 7.38 (t, *J* = 7 Hz, 2 H,4-HAr3), 7.35 (d, *J* = 8 Hz, 1 H, 4-H6), 7.33 (d, *J* = 7.5 Hz, 2 H, 3-Phe-HAr2), 7.32 (s, 1H, 2-NH), 7.24 (t, *J* = 7.5 Hz, 3 H, 3-Phe-HAr3, 4-HAr4), 7.15 (t, *J* = 7.5 Hz, 1H, 3-Phe-HAr4), 6.63 (d, *J* = 8 Hz, 1 H, 4-H5), 5.37 (br, 2H, 4-NH_2), 5.11 (s, 2 H, 4-Hα), 4.86-4.82 (dd, *J* = 8, 4.5 Hz, 1 H, 3-Phe-Hα), 4.66-4.61 (apparent quin, *J* = 6 Hz, 1 H, 2-Hα), 3.87 (d, *J* = 5.5 Hz, 2 H, 1-Gly-H1), 3.12-3.07 (dd, *J* = 10.5 , 4.5 Hz, 2 H, 3-Phe-Hβ), 1.16-1.13 (dd, *J* = 8.5, 6 Hz, 6 H, 2-Hβ) ppm; ^{13}C NMR (DMSO-d_6, 126 MHz) δ: 171.3 (1-Gly-CO), 170.4 (2-CO), 166.7 (4-CO), 165.7 (3-Phe-CO), 145.7 (2-C4), 144.1 (4-C4), 141.9 (4-C3), 138.5 (2-C1), 137.1 (4-C4), 131.3 (2-C3), 129.1 (3-Phe-CAr2), 128.4 (4-CAr2, 4-CAr4), 128.1 (4-CAr3), 127.7 (4-CAr1), 127.3 (3-Phe-CAr3, 3-Phe-CAr4), 126.2 (3-Phe-CAr1), 121.8 (4-C6), 120.2 (2-C5), 118.4 (2-C6), 112.3 (4-C5, 2-C2), 111.4 (4-C2), 71.4 (2-Cα), 69.4 (4-Cα), 55.6 (3-Phe-Cα), 41.73 (1-Gly-C1), 35.5 (3-Phe-Cβ), 21.4 (2-Cβ) ppm; IR

(neat) ν (cm^{-1}): 3286, 3034, 2980, 2930, 1680, 1614, 1494, 1273, 1210; ESI-MS found: 625 $(M+H)^+$; HRMS *m/z* calculated for $C_{35}H_{36}N_4NaO_7$ $(M+Na)^+$: 647.2476; Found: 647.2480.

H_2N-[O-Bn-(2-HABA)]-Phe-[O-iPr-(3-HABA)]-Gly-CO_2H (10)

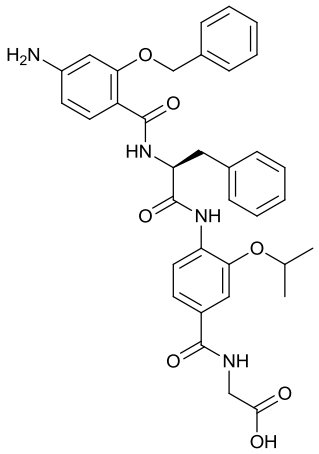

Colourless solid, > 95% pure by NMR; isolated yield: 10 mg, 16%; R_f 0.11 (SiO_2, 20% methanol in acetonitrile);); $[\alpha]_D^{26.5}$ = + 16.2° (c 0.002 g mL^{-1}, methanol); ^{1}H NMR (DMSO-d_6, 500 MHz) δ: 9.28 (s, 1H,1-Gly-CO_2H), 8.67 (t, *J* = 5.5 Hz, 1 H, 1-Gly-NH), 8.23 (d, *J* = 7.5 Hz, 1 H, 3-Phe-NH), 8.21 (d, *J* = 8.5 Hz, 1 H, 2-H6), 7.64 (d, *J* = 8.5 Hz, 1 H, 4-H6), 7.50 (s, 1 H, 2-H2), 7.46 (d, *J* = 8.5 Hz, 1 H, 2-H5), 7.44 (d, *J* = 7 Hz, 2 H, 4-HAr2), 7.41 (s, 1H, 2-NH), 7.40-7.36 (m, 3 H, 4-HAr3, 4-HAr4), 7.16 (t, *J* = 7 Hz, 2 H, 3-Phe-HAr3), 7.13 (t, *J* = 7 Hz, 1 H, 3-Phe-HAr4), 6.96 (d, *J* = 7 Hz, 2H, 3-Phe-HAr2), 6.28 (s, 1H, 4-H3), 6.18 (d, *J* = 8.5 Hz, 1 H, 4-H5), 5.81 (s, 2H, 4-NH_2), 5.19-5.12 (dd, *J* = 23, 12 Hz, 2 H, 4-Hα), 4.88-4.84 (sept, *J* = 4.5 Hz, 1 H, 3-Phe-Hα), 4.65-4.61 (apparent quin, *J* = 6 Hz, 1 H, 2-Hα), 3.87 (d, *J* = 5.5 Hz, 2 H, 1-Gly-H1), 3.15-3.12 (dd, *J* = 9.5 , 4.5 Hz, 1 H, 3-Phe-Hβ), 2.71-2.66 (dd, *J* = 9.5 , 4.5 Hz, 1 H, 3-Phe-Hβ'), 1.15-1.13 (dd, *J* = 8.5, 6 Hz, 6 H, 2-Hβ) ppm; ^{13}C NMR (DMSO-d_6, 126 MHz) δ: 170.1 (1-Gly-CO), 165.7 (2-CO), 165.1 (4-CO), 158.4 (4-C4), 153.8 (3-Phe-CO), 145.9 (2-C4), 137.4 (2-C1), 136.2 (4-C2), 132.8 (4-C6), 131.1 (2-C3), 128.8 (3-Phe-CAr2), 128.6 (4-CAr3, 4-CAr4), 128.2 (3-Phe-CAr1, 3-Phe-CAr3), 127.9 (4-CAr2), 127.3 (4-CAr1), 126.4 (3-Phe-CAr4), 120.03 (2-C5), 118.8 (2-C6), 112.3 (2-C2), 107.4 (4-C1), 106.5 (4-C5), 96.6 (4-C3), 71.3 (2-Cα), 69.8 (4-Cα), 55.2 (3-Phe-Cα), 41.5 (1-Gly-C1), 36.5 (3-Phe-Cβ), 21.4 (2-Cβ) ppm; IR (neat) ν (cm^{-1}): 3692, 3356, 2980, 2921, 1688, 1631, 1598, 1494, 1269, 1209; ESI-MS found: 625 $(M+H)^+$; HRMS *m/z* calculated for $C_{35}H_{36}N_4NaO_7$ $(M+Na)^+$: 647.2476; Found: 647.2481.

H_2N-[*N*-Bn-(ABA)]-Phe-[*O*-*i*Pr-(3-HABA)]-Gly-CO_2H (11)

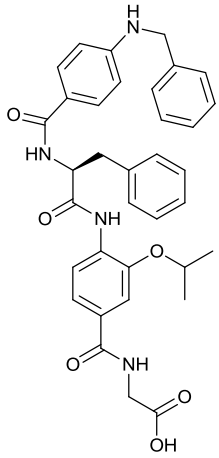

Colourless solid, > 95% pure by NMR; isolated yield: 15 mg, 25%); R_f 0.12 (SiO_2, 20% methanol in acetonitrile); $[\alpha]_D^{26.5}$ = - 13.5° (c 0.003 g mL^{-1}, methanol); ^{1}H NMR (DMSO-d_6, 500 MHz) δ: 9.25 (s, 1H,1-Gly-CO_2H), 8.67 (t, *J* = 5.5 Hz, 1 H, 1-Gly-NH), 8.52 (d, *J* = 8 Hz, 1 H, 3-Phe-NH), 8.29 (d, *J* = 8.5 Hz, 1 H, 2-H6), 7.59 (s, *J* = 8.5 Hz, 2 H, 4-H2), 7.50 (s, 1 H, 2-H2), 7.46 (d, *J* = 8.5 Hz, 1 H, 2-H5), 7.34-7.30 (m, 6 H, 3-Phe-HAr2, 4-HAr2, 4-HAr3), 7.28 (s, 1H, 2-NH), 7.24 (t, *J* = 7.5 Hz, 2 H, 3-Phe-HAr3), 7.23 (t, *J* = 7.5 Hz, 1 H, 4-HAr4), 7.15 (t, *J* = 7.5 Hz, 1H, 3-Phe-HAr4), 6.86 (t, *J* = 6 Hz, 1H, 4-NH), 6.56 (d, *J* = 8.5 Hz, 2 H, 4-H3), 4.83-4.79 (sept, *J* = 7.5 Hz, 1 H, 3-Phe-Hα), 4.65-4.60 (apparent quin, *J* = 6 Hz, 1 H, 2-Hα), 4.31 (d, *J* = 6 Hz, 2 H, 4-Hα), 3.86 (d, *J* = 5.5 Hz, 2 H, 1-Gly-H1), 3.10-3.05 (dd, *J* = 11 , 3.5 Hz, 2 H, 3-Phe-Hβ), 1.13-1.07 (dd, *J* = 11.5, 6 Hz, 6 H, 2-Hβ) ppm; ^{13}C NMR (DMSO-d_6, 126 MHz) δ: 171.3 (1-Gly-CO), 170.4 (2-CO), 166.7 (4-CO), 165.7 (3-Phe-CO), 151.5 (4-C4), 145.7 (2-C4), 138.5 (2-C1), 131.3 (2-C3), 129.0 (4-CAr4), 128.9 (4-C2), 128.3 (4-CAr2, 4-CAr3), 128.1 (3-Phe-CAr1), 127.1 (3-Phe-CAr2, 3-Phe-CAr3), 126.7 (3-Phe-CAr4), 126.2 (4-CAr1), 120.1 (4-C1), 119.8 (2-C5), 118.3 (2-C6), 112.3 (2-C2), 111.1 (4-C3), 71.3 (2-Cα), 55.6 (3-Phe-Cα), 45.8 (4-Cα), 41.4 (1-Gly-C1), 35.5 (3-Phe-Cβ), 21.4 (2-Cβ) ppm; IR (neat) ν (cm^{-1}): 3328, 3030, 2977, 2928, 1685, 1632, 1601, 1494, 1267, 1208; ESI-MS found: 609 $(M+H)^+$; HRMS *m/z* calculated for $C_{35}H_{36}N_4NaO_6$ $(M+Na)^+$: 631.2527; Found: 631.2532.

H_2N-[*O*-Bn-(3-HABA)]-Phe-[*N*-*i*Bu-(ABA)]-Gly-CO_2H (12)

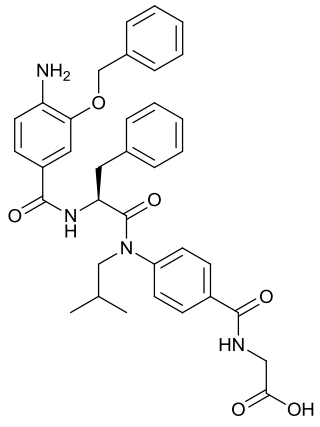

Yellow solid, > 95% pure by NMR; isolated yield: 5.7 mg, 9%; R_f 0.72 (SiO_2, 20% methanol in acetonitrile); $[\alpha]_D^{26.5}$ = + 160.1° (c 0.003 g mL^{-1}, methanol); ^{1}H NMR (DMSO-d_6, 500 MHz) δ: 9.21 (s, 1H,1-Gly-CO_2H), 8.97 (t, *J* = 5.5 Hz, 1 H, 1-Gly-NH), 8.25 (d, *J* = 7.5 Hz, 1 H, 3-Phe-NH), 7.97 (d, *J* = 8 Hz, 2 H, 2-H2), 7.51 (d, *J* = 7 Hz, 2 H, 4-HAr2), 7.48 (br, 2 H, 2-H3), 7.42 (d, *J* = 7 Hz, 2 H, 3-Phe-HAr3), 7.40 (t, *J* = 7 Hz, 1 H 3-Phe-HAr4), 7.35 (d, *J* = 8.5 Hz, 1 H, 4-H6), 7.33 (s, 1 H, 4-H2), 7.16-7.13 (m, , 3 H, 3-Phe-HAr2, 4-H-Ar4), 6.87 (t, *J* = 7 Hz, 2 H, 4-H-Ar3), 6.64 (d, *J* = 8.5 Hz, 1 H, 4-H5), 5.32 (br, 2H, 4-NH_2), 5.17 (s, 2 H, 4-Hα), 4.61-4.57 (dd, *J* = 7, 4.5 Hz, 1 H, 3-Phe-Hα), 3.98 (d, *J* = 5.5 Hz, 2 H, 1-Gly-H1), 3.75-3.71 (m, 1 H, 2-Hα), 3.42-3.38 (m, 1 H, 2-Hα'), 2.92 (d, *J* = 4.5 Hz, 2 H, 3-Phe-Hβ), 1.68-1.63 (apparent quin, *J* = 5.5 Hz, 1 H, 2-Hβ), 0.87-0.85 (dd, *J* = 7.5, 5.5 Hz, 6 H, 2-Hγ) ppm; ^{13}C NMR (DMSO-d_6, 126 MHz) δ: 171.6 (1-Gly-CO), 171.2 (4-CO), 166.2 (3-Phe-CO), 165.8 (2-CO), 144.1 (4-C1), 141.4 (4-C3), 138.0 (2-C1), 137.2 (4-C4), 128.8 (2-C2), 128.4 (3-Phe-CAr2, 3-Phe-CAr3, 3-Phe-CAr4), 128.1 (4-CAr4), 127.7 (2-C3), 127.4 (4-CAr1, 4-CAr2, 4-CAr3), 126.3 (3-Phe-CAr1), 121.8 (4-C6), 120.8 (2-C4), 112.3 (4-C5), 111.3 (4-C2), 72.8 (2-Cα), 69.4 (4-Cα), 55.6 (3-Phe-Cα), 41.2 (1-Gly-C1), 36.5 (3-Phe-Cβ), 26.3 (2-Cγ), 19.8 (2-Cβ) ppm; IR (neat) ν (cm^{-1}): 3367, 2962, 2933, 1701, 1629, 1594, 1495, 1259, 1199; ESI-MS found: 623 $(M+H)^+$; HRMS *m/z* calculated for $C_{36}H_{38}N_4NaO_6$ $(M+Na)^+$: 645.2683; Found: 645.2686.

H_2N-[*O*-Bn-(2-HABA)]-Phe-[*N*-*i*Bu-(ABA)]-Gly-CO_2H (13)

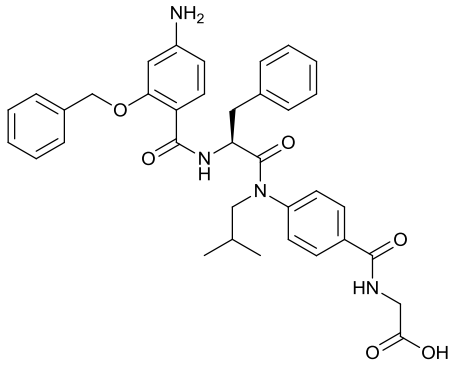

Colourless solid, > 95% pure by NMR; isolated yield: 1 mg, 2%; R_f 0.22 (SiO_2, 20% methanol in acetonitrile); $[\alpha]_D^{26.5}$ = + 57.9° (c 0.003 g mL^{-1}, methanol);^{1}H NMR (DMSO-d_6, 500 MHz) δ: 8.95 (t, *J* = 5.5 Hz, 1 H, 1-Gly-NH), 8.07 (d, *J* = 7 Hz, 1 H, 3-Phe-NH), 7.93 (d, *J* = 8.5 Hz, 2 H, 2-H2), 7.60 (d, *J* = 8.5 Hz, 1 H, 4-H6), 7.58 (d, *J* = 7 Hz, 2 H, 4-HAr2), 7.47 (t, *J* = 7 Hz, 3 H, 4-HAr3, 4-HAr4), 7.40 (d, *J* = 8.5 Hz, 1 H, 2-H3), 7.12-7.10 (m, 3 H, 3-Phe-HAr3, 3-

Phe-HAr4), 6.49 (d, *J* = 7 Hz, 2H, 3-Phe-HAr2), 6.35 (s, 1H, 4-H3), 6.19 (d, *J* = 8.5 Hz, 1 H, 4-H5), 5.80 (s, 2H, 4-NH_2), 5.23-5.15 (dd, *J* = 22, 11 Hz, 2 H, 4-Hα), 4.59-4.55 (dd, *J* = 7, 4.5 Hz, 1 H, 3-Phe-Hα), 3.96 (d, *J* = 5.5 Hz, 2 H, 1-Gly-H1), 3.73-3.69 (dd, *J* = 8.5, 5 Hz, 1 H, 2-Hα), 3.32-3.30 (dd, *J* = 8.5, 5 Hz, 1 H, 2-Hα'), 2.80-2.76 (dd, *J* = 9.5, 4.5 Hz, 1 H, 3-Phe-Hβ), 2.38-2.35 (dd, *J* = 9.5, 4.5 Hz, 1 H, 3-Phe-Hβ'), 1.63-1.58 (apparent quin, *J* = 5 Hz, 1 H, 2-Hβ), 0.84-0.81 (dd, *J* = 7.5, 5 Hz, 6 H, 2-Hγ) ppm; ^{13}C NMR (DMSO-d_6, 126 MHz) δ: 171.2 (1-Gly-CO), 171.1 (4-CO), 165.7 (3-Phe-CO), 164.2 (2-CO), 158.2 (4-C4), 153.5 (4-C2), 144.3 (2-C4), 136.2 (2-C1), 132.9 (4-C6), 128.6 (4-CAr2, 4-CAr3), 128.6 (2-C2), 128.3 (2-C3), 128.2 (3-Phe-CAr2,3-Phe-CAr3, 3-Phe-CAr4), 128.2 (4-CAr4), 128.0 (4-CAr1), 126.4 (3-Phe-CAr1), 108.0 (4-C5), 106.5 (4-C1), 97.1 (4-C3), 69.9 (4-Cα), 55.6 (2-Cα), 52.0 (3-Phe-Cα), 41.2 (1-Gly-C1), 37.6 (3-Phe-Cβ), 26.3 (2-Cβ), 19.8 (2-Cγ) ppm; IR (neat) ν (cm^{-1}): 3359, 2923, 1701, 1631, 1596, 1495, 1259, 1199; ESI-MS found: 623 $(M+H)^+$; HRMS *m/z* calculated for $C_{36}H_{39}N_4O_6$ $(M+Na)^+$: 623.2864; Found: 623.2867.

H_2N-[*N*-Bn-(ABA)]-Phe-[*N*-*i*Bu-(ABA)]-Gly-CO_2H (14)

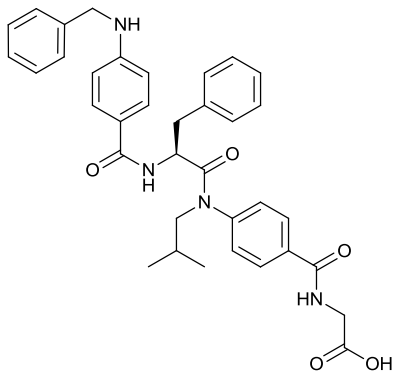

Colourless solid, > 95% pure by NMR; isolated yield: 4 mg, 7%; R_f 0.30 (SiO_2, 20% methanol in acetonitrile); $[\alpha]_D^{26.6}$ = + 113.1° (c 0.002 g mL^{-1}, methanol); ^{1}H NMR (DMSO-d_6, 500 MHz) δ: 8.97 (t, *J* = 5.5 Hz, 1 H, 1-Gly-NH), 8.17 (d, *J* = 7 Hz, 1 H, 3-Phe-NH), 7.97 (d, *J* = 8.5 Hz, 2 H, 2-H2), 7.60 (d, *J* = 8.5 Hz, 2 H, 4-H2), 7.48 (br, 2 H, 2-H3), 7.36-7.31 (m, 5 H, 3-Phe-HAr2, 3-Phe-HAr3, 4-NH), 7.24 (t, *J* = 7 Hz, 1 H 3-Phe-HAr4), 7.13 -7.11 (m, 3 H, 4-HAr3, 4-HAr4), 6.83 (d, *J* = 7.5 Hz, 2 H, 4-HAr2), 6.56 (d, *J* = 8.5 Hz, 1 H, 4-H3), 4.56-4.52 (dd, *J* = 7, 4.5 Hz, 1 H, 3-Phe-Hα), 4.33 (s, 2 H, 4-Hα), 3.97 (d, *J* = 5.5 Hz, 2 H, 1-Gly-H1), 3.74-3.69 (dd, *J* = 8.5, 5 Hz, 1 H, 2-Hα), 3.38-3.36 (dd, *J* = 8.5, 5 Hz, 1 H, 2-Hα'), 2.88 (d, *J* = 4.5 Hz, 2 H, 3-Phe-Hβ), 1.66-1.61 (apparent quin, *J* = 5 Hz, 1 H, 2-Hβ), 0.85-0.83 (dd, *J* = 7.5, 5 Hz, 6 H, 2-Hγ) ppm; ^{13}C NMR (DMSO-d_6, 126 MHz) δ: 171.6 (1-Gly-CO), 171.2 (4-CO), 166.2 (3-Phe-CO), 165.8 (2-CO), 151.2 (4-C4), 139.6 (2-C4), 138.1 (2-C1), 129.0 (4-CAr4), 128.8 (2-C2), 128.4 (4-C2), 128.3 (3-Phe-CAr2, 3-Phe-CAr3, 3-Phe-CAr4), 128.1 (3-Phe-CAr1), 127.1 (4-CAr2, 4-CAr3), 126.7 (2-C3), 126.3 (4-CAr1), 120.5 (4-C1), 111.0 (4-C3), 72.6 (2-Cα), 55.6 (3-Phe-Cα), 45.9 (4-Cα),

41.2 (1-Gly-C1), 37.3 (3-Phe-Cβ), 26.3 (2-Cγ), 19.8 (2-Cβ) ppm; IR (neat) ν (cm^{-1}): 3359, 3243, 2960, 2931, 1701, 1630, 1595, 1495, 1260, 1199; ESI-MS found: 607 $(M+H)^+$; HRMS *m/z* calculated for $C_{36}H_{38}N_4NaO_5$ $(M+Na)^+$: 629.2734; Found: 629.2741.

H_2N-[*O*-Bn-(3-HABA)]-D-Phe-[*O*-*i*Pr-(2-HABA)]-Gly-CO_2H (15)

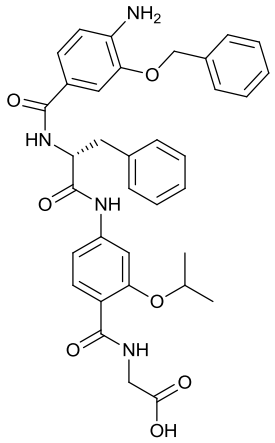

Colourless solid, > 95% pure by NMR; isolated yield: 10.3 mg, 17%; R_f 0.82 (SiO_2, 20% methanol in acetonitrile); $[\alpha]_D^{27.5}$ = - 23.4° (c 0.008 g mL^{-1}, methanol); ^{1}H NMR (DMSO-d_6, 500 MHz) δ: 10.46 (s, 1H,1-Gly-CO_2H), 8.47 (t, *J* = 5 Hz, 1 H, 1-Gly-NH), 8.35 (d, *J* = 8 Hz, 1 H, 3-D-Phe-NH), 7.89 (d, *J* = 8.5 Hz, 1 H, 2-H6), 7.64 (s, 1 H, 2-H3), 7.50 (d, *J* = 8.5 Hz, 2 H, 3- D-Phe-HAr2), 7.42 (s, 1 H, 4-H2), 7.40-7.37 (m, 5 H, 4-HAr2, 4-H-Ar3, 4-HAr4), 7.32 (t, *J* = 8.5 Hz, 2 H, 3- D-Phe-HAr3), 7.26 (d, *J* = 8.5 Hz, 2 H, 4-H6, 2-H5), 7.25 (s, 1H, 2-NH), 7.17 (t, *J* = 8.5 Hz, 1H, 3- D-Phe-HAr4), 6.62 (d, *J* = 8.5 Hz, 1 H, 4-H5), 5.32 (br, 2H, 4-NH_2), 5.15 (s, 2 H, 4-Hα), 4.82-4.77 (dd, *J* = 8.5 , 5.5 Hz, 1 H, 3-D-Phe-Hα), 4.73-4.68 (apparent quin, *J* = 6 Hz, 1 H, 2-Hα), 4.01 (d, *J* = 5 Hz, 2 H, 1-Gly-H1), 3.13-3.09 (dd, *J* = 8.5 , 5.5 Hz, 2 H, 3- D-Phe-Hβ), 1.45-1.43 (dd, *J* = 8.5, 6 Hz, 6 H, 2-Hβ), ppm; ^{13}C NMR (DMSO-d_6, 126 MHz) δ: 171.5 (1-Gly-CO), 166.4 (4-CO), 163.9 (2-CO), 156.2 (3-D-Phe-CO), 144.0 (4-C3), 143.0 (2-C2), 141.5 (4-C4), 138.2 (2-C4), 137.2 (2-C6), 131.9 (4-CAr1), 129.2 (3- D-Phe-CAr3), 128.4 (4-CAr2, 4-CAr3), 128.1 (4-CAr4), 127.7 (4-C2), 127.4 (3- D-Phe-CAr2, 3- D-Phe-CAr4), 126.3 (3- D-Phe-CAr1), 121.8 (4-C6), 120.8 (4-C1), 116.6 (2-C1), 112.3 (4-C5), 111.4 (2-C5), 104.7 (2-C3), 71.9 (2-Cα), 69.4 (4-Cα), 55.9 (3- D-Phe-Cα), 41.9 (1-Gly-C1), 37.1 (3- D-Phe-Cβ), 21.6 (2-Cβ) ppm; IR (neat) ν (cm^{-1}): 3358, 3032, 2979, 2929, 1682, 1596, 1494, 1258, 1211; ESI-MS found: 625 $(M+H)^+$; HRMS *m/z* calculated for $C_{35}H_{37}N_4O_7$ $(M+H)^+$: 625.2657; Found: 625.2668.

H_2N-[*O*-Bn-(3-HABA)]-Trp-[*O*-*i*Pr-(2-HABA)]-Gly-CO_2H (16)

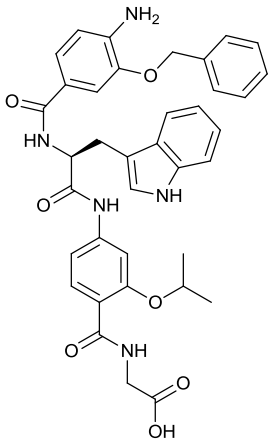

Yellow solid, > 90% pure by NMR; isolated yield: 9.8 mg, 15%; R_f 0.53 (SiO_2, 20% methanol in acetonitrile); $[\alpha]_D^{26.6}$ = + 91.1° (c 0.006 g mL^{-1}, methanol);^{1}H NMR (DMSO-d_6, 500 MHz) δ: 10.83 (s, 1 H, 3-Trp-NH1), 10.46 (s, 1H,1-Gly-CO_2H), 8.51 (t, *J* = 5 Hz, 1 H, 1-Gly-NH), 8.26 (d, *J* = 7.5 Hz, 1 H, 3-Trp-NH), 7.90 (d, *J* = 8.5 Hz, 1 H, 2-H6), 7.75 (d, *J* = 7.5 Hz, 1 H, 3-Trp-HAr4), 7.65 (s, 1 H, 2-H3), 7.51 (d, *J* = 7.5 Hz, 2 H, 4-HAr2), 7.45 (s, 1 H, 4-H2), 7.41 (t, *J* = 7.5 Hz, 3 H, 4-HAr3, 4-HAr4), 7.33-7.31 (m, 3 H, 4-H6, 3-Trp-HAr7, 2-NH), 7.28 (s, 1 H, 3-TrpHAr2), 7.27 (d, *J* = 8.5 Hz, 1 H, 2-H5), 7.07 (t, *J* = 7.5 Hz, 1H, 3-Trp-HAr6), 6.99 (t, *J* = 7.5 Hz, 1H, 3-Trp-HAr5), 6.64 (d, *J* = 8Hz, 1 H, 4-H5), 5.33 (br, 2H, 4-NH_2), 5.17-5.13 (dd, *J* = 12, 4 Hz, 2 H, 4-Hα), 4.89-4.85 (dd, *J* = 9 , 5 Hz, 1 H, 3-Trp-Hα), 4.74-4.69 (apparent quin, *J* = 6 Hz, 1 H, 2-Hα), 4.00 (d, *J* = 5 Hz, 2 H, 1-Gly-H1), 3.27-3.24 (dd, *J* = 11 , 5 Hz, 2 H, 3-Trp-Hβ), 1.43-1.41 (dd, *J* = 9.5, 6 Hz, 6 H, 2-Hβ) ppm; ^{13}C NMR (DMSO-d_6, 126 MHz) δ: 171.2 (1-Gly-CO), 166.3 (4-CO), 163.8 (2-CO), 156.2 (3-Trp-CO), 144.1 (4-C1), 143.1 (2-C2), 141.5 (4-C4), 138.2 (2-C4), 137.2 (4-C3, 3-Trp-CAr7a), 136.0 (3-Trp-CAr3a), 131.9 (2-C6), 128.4 (4-CAr3, 4-CAr4), 127.7 (4-CAr1), 127.5 (4-CAr2, 3-Trp-CAr3), 124.5 (3-Trp-CAr2), 123.7 (4-C6), 121.8 (3-Trp-CAr7), 120.8 (3-Trp-CAr5), 118.6 (3-Trp-CAr4), 118.2 (3-Trp-CAr6), 115.1 (2-C1), 112.3 (4-C5), 111.4 (4-C2), 110.2 (2-C5), 104.8 (2-C3), 71.9 (2-Cα), 69.4 (4-Cα), 55.1 (3-Trp-Cα), 41.0 (1-Gly-C1), 27.5 (3-Trp-Cβ), 21.6 (2-Cβ) ppm; IR (neat) ν (cm^{-1}): 3259, 3143, 2921, 2810, 1686, 1617, 1591, 1494, 1298, 1209; ESI-MS found: 664 $(M+H)^+$; HRMS *m/z* calculated for $C_{37}H_{37}N_5NaO_7$ $(M+Na)^+$: 686.2585; Found: 686.2599.

H_2N-[*O*-Bn-(3-HABA)]-D-Trp-[*O*-*i*Pr-(2-HABA)]-Gly-CO_2H (17)

Pale brown solid, > 90% pure by NMR; isolated yield: 5 mg, 8%; R_f 0.083 (SiO_2, 20% methanol in acetonitrile); $[\alpha]_D^{28.3}$ = - 137.6° (c 0.007 g mL^{-1}, methanol); ^{1}H NMR (DMSO-d_6, 500 MHz) δ: 10.83 (s, 1 H, 3-D-Trp-NH'), 10.45 (s, 1H,1-Gly-CO_2H), 8.48 (t, *J* = 5 Hz, 1 H, 1-Gly-NH), 8.24 (d, *J* = 7.5 Hz, 1 H, 3-D -Trp-NH), 7.90 (d, *J* = 8.5 Hz, 1 H, 2-H6), 7.75 (d, *J* = 7.5 Hz, 1 H, 3-D-Trp-HAr4), 7.65 (s, 1 H, 2-H3), 7.51 (d, *J* = 7.5 Hz, 2 H, 4-HAr2), 7.45 (s, 1 H, 4-H2), 7.41 (t, *J* = 7.5 Hz, 3 H, 4-HAr3, 4-HAr4), 7.35-7.32 (m, 3 H, 4-H6, 3-D-Trp-HAr7, 2-NH), 7.28 (s, 1 H, 3-D-Trp-HAr2), 7.26 (d, *J* = 8.5 Hz, 1 H, 2-H5), 7.07 (t, *J* = 7.5 Hz, 1H, 3-D-Trp-HAr6), 6.99 (t, *J* = 7.5 Hz, 1H, 3-D-Trp-HAr5), 6.64 (d, *J* = 8Hz, 1 H, 4-H5), 5.33 (br, 2H, 4-NH_2), 5.18-5.11 (dd, *J* = 12, 4 Hz, 2 H, 4-Hα), 4.89-4.84 (dd, *J* = 9, 5 Hz, 1 H, 3-D-Trp-Hα), 4.74-4.69 (apparent quin, *J* = 6 Hz, 1 H, 2-Hα), 4.04 (d, *J* = 5 Hz, 2 H, 1-Gly-H1), 3.28-3.24 (dd, *J* = 11 , 5 Hz, 2 H, 3-D-Trp-Hβ), 1.43-1.41 (dd, *J* = 9.5, 6 Hz, 6 H, 2-Hβ) ppm; ^{13}C NMR (DMSO-d_6, 126 MHz) δ: 171.2 (1-Gly-CO), 164.5 (4-CO), 163.9 (2-CO), 158.2 (3-D-Trp-CO), 156.2 (4-C1), 155.9 (2-C2), 153.5 (4-C4), 143.1 (2-C4), 136.1 (4-C3), 132.7 (3-D-Trp-CAr7a), 131.8 (2-C6), 129.6 (3-D-Trp-CAr3a), 128.5 (4-CAr3, 4-CAr4), 128.1 (4-CAr1), 128.0 (4-CAr2, 3-D-Trp-CAr3), 127.1 (3-D-Trp-CAr2), 125.2 (4-C6), 123.3 (3-D-Trp-CAr7), 120.9 (3-D-Trp-CAr5), 118.2 (3-D-Trp-CAr4), 116.5 (3-D-Trp-CAr6), 111.3 (2-C1), 109.4 (4-C5), 108.2 (4-C2), 106.5 (2-C5), 97.2 (2-C3), 71.9 (2-Cα), 69.8 (4-Cα), 48.6 (3-D-Trp-Cα), 41.6 (1-Gly-C1), 28.0 (3-D -Trp-Cβ), 21.6 (2-Cβ) ppm; IR (neat) ν (cm^{-1}): 3384, 2922, 1634, 1597, 1494, 1259, 1216; ESI-MS found: 664 $(M+H)^+$; HRMS *m/z* calculated for $C_{37}H_{37}N_5NaO_7$ $(M+Na)^+$: 686.2585; Found: 686.2590.

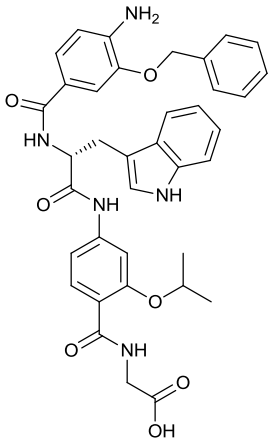

^{1}H and ^{13}C NMR Spectra

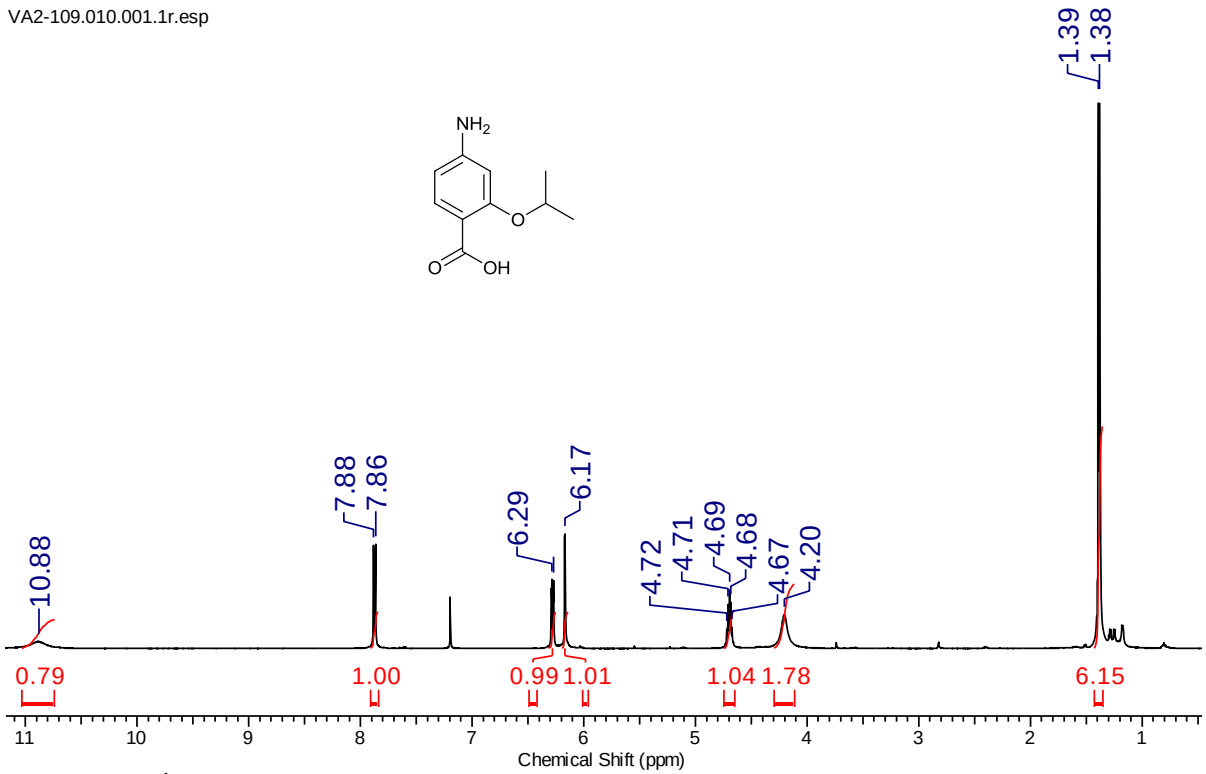

Figure S 2. ^{1}H NMR spectrum of 27 ($CDCl_3$, 500 MHz).

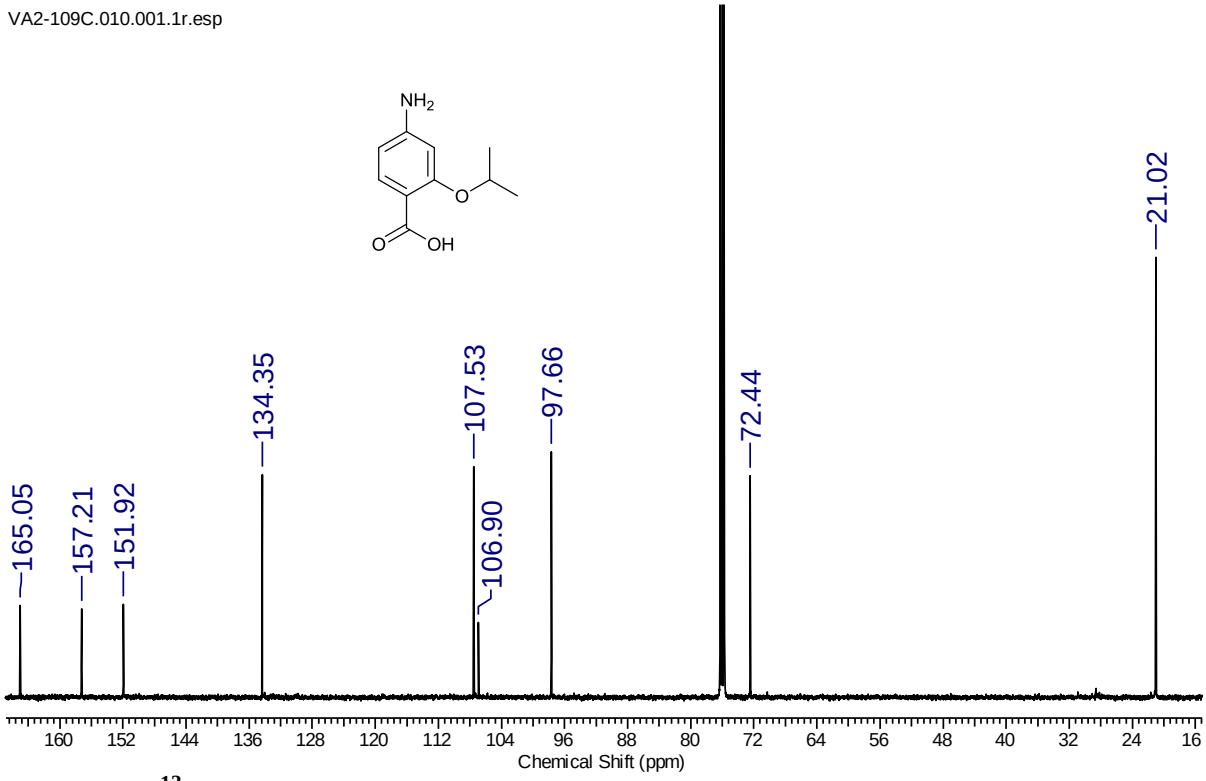

Figure S 3. ^{13}C NMR spectrum of 27 ($CDCl_3$, 500 MHz).

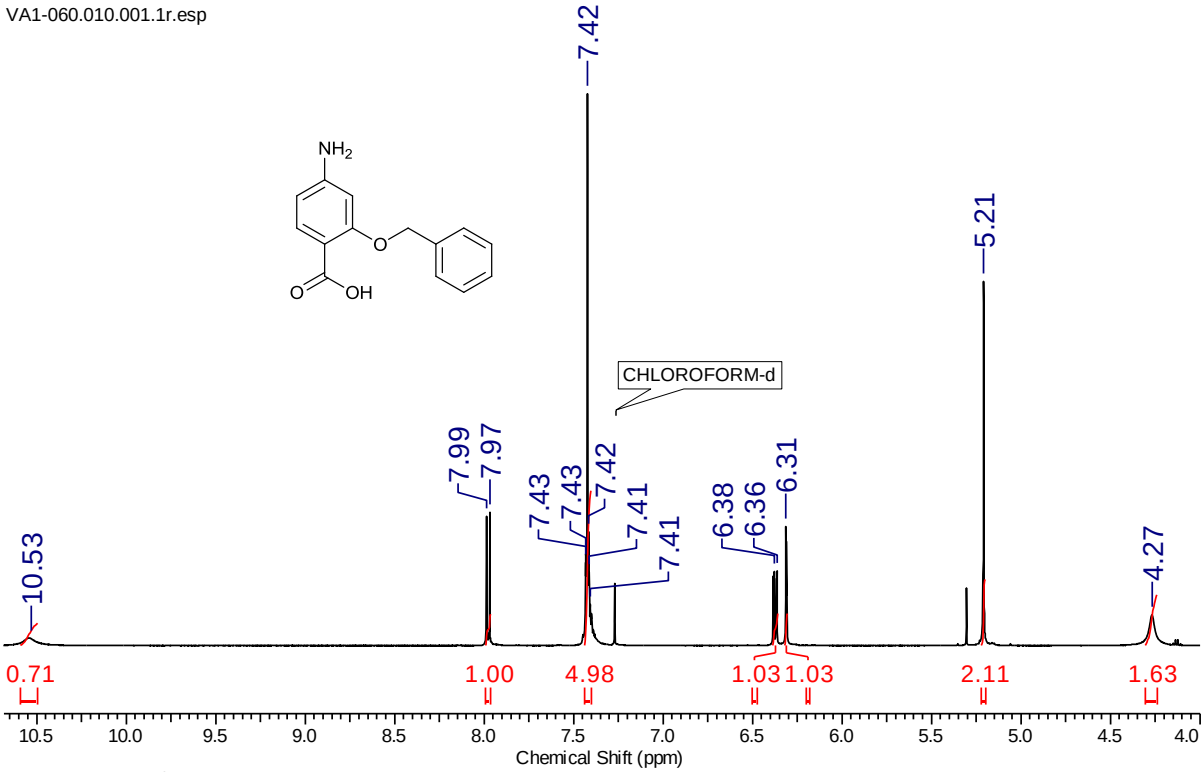

Figure S 4. ^{1}H NMR spectrum of 29 ($CDCl_3$, 500 MHz).

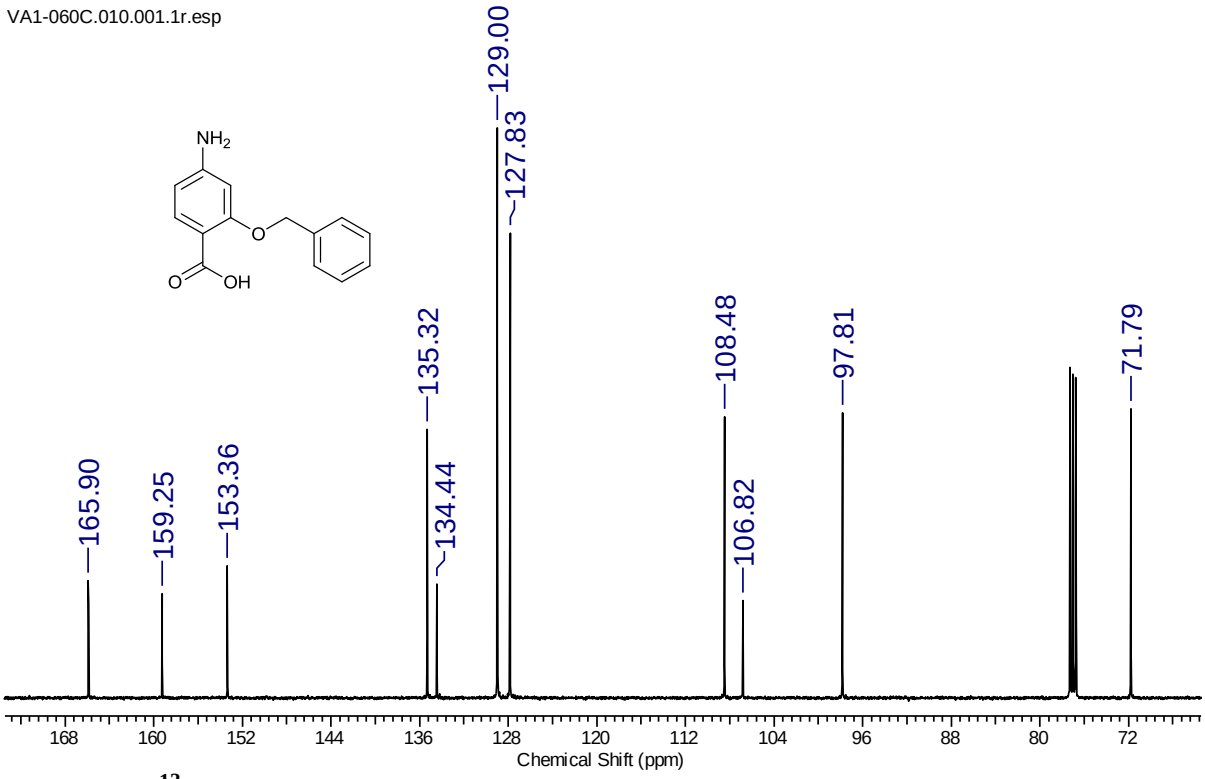

Figure S 5. ^{13}C NMR spectrum of 29 ($CDCl_3$, 500 MHz).

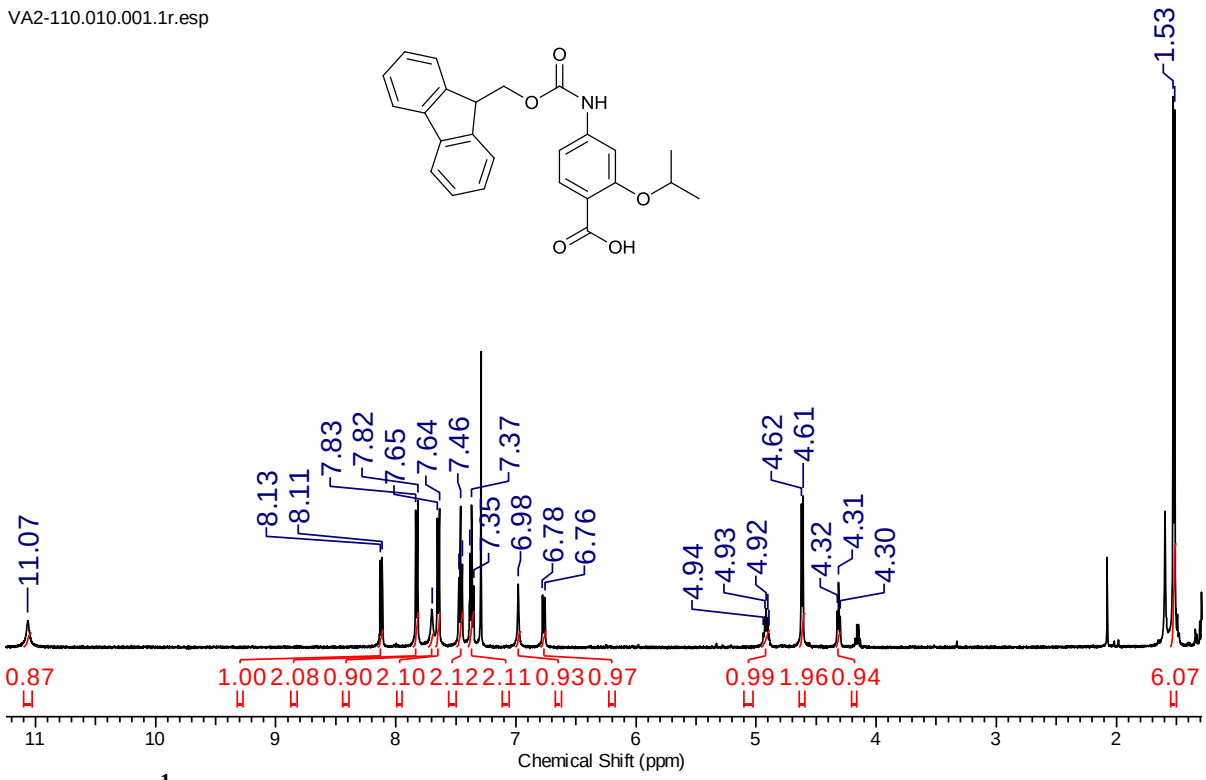

Figure S 6. ^{1}H NMR spectrum of 31 ($CDCl_3$, 500 MHz).

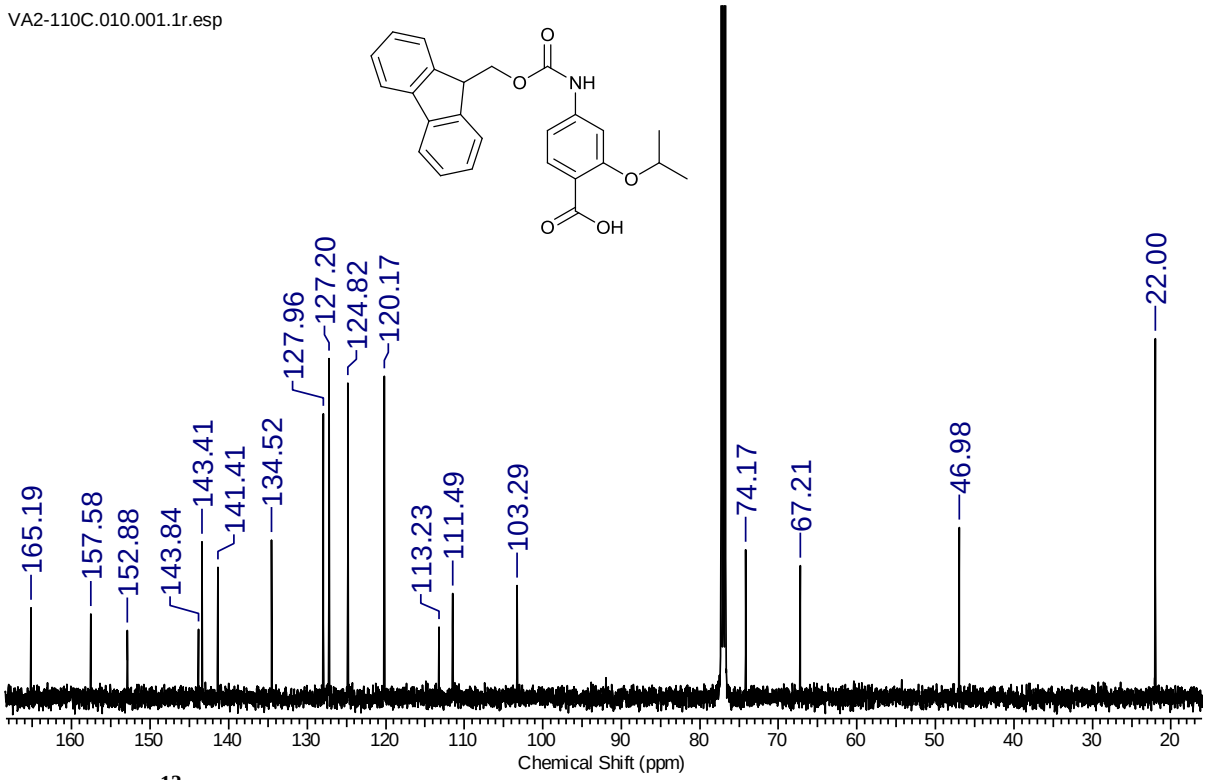

Figure S 7. ^{13}C NMR spectrum of 31 ($CDCl_3$, 500 MHz).

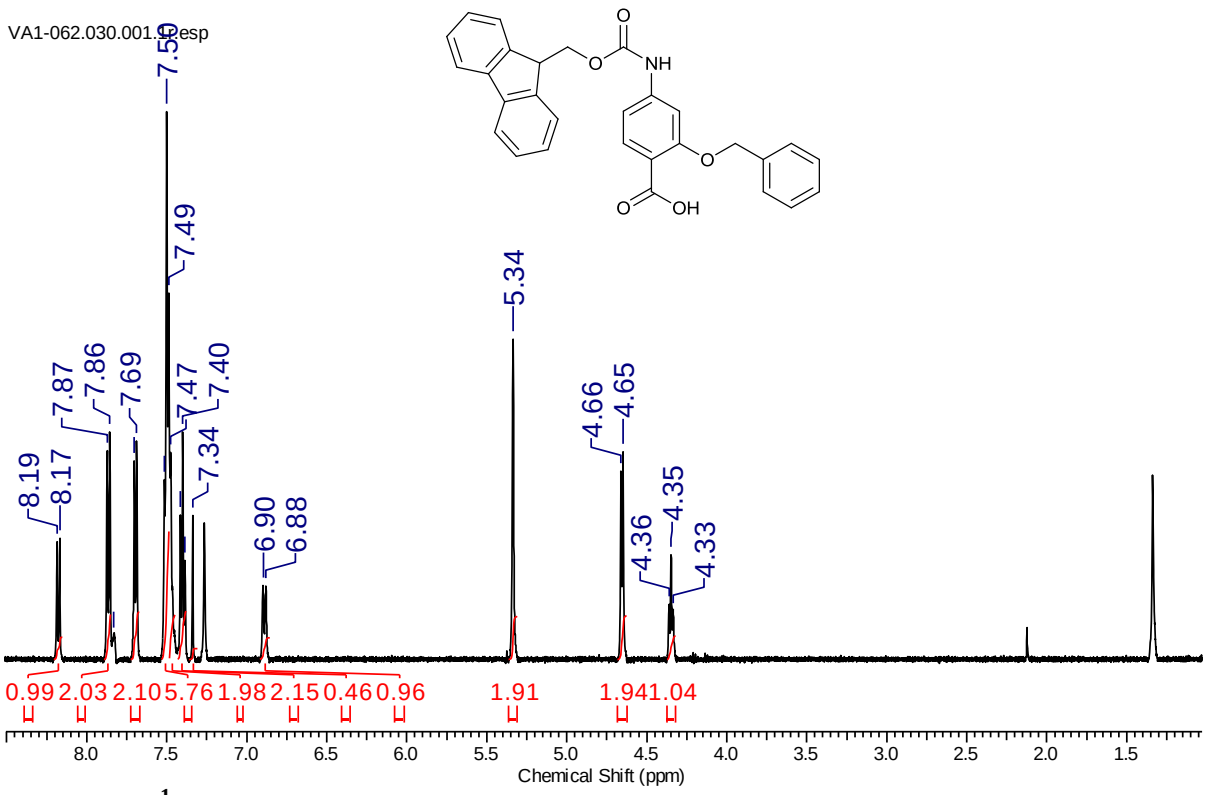

Figure S 8. ^{1}H NMR spectrum of 33 ($CDCl_3$, 500 MHz).

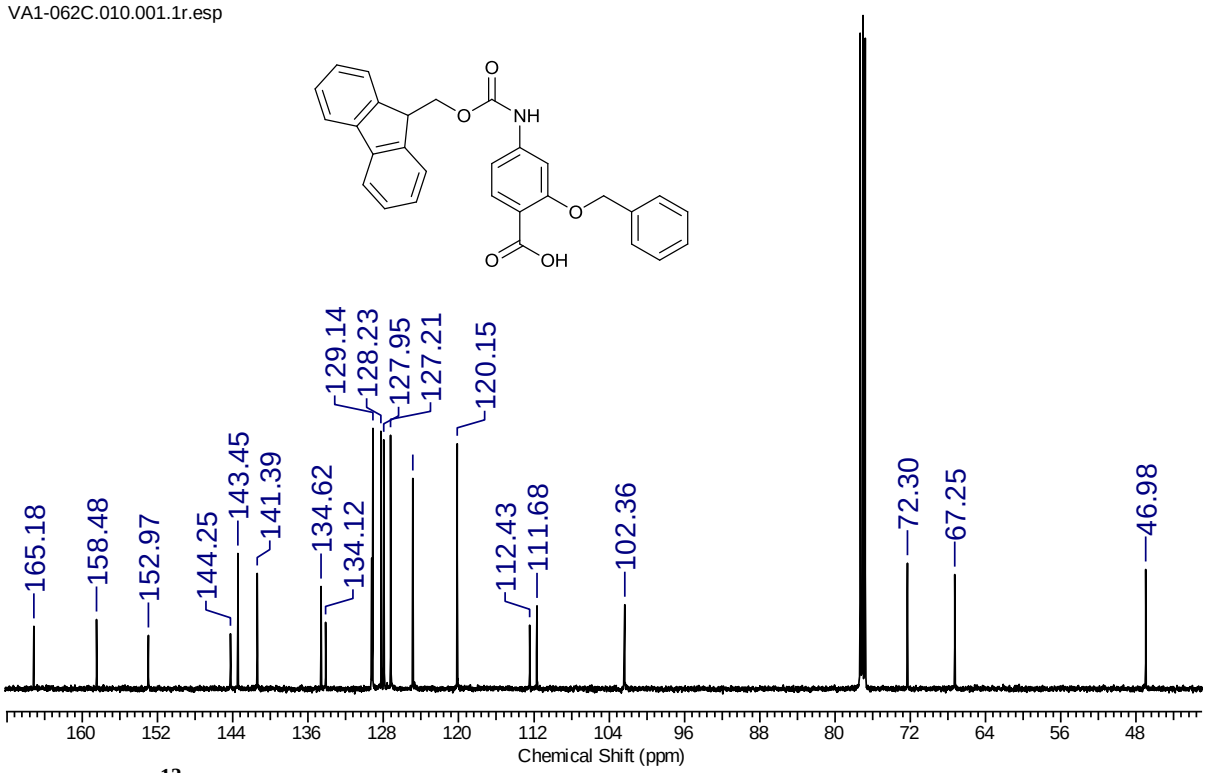

Figure S 9. ^{13}C NMR spectrum of 33 ($CDCl_3$, 500 MHz).

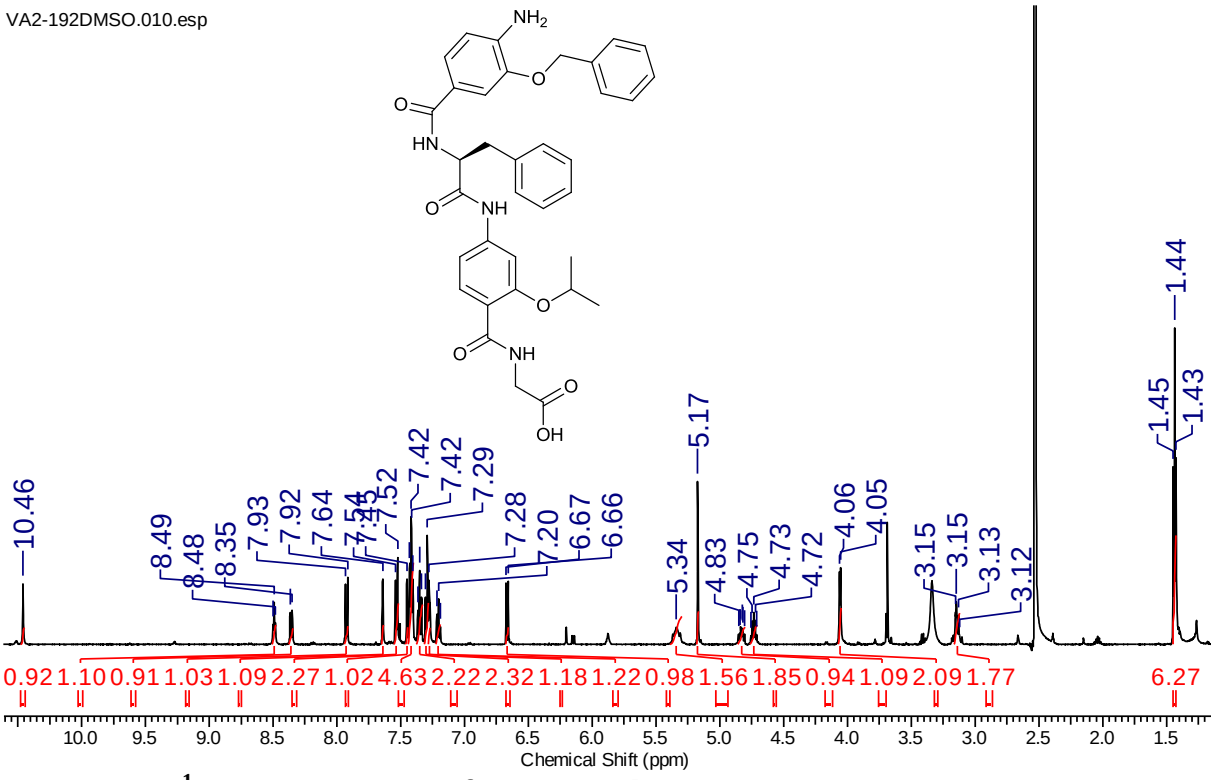

Figure S 10. ^{1}H NMR spectrum of 1 (DMSO-d$_6$, 500 MHz).

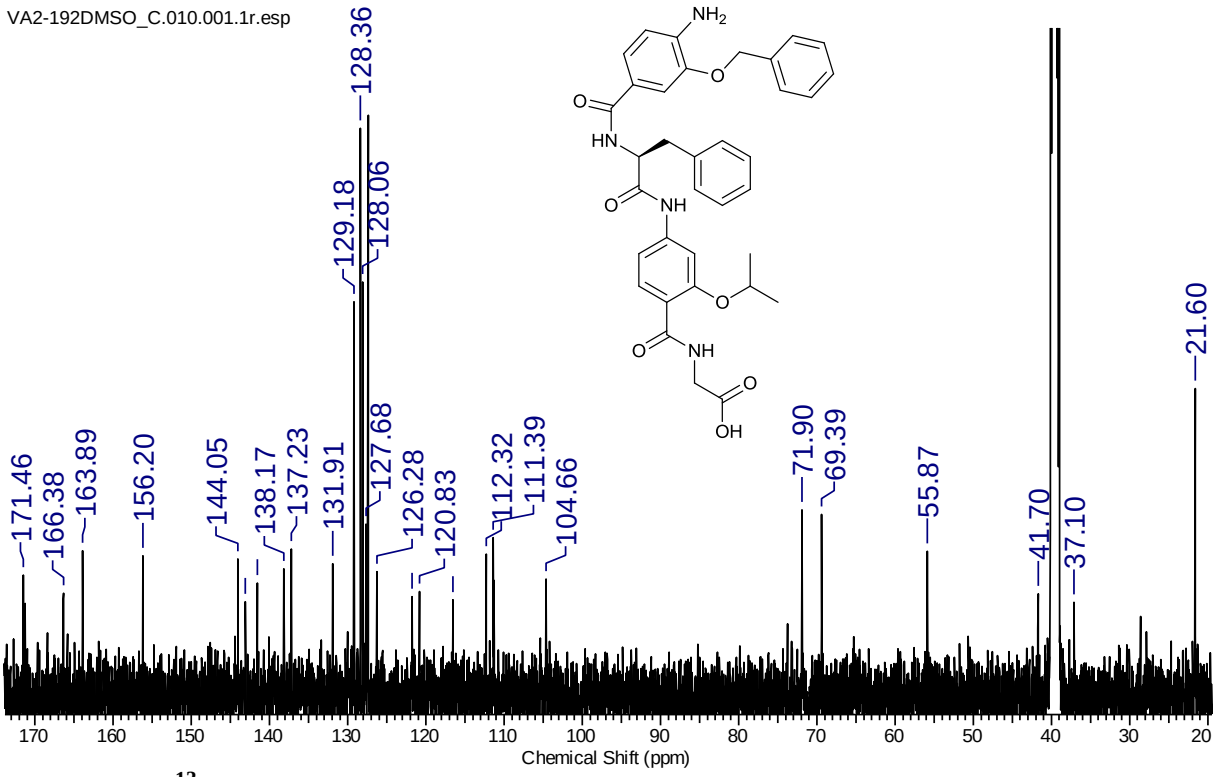

Figure S 11. ^{13}C NMR spectrum of 1 (DMSO-d$_6$, 500 MHz).

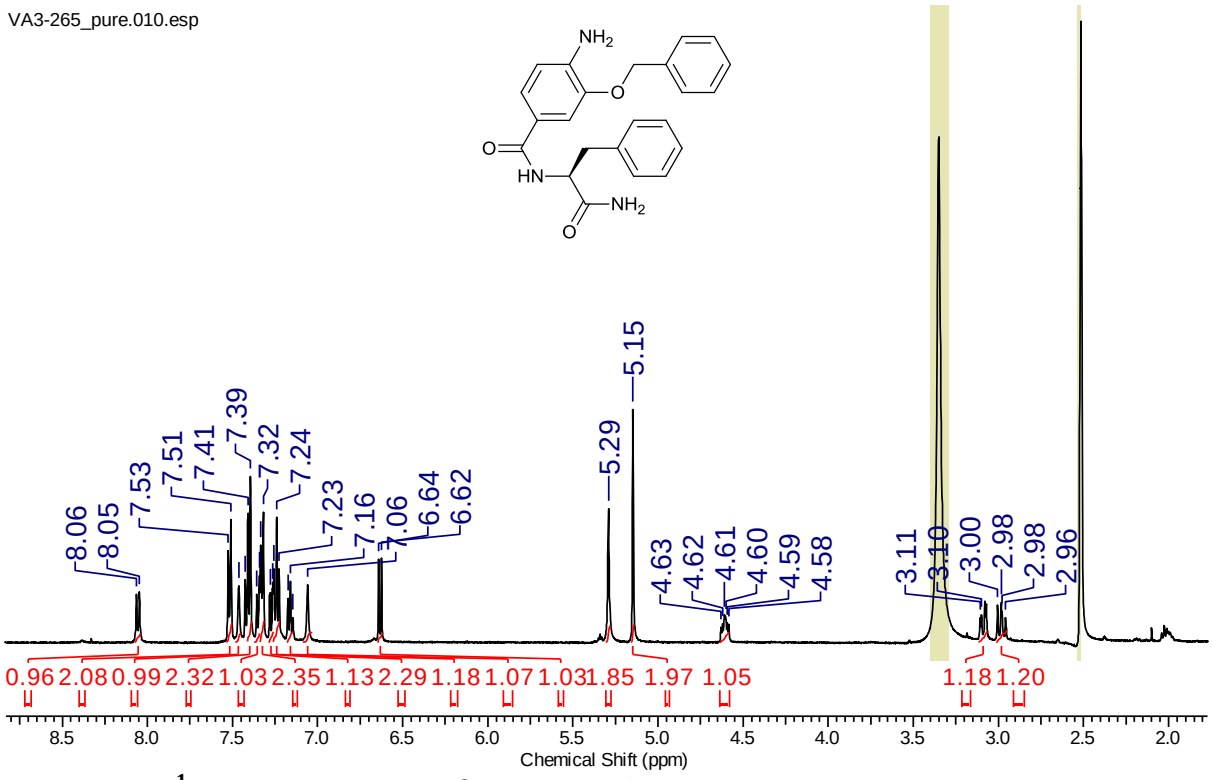

Figure S 12. ^{1}H NMR spectrum of 2 (DMSO-d$_6$, 500 MHz).

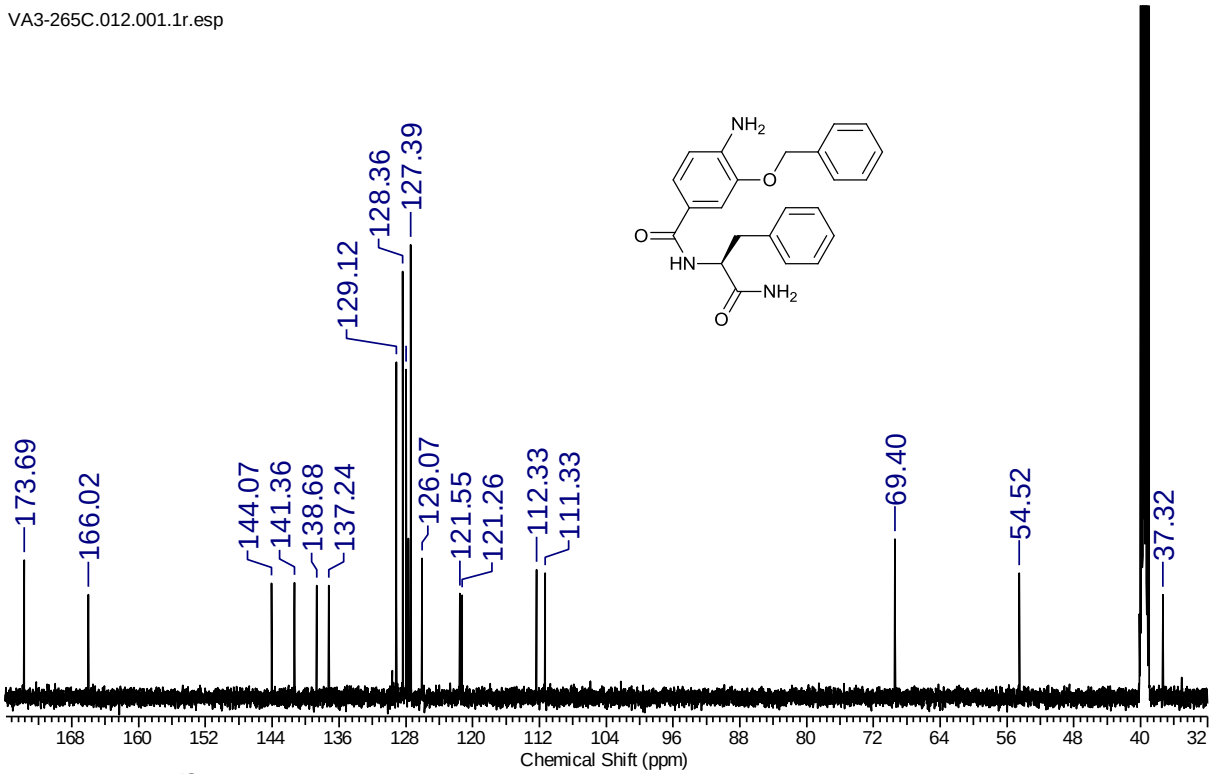

Figure S 13. ^{13}C NMR spectrum of 2 (DMSO-d$_6$, 500 MHz).

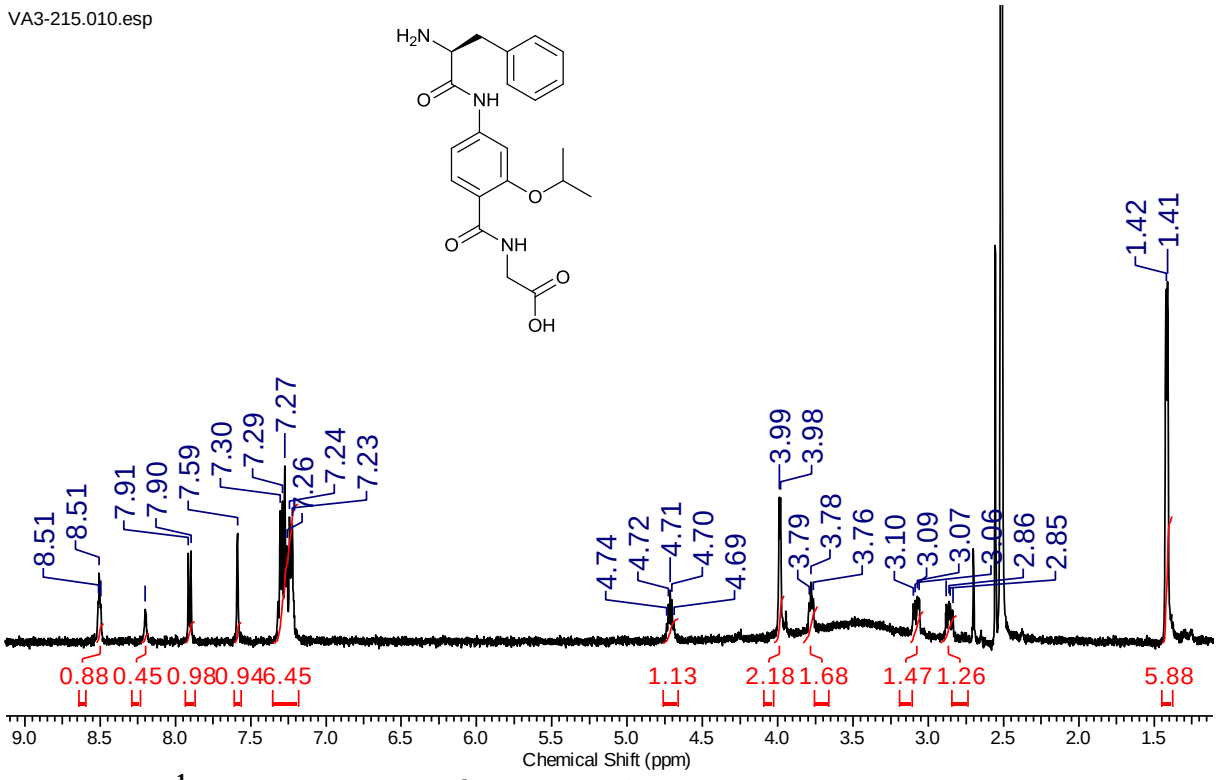

Figure S 14. ^{1}H NMR spectrum of 3 (DMSO-d$_6$, 500 MHz).

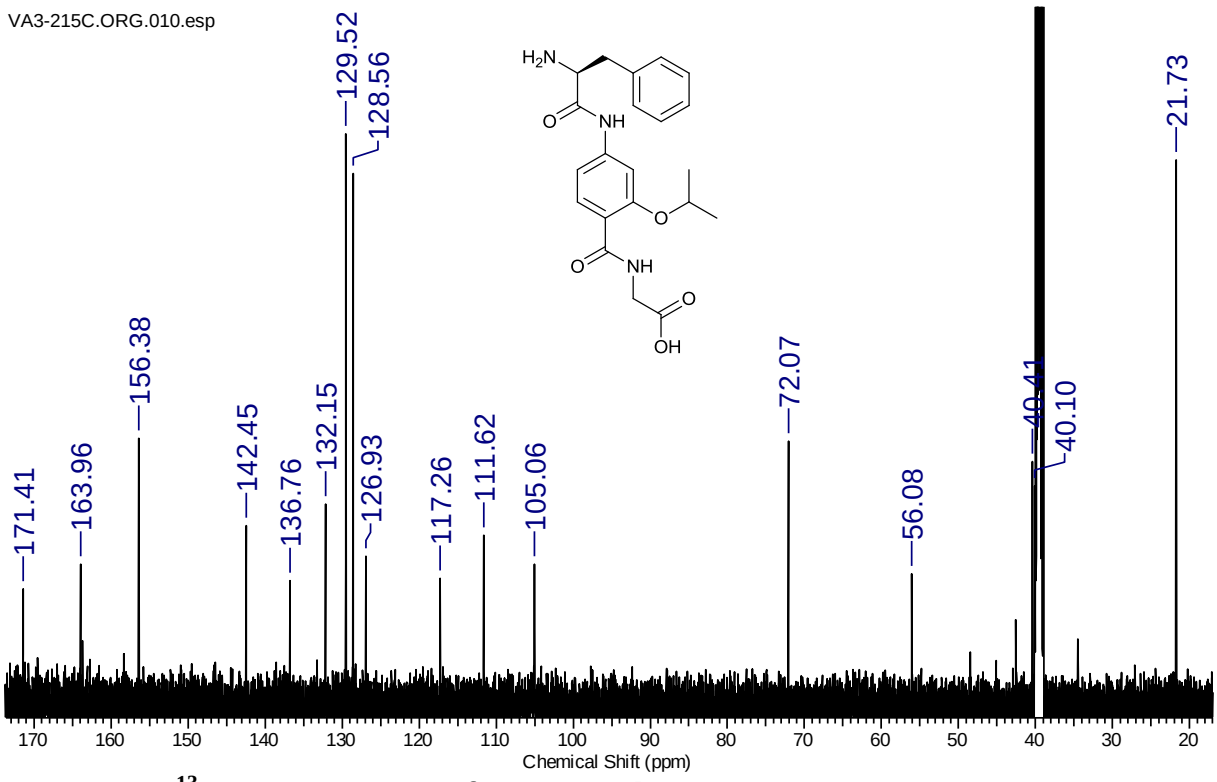

Figure S 15. ^{13}C NMR spectrum of 3 (DMSO-d$_6$, 500 MHz).

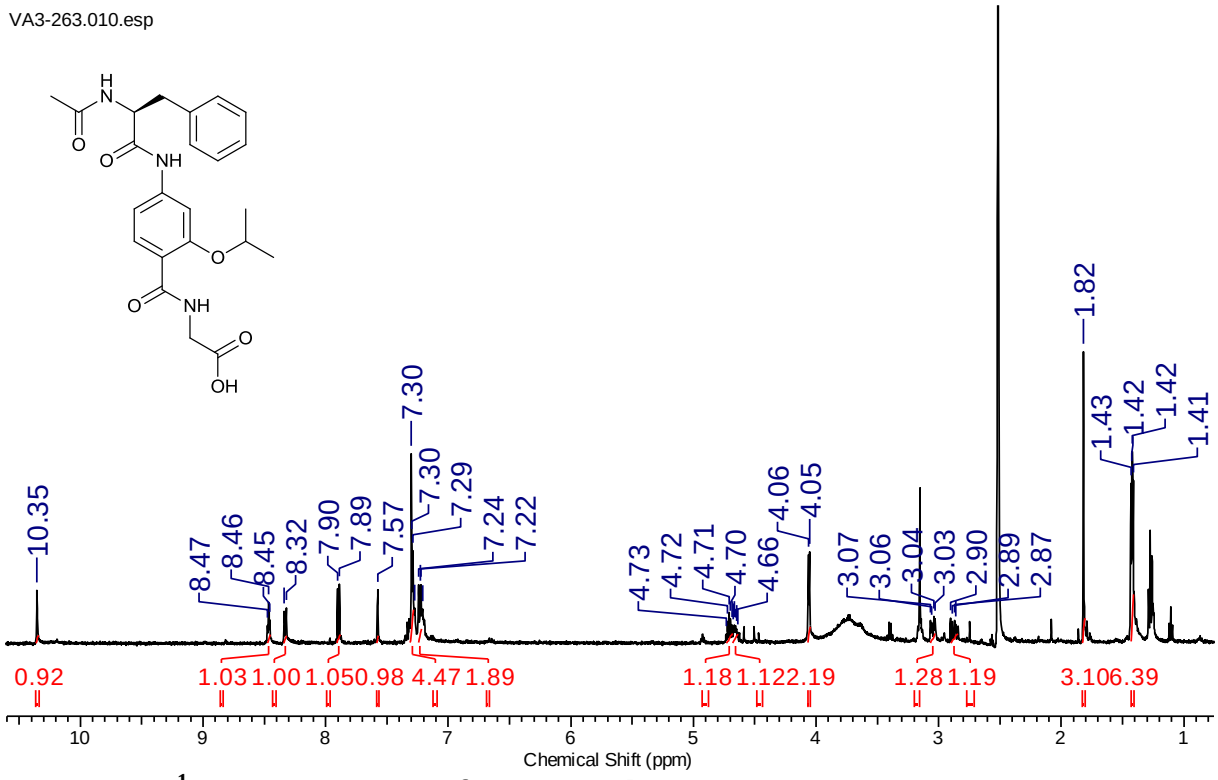

Figure S 16. ^{1}H NMR spectrum of 4 (DMSO-d$_6$, 500 MHz).

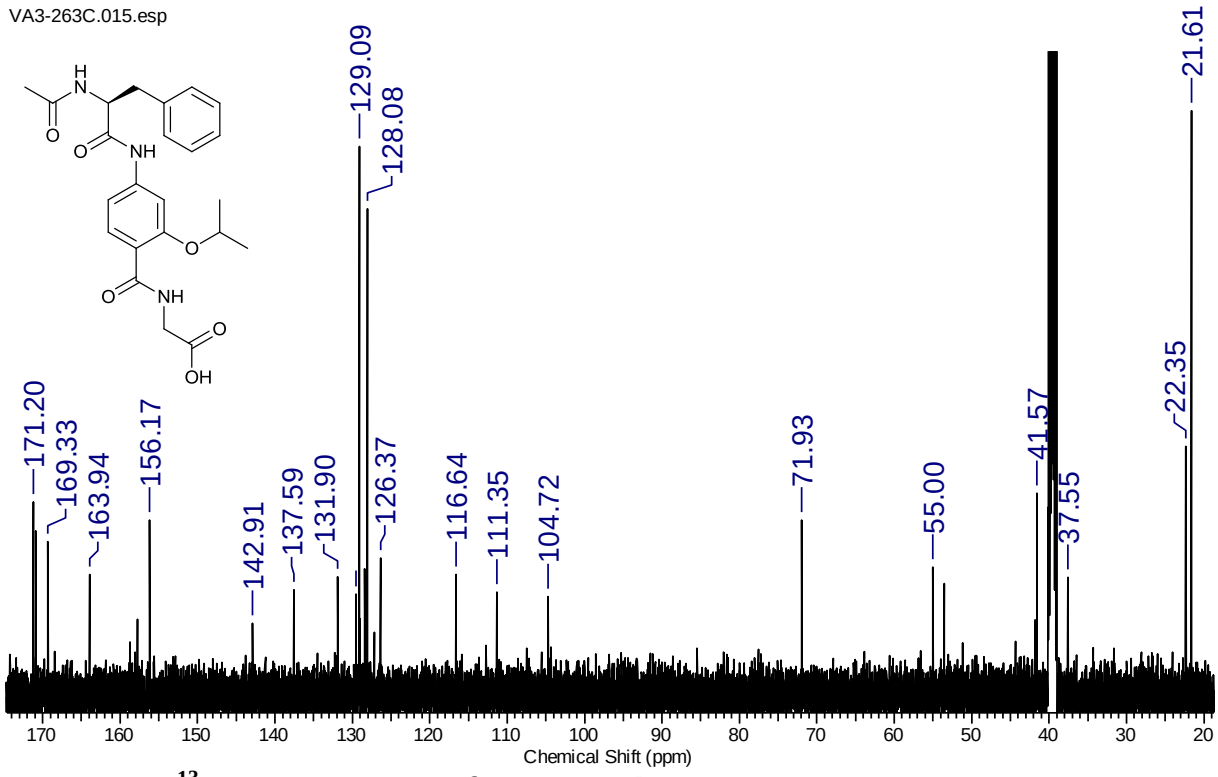

Figure S 17. ^{13}C NMR spectrum of 4 (DMSO-d$_6$, 500 MHz).

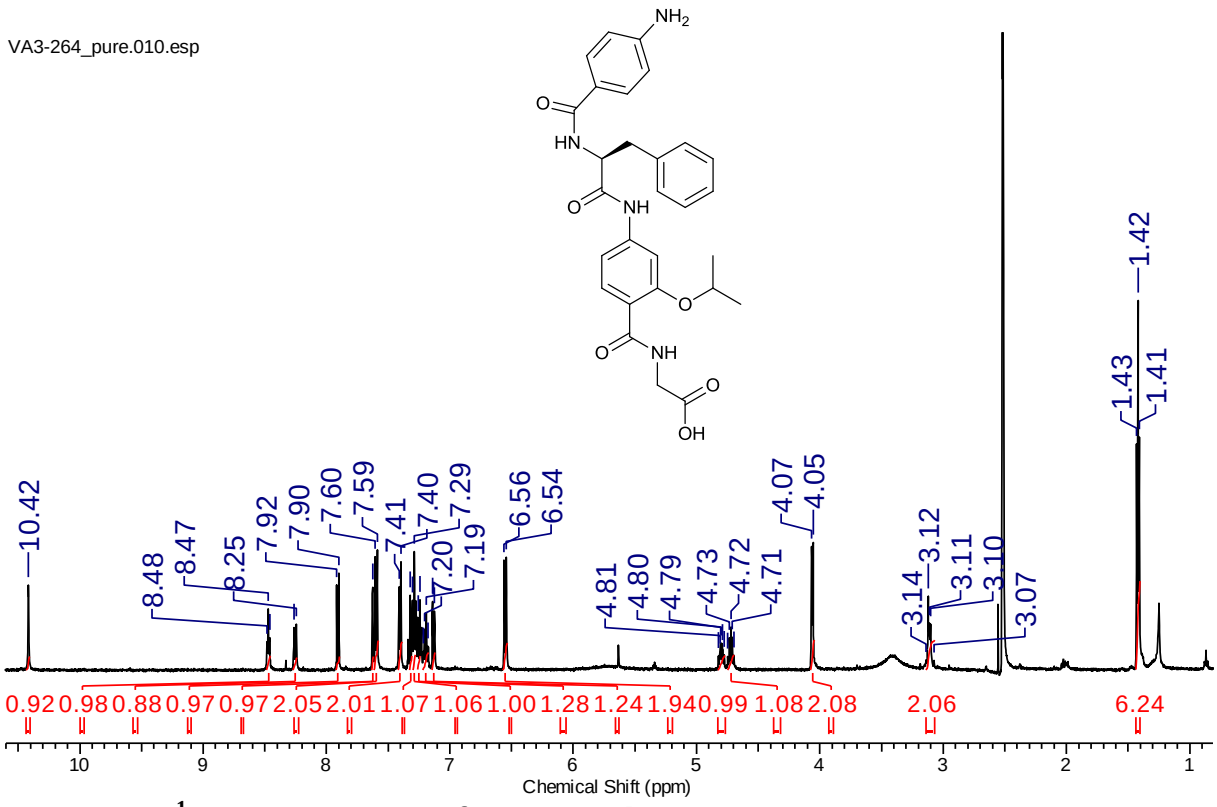

Figure S 18. ^{1}H NMR spectrum of 5 (DMSO-d$_6$, 500 MHz).

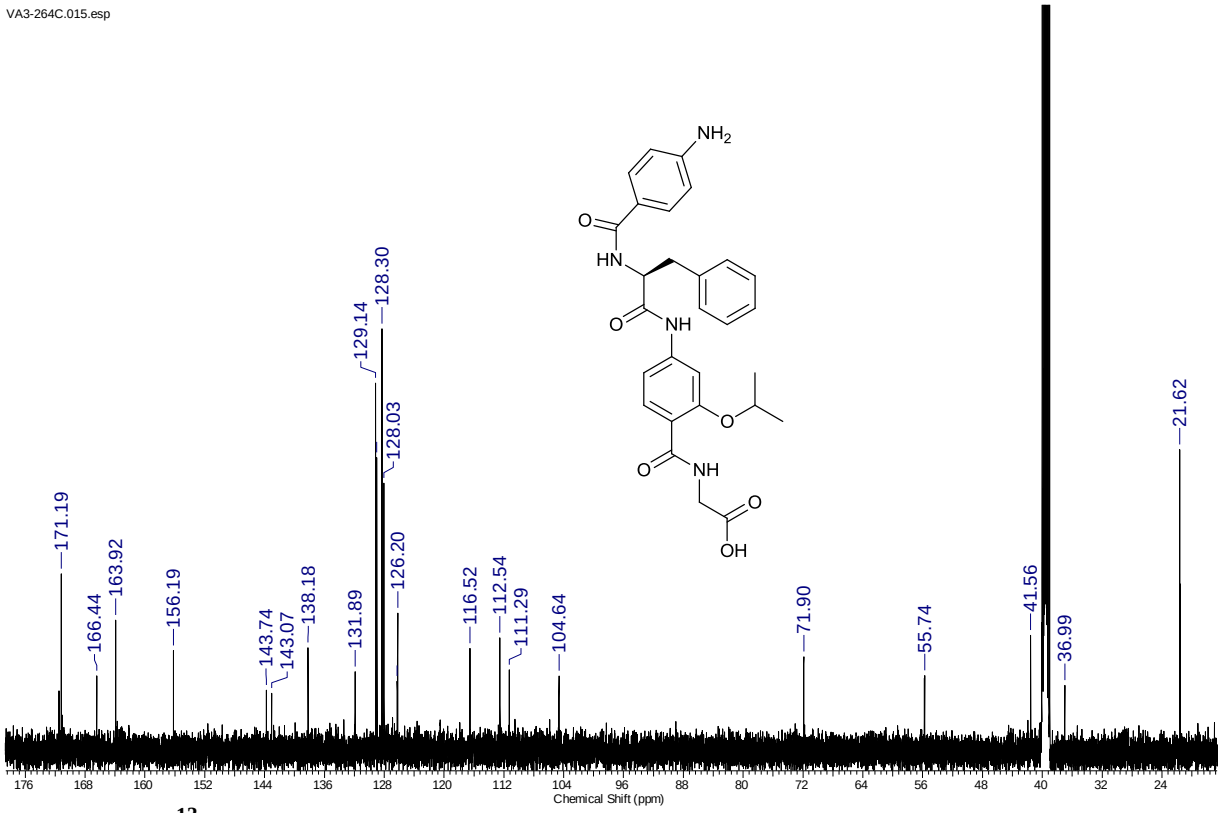

Figure S 19. ^{13}C NMR spectrum of 5 (DMSO-d$_6$, 500 MHz).

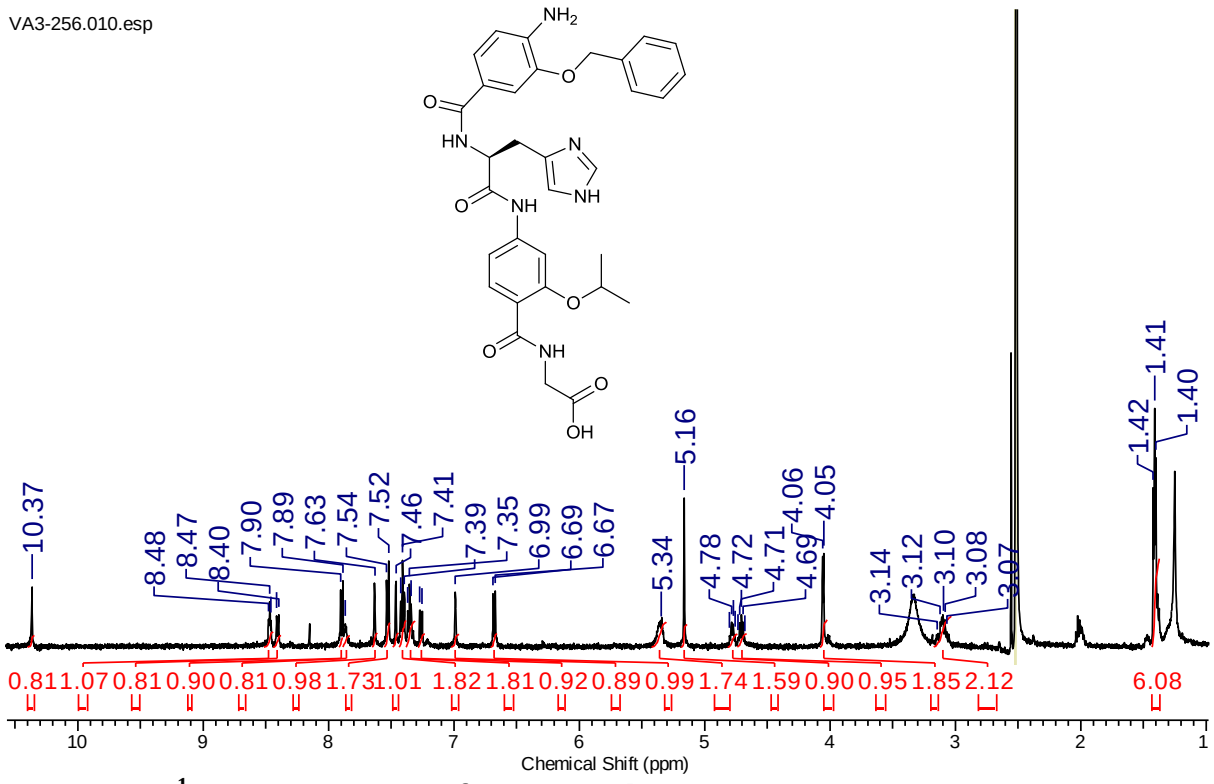

Figure S 20. ^{1}H NMR spectrum of 6 (DMSO-d$_6$, 500 MHz).

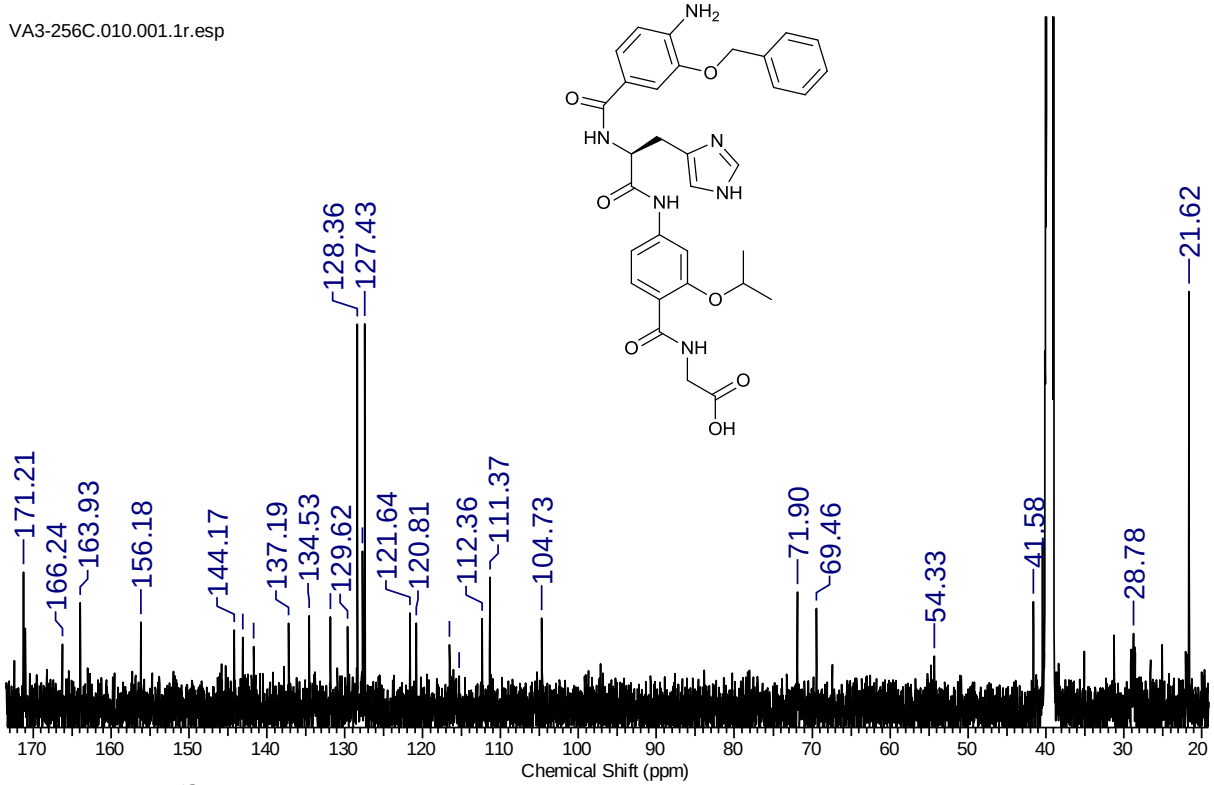

Figure S 21. ^{13}C NMR spectrum of 6 (DMSO-d$_6$, 500 MHz).

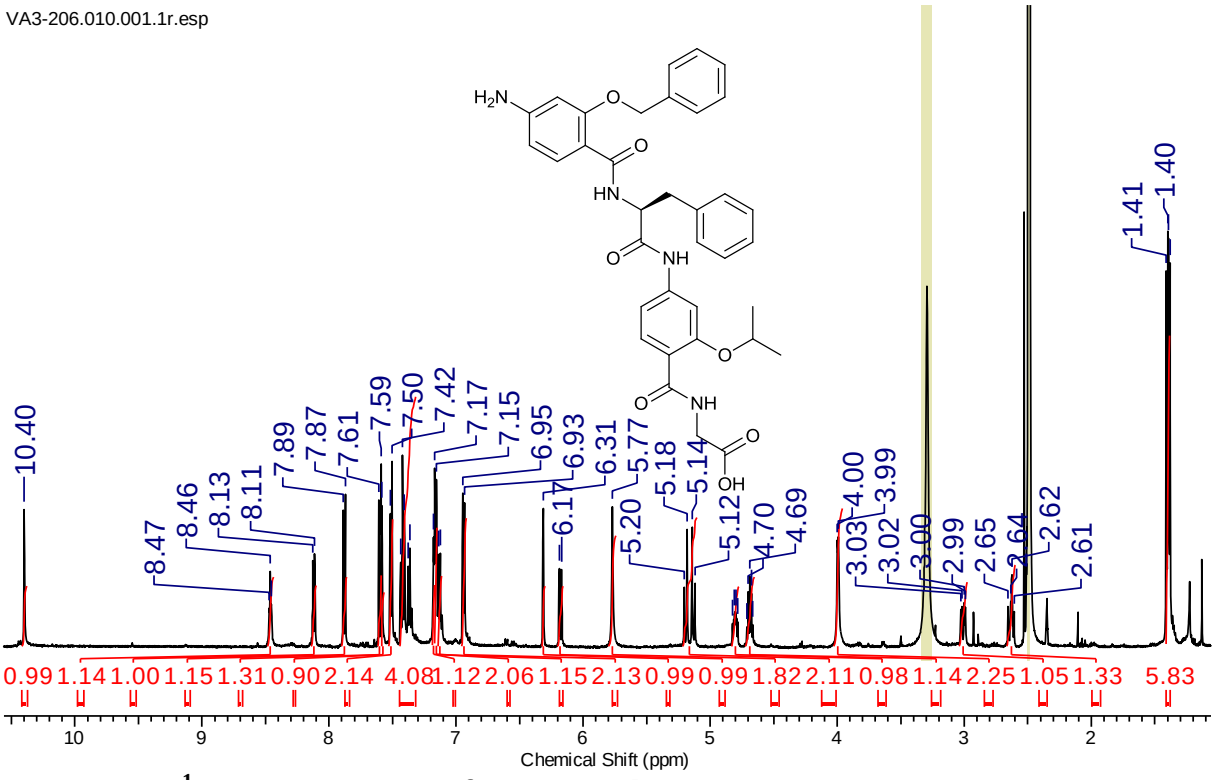

Figure S 22. ^{1}H NMR spectrum of 7 (DMSO-d$_6$, 500 MHz).

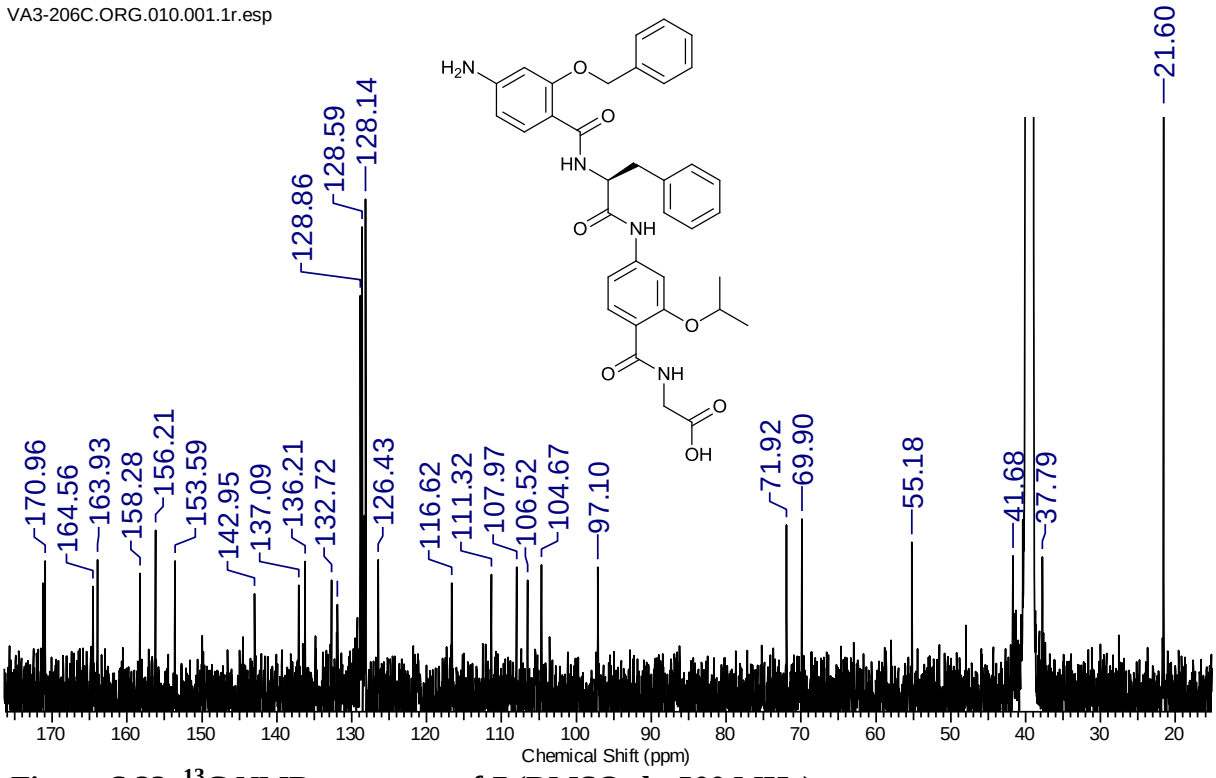

Figure S 23. ^{13}C NMR spectrum of 7 (DMSO-d$_6$, 500 MHz).

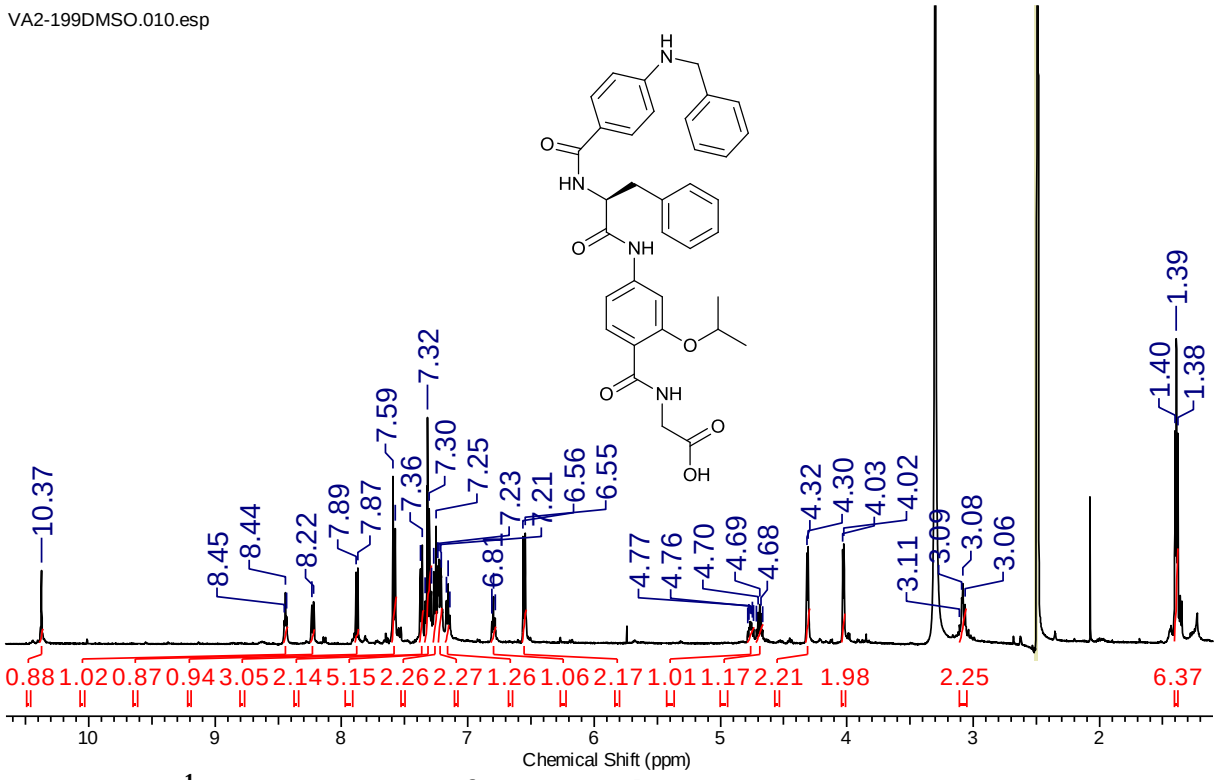

Figure S 24. ^{1}H NMR spectrum of 8 (DMSO-d$_6$, 500 MHz).

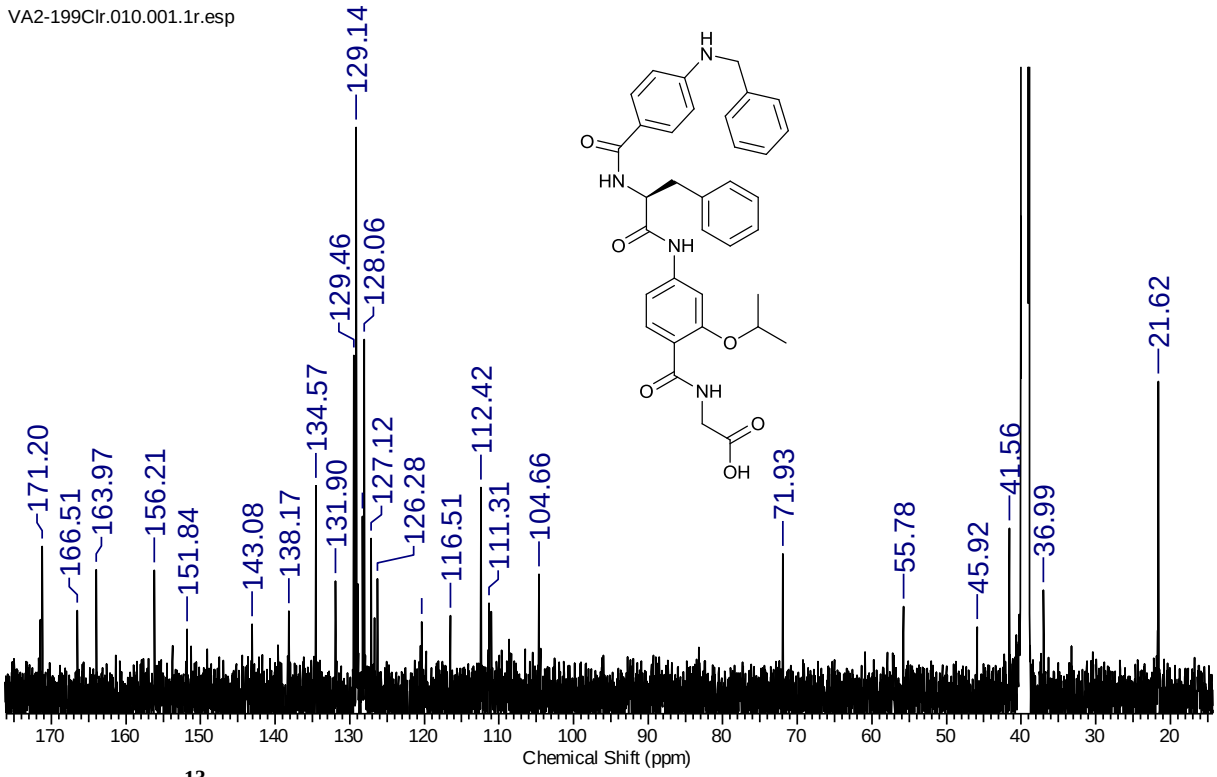

Figure S 25. ^{13}C NMR spectrum of 8 (DMSO-d$_6$, 500 MHz).

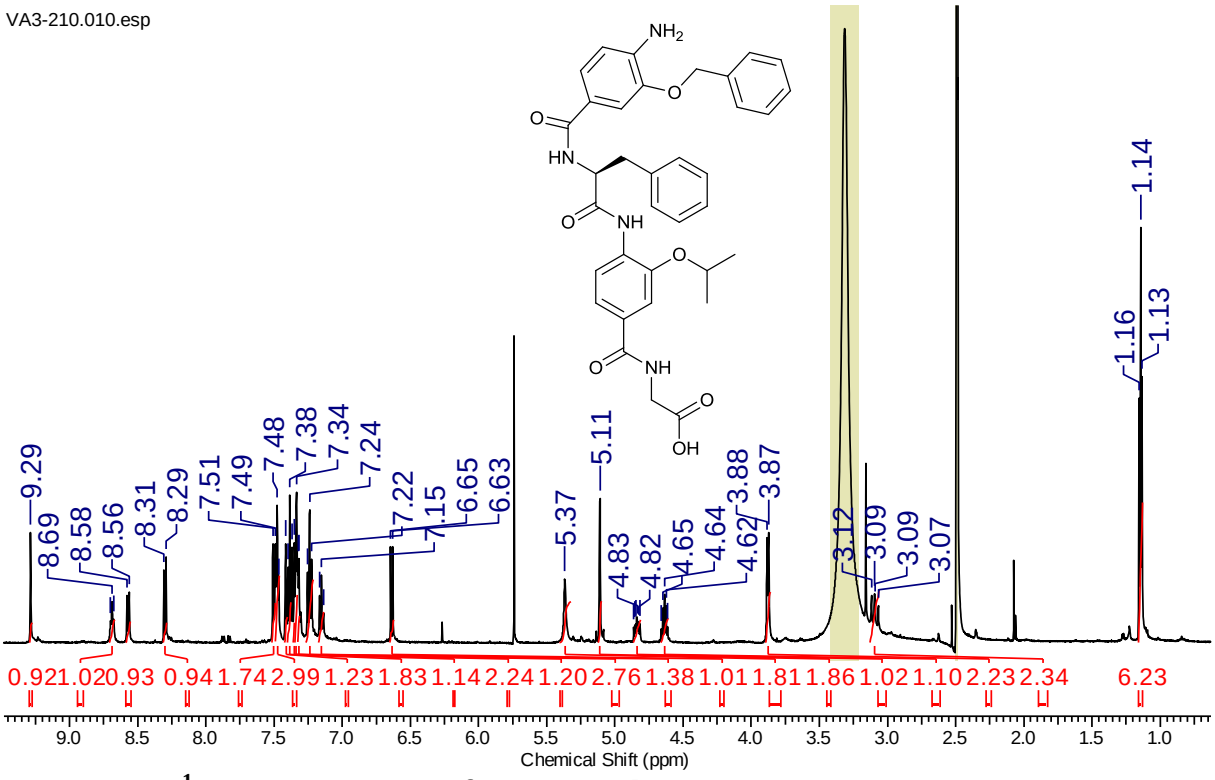

Figure S 26. ^{1}H NMR spectrum of 9 (DMSO-d$_6$, 500 MHz).

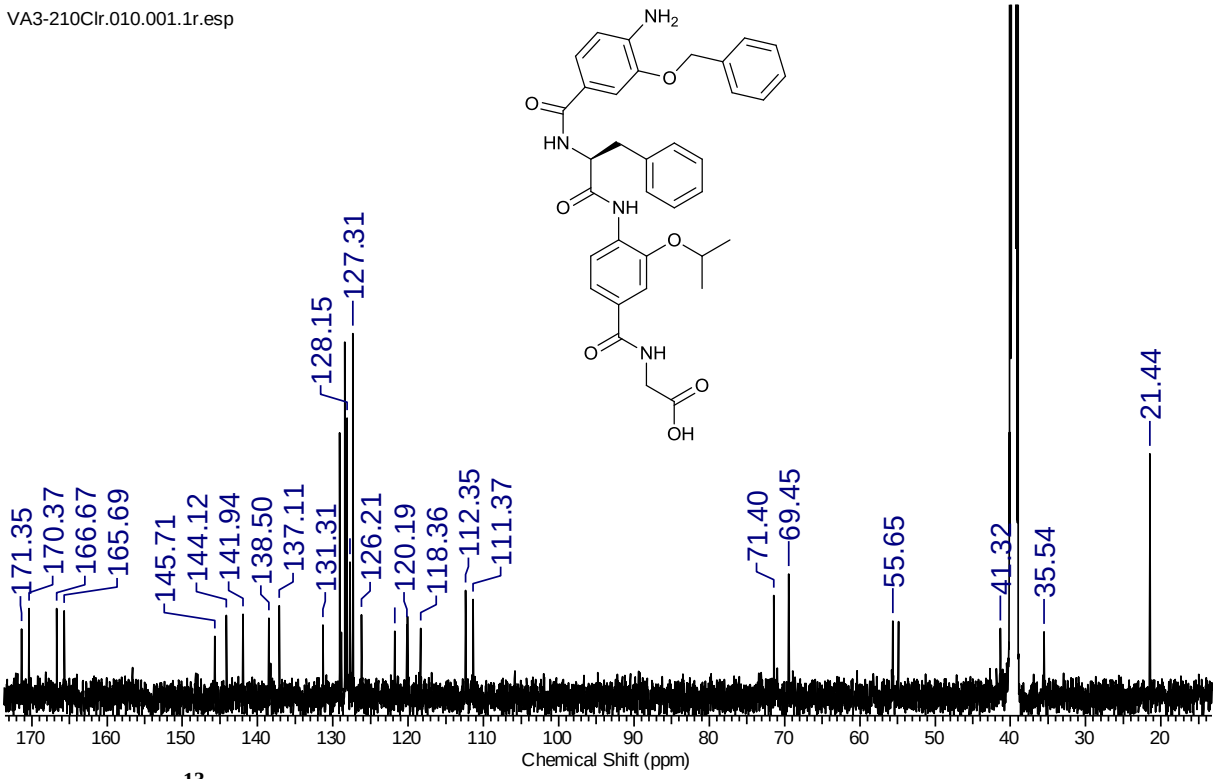

Figure S 27. ^{13}C NMR spectrum of 9 (DMSO-d$_6$, 500 MHz).

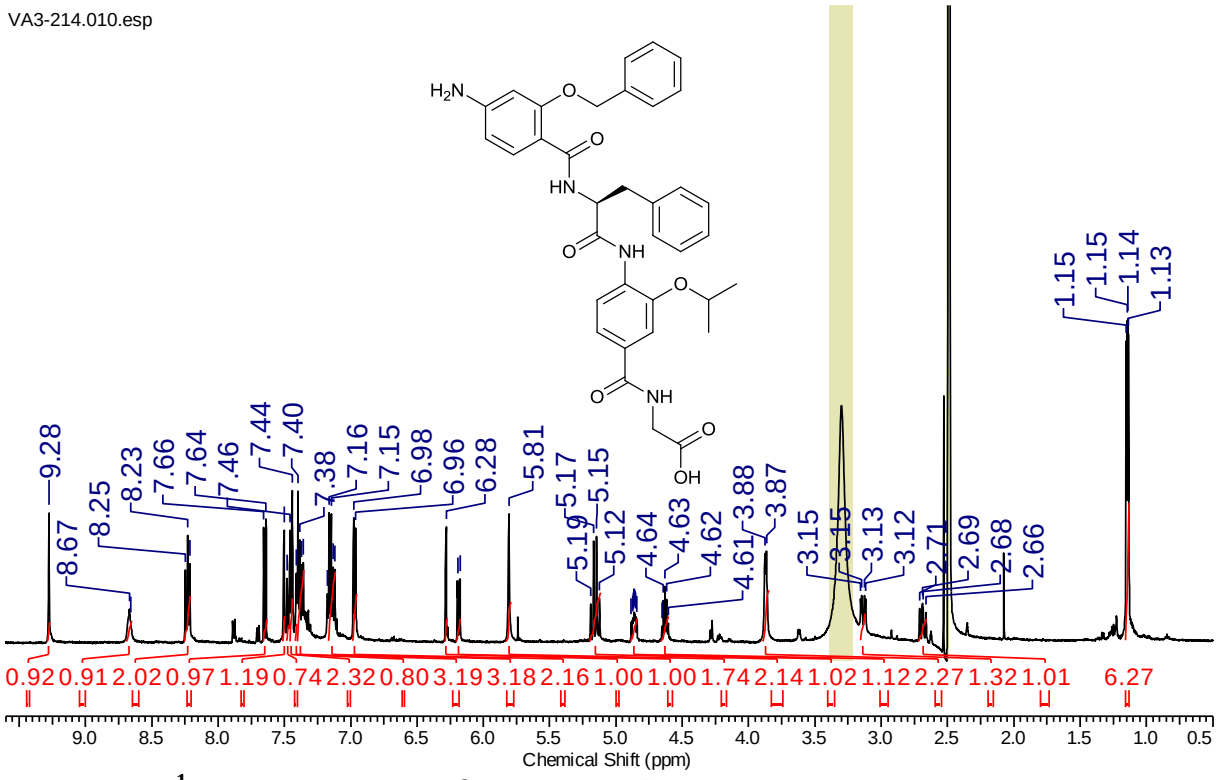

Figure S 28. ^{1}H NMR spectrum of 10 (DMSO-d$_6$, 500 MHz).

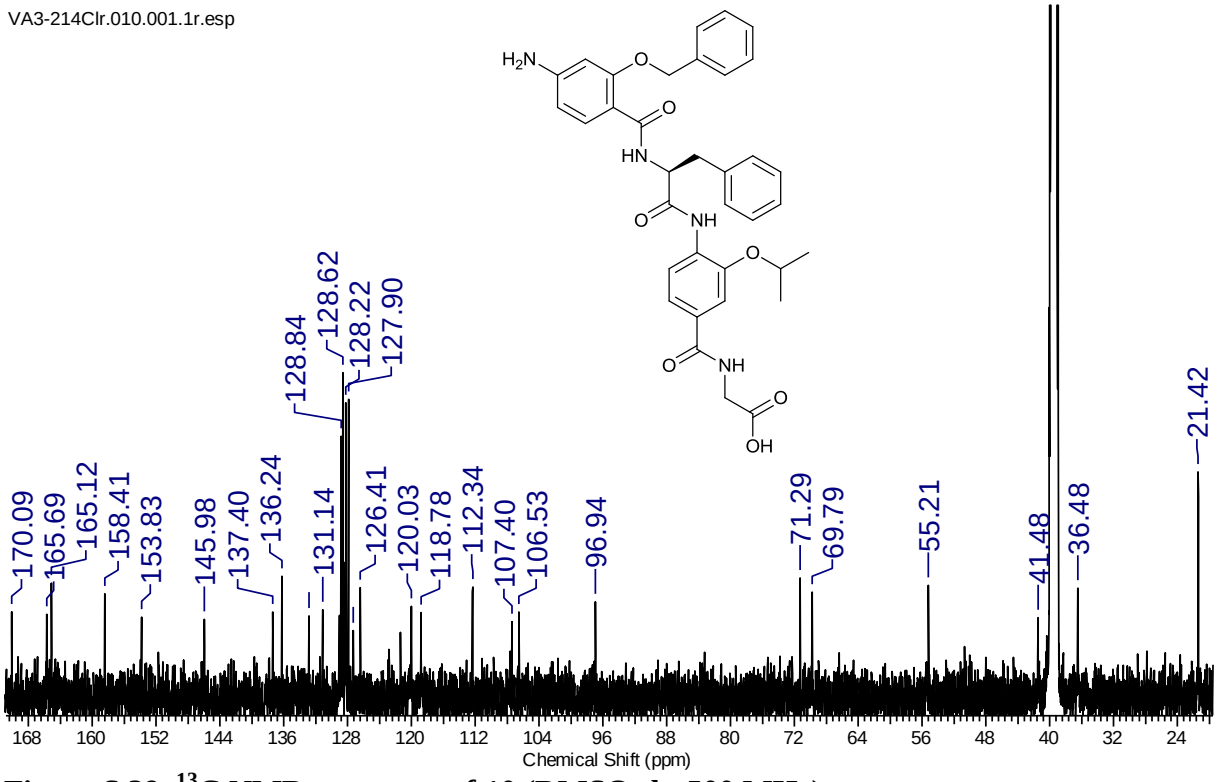

Figure S 29. ^{13}C NMR spectrum of 10 (DMSO-d$_6$, 500 MHz).

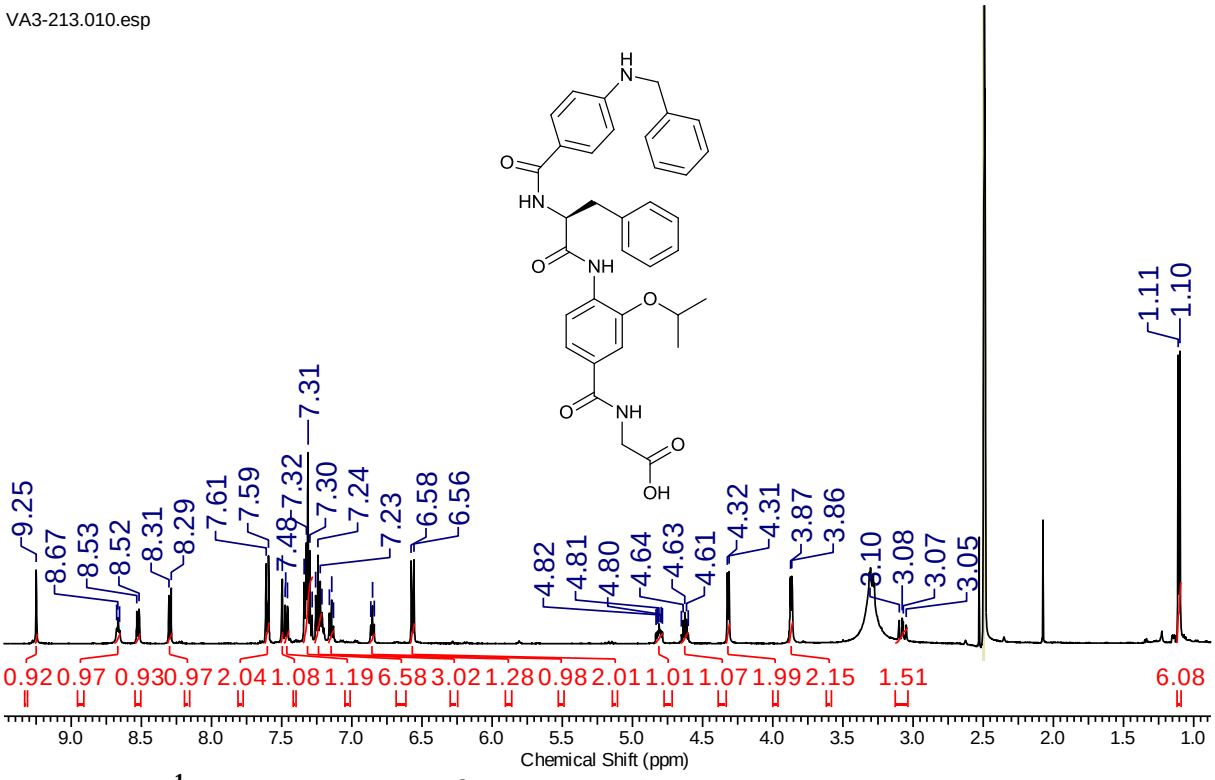

Figure S 30. ^{1}H NMR spectrum of 11 (DMSO-d$_6$, 500 MHz).

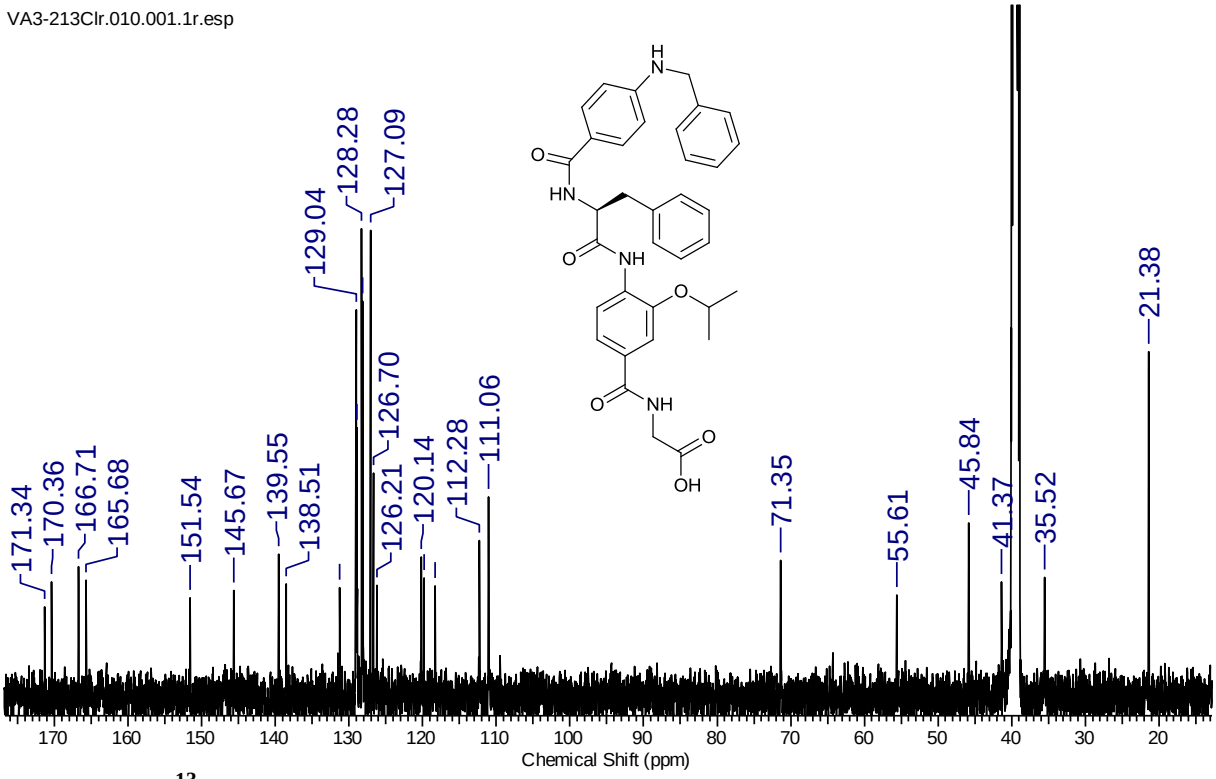

Figure S 31. ^{13}C NMR spectrum of 11 (DMSO-d$_6$, 500 MHz).

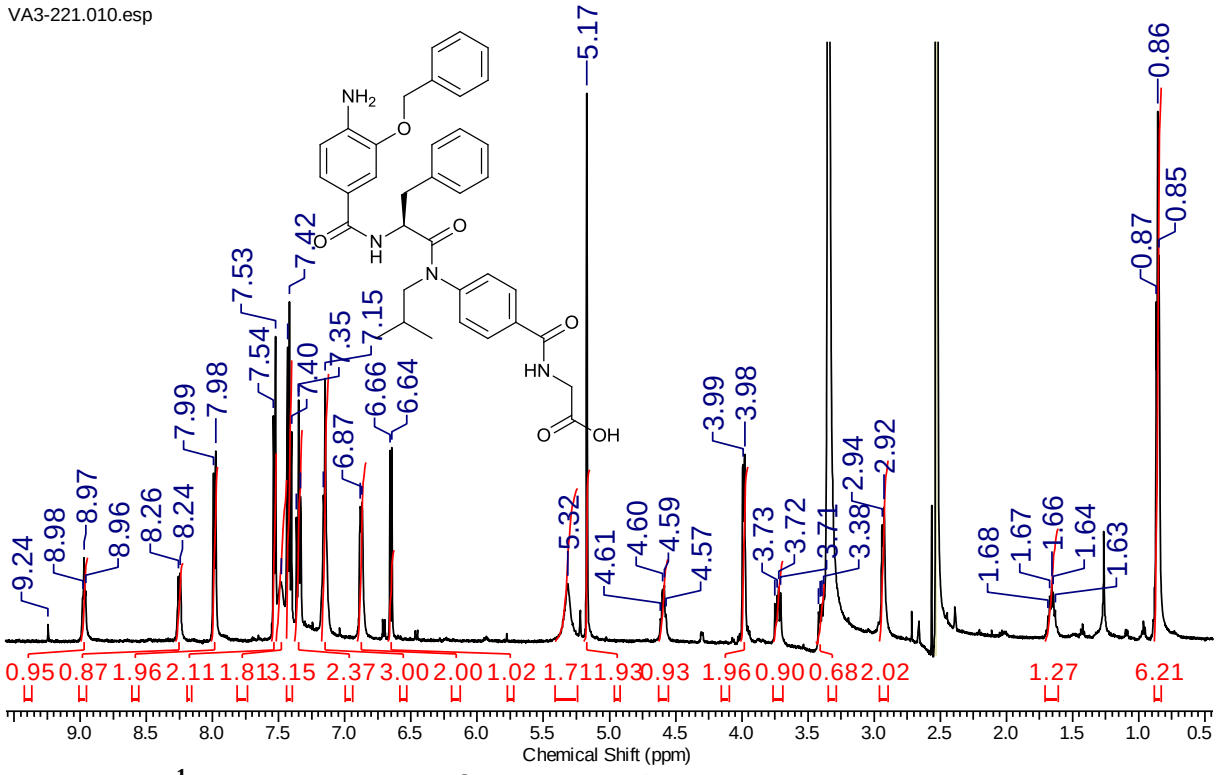

Figure S 32. ^{1}H NMR spectrum of 12 (DMSO-d$_6$, 500 MHz).

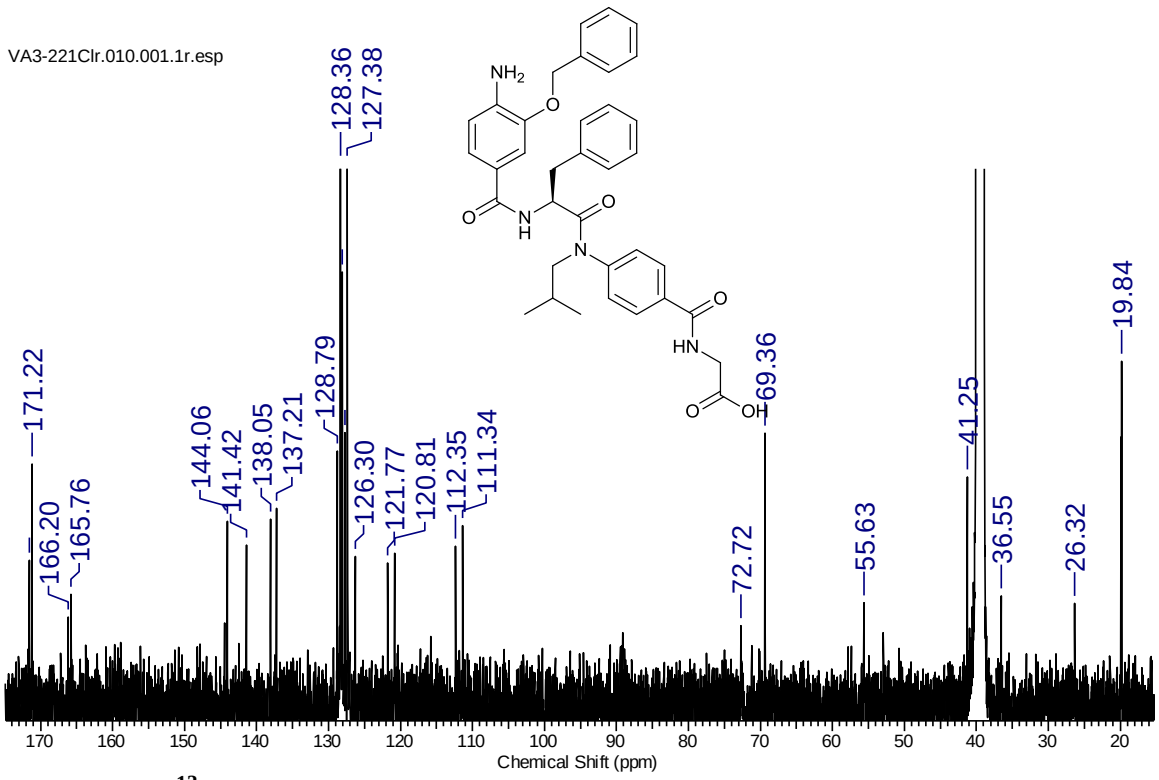

Figure S 33. ^{13}C NMR spectrum of 12 (DMSO-d$_6$, 500 MHz).

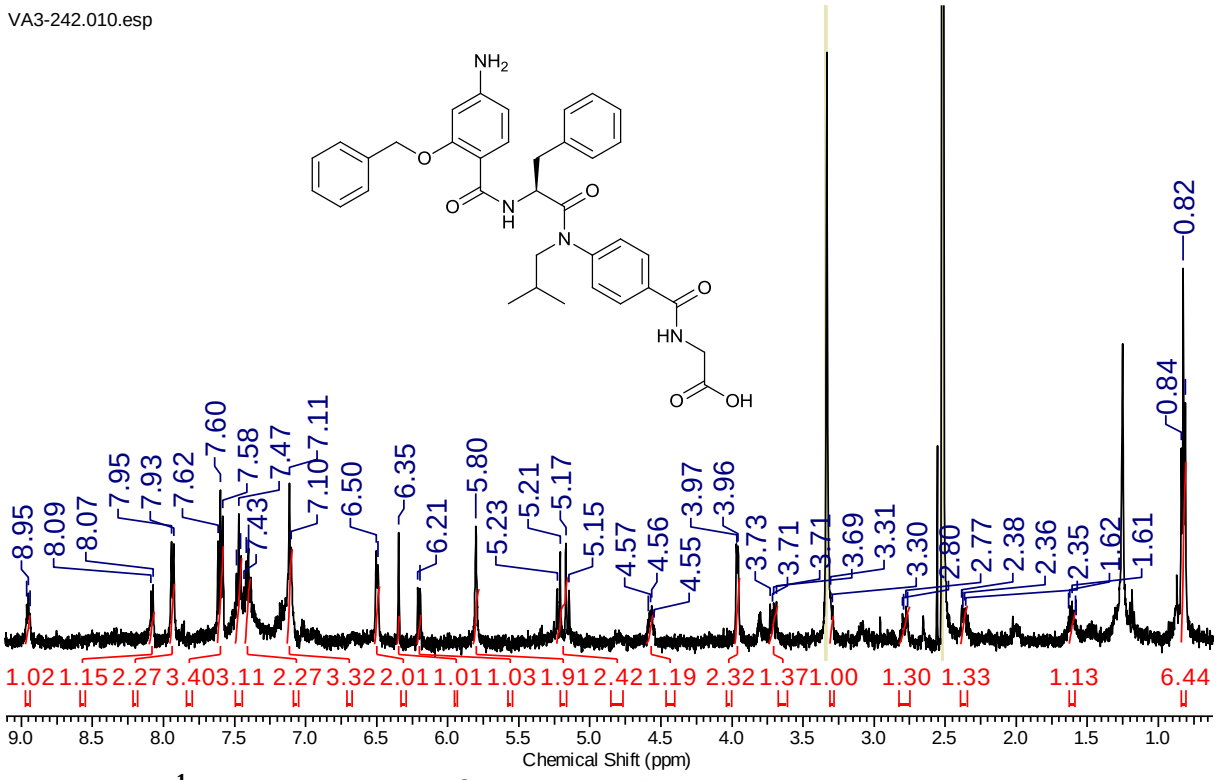

Figure S 34. ^{1}H NMR spectrum of 13 (DMSO-d$_6$, 500 MHz).

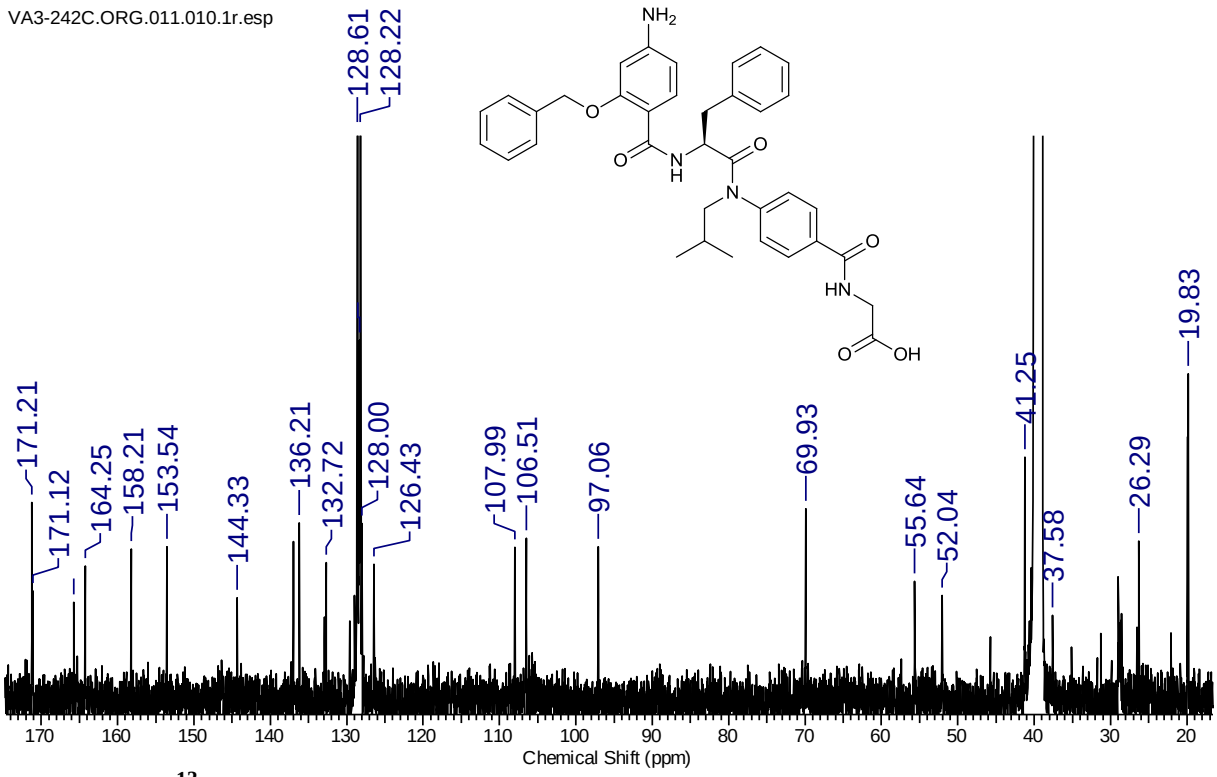

Figure S 35. ^{13}C NMR spectrum of 13 (DMSO-d$_6$, 500 MHz).

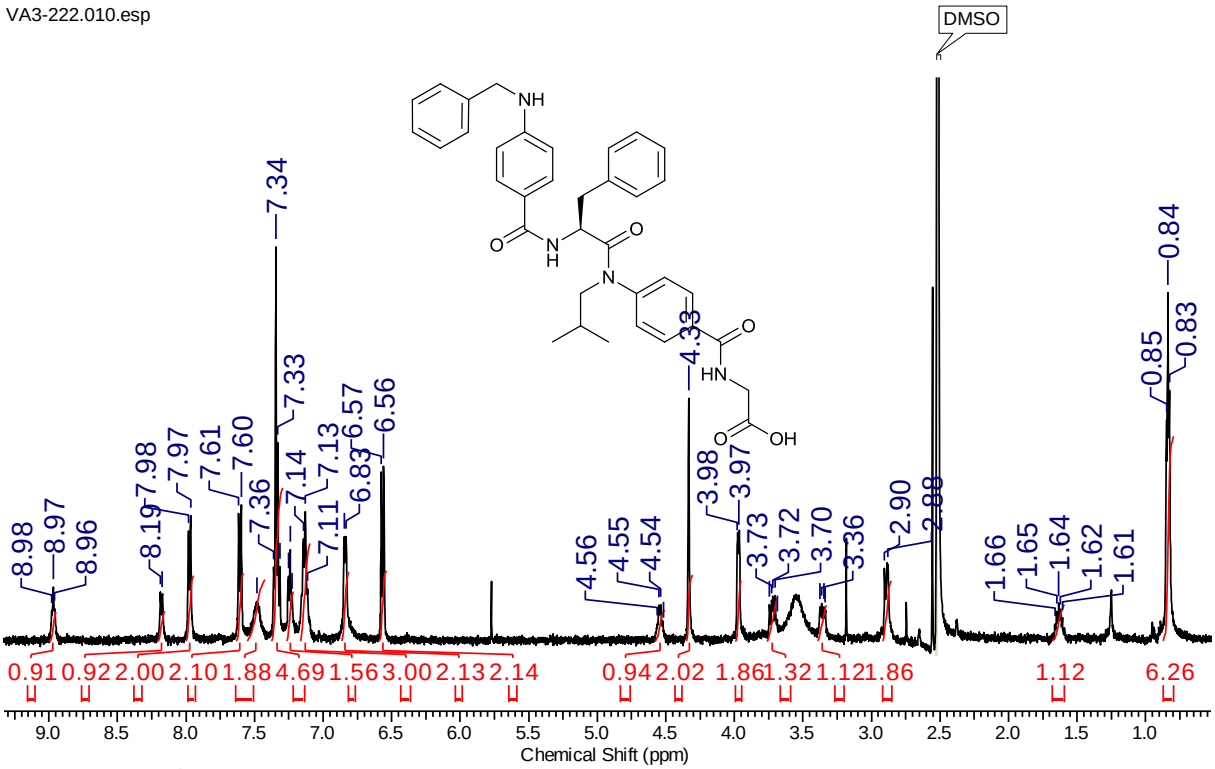

Figure S 36. ^{1}H NMR spectrum of 14 (DMSO-d$_6$, 500 MHz).

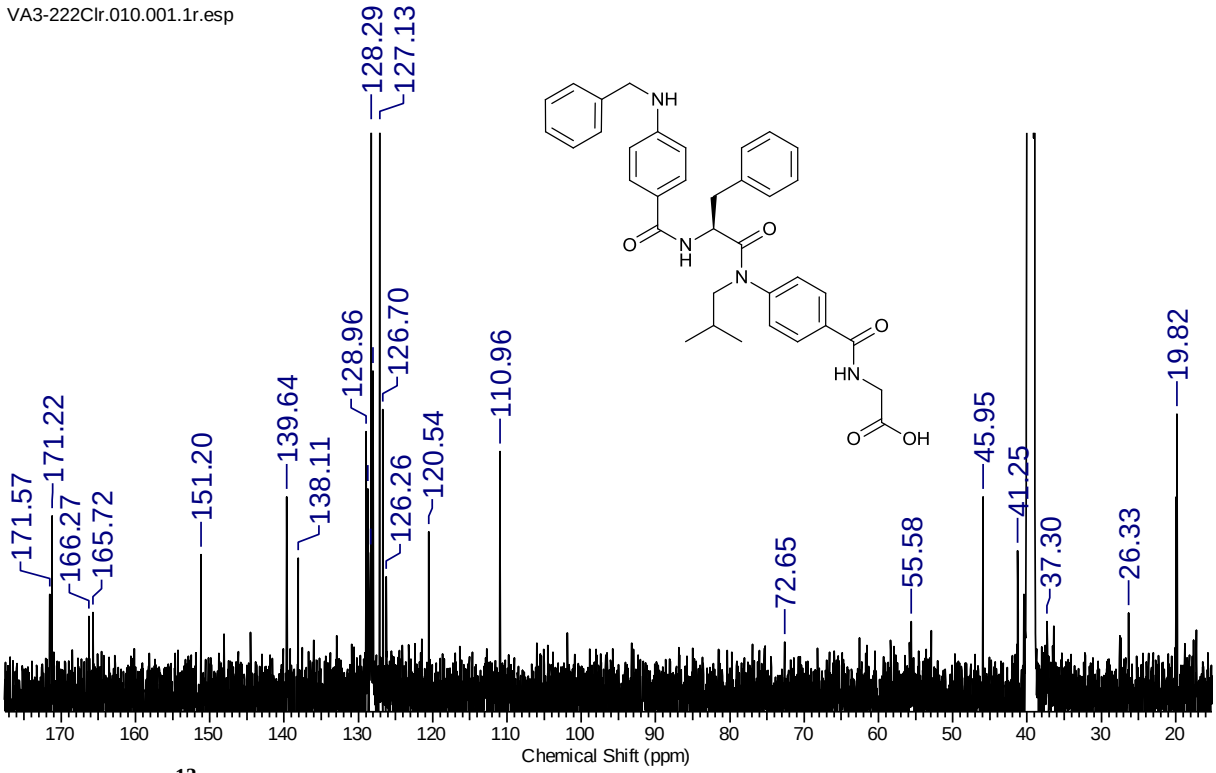

Figure S 37. ^{13}C NMR spectrum of 14 (DMSO-d$_6$, 500 MHz).

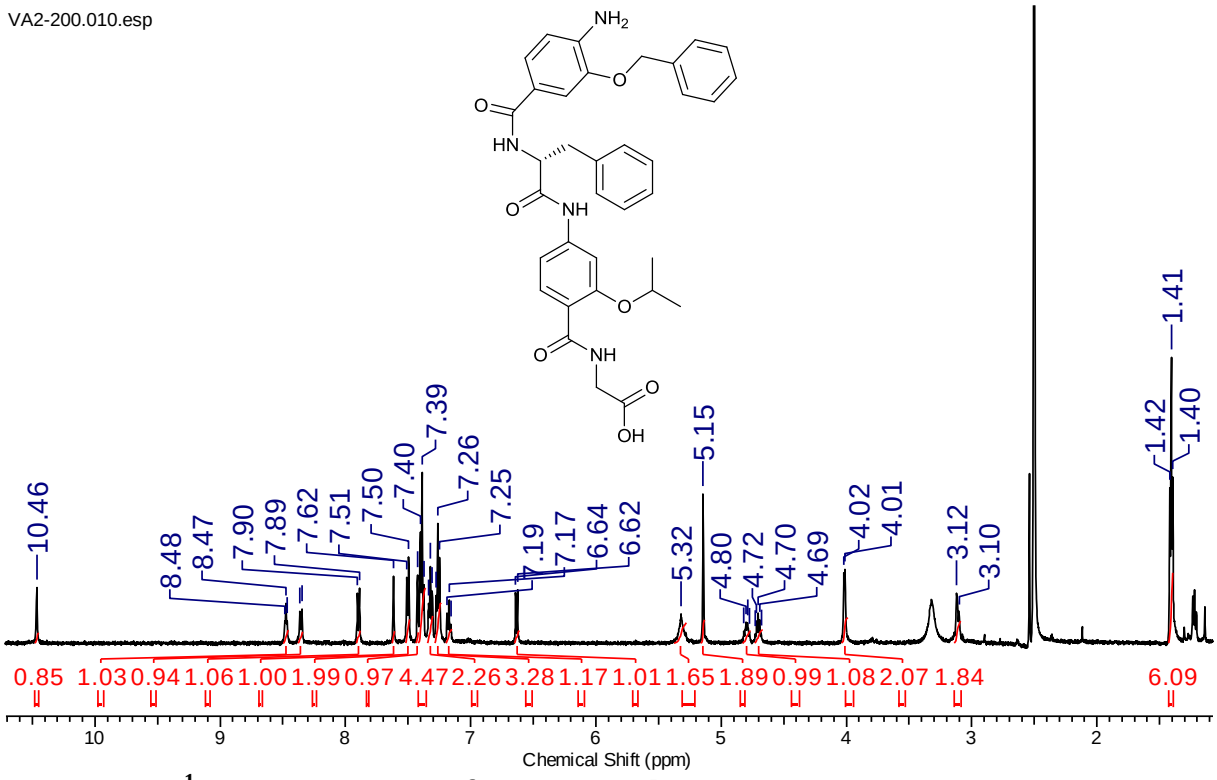

Figure S 38. ^{1}H NMR spectrum of 15 (DMSO-d$_6$, 500 MHz).

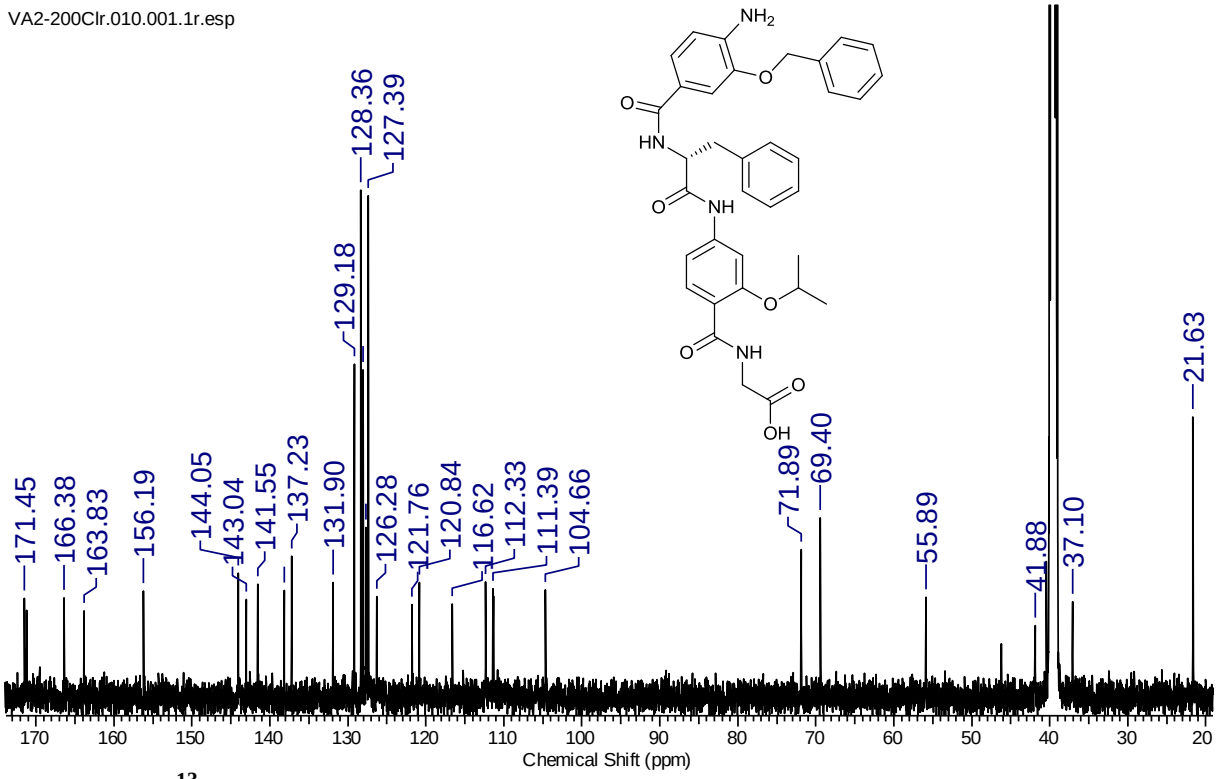

Figure S 39. ^{13}C NMR spectrum of 15 (DMSO-d$_6$, 500 MHz).

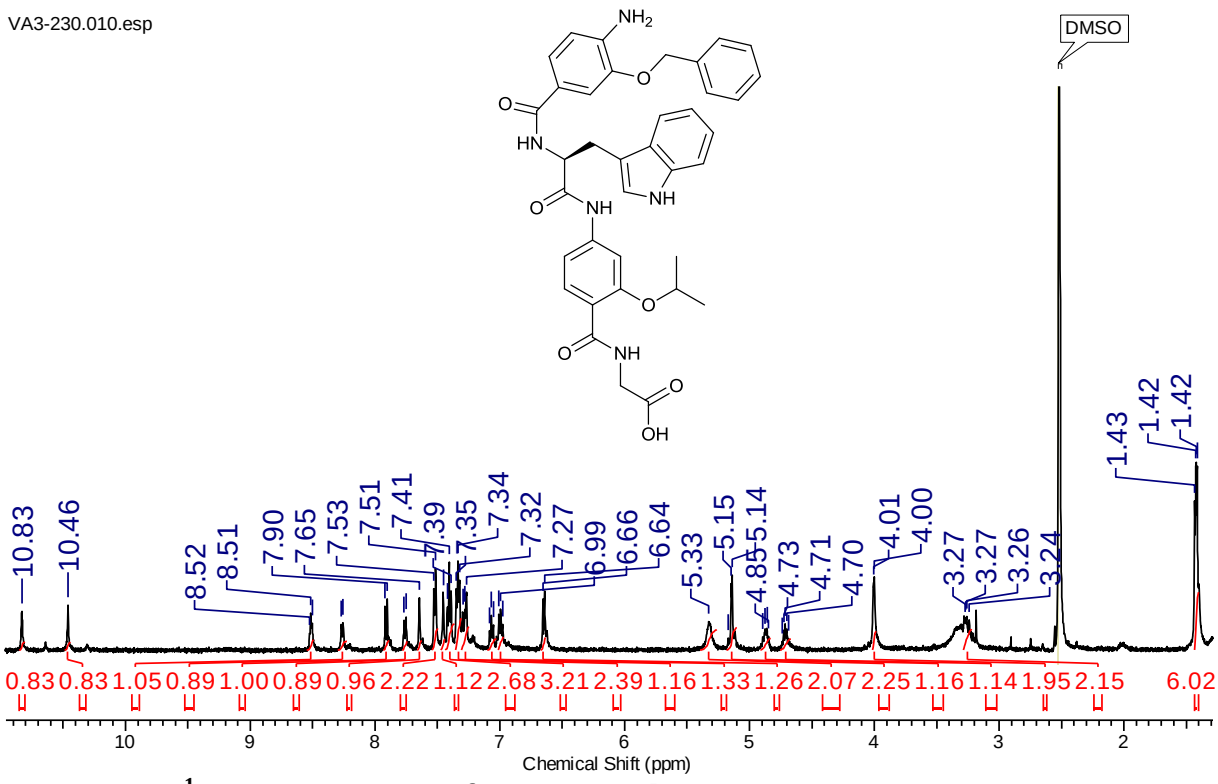

Figure S 40. ^{1}H NMR spectrum of 16 (DMSO-d$_6$, 500 MHz).

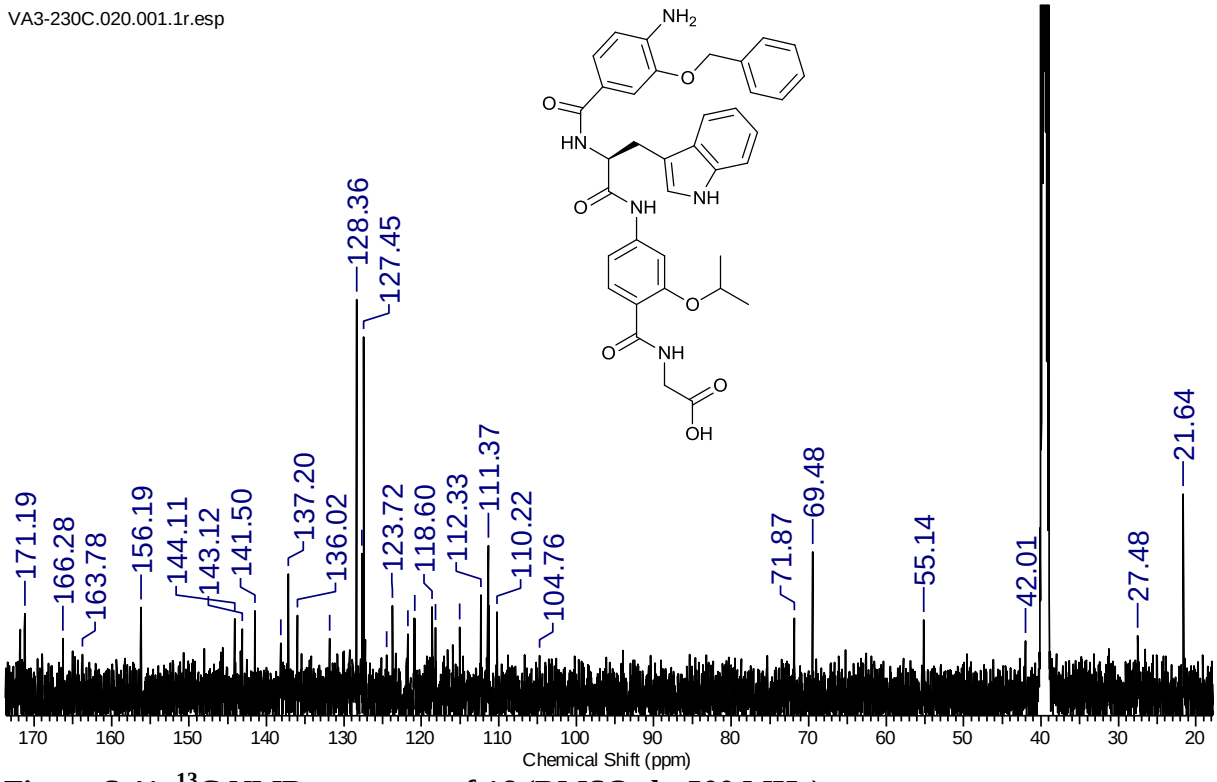

Figure S 41. ^{13}C NMR spectrum of 16 (DMSO-d$_6$, 500 MHz).

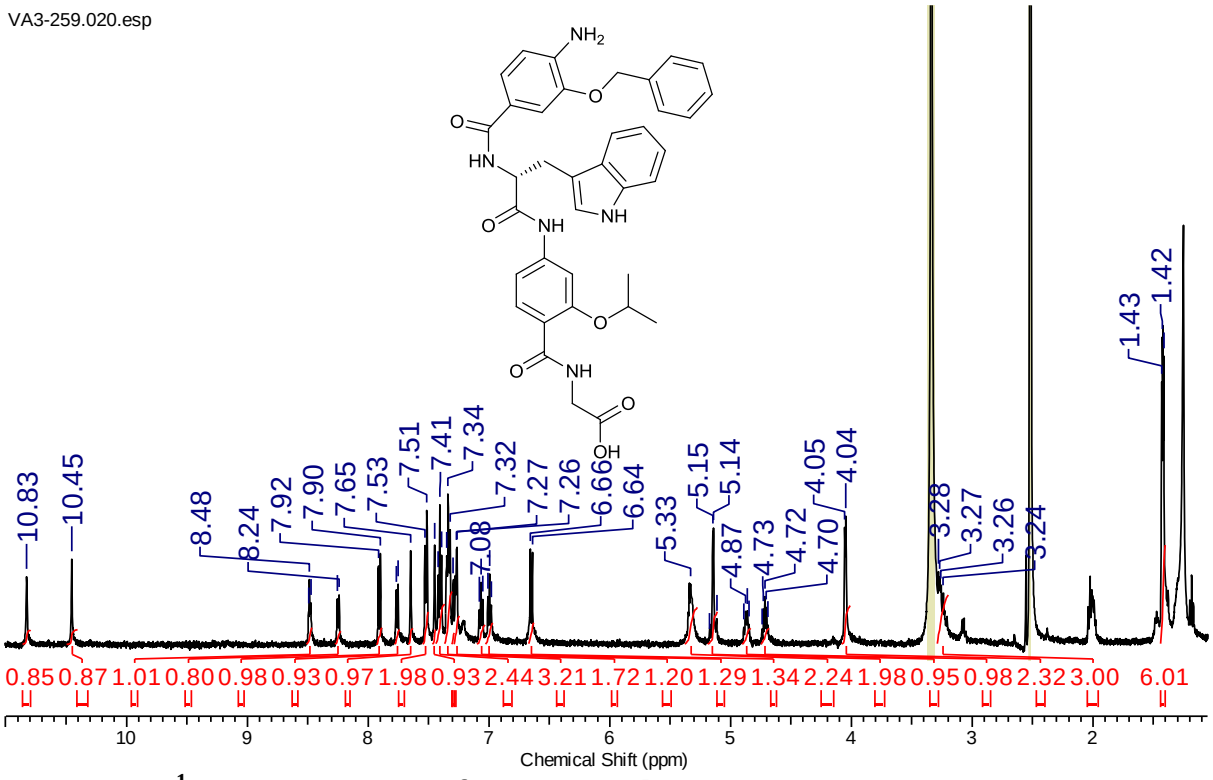

Figure S 42. ^{1}H NMR spectrum of 17 (DMSO-d$_6$, 500 MHz).

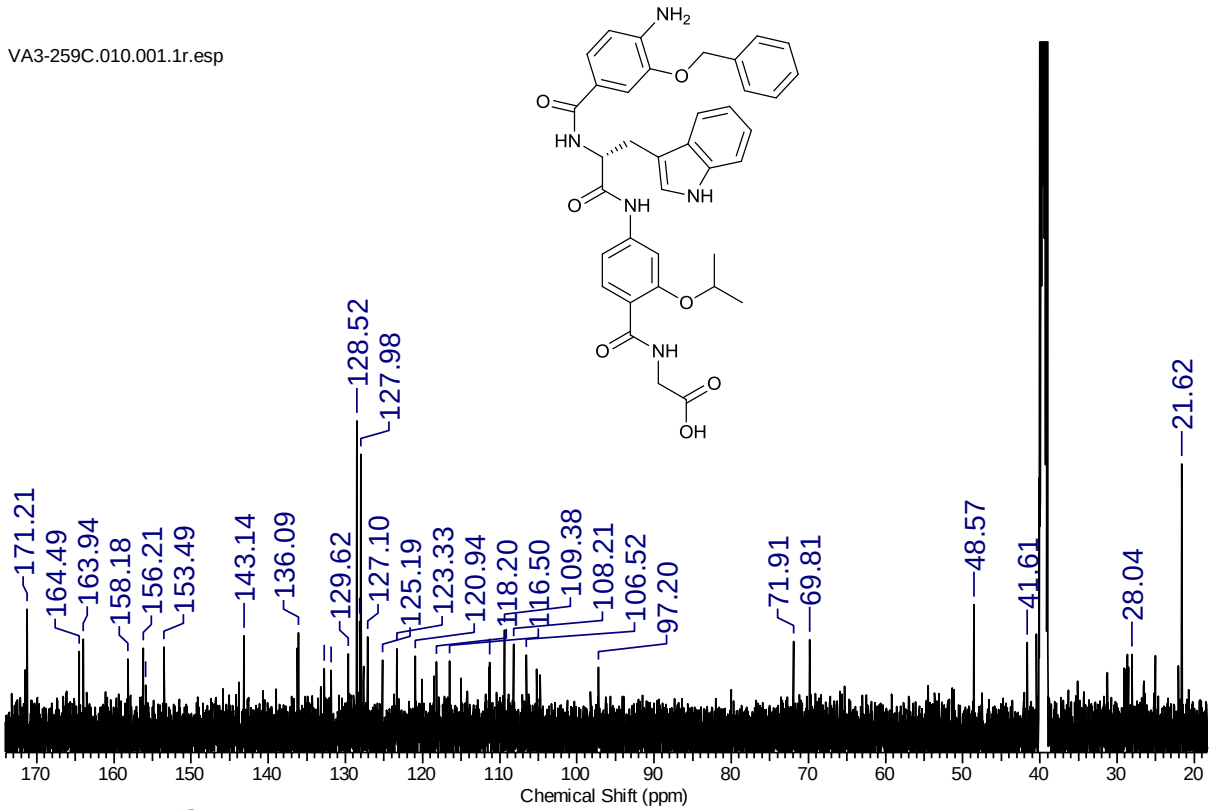

Figure S 43. ^{13}C NMR spectrum of 17 (DMSO-d$_6$, 500 MHz).

2D HMQC, HMBC, COSY and NOESY NMR Spectra

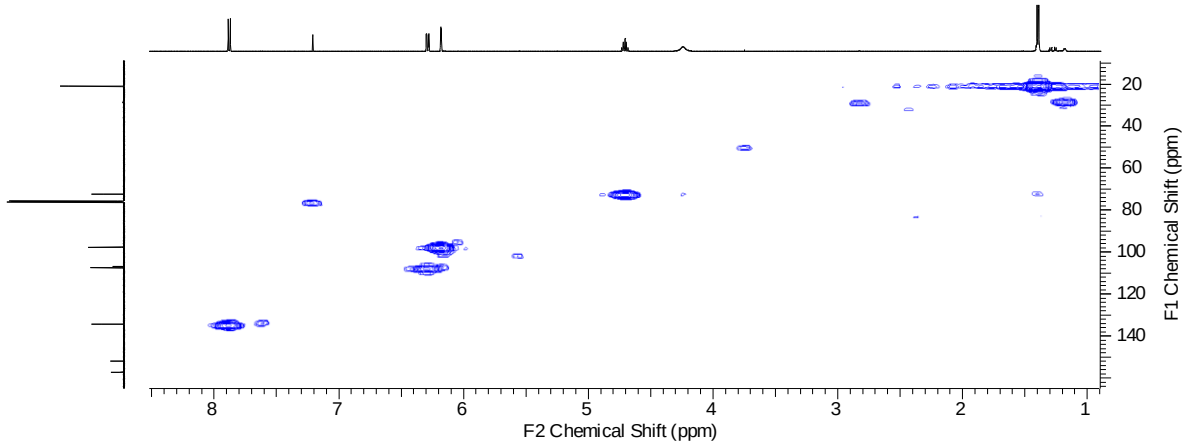

Figure S 44. HMQC spectrum of 27 ($CDCl_3$, 500 MHz).

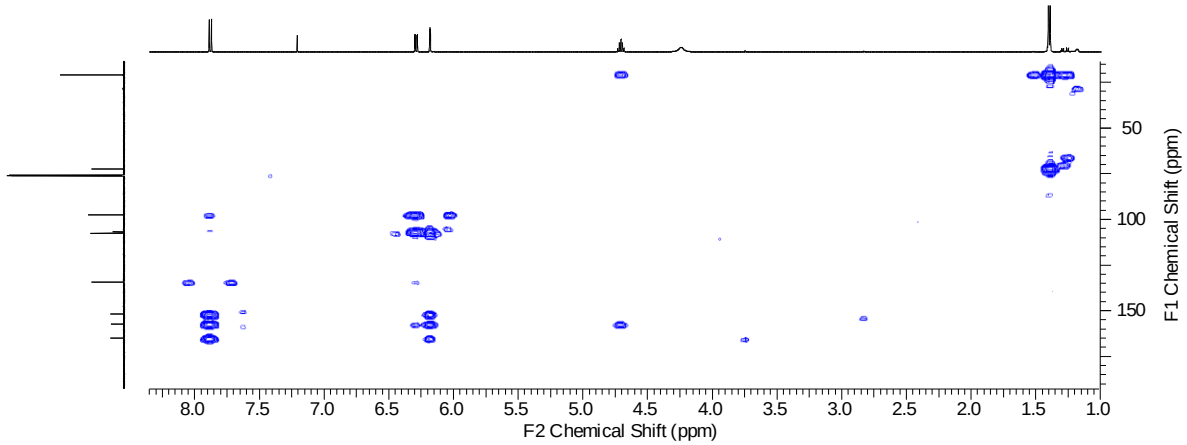

Figure S 45. HMBC spectrum of 27 ($CDCl_3$, 500 MHz).

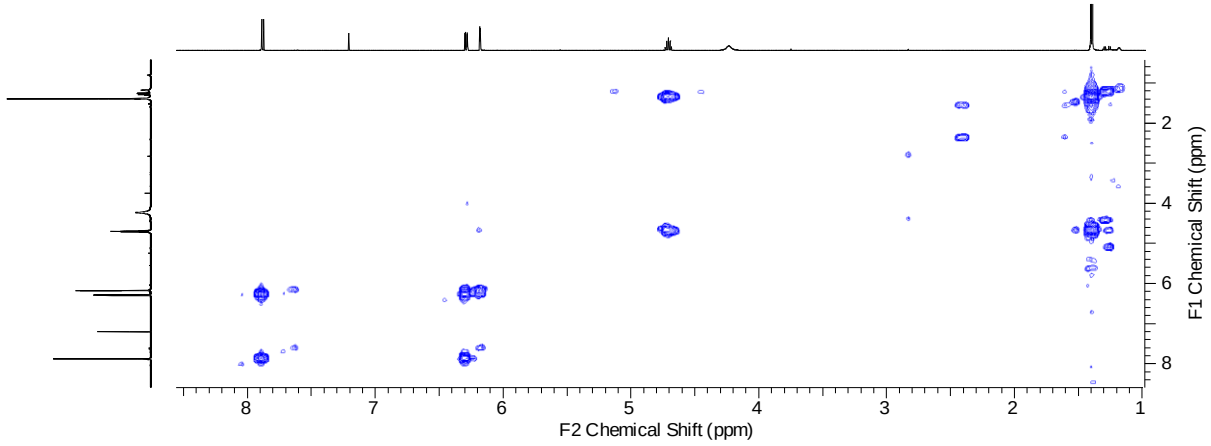

Figure S 46. COSY spectrum of 27 ($CDCl_3$, 500 MHz).

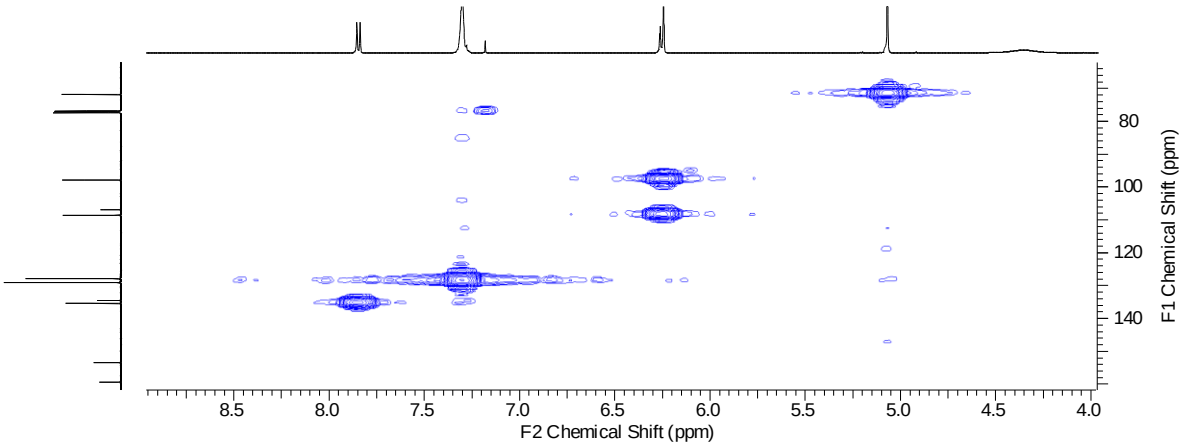

Figure S 47. HMQC spectrum of 29 ($CDCl_3$, 500 MHz).

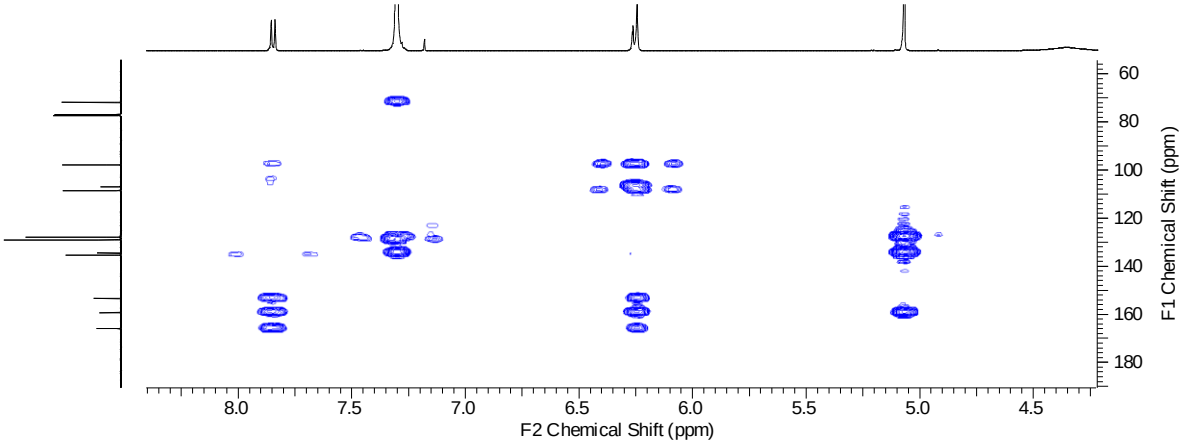

Figure S 48. HMBC spectrum of 29 ($CDCl_3$, 500 MHz).

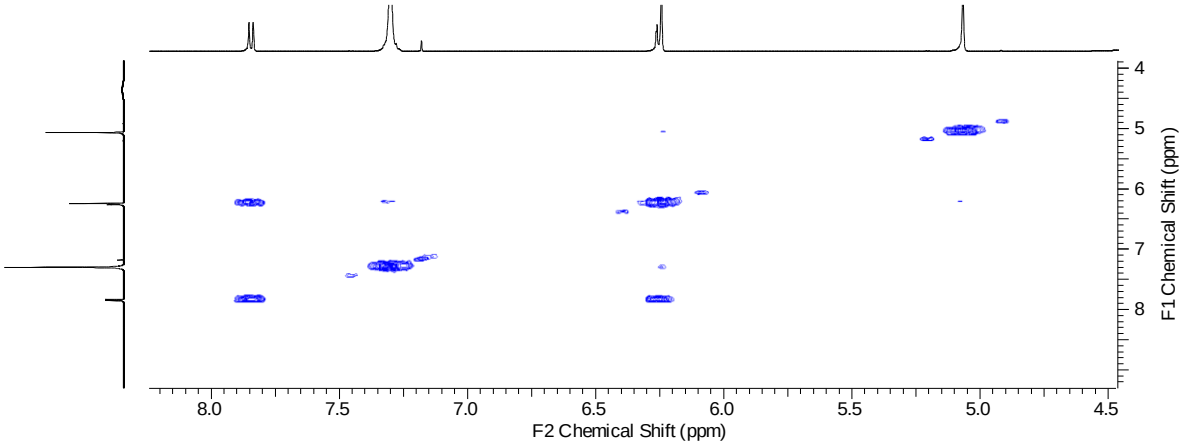

Figure S 49. COSY spectrum of 29 ($CDCl_3$, 500 MHz).

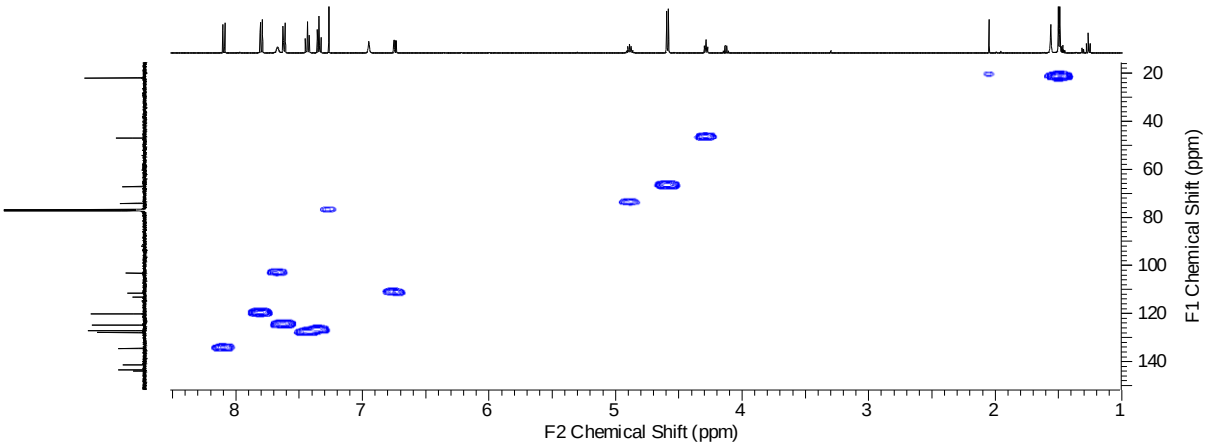

Figure S 50. HMQC spectrum of 31 ($CDCl_3$, 500 MHz).

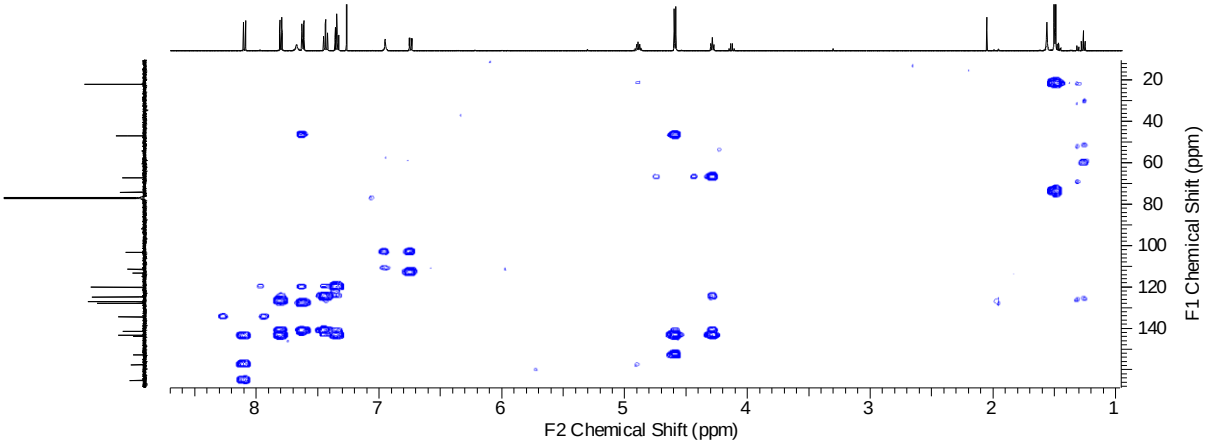

Figure S 51. HMBC spectrum of 31 ($CDCl_3$, 500 MHz).

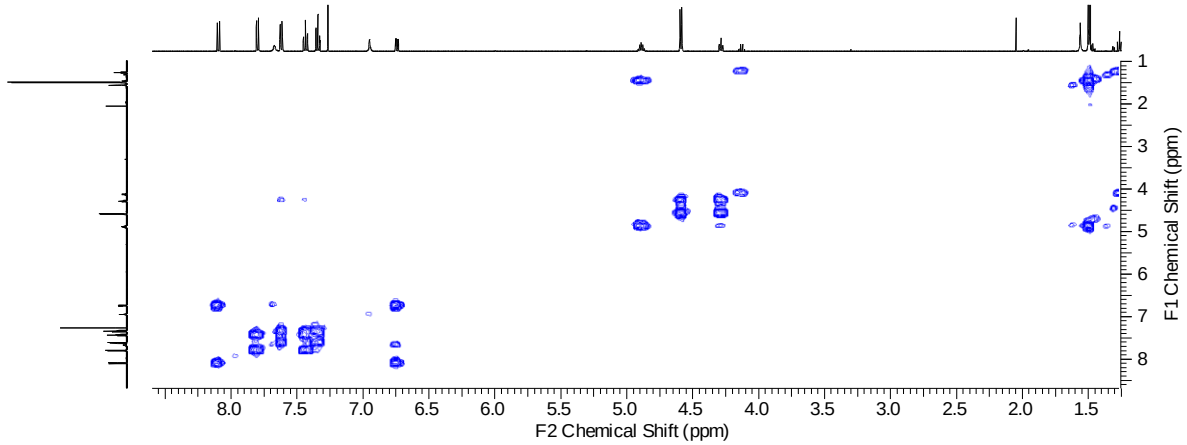

Figure S 52. COSY spectrum of 33 ($CDCl_3$, 500 MHz).

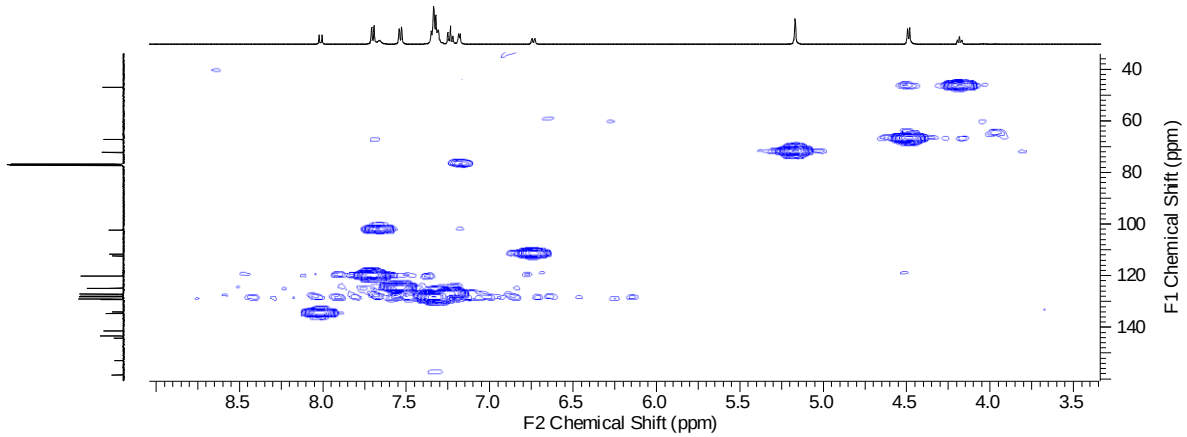

Figure S 53. HMQC spectrum of 33 ($CDCl_3$, 500 MHz).

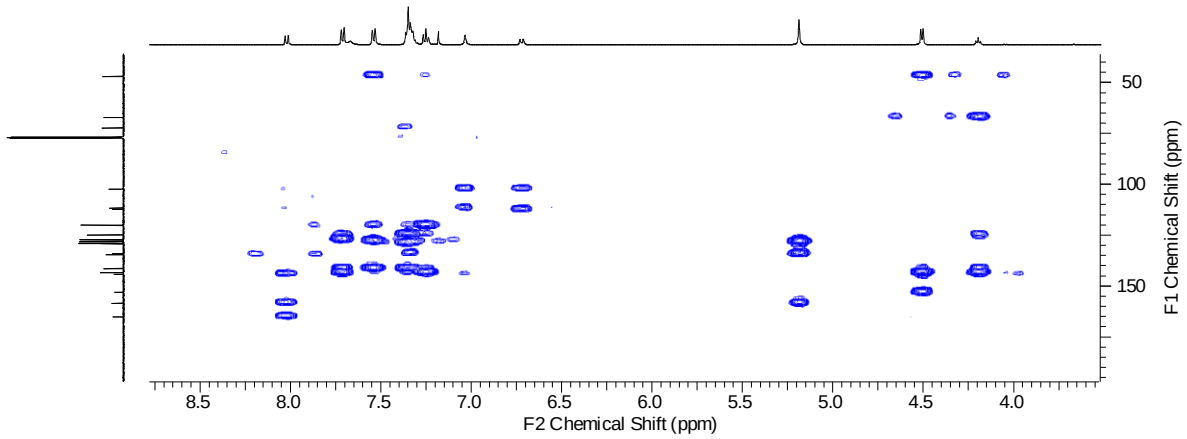

Figure S 54. HMBC spectrum of 33 ($CDCl_3$, 500 MHz).

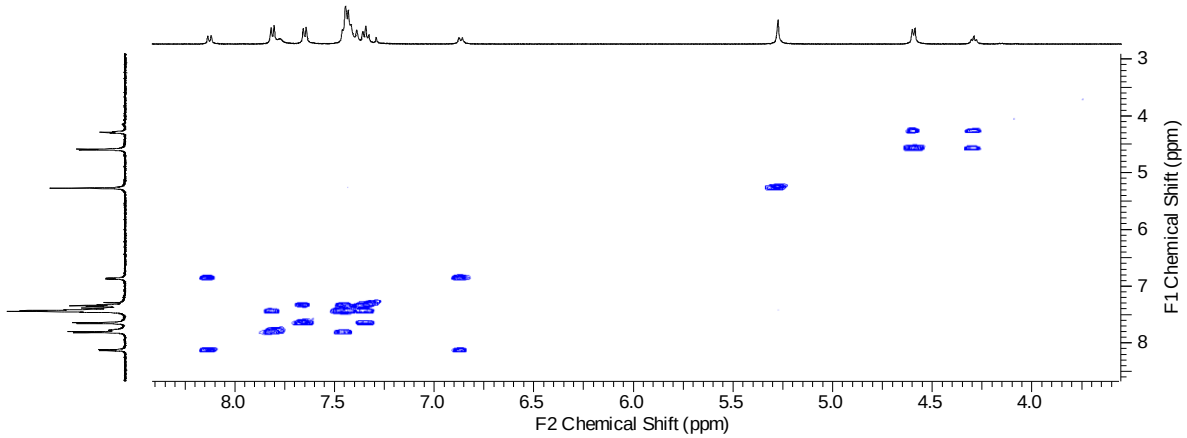

Figure S 55. COSY spectrum of 33 ($CDCl_3$, 500 MHz).

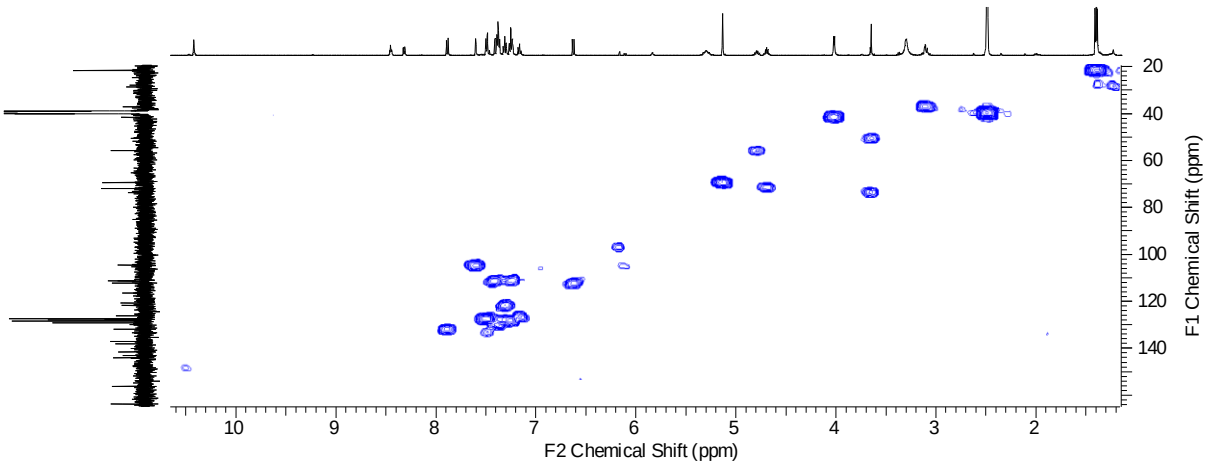

Figure S 56. HMQC spectrum of 1 (DMSO-d_6, 500 MHz).

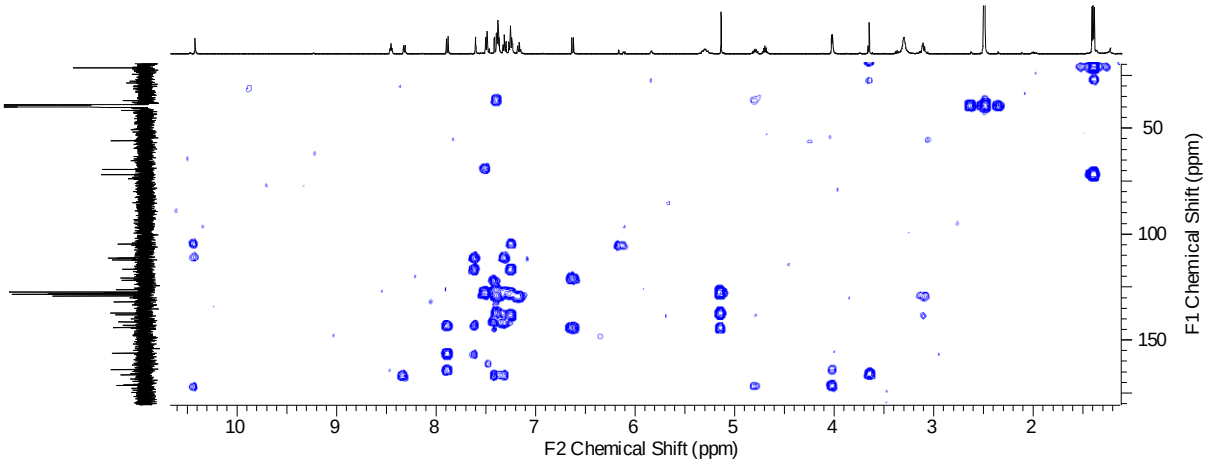

Figure S 57. HMBC spectrum of 1 (DMSO-d_6, 500 MHz).

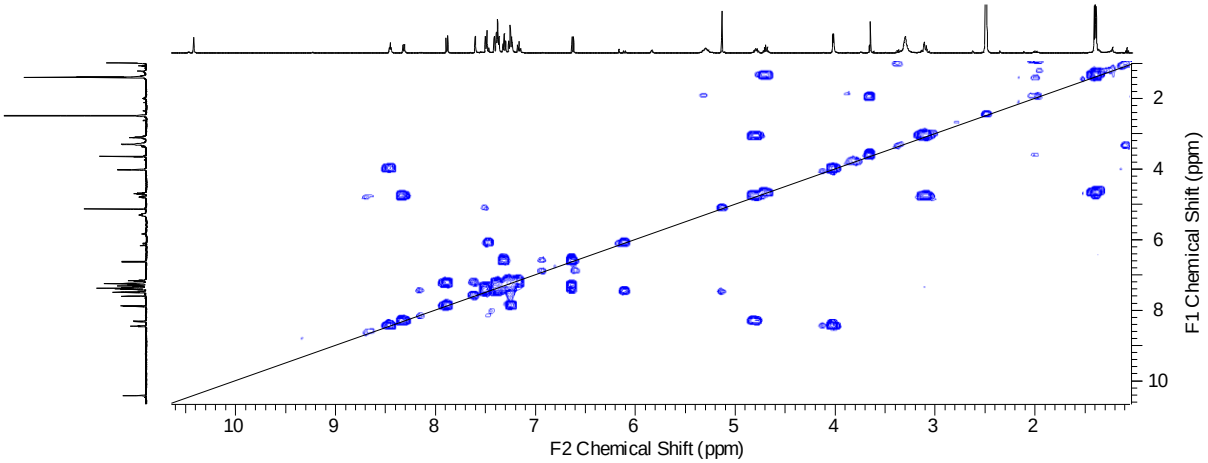

Figure S 58. COSY spectrum of 1 (DMSO-d_6, 500 MHz).

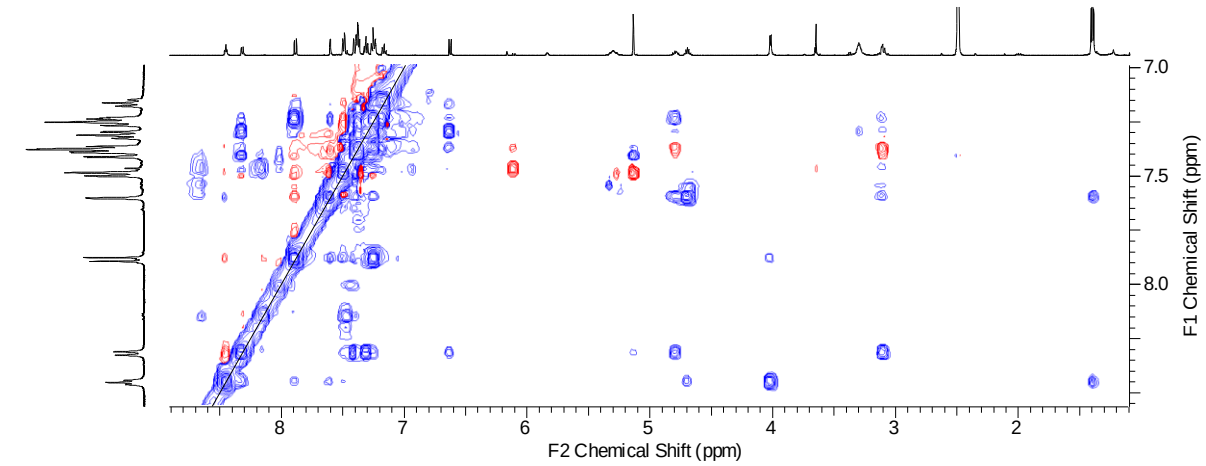

Figure S 59. Partial NOESY spectrum of 1 (DMSO-d_6, 500 MHz).

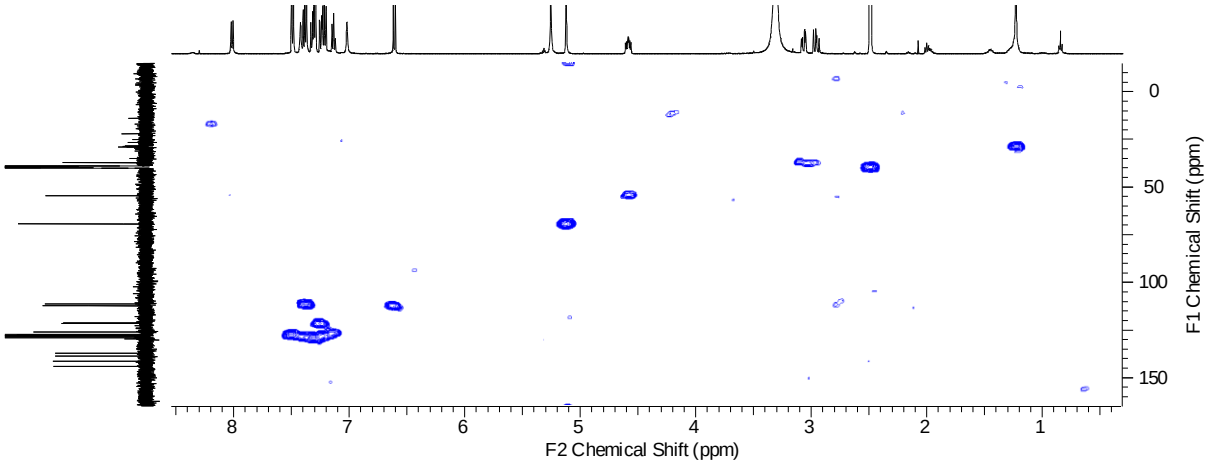

Figure S 60. HMQC spectrum of 2 (DMSO-d_6, 500 MHz).

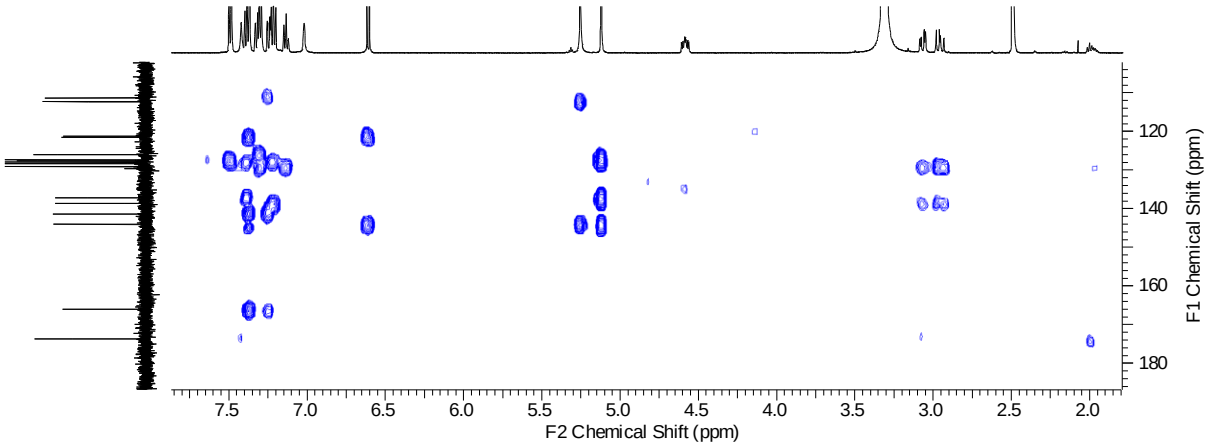

Figure S 61. HMBC spectrum of 2 (DMSO-d_6, 500 MHz).

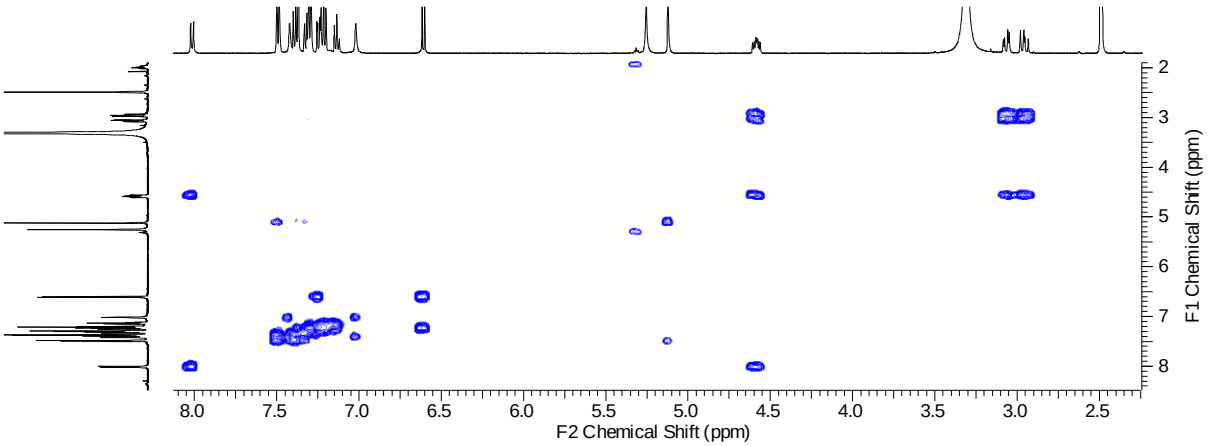

Figure S 62. COSY spectrum of 2 (DMSO-d_6, 500 MHz).

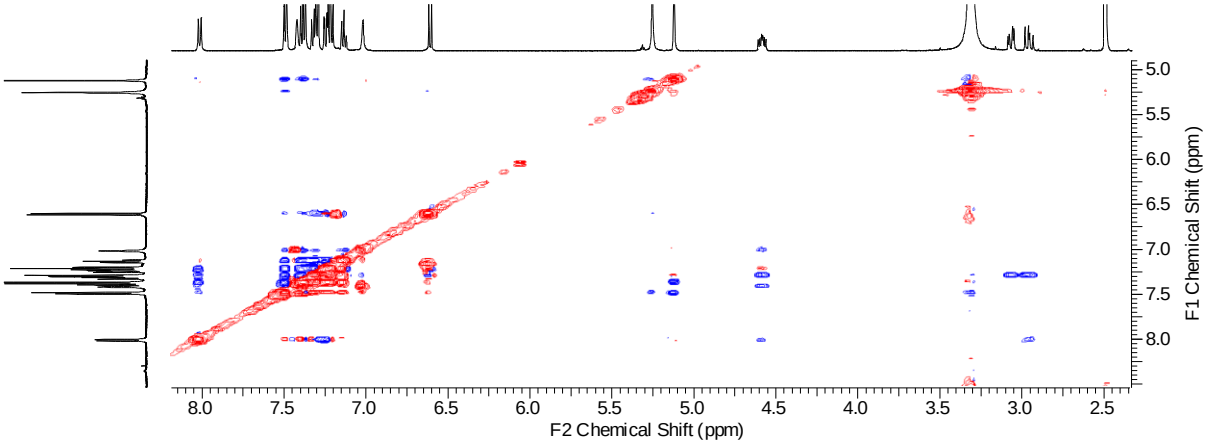

Figure S 63. Partial NOESY spectrum of 2 (DMSO-d_6, 500 MHz).

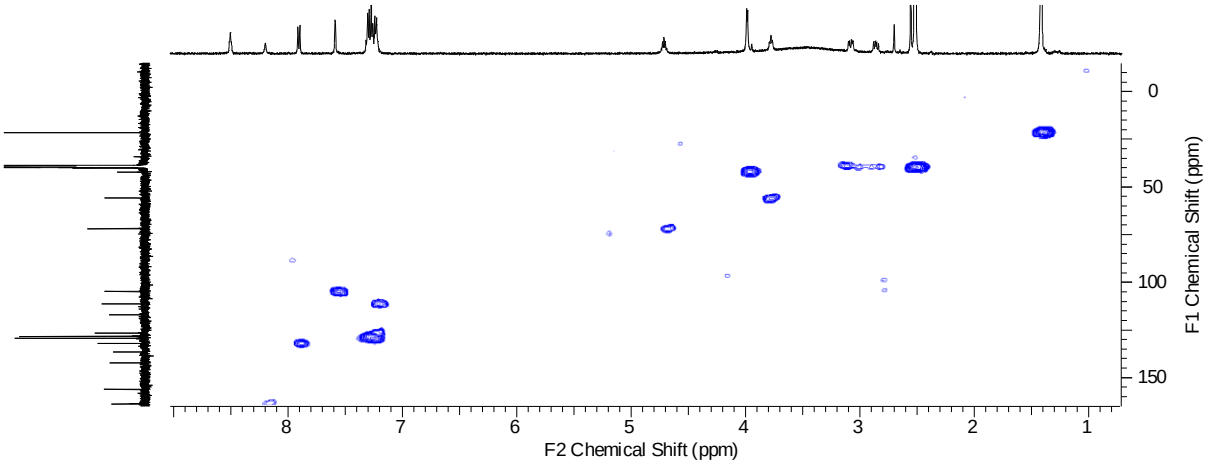

Figure S 64. HMQC spectrum of 3 (DMSO-d_6, 500 MHz).

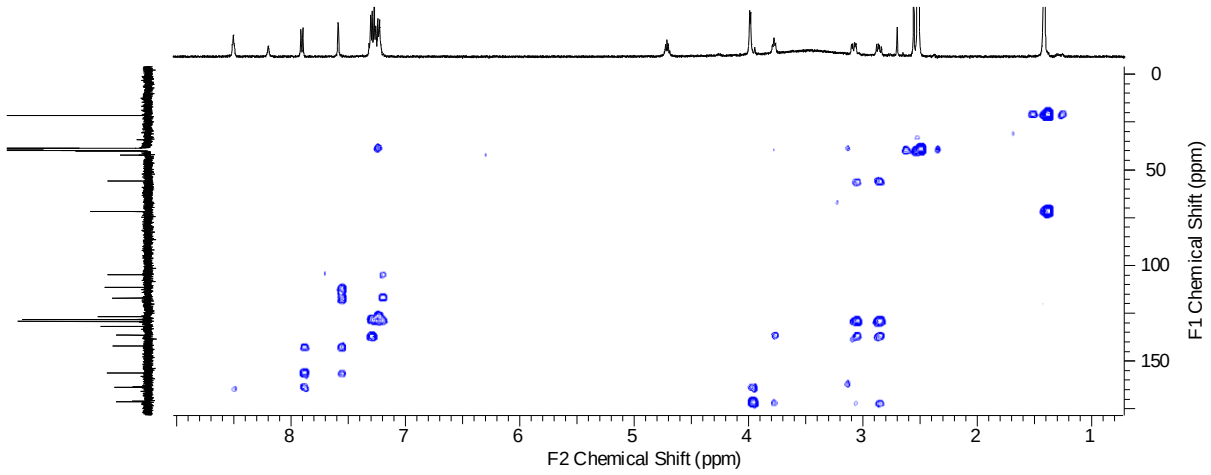

Figure S 65. HMBC spectrum of 3 (DMSO-d_6, 500 MHz).

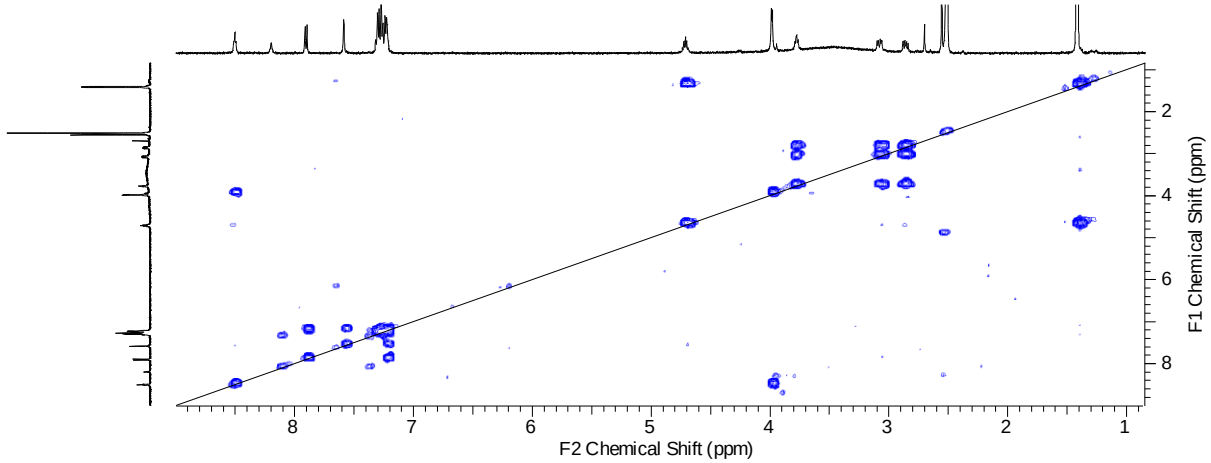

Figure S 66. COSY spectrum of 3 (DMSO-d_6, 500 MHz).

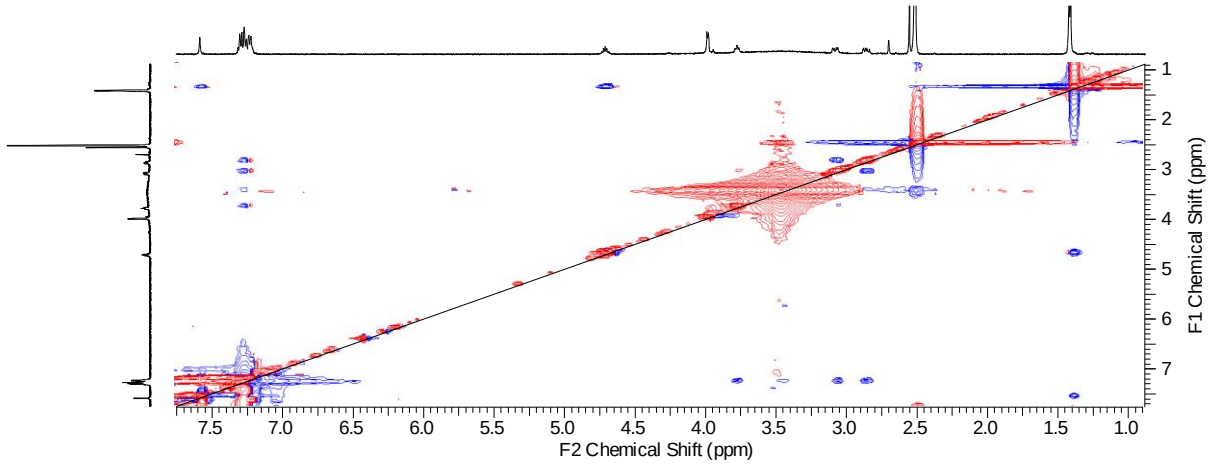

Figure S 67. Partial NOESY spectrum of 3 (DMSO-d_6, 500 MHz).

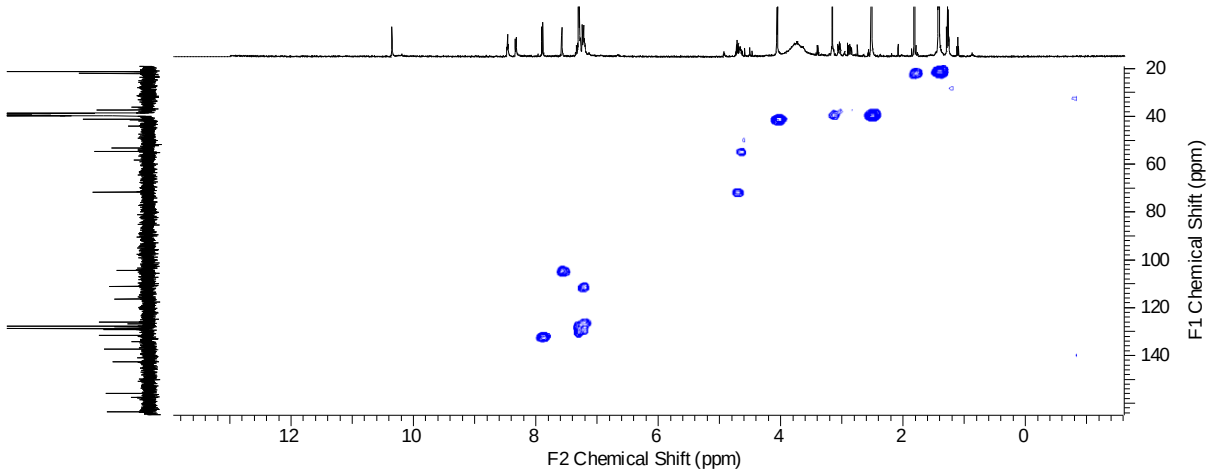

Figure S 68. HMQC spectrum of 4 (DMSO-d_6, 500 MHz).

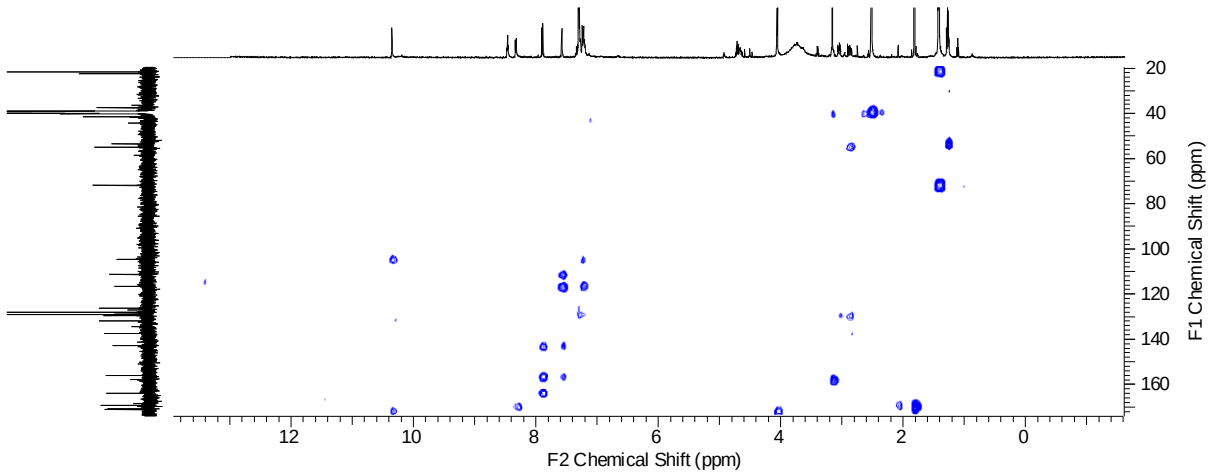

Figure S 69. HMBC spectrum of 4 (DMSO-d_6, 500 MHz).

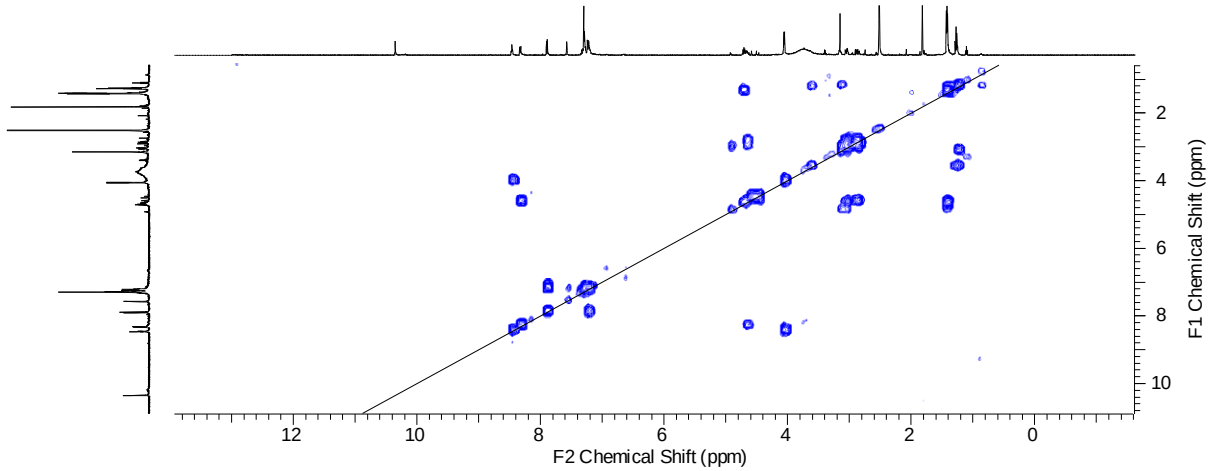

Figure S 70. COSY spectrum of 4 (DMSO-d_6, 500 MHz).

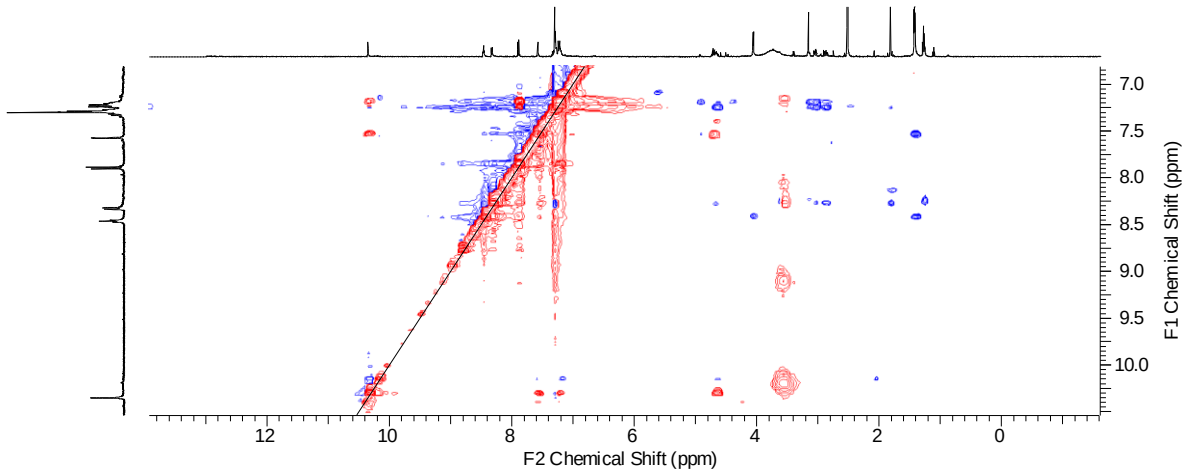

Figure S 71. Partial NOESY spectrum of 4 (DMSO-d_6, 500 MHz).

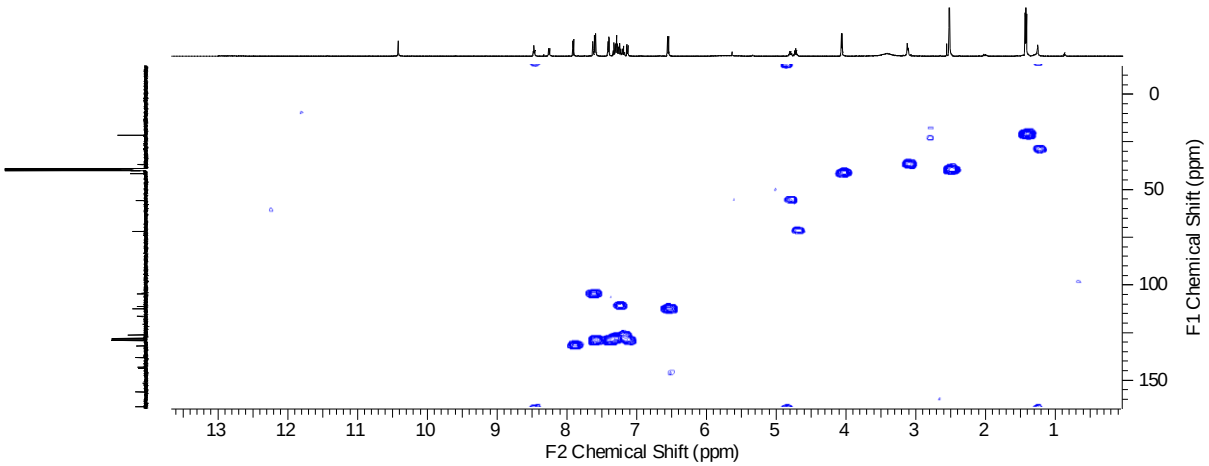

Figure S 72. HMQC spectrum of 5 (DMSO-d_6, 500 MHz).

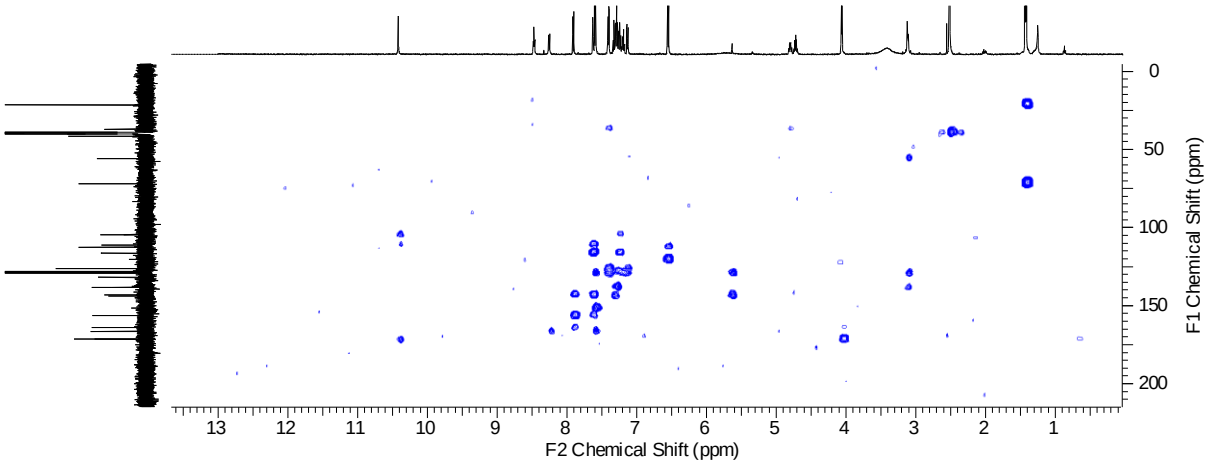

Figure S 73. HMBC spectrum of 5 (DMSO-d_6, 500 MHz).

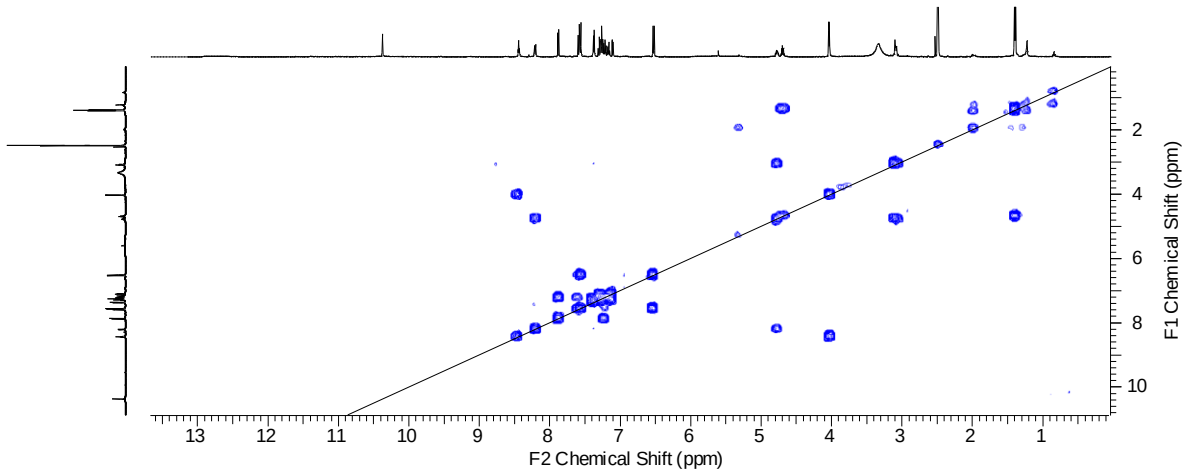

Figure S 74. COSY spectrum of 5 (DMSO-d_6, 500 MHz).

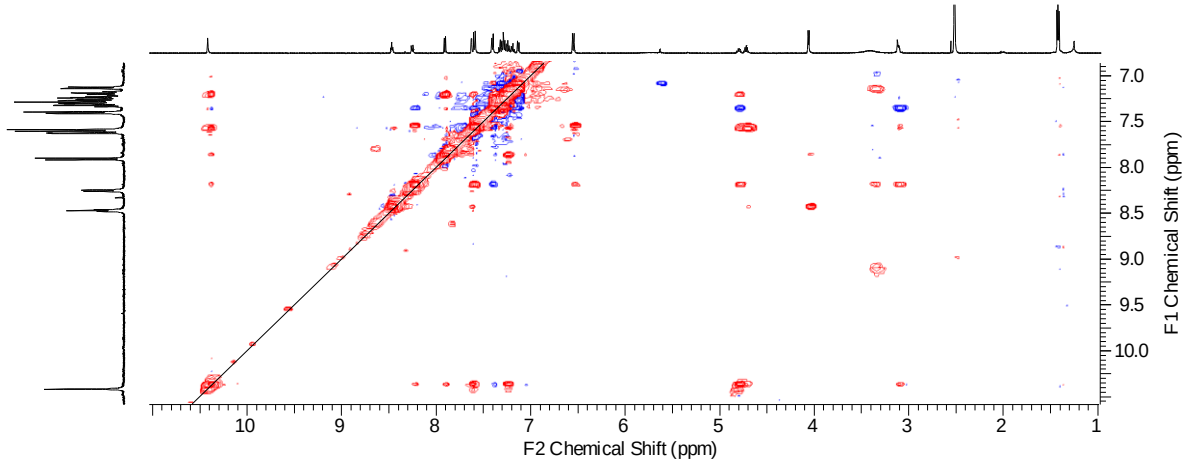

Figure S 75. Partial NOESY spectrum of 5 (DMSO-d_6, 500 MHz).

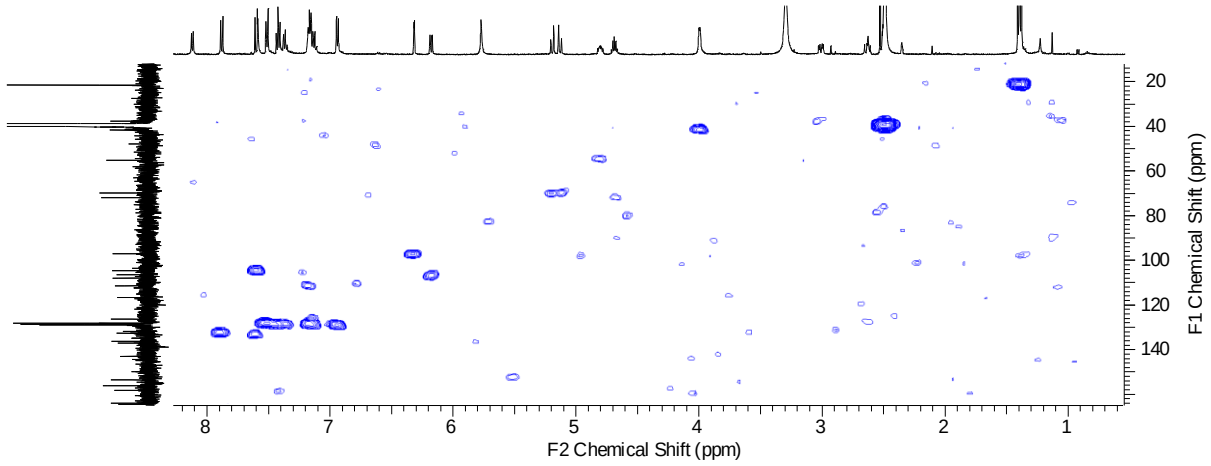

Figure S 76. HMQC spectrum of 6 (DMSO-d_6, 500 MHz).

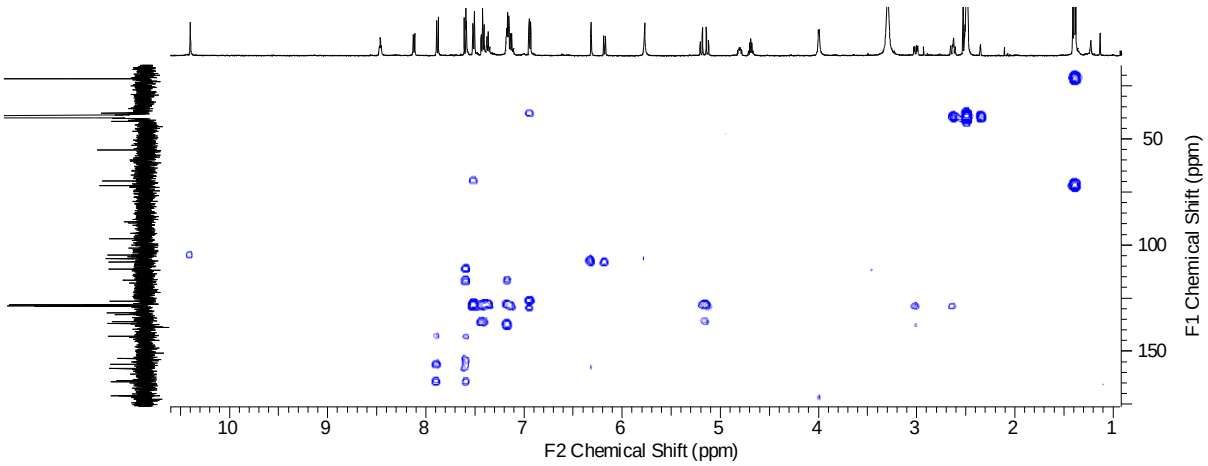

Figure S 77. HMBC spectrum of 6 (DMSO-d_6, 500 MHz).

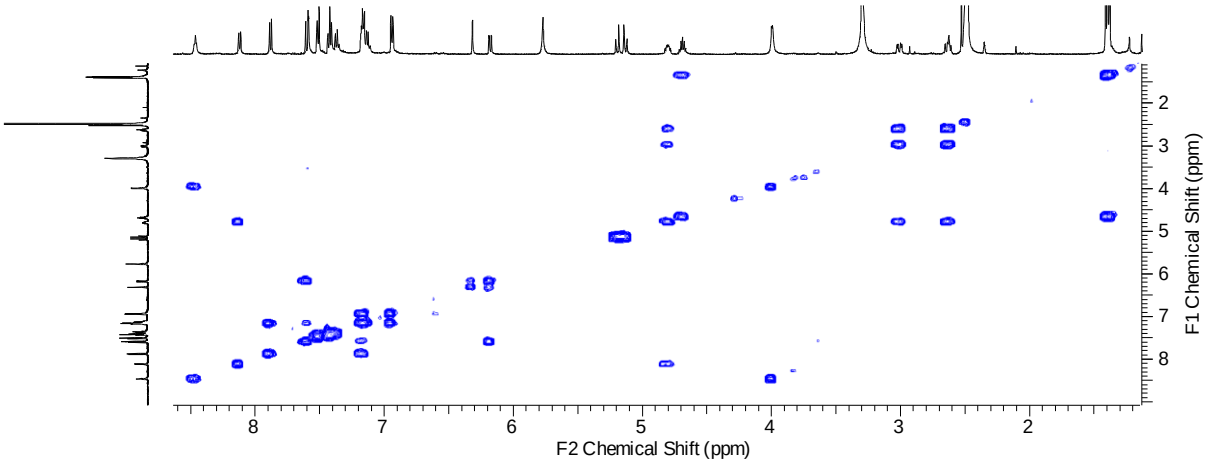

Figure S 78. COSY spectrum of 6 (DMSO-d_6, 500 MHz).

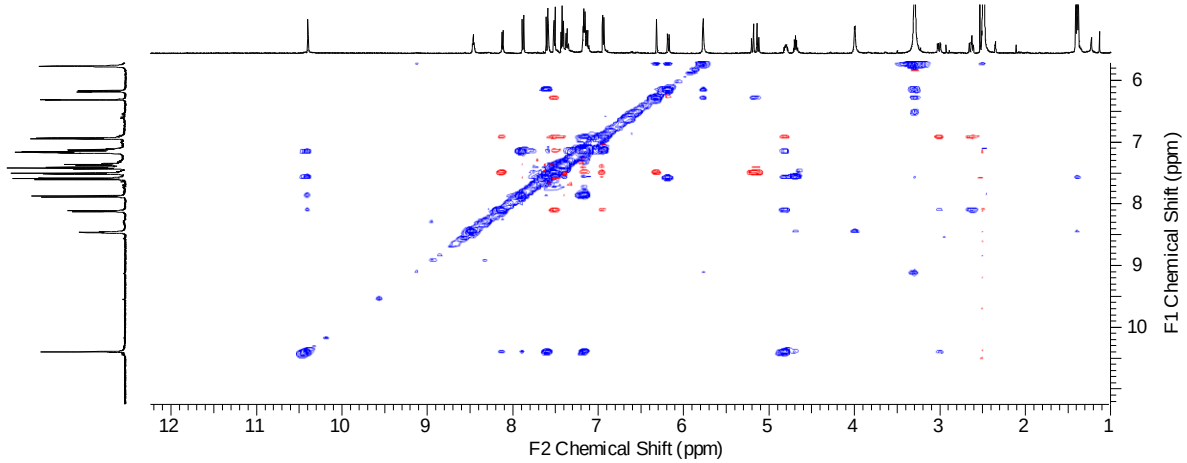

Figure S 79. Partial NOESY spectrum of 6 (DMSO-d_6, 500 MHz).

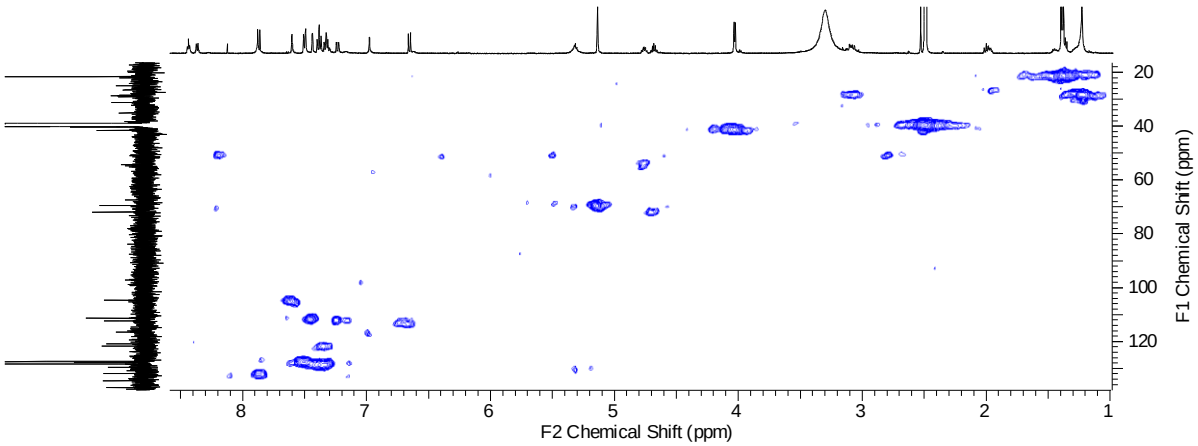

Figure S 80. HMQC spectrum of 7 (DMSO-d_6, 500 MHz).

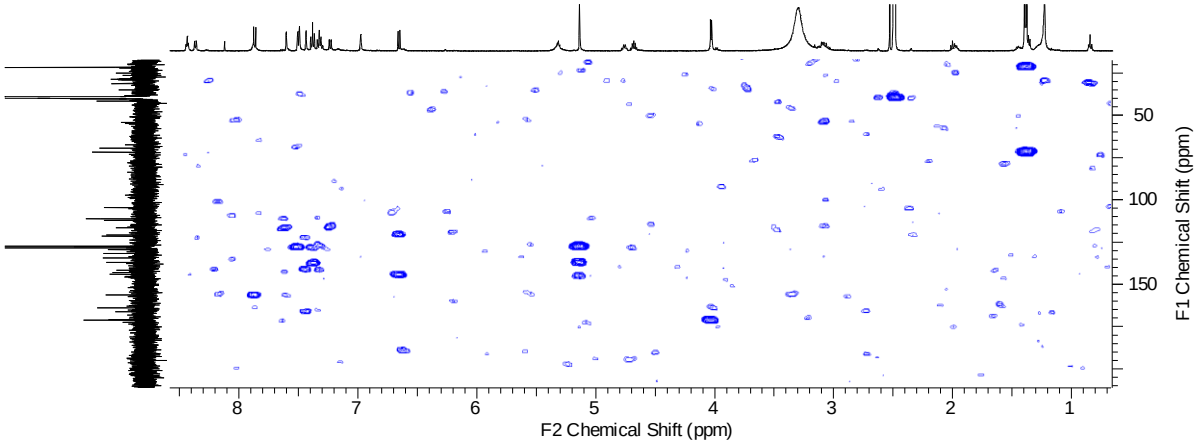

Figure S 81. HMBC spectrum of 7 (DMSO-d_6, 500 MHz).

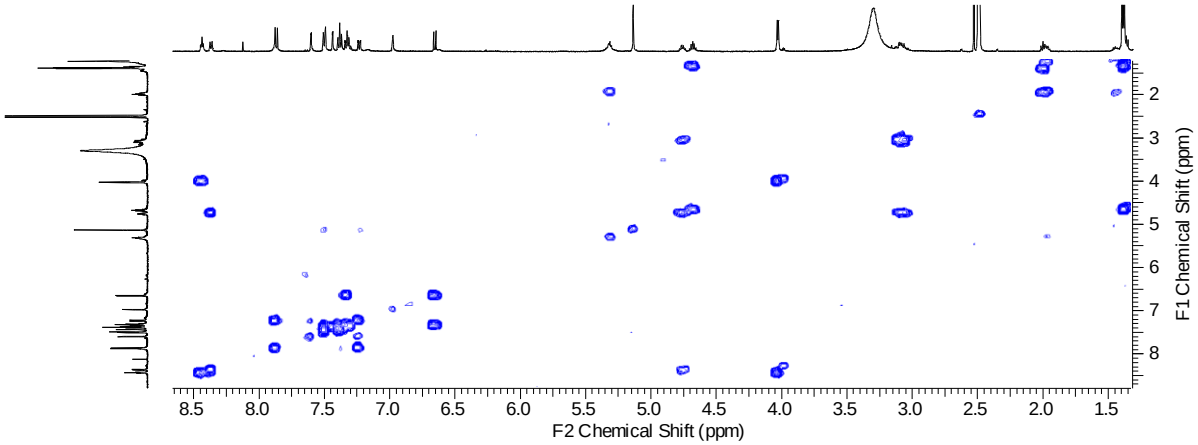

Figure S 82. COSY spectrum of 7 (DMSO-d_6, 500 MHz).

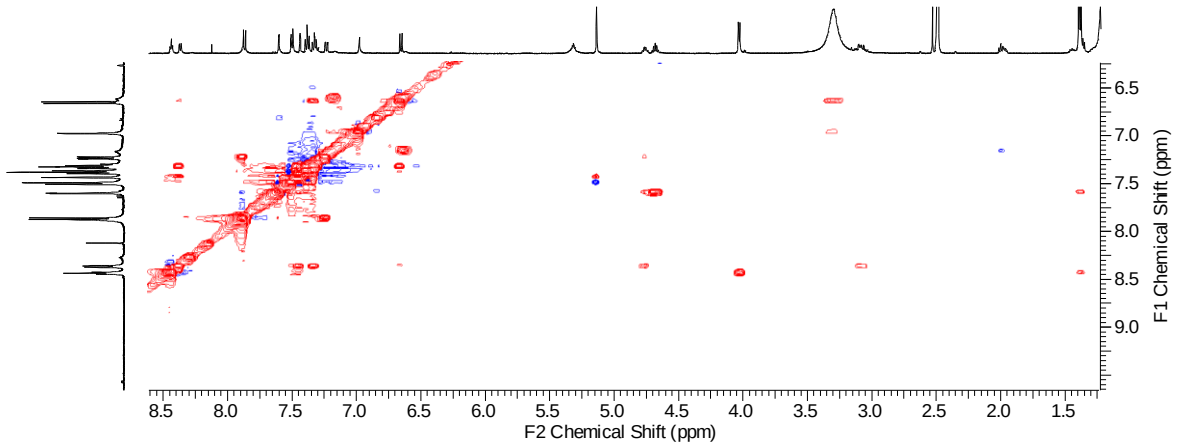

Figure S 83. Partial NOESY spectrum of 7 (DMSO-d_6, 500 MHz).

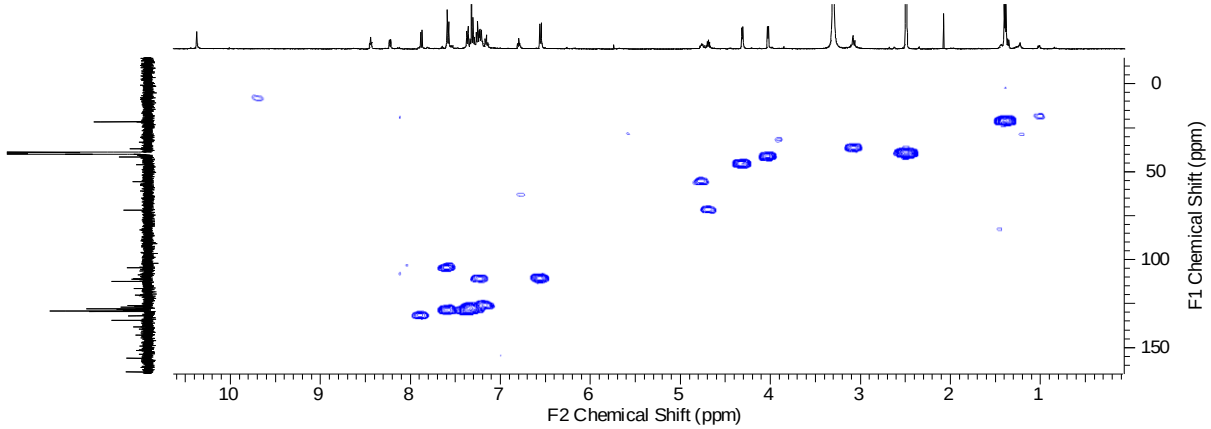

Figure S 84. HMQC spectrum of 8 (DMSO-d_6, 500 MHz).

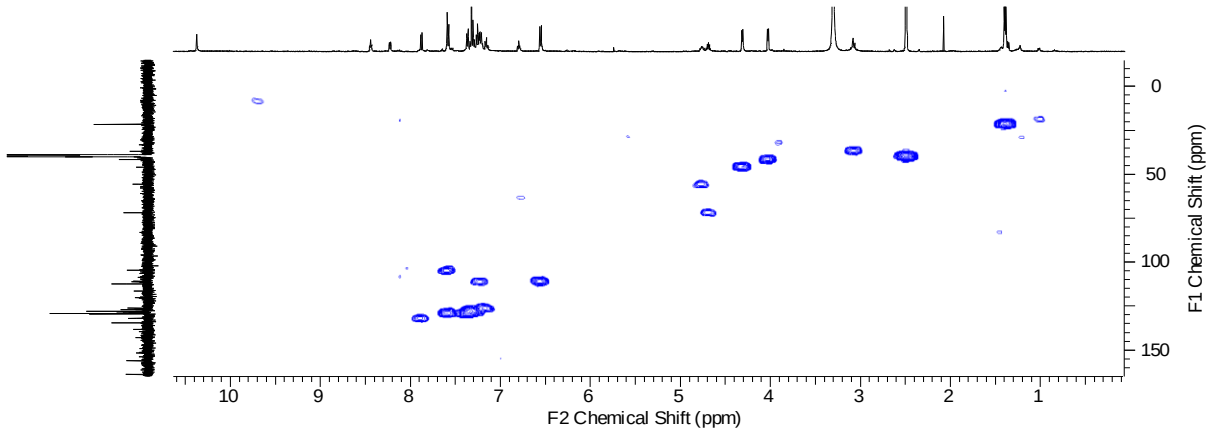

Figure S 85. HMBC spectrum of 8 (DMSO-d_6, 500 MHz).

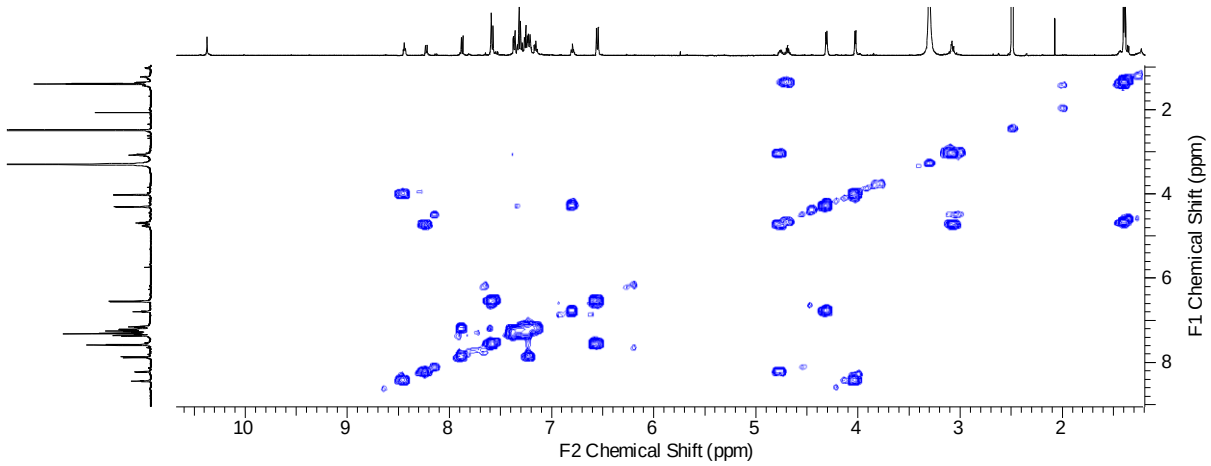

Figure S 86. COSY spectrum of 8 (DMSO-d_6, 500 MHz).

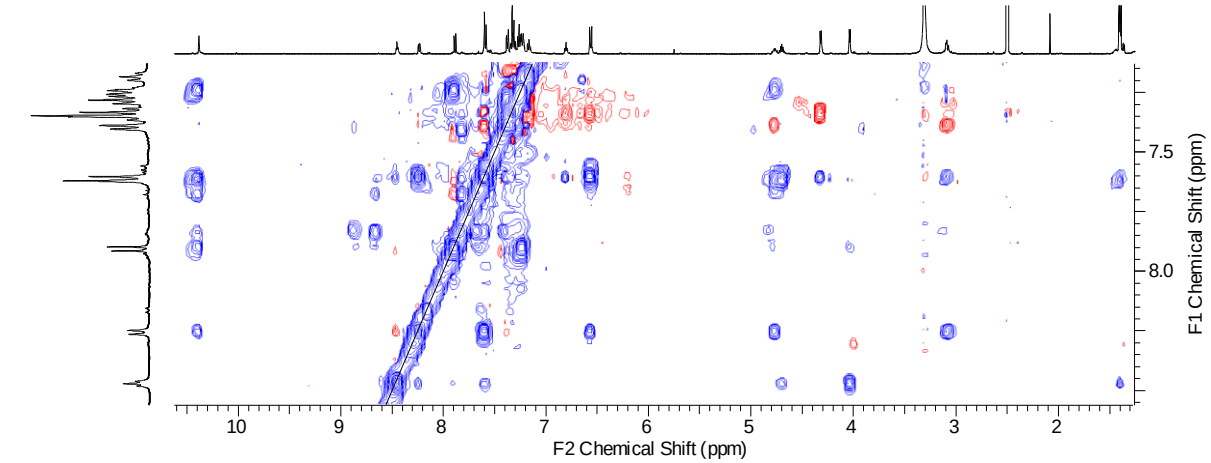

Figure S 87. Partial NOESY spectrum of 8 (DMSO-d_6, 500 MHz).

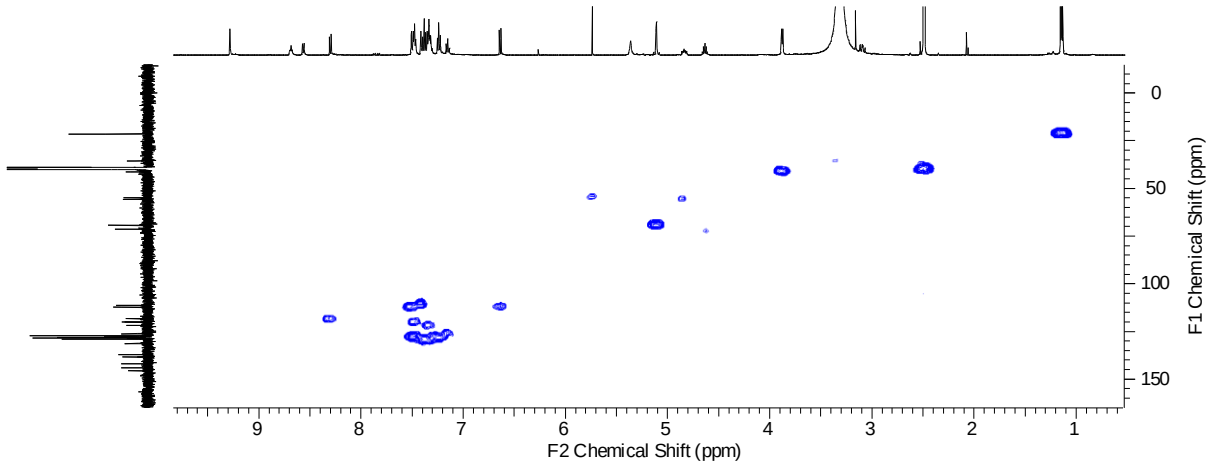

Figure S 88. HMQC spectrum of 9 (DMSO-d_6, 500 MHz).

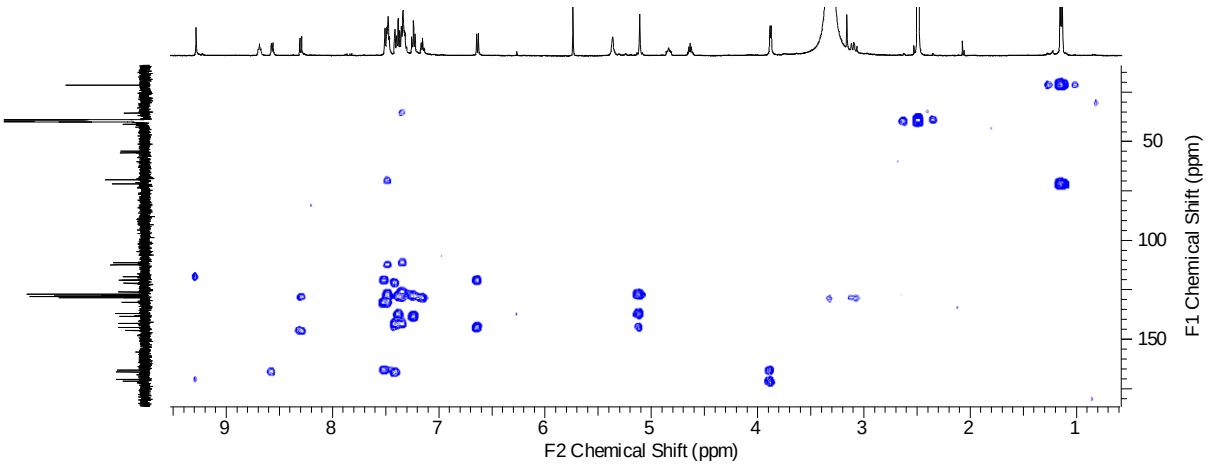

Figure S 89. HMBC spectrum of 9 (DMSO-d_6, 500 MHz).

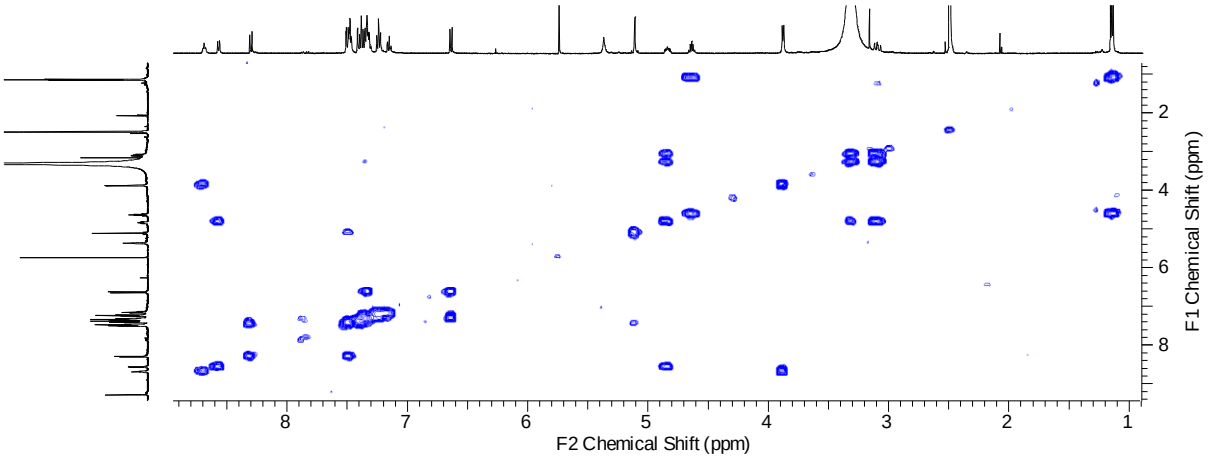

Figure S 90. COSY spectrum of 9 (DMSO-d_6, 500 MHz).

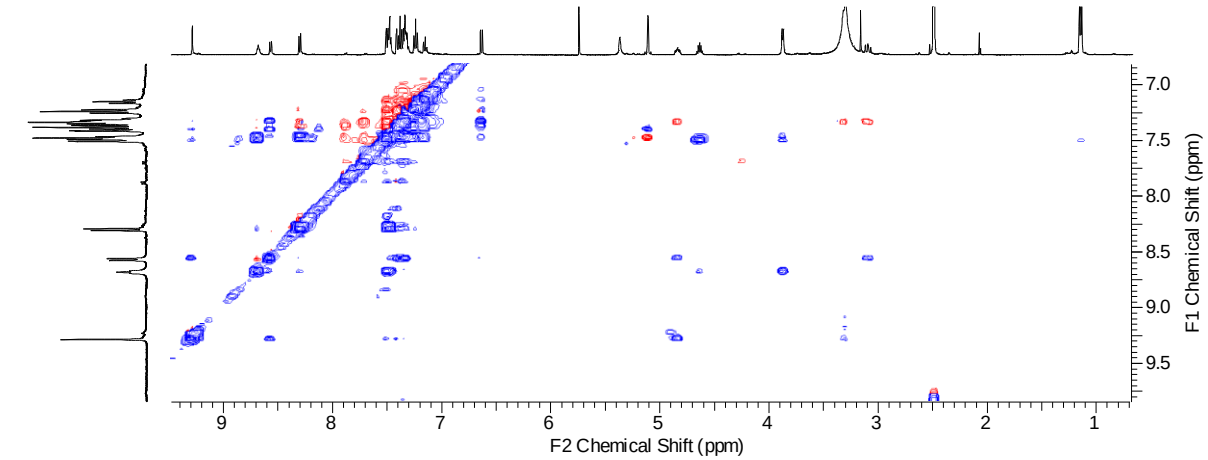

Figure S 91. Partial NOESY spectrum of 9 (DMSO-d_6, 500 MHz).

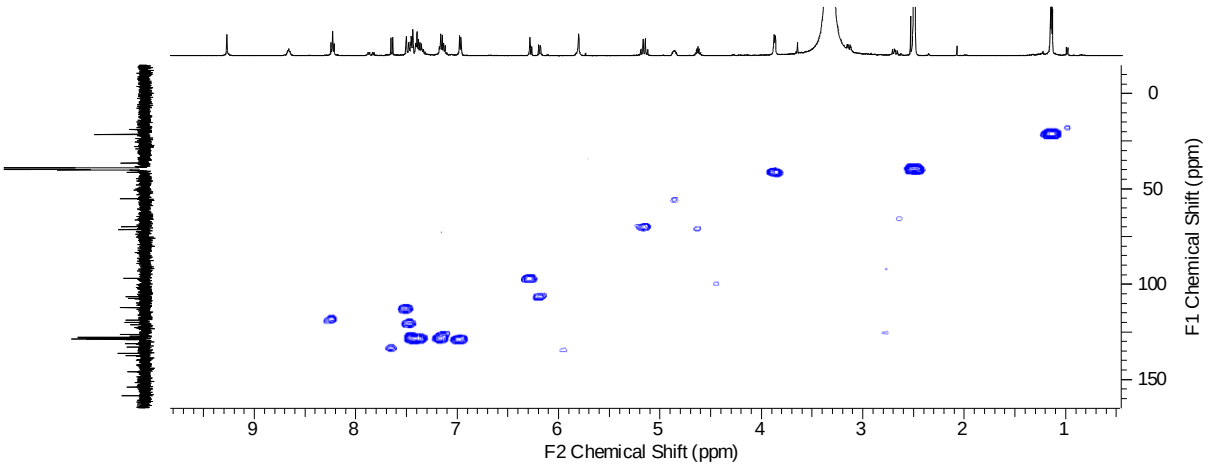

Figure S 92. HMQC spectrum of 10 (DMSO-d_6, 500 MHz).

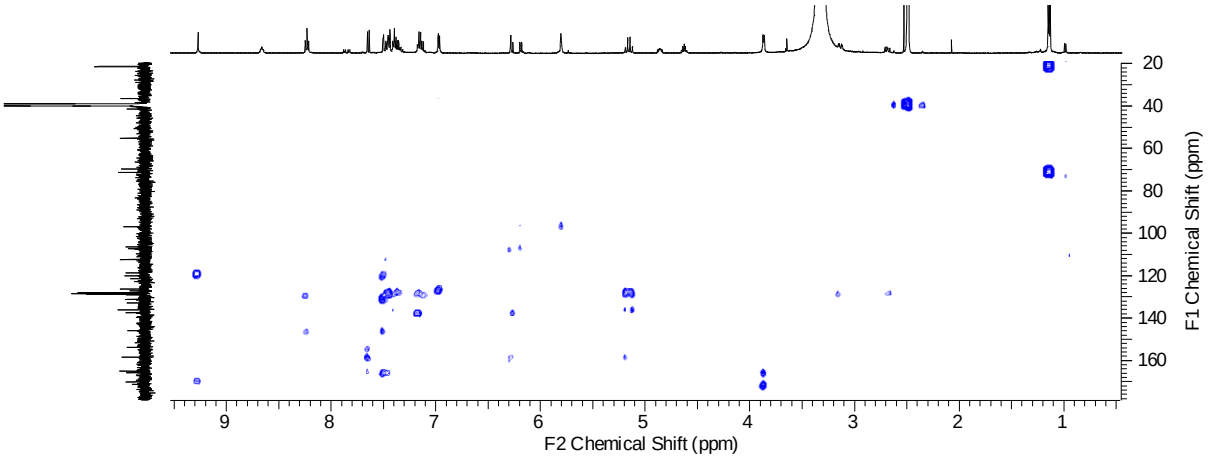

Figure S 93. HMBC spectrum of 10 (DMSO-d_6, 500 MHz).

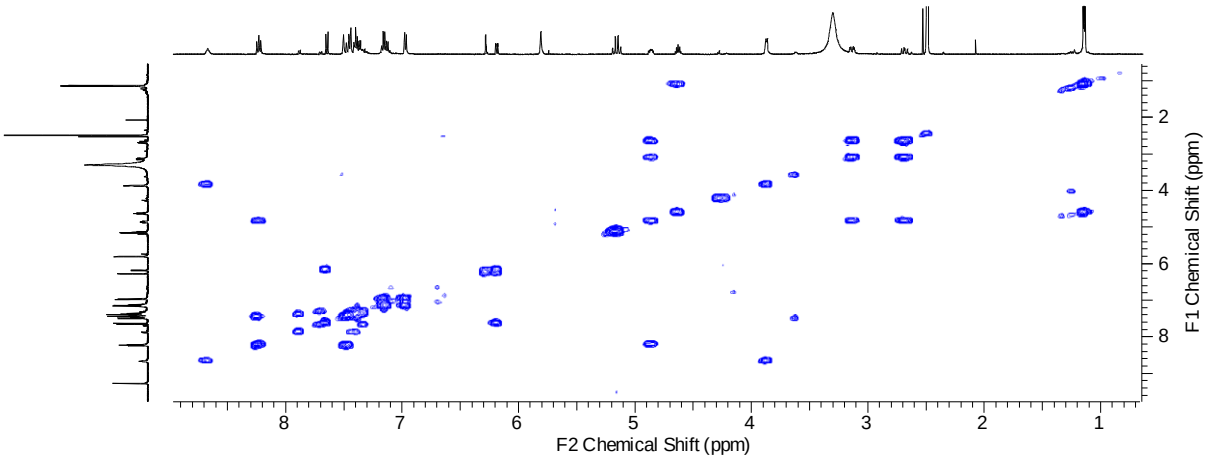

Figure S 94. COSY spectrum of 10 (DMSO-d_6, 500 MHz).

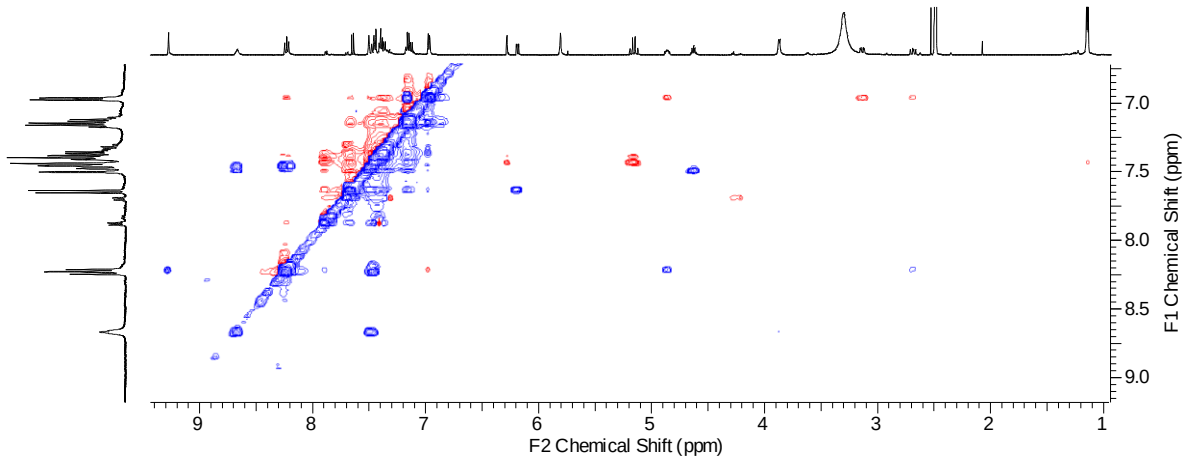

Figure S 95. Partial NOESY spectrum of 10 (DMSO-d_6, 500 MHz).

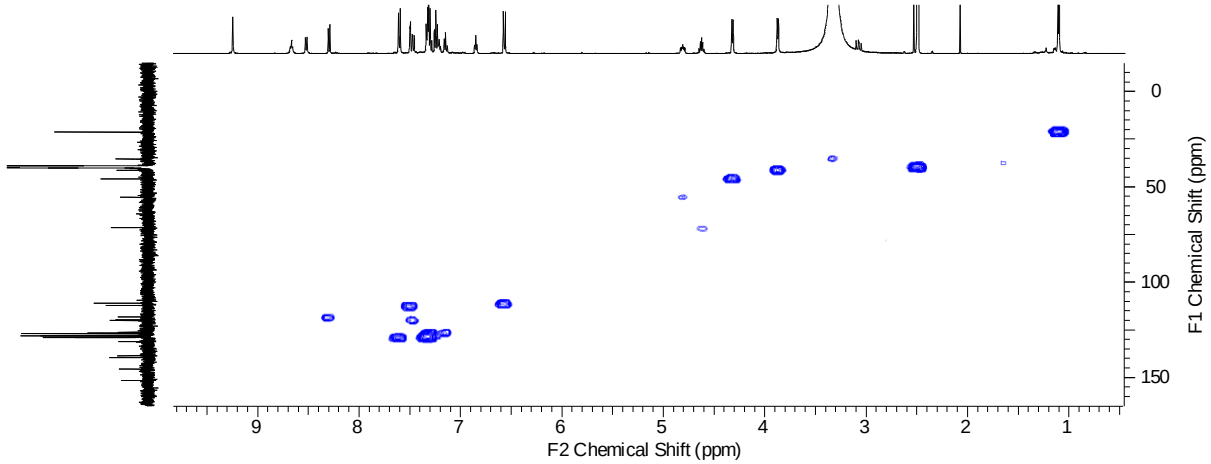

Figure S 96. HMQC spectrum of 11 (DMSO-d_6, 500 MHz).

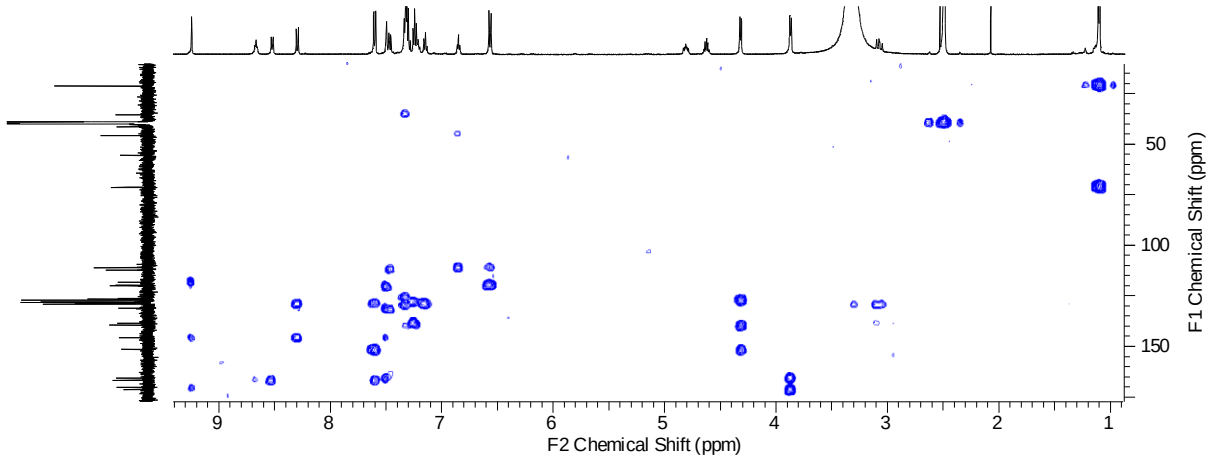

Figure S 97. HMBC spectrum of 11 (DMSO-d_6, 500 MHz).

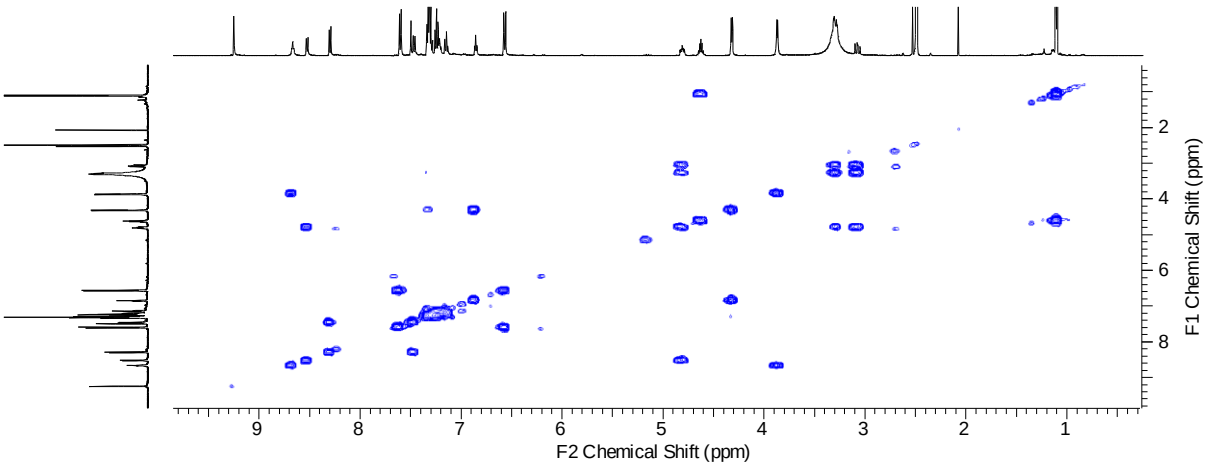

Figure S 98. COSY spectrum of 11 (DMSO-d_6, 500 MHz).

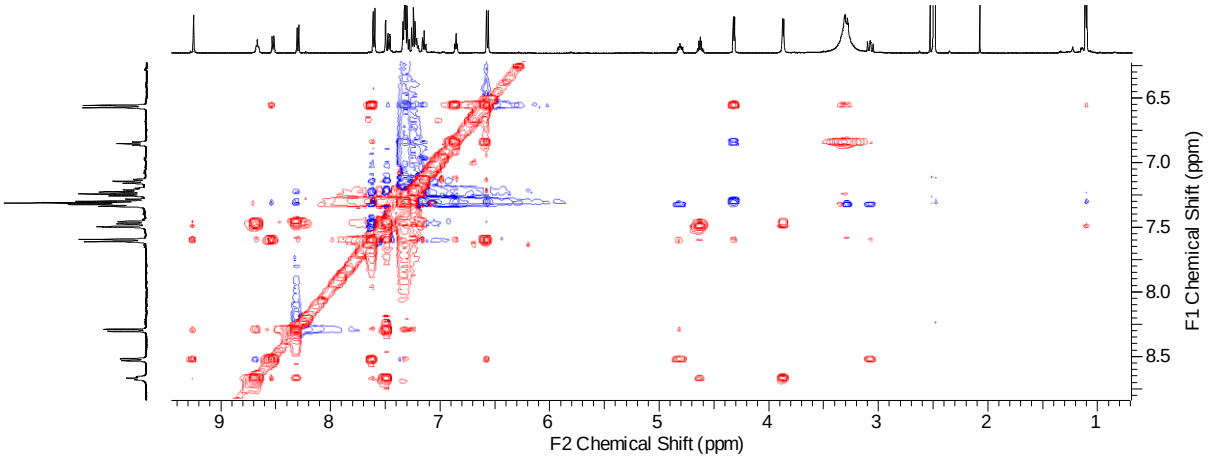

Figure S 99. Partial NOESY spectrum of 11 (DMSO-d_6, 500 MHz).

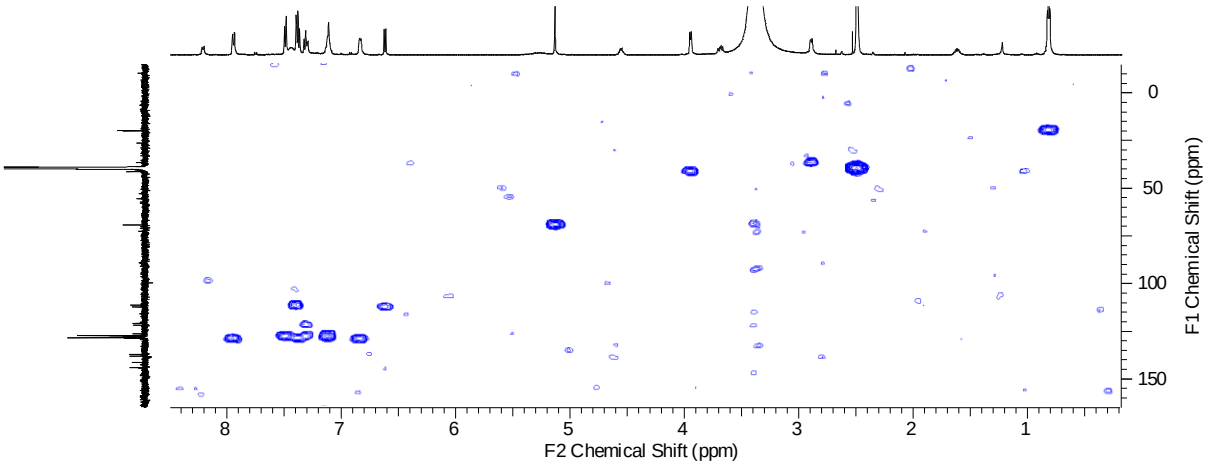

Figure S 100. HMQC spectrum of 12 (DMSO-d_6, 500 MHz).

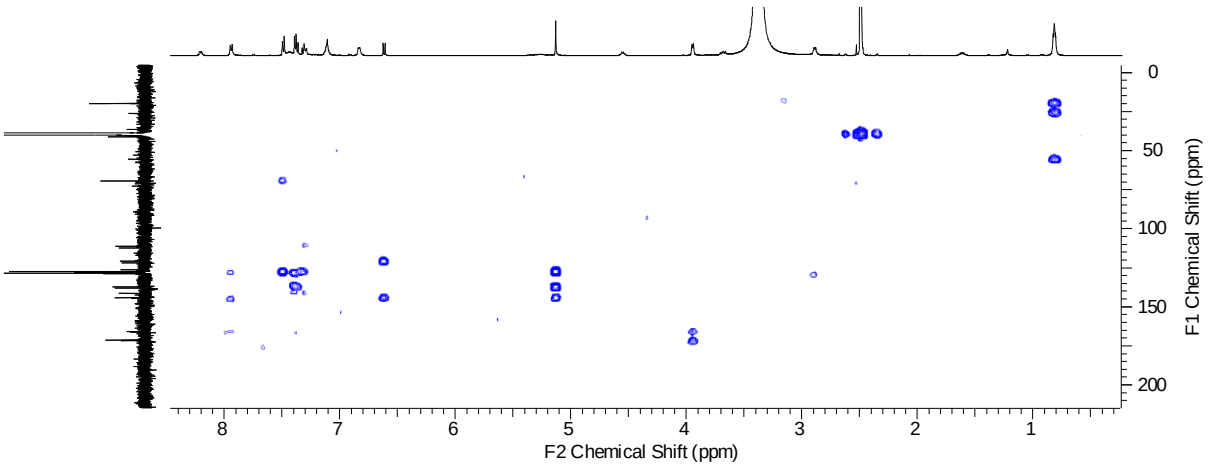

Figure S 101. HMBC spectrum of 12 (DMSO-d_6, 500 MHz).

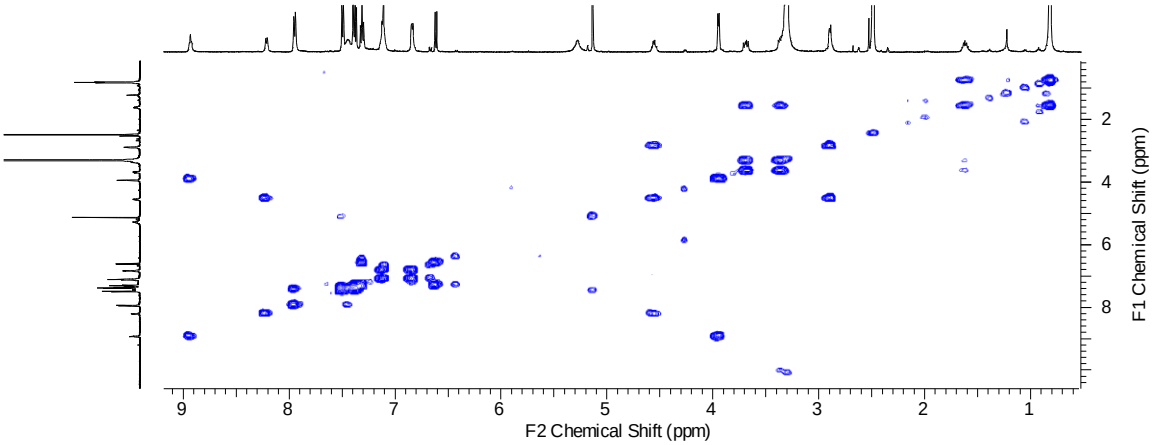

Figure S 102. COSY spectrum of 12 (DMSO-d_6, 500 MHz).

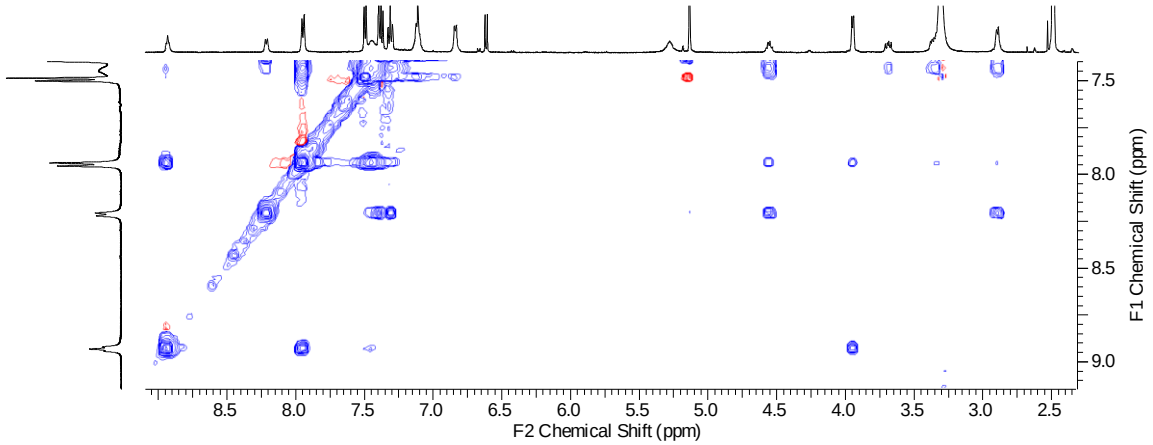

Figure S 103. Partial NOESY spectrum of 12 (DMSO-d_6, 500 MHz).

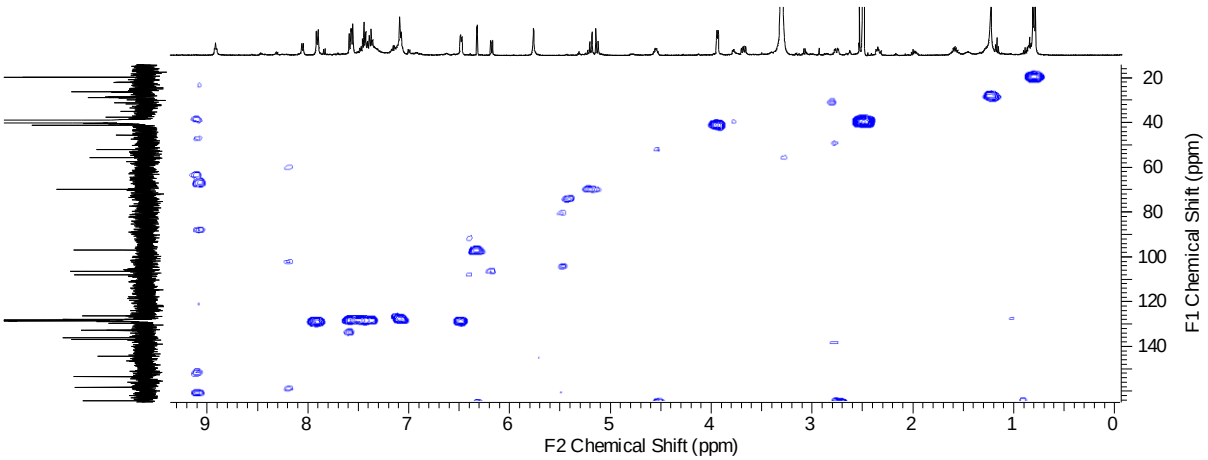

Figure S 104. HMQC spectrum of 13 (DMSO-d_6, 500 MHz).

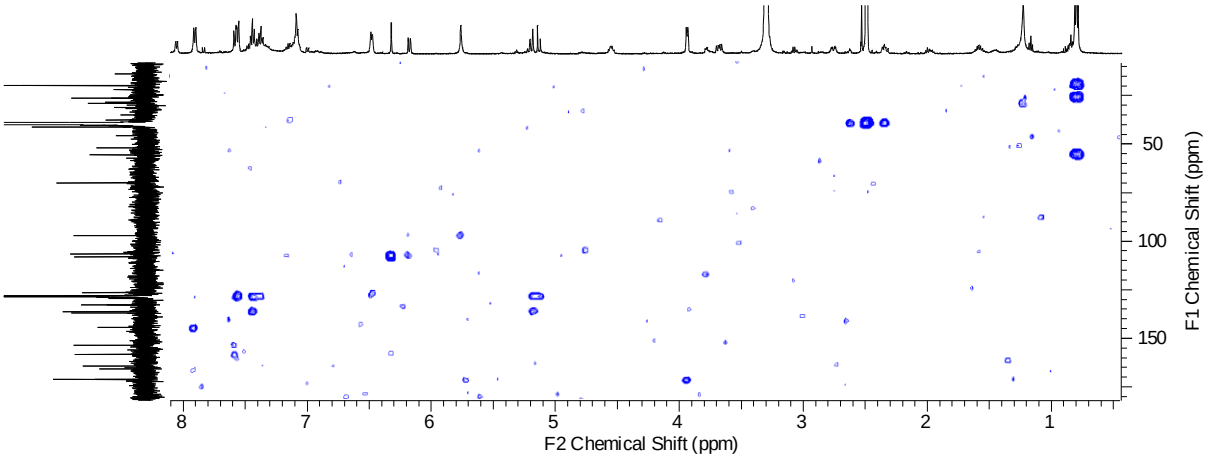

Figure S 105. HMBC spectrum of 13 (DMSO-d_6, 500 MHz).

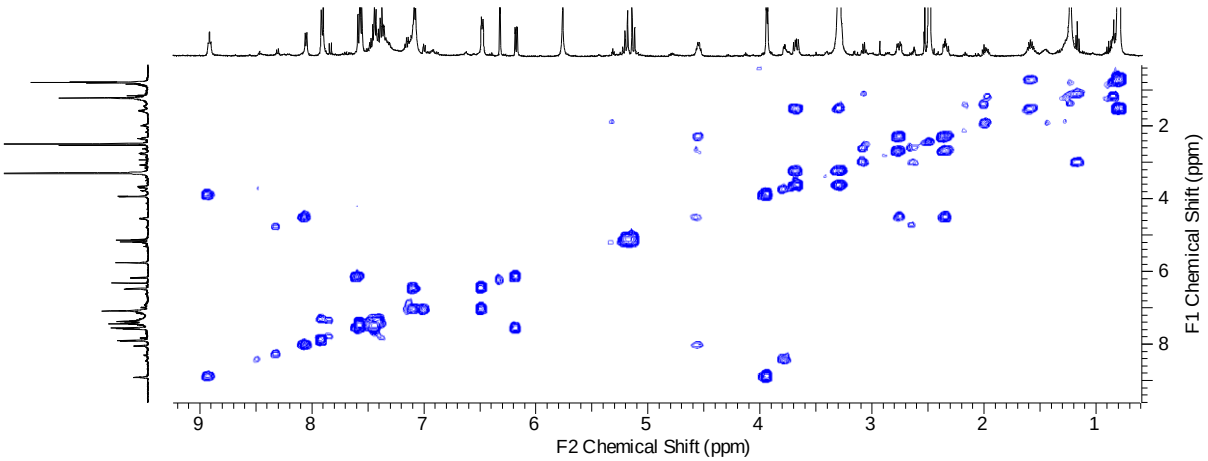

Figure S 106. COSY spectrum of 13 (DMSO-d_6, 500 MHz).

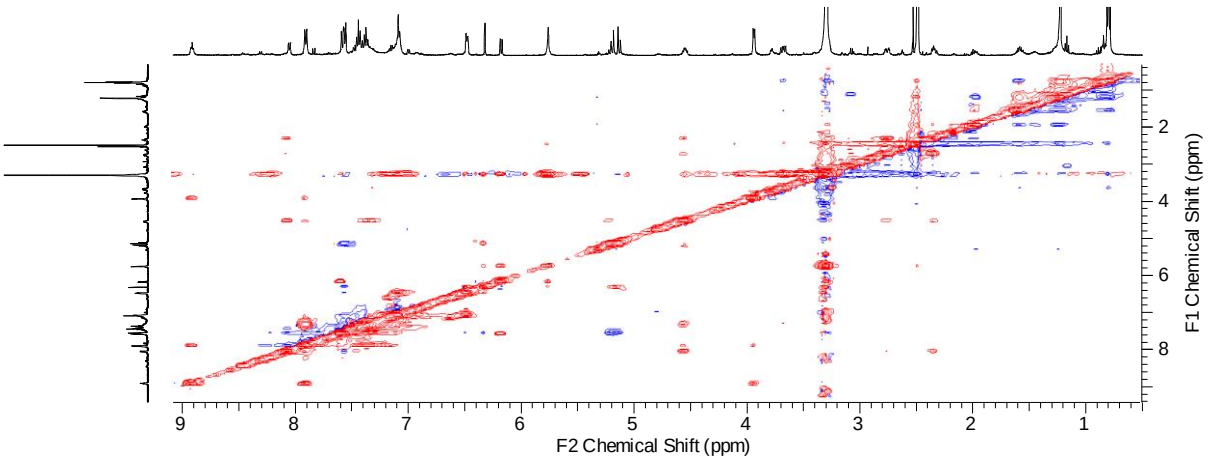

Figure S 107. Partial NOESY spectrum of 13 (DMSO-d_6, 500 MHz).

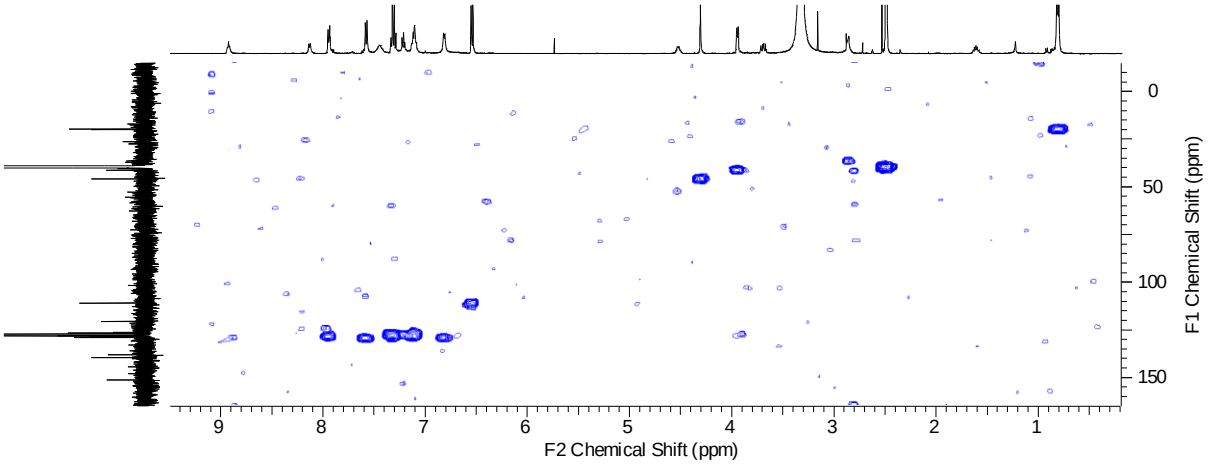

Figure S 108. HMQC spectrum of 14 (DMSO-d_6, 500 MHz).

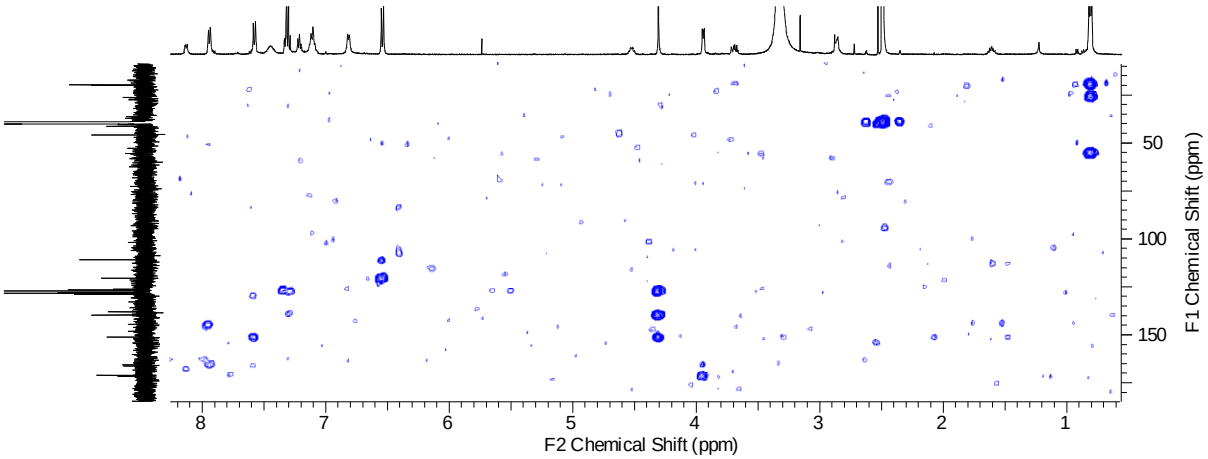

Figure S 109. HMBC spectrum of 14 (DMSO-d_6, 500 MHz).

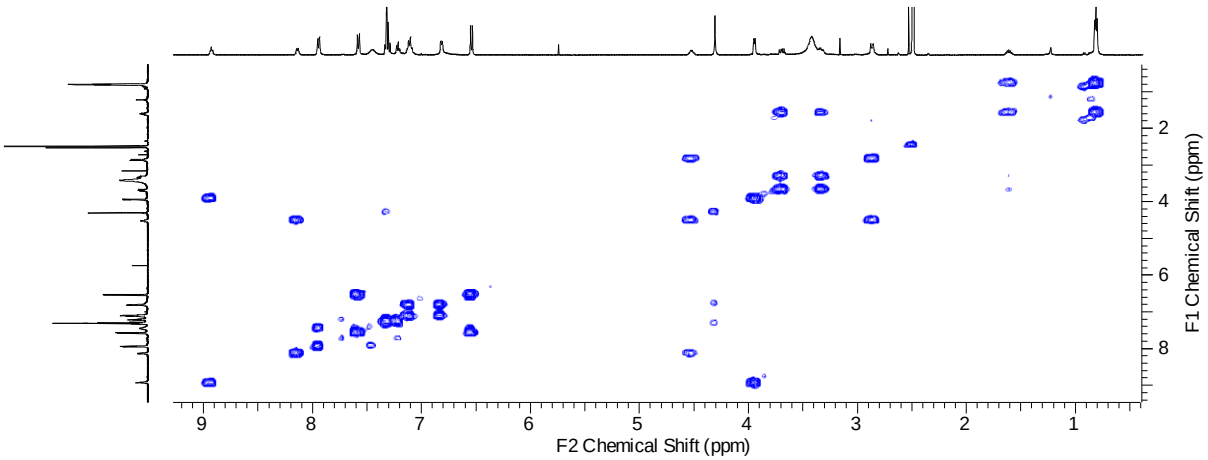

Figure S 110. COSY spectrum of 14 (DMSO-d_6, 500 MHz).

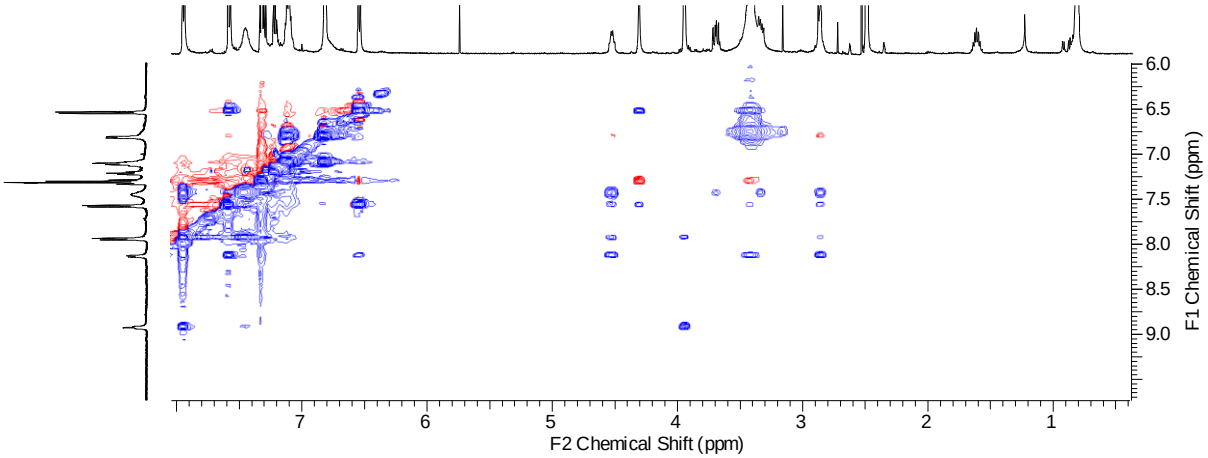

Figure S 111. Partial NOESY spectrum of 14 (DMSO-d_6, 500 MHz).

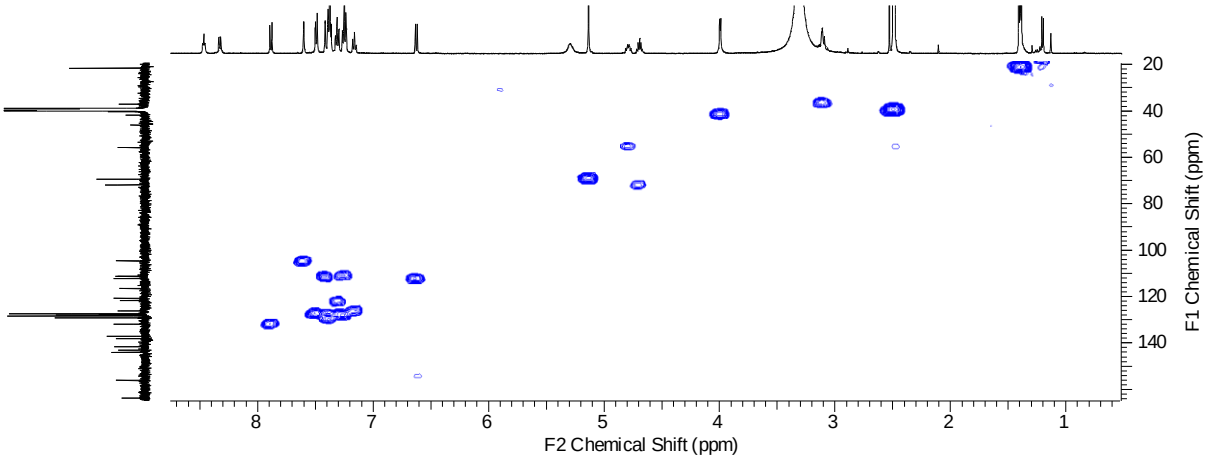

Figure S 112. HMQC spectrum of 15 (DMSO-d_6, 500 MHz).

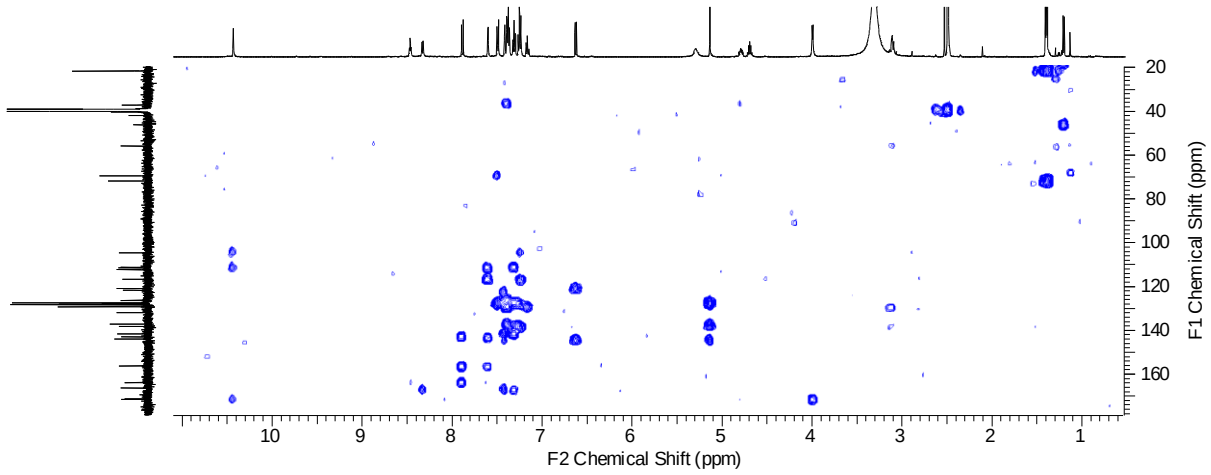

Figure S 113. HMBC spectrum of 15 (DMSO-d_6, 500 MHz).

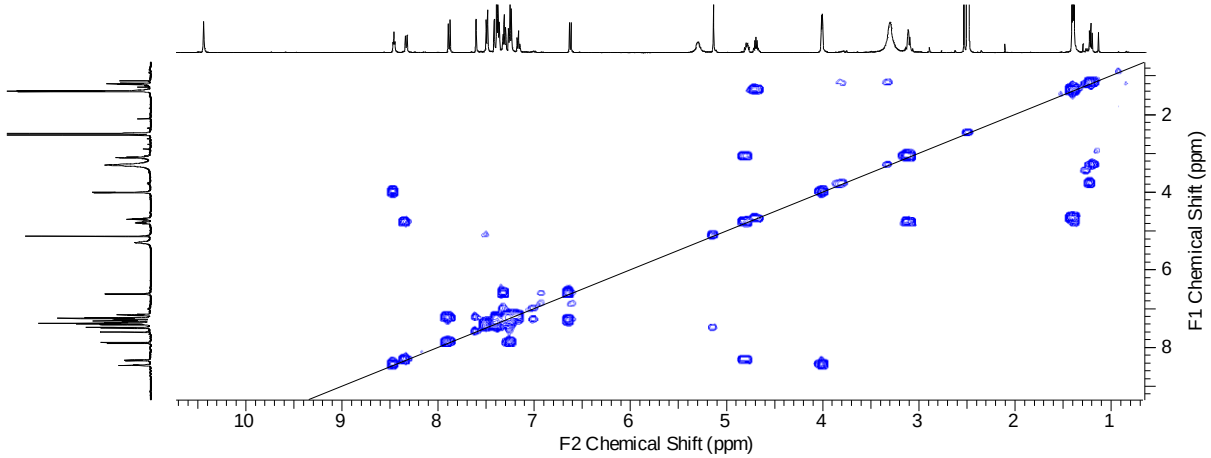

Figure S 114. COSY spectrum of 15 (DMSO-d_6, 500 MHz).

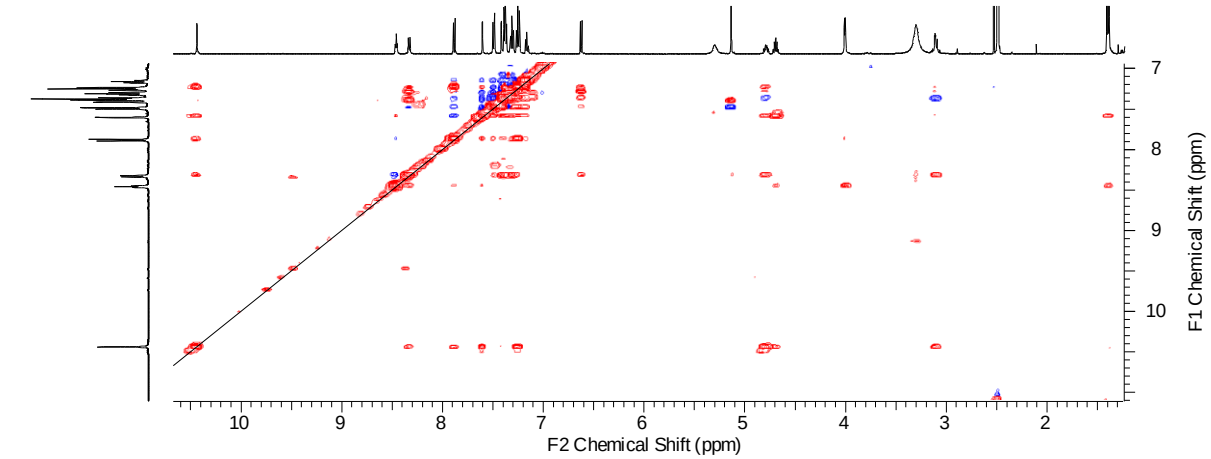

Figure S 115. Partial NOESY spectrum of 15 (DMSO-d_6, 500 MHz).

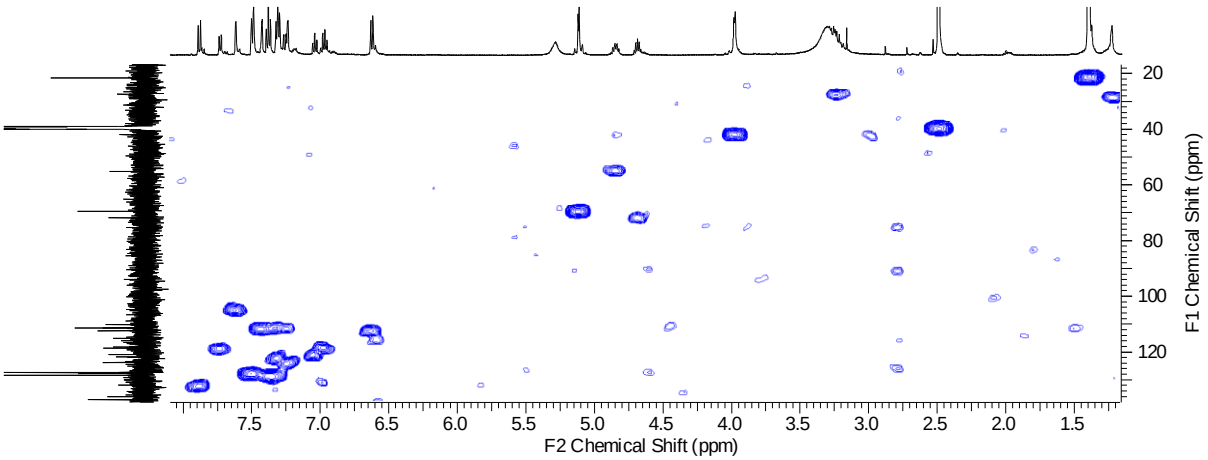

Figure S 116. HMQC spectrum of 16 (DMSO-d_6, 500 MHz).

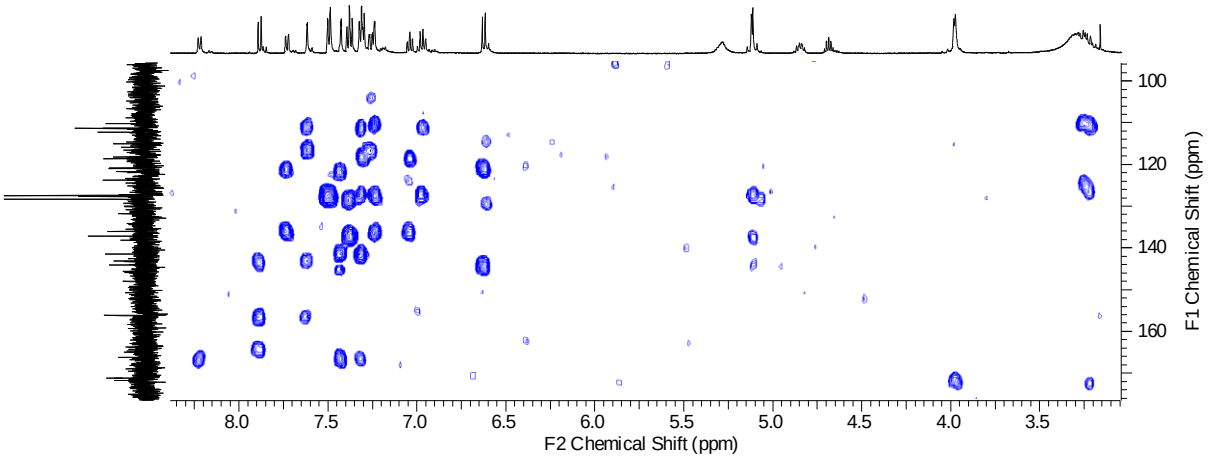

Figure S 117. HMBC spectrum of 16 (DMSO-d_6, 500 MHz).

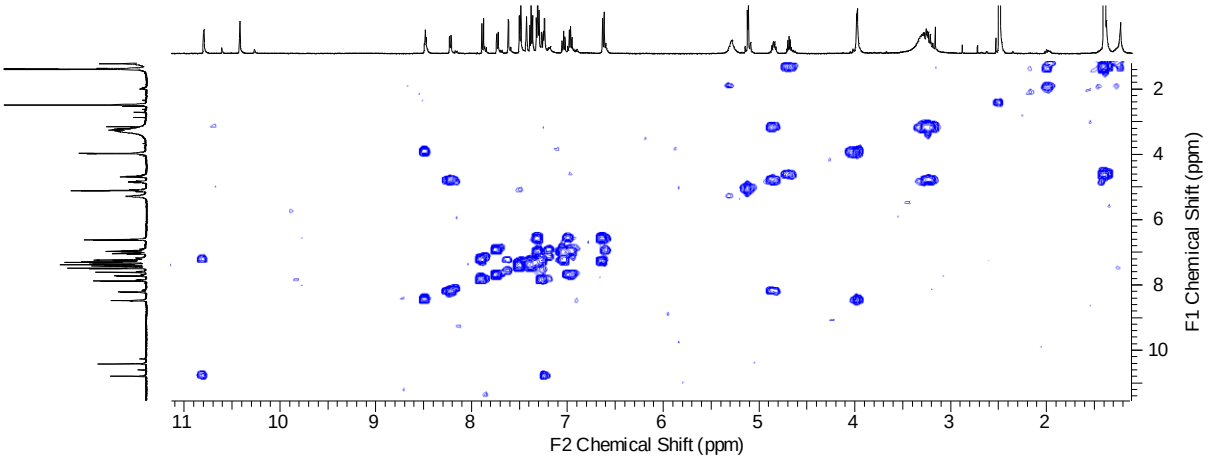

Figure S 118. COSY spectrum of 16 (DMSO-d_6, 500 MHz).

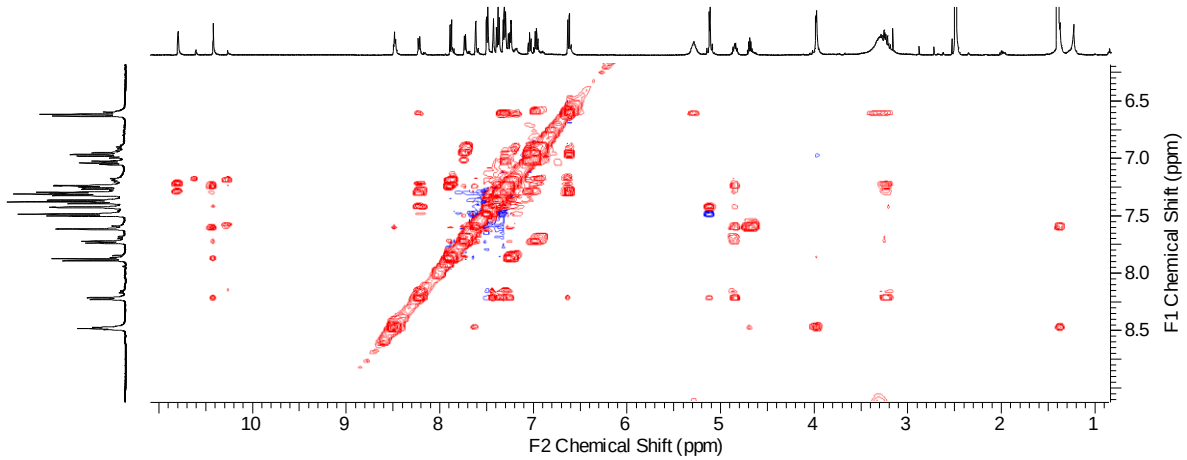

Figure S 119. Partial NOESY spectrum of 16 (DMSO-d_6, 500 MHz).

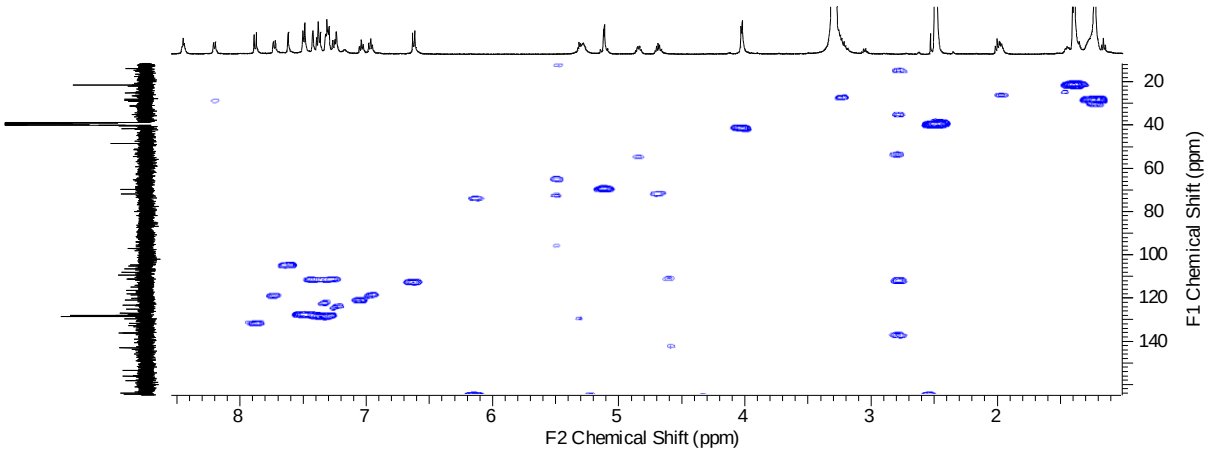

Figure S 120. HMQC spectrum of 17 (DMSO-d_6, 500 MHz).

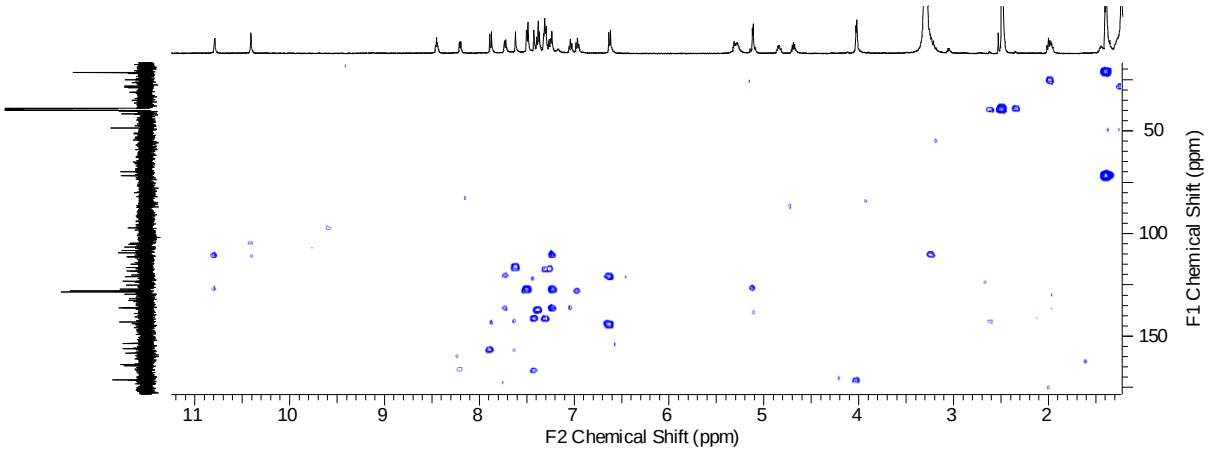

Figure S 121. HMBC spectrum of 17 (DMSO-d_6, 500 MHz).

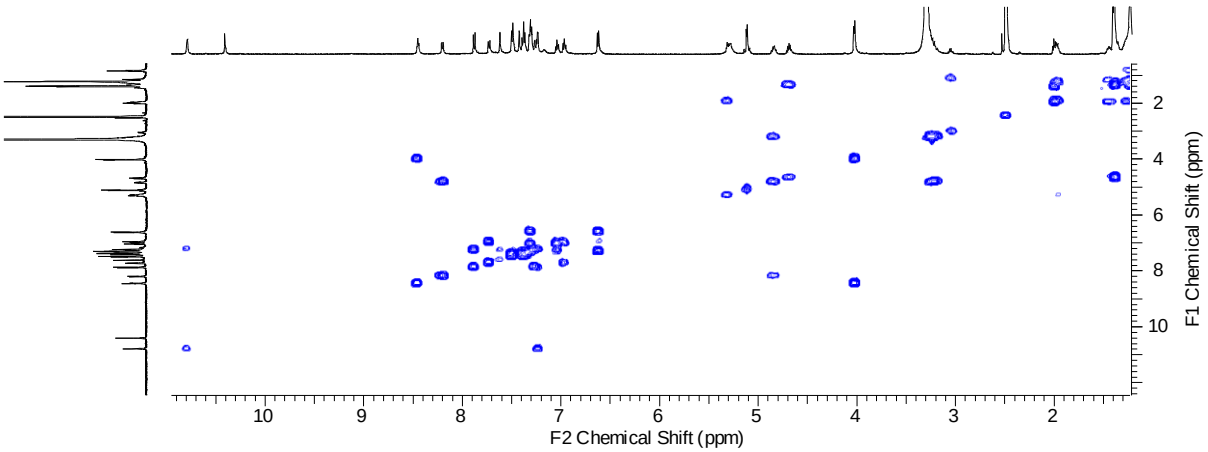

Figure S 122. COSY spectrum of 17 (DMSO-d_6, 500 MHz).

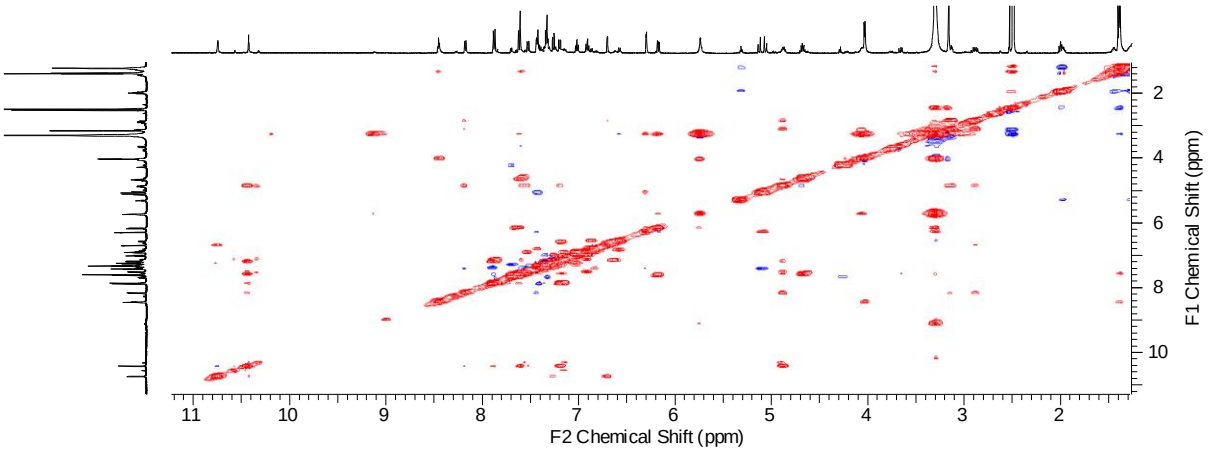

Figure S 123. Partial NOESY spectrum of 17 (DMSO-d_6, 500 MHz).

LC-MS UV traces

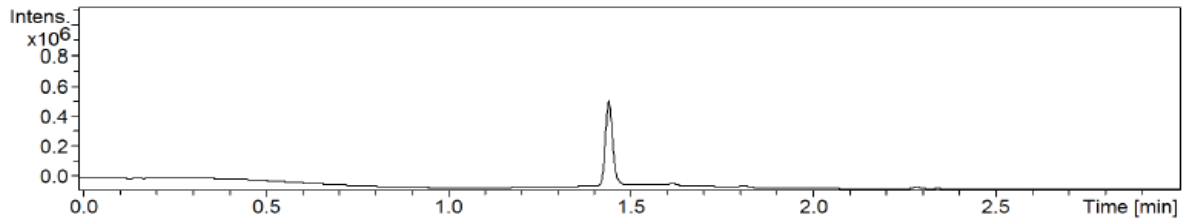

Figure S 124. LC-MS UV trace of 27.

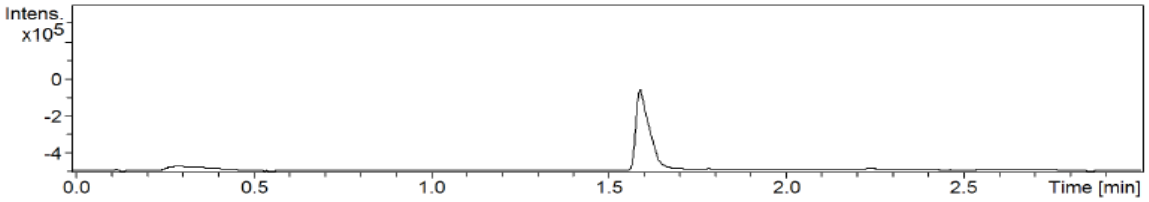

Figure S 125. LC-MS UV trace of 29.

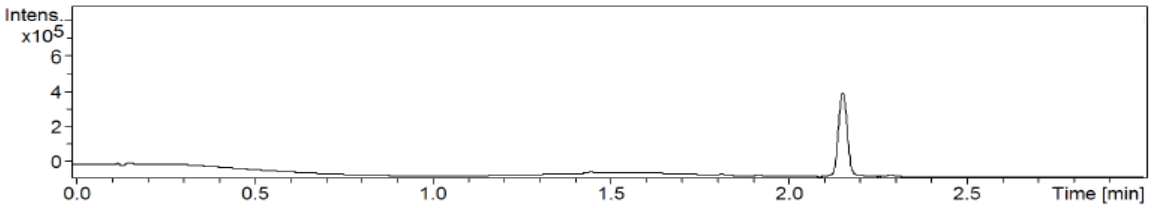

Figure S 126. LC-MS UV trace of 31.

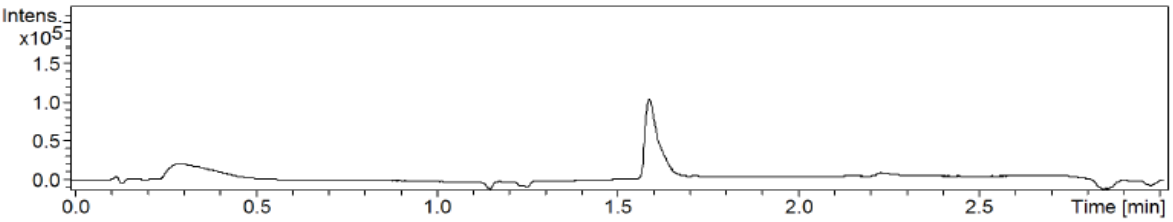

Figure S 127. LC-MS UV trace of 33.

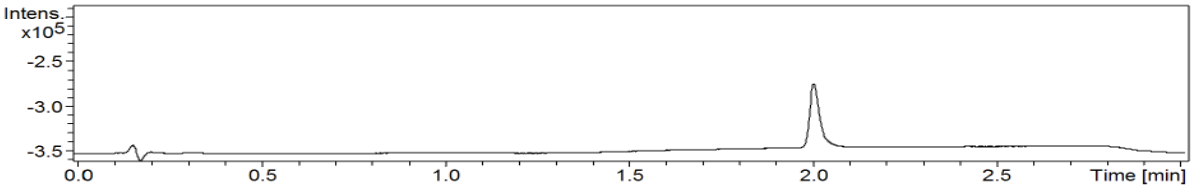

Figure S 128 LC-MS UV trace of 1.

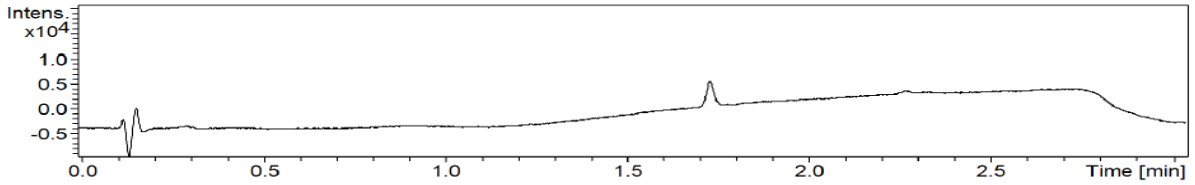

Figure S 129. LC-MS UV trace of 2.

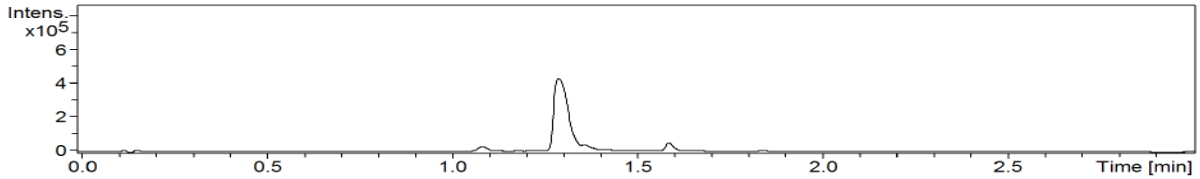

Figure S 130. **LC-MS UV trace of** 3.

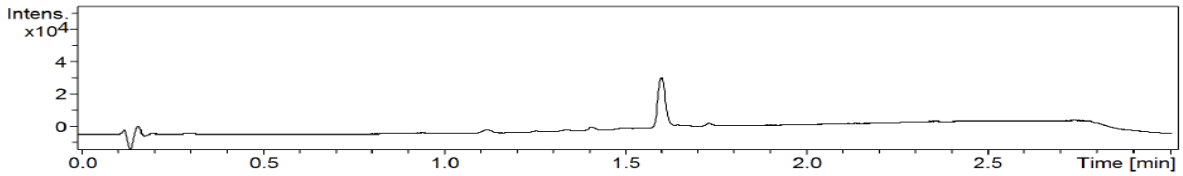

Figure S 131. LC-MS UV trace of 4.

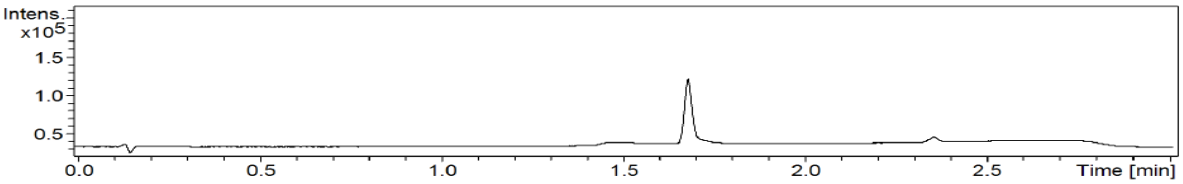

Figure S 132. LC-MS UV trace of 5.

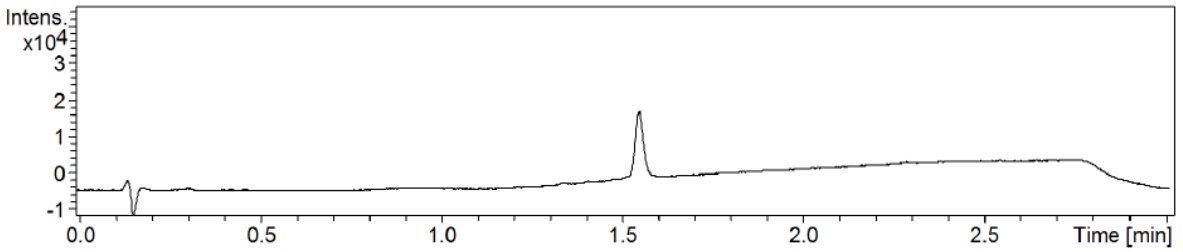

Figure S 133. LC-MS UV trace of 6.

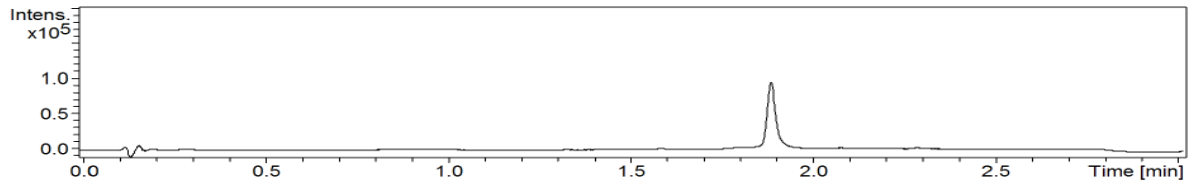

Figure S 134. LC-MS UV trace of 7.

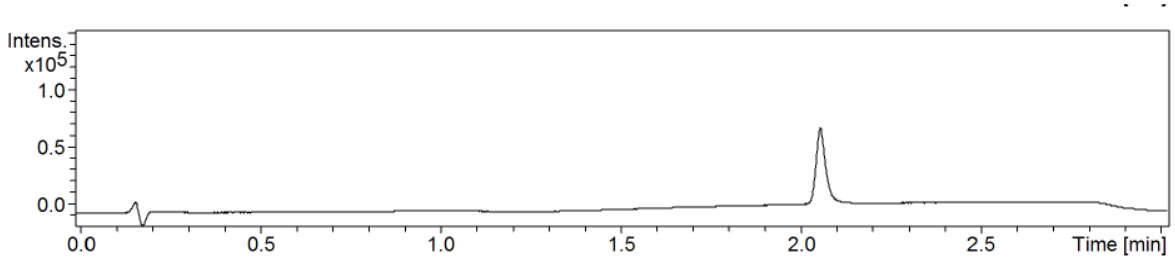

Figure S 135. LC-MS UV trace of 8.

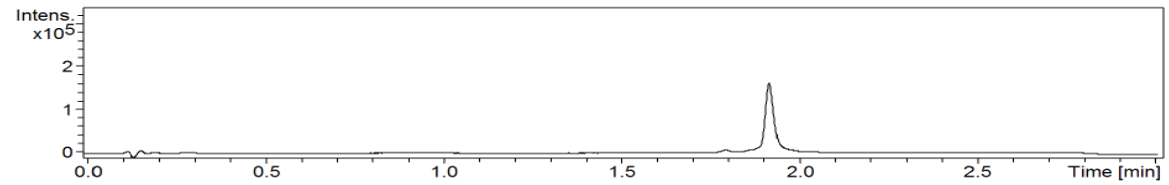

Figure S 136. LC-MS UV Trace of 9.

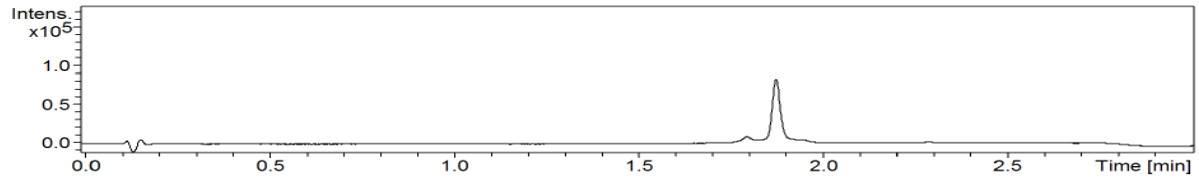

Figure S 137. LC-MS UV Trace of 10.

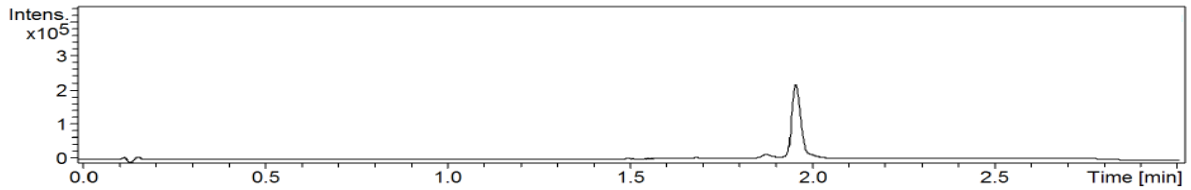

Figure S 138. LC-MS UV trace of 11.

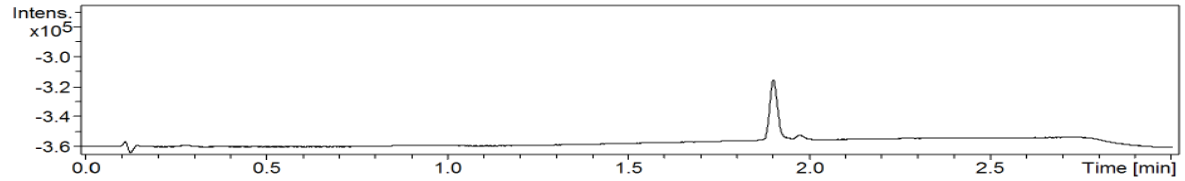

Figure S 139. LC-MS UV trace of 12.

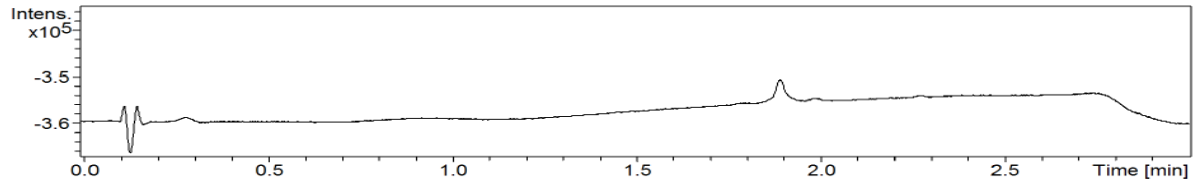

Figure S 140. LC-MS UV trace of 13.

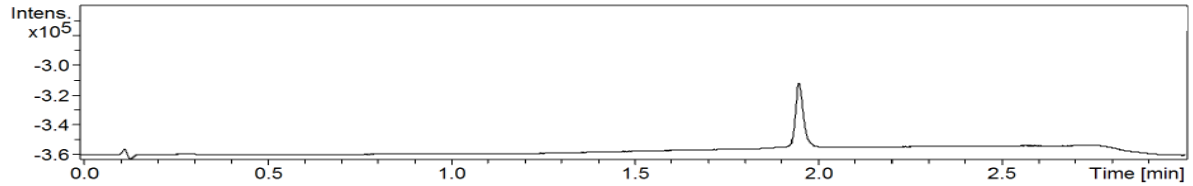

Figure S 141. LC-MS UV trace of 14.

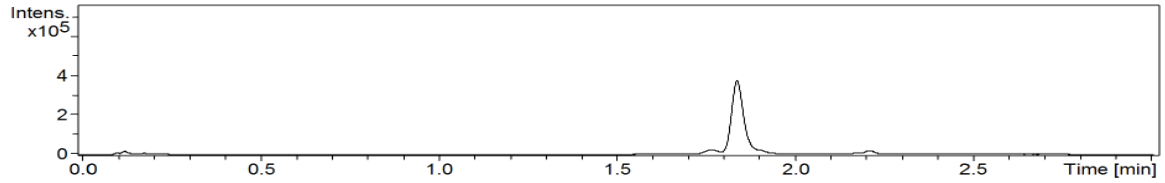

Figure S 142. LC-MS UV trace of 15.

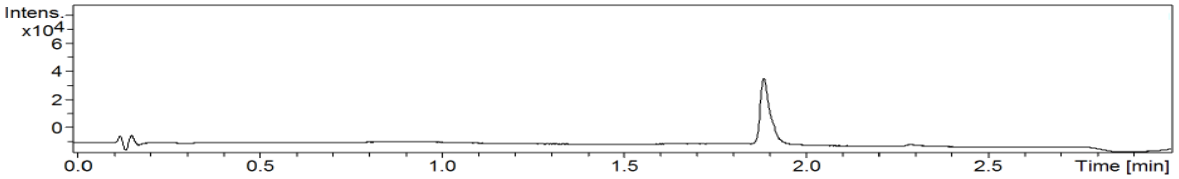

Figure S 143. LC-MS UV trace of 16.

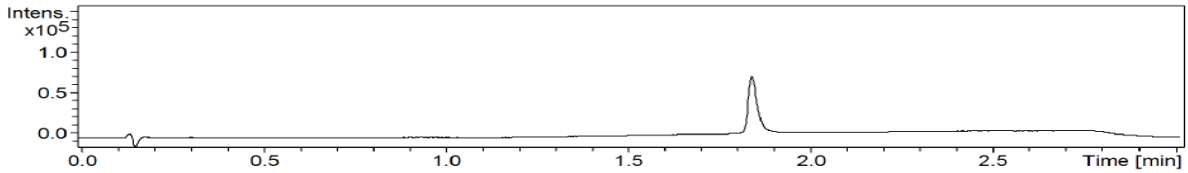

Figure S 144. LC-MS UV trace of 17.

NMR Structure Determination

Additional correlations observed in the NOESY spectrum are highlighted in Figure S150

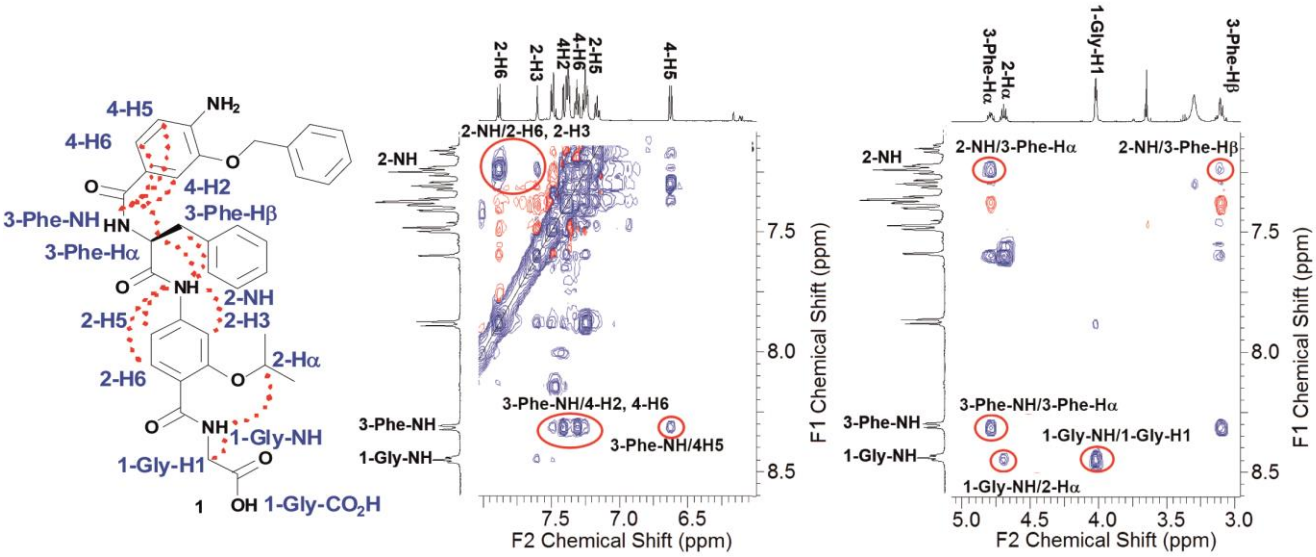

Figure S 145. Partial NOESY spectrum of 1 (DMSO-d6, 500 MHz) together with an illustration showing key nOes.

A number of through-space connections were identified in the 2D ROESY spectrum for peptide mimetic **1** in dmso-d_6 solution at 293K. Assigned ROESY cross-peaks were integrated using SPARKY 3.111 (T.D. Goddard and D.G. Kneller, *Sparky 3*. (2006): University of California, San Fransisco, USA) and volumes converted to distances with reference to the fixed and know distance between the H5 and H6 protons of the residue 4. These distances were then used within CNS-solve[8] to generate a set of low energy structures, following a simulated annealing process, all satisfying the distance constraints, in a similar manner to that adopted recently for a similar sized peptide.[9] Of particular note are strong, inter-residue rOes (indicative of short inter-proton separations) between 4-H2 and 3-Phe-NH, 4-H2 and 3-Phe-Hβ, and between 3-Phe-Hα and 1-Gly-NH and a weaker rOe between. Distances between sets of protons (as indicated in Figure S1) were estimated from cross-peak volumes in the ROESY spectrum for the peptide measured using SPARKY 3.111. These volumes were converted to distances using equation (1); where r_{ij} is the distance between protons H_i and H_j, r_{ref} is a reference distance (in this case the separation between 4-H5 and 4-H6 which was measured as 2.35 Å from the structure built from the x-ray crystallographic analysis of a derivative of residue 4.[10] v_{ij} and v_{ref} are the associated cross-peak volumes.

$$r_{ij} = r_{ref} \sqrt[6]{v_{ref} / v_{ij}}$$

A list of the distances utilised is provided below.

Entry	Proton 1	Proton 2	Distance (Å) from volumes	bounds
1	4-NH2	4-H5	2.6	+/- 0.2
2	4-H6	4-H5	2.3(5)	+/- 0.2
3	4-H2	4-O-CH2	2.3	+0.5/-0.2*
4	4-O-CH2	4-O-orthos	2.5	+1.5/ -0.2*
5	4-H2	3-Phe-NH	1.9	+/- 0.5
6	4-H6	3-Phe-NH	4.3	+/- 1.5
7	4-H2	3-Phe-Hα	3.5	+/- 0.8
8	4-H para of o	3-Phe-NH	3.0	+/- 0.5
9	4-H2	3-Phe-Hβ	2.8	+/- 1.0*
10	4-O-CH2	3-Phe-ortho	3.0	+/- 1.5*
11	3-Phe-ortho	1-Gly-NH	5.5	+/- 1.5*
12	3-Phe-NH	3-Phe- Hα	2.5	+/- 0.5
13	3-Phe- Hα	3-Phe- Hβ	2.5	+/-0.5
14	3-Phe- Hβ	3-Phe-NH	3.0	+/- 0.2
15	3-Phe- Hβ	3-Phe ortho	3.0	+/- 1.5
16	3-Phe- Hα	2-H-NH	3.0	+/- 0.7
17	3-Phe- Hβ	2-H-NH	4.0	+/- 1.3*
18	2-H-NH	2-H-H5	2.5	+/- 0.5
19	2-H-H5	2-H-H6	2.3(5)	+/-0.2
20	2-H-H3	2-H - OCH	2.2	+/- 0.2
21	2-H-OCH	2-H-CH3	2.5	+/- 1.5*
22	2-H-H3	2-H-CH3	3.0	+ 0.5/-1.0*
23	1-Gly-NH	1-Gly-Hα	3.0	+/- 0.5

* wide bounds to accommodate, for example the ortho protons being indistinguishable from each other, and likewise the O-CH2 protons.

Topology files for residues 4 and 2 were built using bond angles, torsion angles and bond lengths taken from the x-ray crystallographic structures of analogues of the two residues. For each simulated annealing run 100 structures were generated and this was repeated 10 times. The 10 lowest energy structures from each run were then tested for acceptability (rather than trial structures) and the 10 lowest energy accepted structures satisfy all of the rOe constraints with the bounds shown.

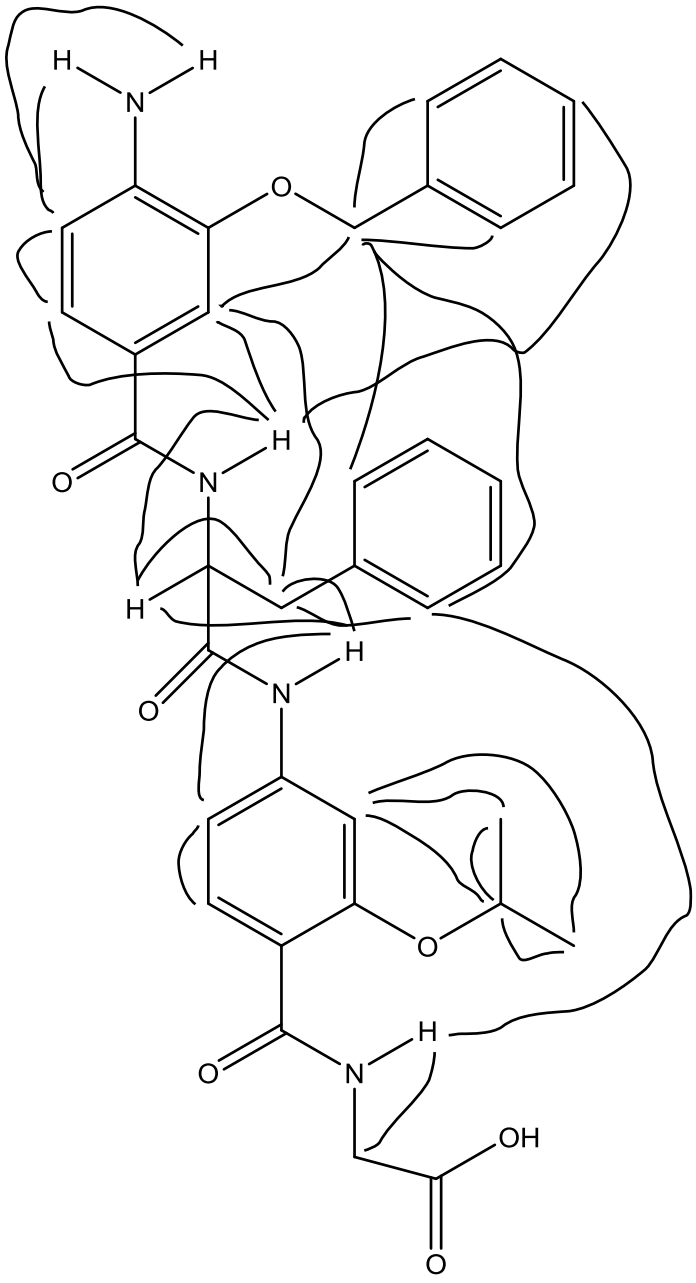

Figure S 146. Structure of 1 illustrating cross-peaks observed in the ROESY spectrum.

Variable Temperature and dilution ^{1}H NMR studies

Dilution NMR studies on the model hybrid **1** were performed acquiring ^{1}H NMR spectra at concentrations ranging from 10 to 1 mM (Figure S 152).

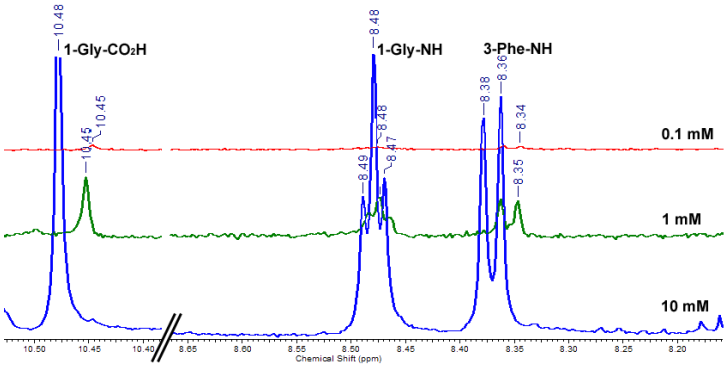

Figure S 147 Partial ^{1}H-NMR spectra of hybrid 1 (DMSO-d_6, 500 MHz) at concentrations of 10 mM (blue), 1 mM (green) and 0.1 mM (red) showing the acid proton (1-Gly-CO_2H), the Gly-NH proton (1-Gly-NH) and the top amide proton of the sequence (3-Phe-NH).

As expected, a resonance shift was observed for the acid and the top amide protons, but no change was detected for the Gly-NH. This concentration independence confirmed this proton is engaged in an intramolecular H-bond.

Intramolecular H-bonding was further confirmed by VT NMR studies and the results are summarised in Figure S 153.

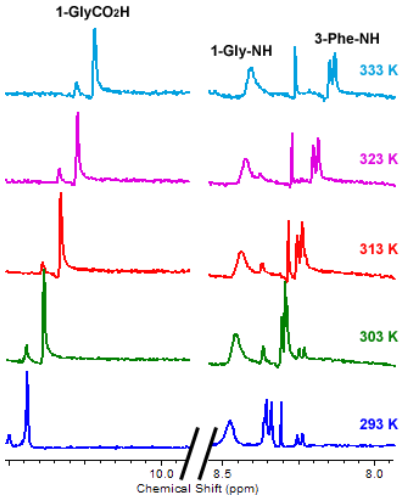

Figure S 148 Partial ^{1}H-NMR spectra of hybrid 1 (10 mM DMSO-d_6, 500 MHz) at 293 K (blue), 303 K (green) 313 K (red), 323 K (magenta) and 333 K (light blue) showing the acid proton (1-Gly-CO_2H), the Gly-NH proton (1-Gly-NH) and the top amide proton of the sequence (3-Phe-NH).

Analysis of temperature coefficients (T_{coeff}, calculated following Equation S1)[11] revealed T_{coeff} of – 5.5 ppb K^{-1} and - 5 ppb K^{-1} for the acid (1-GlyCO_2H) and the top amide (3-Phe-NH) protons respectively and T_{coeff} of – 1.75 ppb K^{-1} for the 1-Gly-NH proton. These data further supported the hypothesis that the Gly-NH proton engages in a S(6) intramolecular H-bond, as internally hydrogen bonded amides are expected to show much smaller shifts with temperature than protons which are accessible for H-bonding to external polar solvents.

$$T_{coeff} = \frac{\delta_2 - \delta_1}{T_2 - T_1} \times 10^3 \quad \delta = \text{chemical shift in ppm, } T = \text{temperature in K}$$

Equation S 1

Proteolytic studies

α-Chymotrypsin Type II from bovine pancreas (lyophilized powder, MW = 25 kDa, ≥ 40 units/mg protein), Proteinase K from *Tritirachium album* (lyophilized powder, MW = 28.93 kDa, ≥ 30 units/mg protein) and Trypsin IV-O from chicken egg white (lyophilized powder, MW = 20 kDa, ≥ 20 units/mg protein) were purchased from Sigma-Aldrich and used without further purification.

Hybrid **1** (Figure S 154 b-d) and WT-p53 (Figure S 155 b-d) (200 μM stock in PBS buffer pH 7.50, 2% DMSO) were treated with the chosen enzyme (0.02 μM stock solutions in PBS buffer pH 7.50) in a 1:10000 enzyme/substrate ratio. A control was also run treating hybrid **1** and WT-p53 with no enzyme (Figure S154a and S155 a). The degradation was followed with analytical HPLC (Ascentis® Express Peptide Column, injection volume: 20 μL, acetonitrile/water (0.1% TFA) 5-95% gradient) and the data was analysed to extract kinetic values. To minimize variability, the area of the peak corresponding to DMSO was used as internal reference for correction. Rate constants were determined from a linear fit following Equation S2 and the half-life of the proteolysis was determined using Equation S3.

$$\ln\left(\frac{A_t}{A_0}\right) = -kt$$

A_t = Substrate areas at time t; A_0 = Substrate area at time zero; k = reaction rate coefficient

Equation S 2

$$t_{1/2} = \frac{\ln 2}{k}$$

Equation S 3

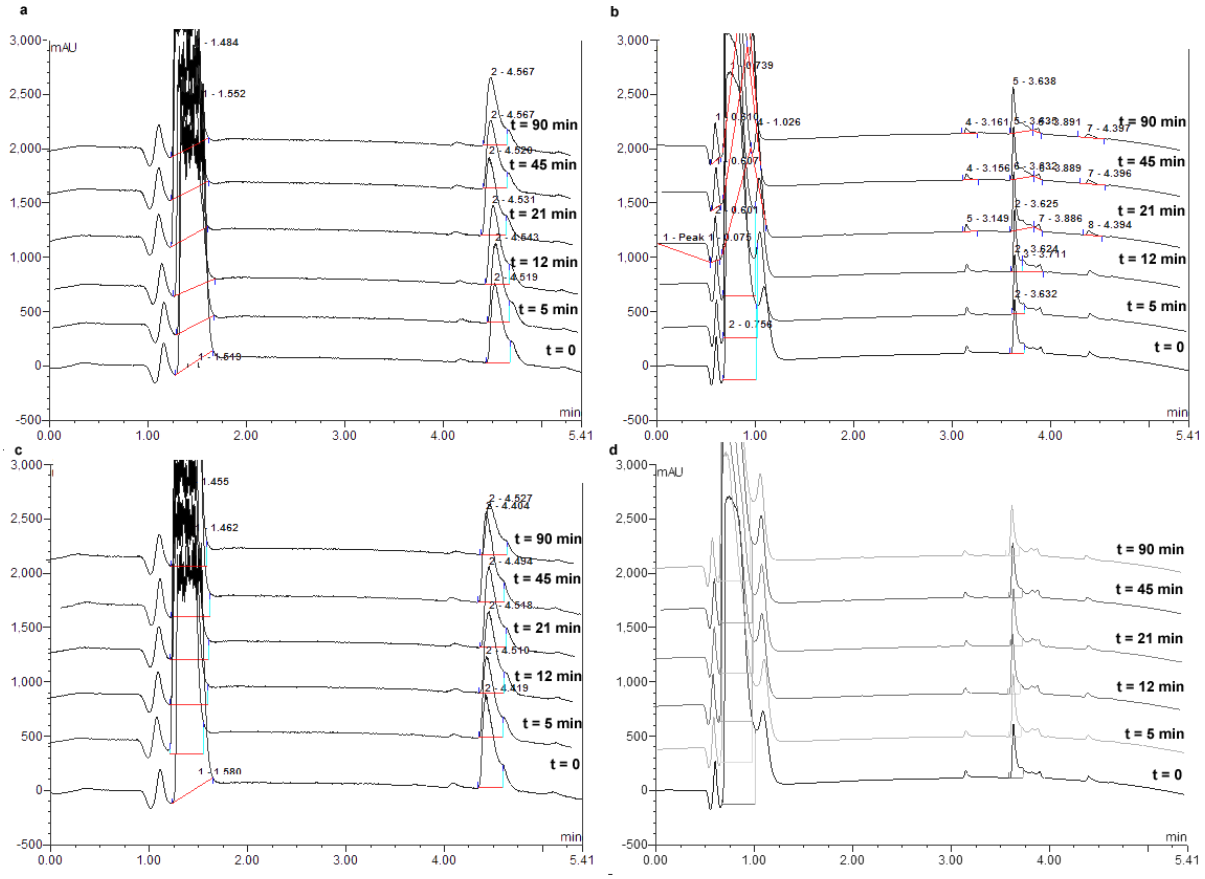

Figure S 149. Proteolytic study on hybrid 1 a Analytical HPLC trace for 1 treated with no enzyme; b Analytical HPLC trace for 1 treated with Trypsin; c Analytical HPLC trace for 1 treated with Proteinase K; d Analytical HPLC trace for 1 treated with α-Chymotrypsin.

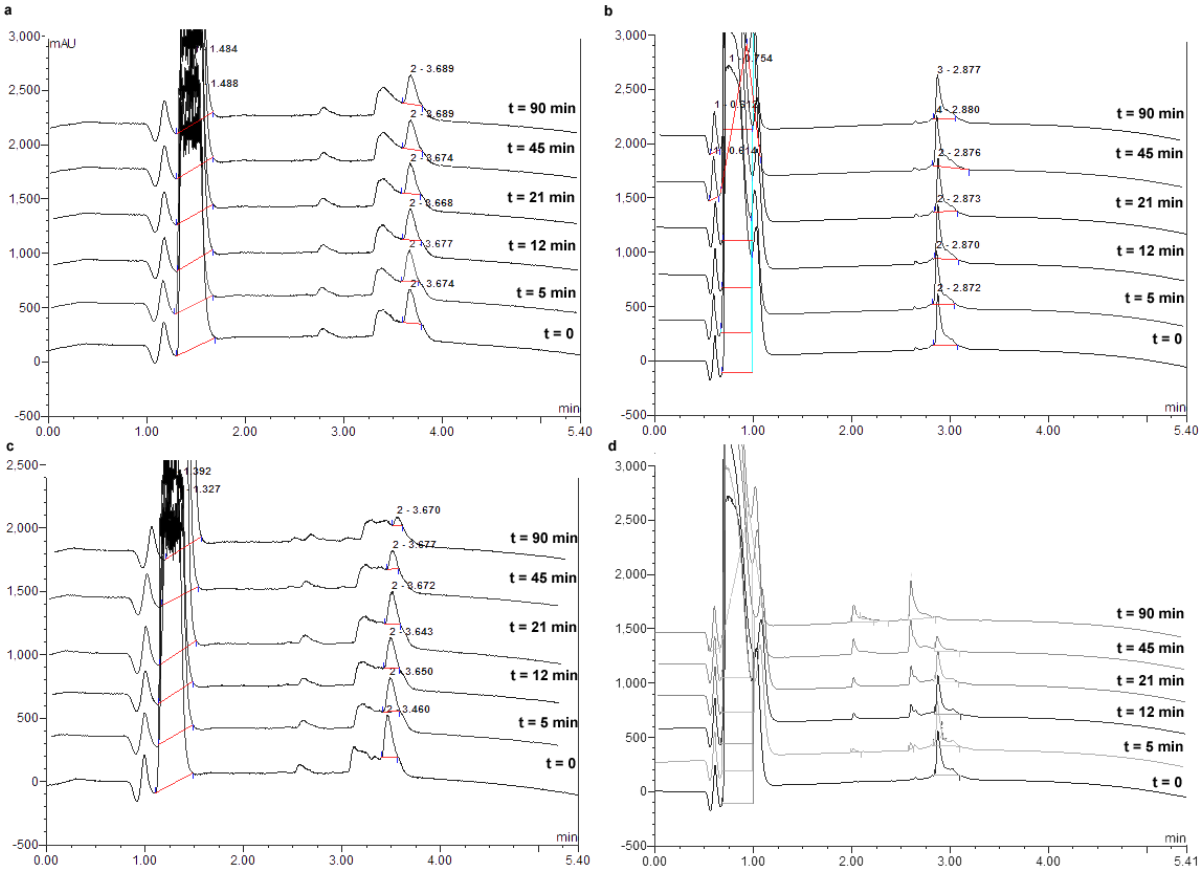

Figure S 150. Proteolytic study on WT-p53 a Analytical HPLC trace for WT-p53 treated with no enzyme; b Analytical HPLC trace for WT-p53 treated with Trypsin; c Analytical HPLC trace for WT-p53 treated with Proteinase K; d Analytical HPLC trace for WT-p53 treated with α-Chymotrypsin.

Hybrid **1** was further treated with α-Chymotrypsin increasing the ratio enzyme/substrate to 1:1000 and 1:100 (Figure S156, α-chymotripsin 0.2 μM and 2 μM stock solutions in PBS buffer pH 7.50).

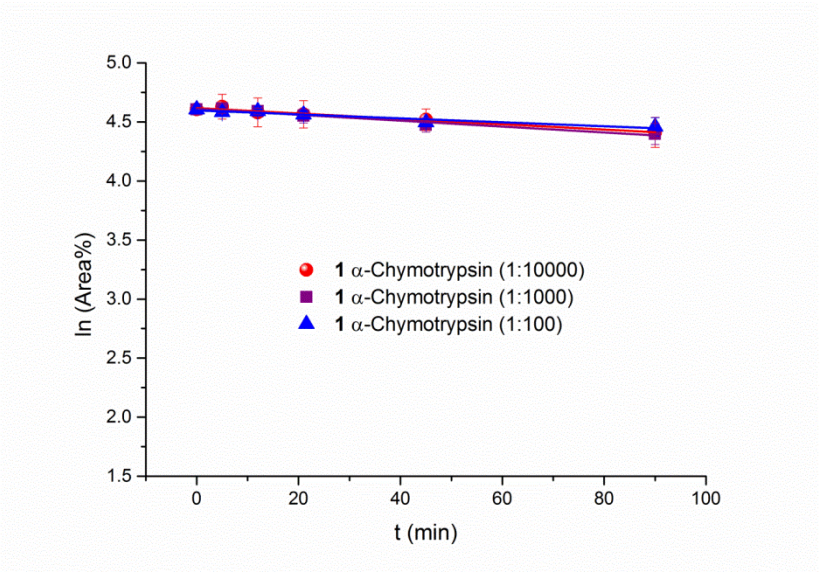

Figure S 151. Kinetics of degradation from proteolytic studies of hybrid 1 at 1:10000 (red), 1:1000 (purple) and 1:100 (blue) α-Chymotrypsin /substrate ratio.

Biophysical assessment of proteomimetics

Proteins expression and purification

The protein was expressed as previously described[2] in *E.coli* BL21 (DE3) GOLD and purified following previously published methods. The purified *h*DM2 (17-126) L33E was concentrated (typically to ~ 100 μM) and stored at – 80 °C.

The pet28a His-SUMO Mcl-1 (172-327) construct was over-expressed in the *E.coli* strain Rosetta 2. 10 ml of overnight starter culture was used to inoculate 1 L 2 xYT containing 50 μg/ml Kanamycin and 50ug/ml Chloramphenicol. Cultures were grown at 37 °C plus shaking until OD_{600} ~ 0.6 – 0.8, the temperature was then switched to 18 °C and protein expression induced by the addition of 0.8mM IPTG. Induced cultures were grown at 18 °C plus shaking overnight before harvesting by centrifugation. Cells were resuspended in 50mM TRIS pH 8.0, 500mM NaCl, 15mM Imidazole and lysed by sonication in the presence of 10 μL of 1 $U.ml^{-1}$ DNase I per litre of over-expression culture and 5mM $MgCl_2$. The cell lysate was centrifuged (Beckman JA25.50 rotor, 17,000 rpm, 45 min, 4 °C) and the supernatant filtered (0.22 μM syringe filter) before application onto a 5ml HisTrap that had previously been equilibrated with 50mM TRIS pH 8.0, 500mM NaCl, 15mM Imidazole. The cleared cell

lysate was then allowed to flow through the HisTrap with the aid of a peristaltic pump. The HisTrap was then washed with 10 CV of 50mM TRIS pH 8.0, 500mM NaCl, 15mM Imidazole followed by 10 CV 50mM TRIS pH 8.0, 500mM NaCl, 50mM Imidazole. The His-SUMO-Mcl-1 fusion protein was then eluted from the HisTrap with 50mM TRIS pH 8.0, 500mM NaCl, 300mM Imidazole. The His-SUMO-Mcl-1 fusion protein was cleaved overnight in dialysis into 50mM TRIS pH 8.0, 250mM NaCl in the presence of Smt3 protease, Ulp1, overnight at 4°C. To remove any uncleaved Mcl-1, His-SUMO and Ulp1, the sample was reapplied to a HisTrap in 50mM TRIS pH 8.0, 250mM NaCl and the flow through containing Mcl-1 collected. The flow through containing cleaved Mcl-1 was concentrated (Amicon Ultra centrifugal filter, MWCO 10,000) to approximately 5 ml. The sample was then filtered before being loaded onto a Superdex 75 column (GE healthcare) equilibrated in 50mM TRIS pH 8.0, 250mM NaCl, 0.5mM DTT, 2.5% Glycerol. The purified was concentrated to ~ 6 mg/ml and stored at – 80 °C.

Fluorescence anisotropy assays

WT-p53(15-31) transactivation domain peptide and its fluorescein-labelled analogue p53 (15-31) Flu were purchased from Peptide Protein Research Ltd and used without further purification. WT-NOXA B (68-87) and its fluorescein-labelled analogue FITC-NOXA B (68-87) were synthesised and purified. Fluorescence anisotropy assays were performed in 384-well plates (Greiner Bio-one). Each experiment was run in triplicate and the fluorescence anisotropy measured using a Perkin Elmer EnVision^{TM} 2103 MultiLabel plate reader, with excitation at 480 nm (30 nM bandwidth), polarised dichroic mirror at 505 nm and emission at 535 nm (40 nM bandwidth, *S* and *P* polarised).

All experiments were performed in assay buffer: 40 mM phosphate buffer at pH 7.50, containing 200 mM NaCl and 0.02 mg mL^{-1} *bovine serum albumin* (BSA) and data analysed following previously published methods.[2,12] Assays for HIF-1α/p300,[13] eIF4E/eIF4G[13] and Bcl-x_L/BAK[14] were performed as previously described.

Competition assays

Stocks of hybrid α-helix mimetics (400 μM in 90:10 (v/v) assay buffer: DMSO) were used to prepare serial dilution across the plate (starting point: 100 μM; 18-points, 3/4 serial dilution).

For the p53/*h*DM2 FA competition assay, p53 (15-31) Flu and *h*DM217-126 L33E were then added to each well to give a final concentration of 54.5 nM and 154.2 nM, respectively. For the Mcl-1/NOXAB FA competition assay, FITC-NOXAB (68-87) and Mcl-1 (172-327) were added to each well to give a final concentration of 50 nM and 150 nM, respectively. For control wells the tracer peptide was replaced with an identical volume of assay buffer. The total volume in each well was 60 µL.

The data for both the *P* (perpendicular intensity) and *S* (parallel (same) intensity) channels, resulting from this measurement and corrected by subtracting the corresponding control wells, were used to calculate the intensity and anisotropy for each well following Equations S 4 and S 5:

$$I = (2PG) + S$$

Equation S 4

$$r = \frac{S - PG}{I}$$

Equation S 5

Where *I* is the total intensity, *G* is an instrument factor which was set to 1 for all experiments and *r* is the anisotropy.

The average anisotropy (across three experimental replicates) and the standard deviation of these values were then calculated and fit to a sigmoidal logistic model (Equation S 6) using OriginPro 9.0 which provided the IC_{50} and error values.

$$y = r_{\max} + \frac{r_{\min} - r_{\max}}{1 + \left(x / x_0 \right)^p}$$

Equation S 6

FA competition assays of mimetics 1 and 6-13 and Nutlin-3a against p53/*h*DM2

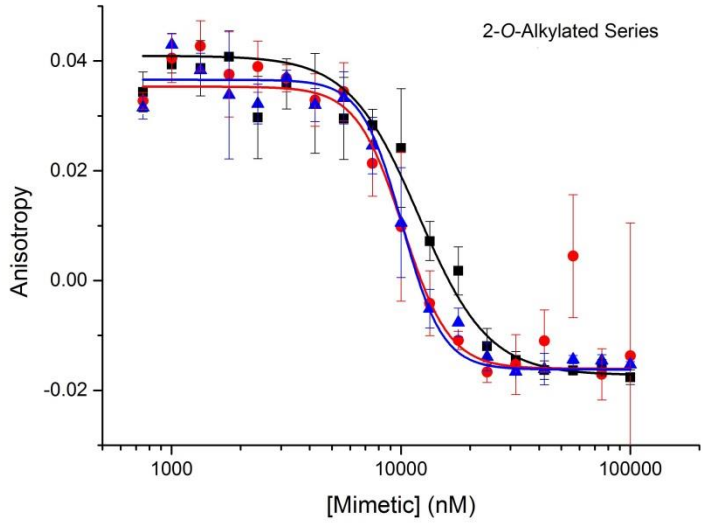

Figure S 152. Side-chain spacing studies targeting the p53/*h*DM2 PPI: dose-response curves of hybrid mimetics of the 2-*O*-alkylated series (black 1, red 7 and blue 8).

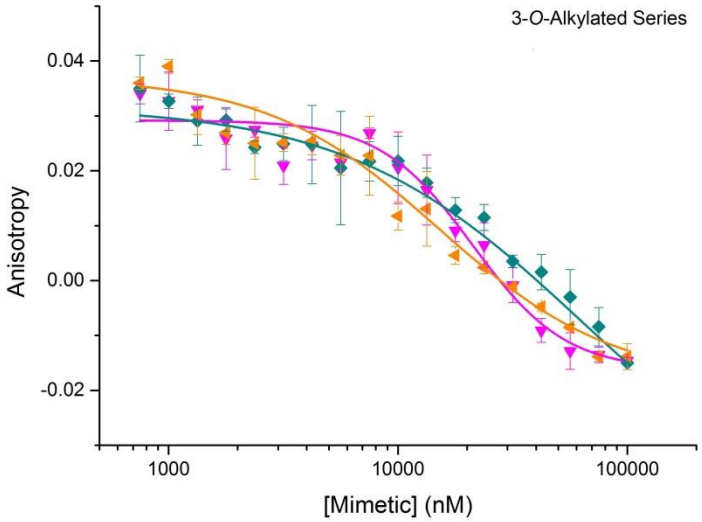

Figure S 153. Side-chain spacing studies targeting the p53/*h*DM2 PPI: dose-response curves of hybrid mimetics of the 3-*O*-alkylated series (pink 9, turquoise 10, orange 11).

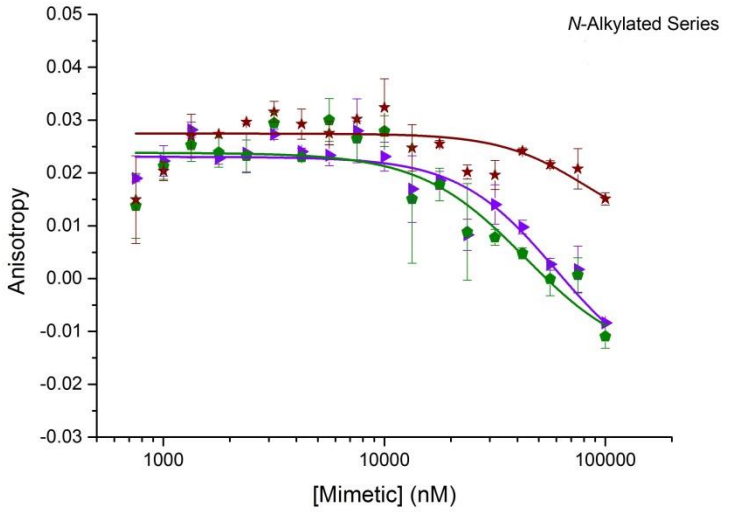

Figure S 154. Side-chain spacing studies targeting the p53/*h*DM2 PPI: dose-response curves of hybrid mimetics of the *N*-alkylated series (purple 12, green 13, brown 14).

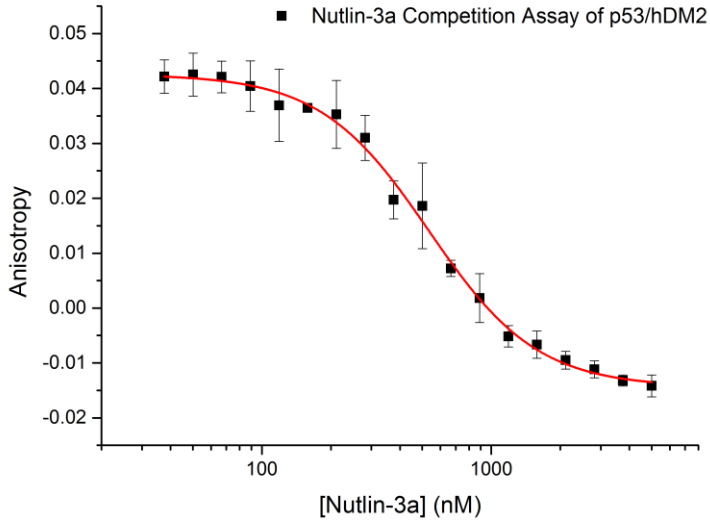

Figure S 155. Dose-response curves of Nutlin-3a[15] against the p53/*h*DM2 PPI

Table S1. IC_{50} values obtained from fitting the fluorescence anisotropy competition assay data against p53/*h*DM2.

Compound	IC_{50} (μM)
Nutlin-3a	0.534 ± 0.024
1	11.9 ± 0.6
7	10.1 ± 1.1
8	10.2 ± 1.0
9	21.2 ± 2.5
10	62.3 ± 5.6
11	15.2 ± 2.0
12	59.7 ± 31.9
13	> 100
14	> 100

FA competition assays of mimetics 1 and 7-14 against Mcl-1/NOXA B

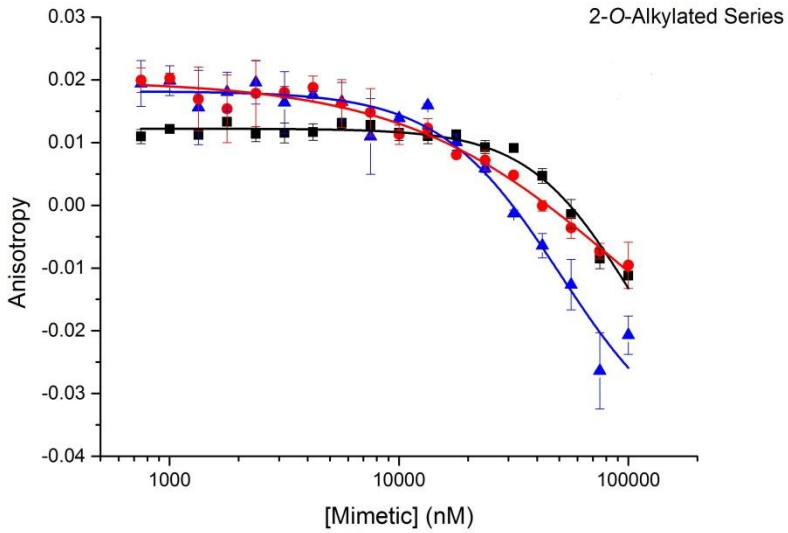

Figure S 156. Side-chain spacing studies targeting the Mcl-1/NOXA B PPI: dose-response curves of hybrid mimetics of the 2-*O*-alkylated series(black 1, red 7 and blue 8).

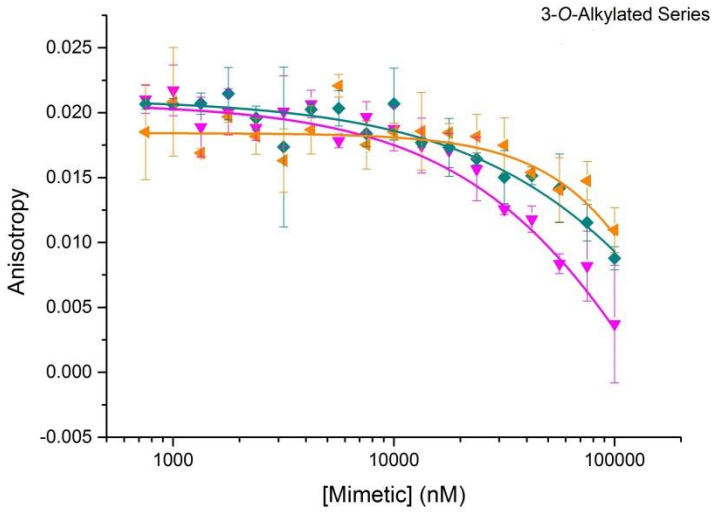

Figure S 157. Side-chain spacing studies targeting the Mcl-1/NOXA B PPI: dose-response curves of hybrid mimetics of the3-*O*-alkylated series (pink 9, turquoise 10, orange 11).

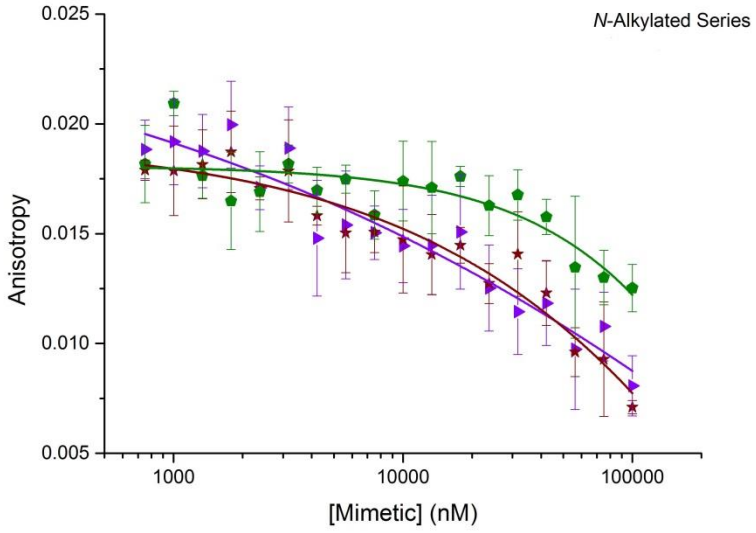

Figure S 158. Side-chain spacing studies targeting the Mcl-1/NOXA B PPI: dose-response curves of hybrid mimetics of the *N*-alkylated series.

Table S2. IC_{50} values obtained from fitting the fluorescence anisotropy competition assay data against Mcl-1/NOXA-B.

Compound	IC_{50} (μM)
1	> 100
7	> 100
8	> 100
9	> 100
10	> 100
11	> 100
12	> 100
13	> 100
14	> 100

FA competition assays of mimetic 1 against Bcl-x_L/BAK, HIF-1α/p300 and eIF4E/4G

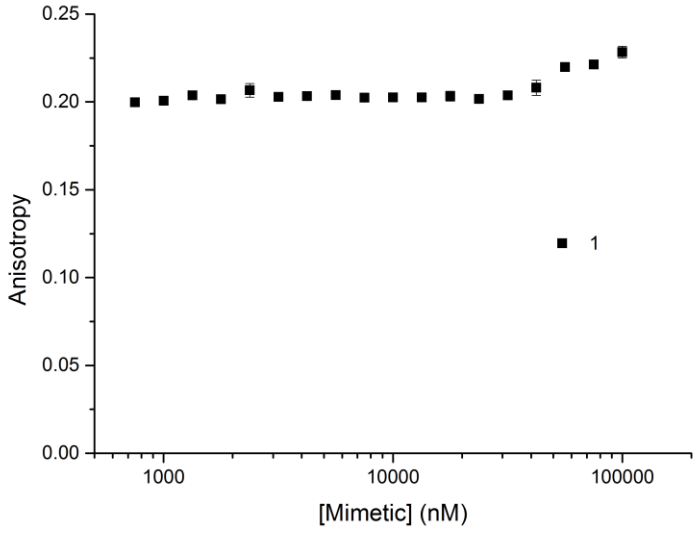

Figure S 159. Dose-response of 1 against the Bcl-x_L/BAK PPI

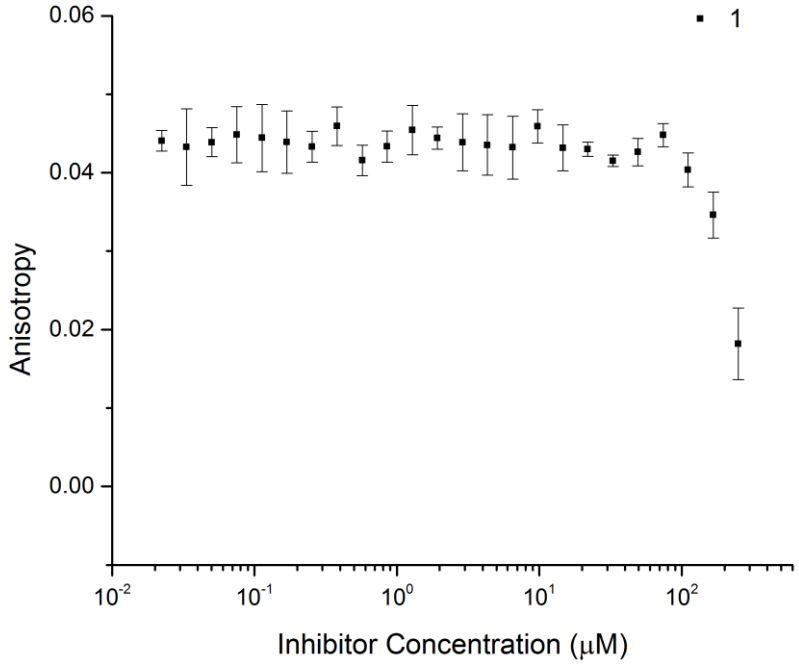

Figure S 160. Dose-response of 1 against the HIF-1α/p300 PPI.

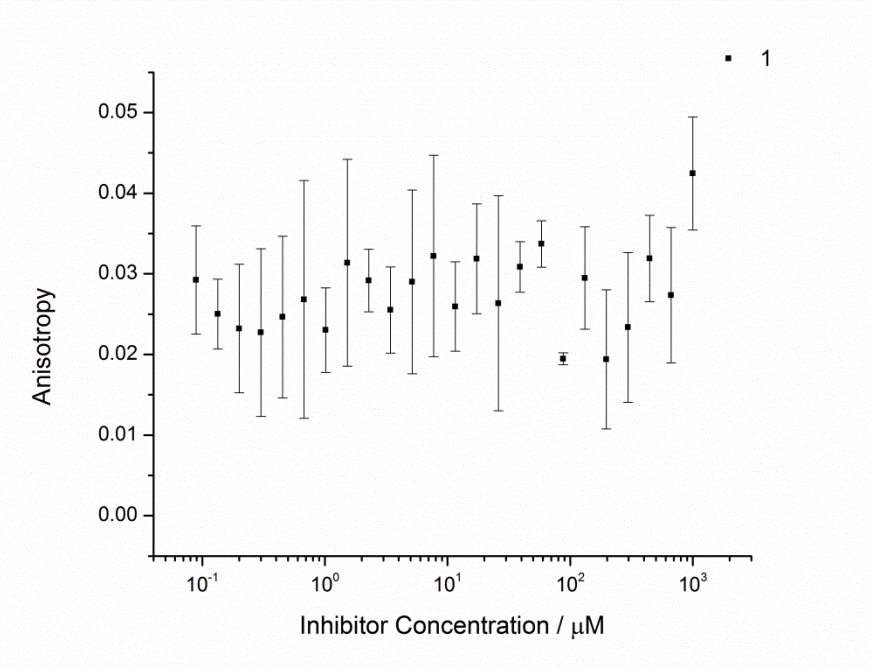

Figure S 161. Dose-response of 1 against the eIF4E/4G PPI.

^{1}H-^{15}N HSQC Studies.

*h*DM2 (17-126) L33E and Mcl-1 (172-327) C286S were overexpressed in minimal media enriched with ^{15}N Ammonium Chloride to produce isotopically labelled protein. The C286S mutant of Mcl-1 was used in place of the wild type as this has previously shown to be more stable.[16] The proteins were purified as described for the unlabelled material.

Each ^{1}H-^{15}N HSQC was obtained using 100μM protein that had been incubated in the absence or presence of 200μM compound overnight at 4°C. The buffer used for hDM2 spectra contained 100mM Sodium Phosphate pH 7.3, 2.5% glycerol, 1mM DTT and 5% DMSO, whilst the buffer for Mcl-1 contained 20mM HEPES pH 7.0, 50mM NaCl, 0.5mM DTT, 2.5% Glycerol, 5% DMSO. Sample volumes of 330 μL were placed in Shigemi BMS-005V tubes and included 10% D_2O v/v. All NMR datasets were acquired at 25 °C.

All HSQC experiments were performed on a Varian Inova spectrometer at 600MHz. A gradient filtered pulse sequence was used and the data was phased using NMRpipe and visualised using NMRview**.** The crosspeaks were assigned from published structures, with BMRB entry 6621 used for hDM2[17] and BMRB entry 19654 used for Mcl-1.[16] The difference in chemical shift was as described previously.[12] Large shifts were defined as greater than 0.3 ppm, medium as between 0.2 to 0.3 and weak shifts those above 0.1ppm.

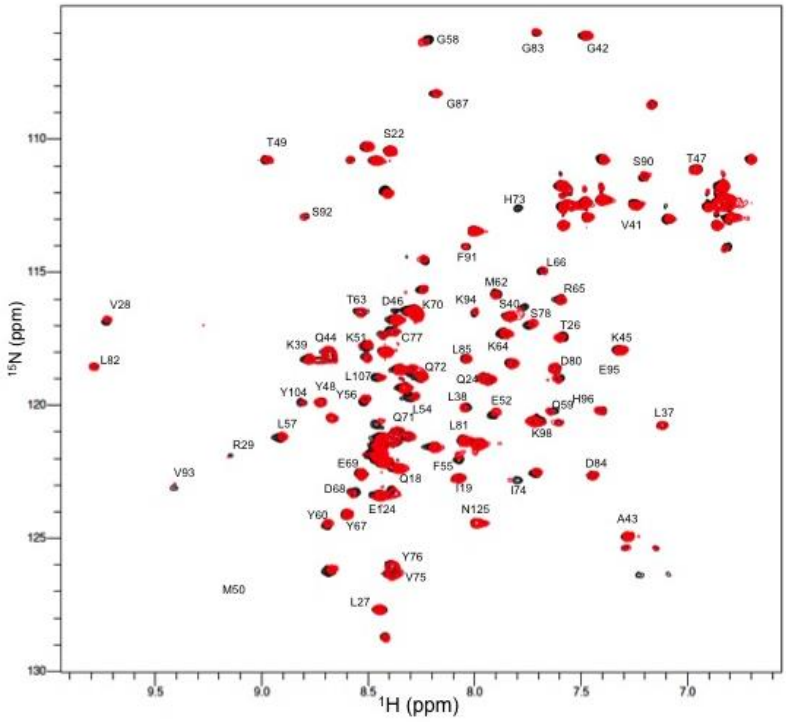

Figure S 162. ^{1}H-^{15}N HSQC of *h*DM2 in the absence and presence of Compound 1. Black is from the protein alone, with red showing the crosspeaks upon inclusion of Compound 1.

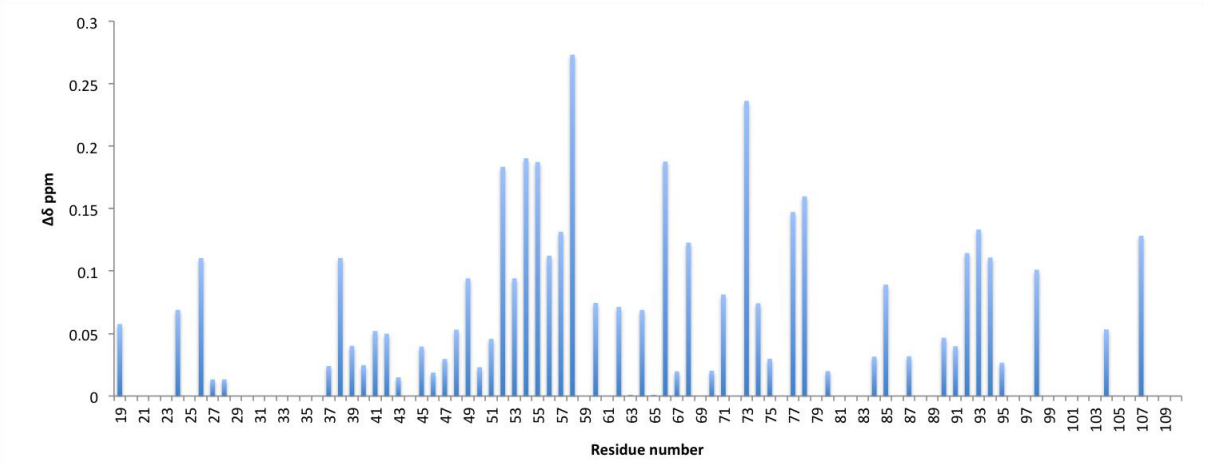

Figure S 163. Plot of chemical shifts perturbations of *h*DM2 in the presence of compound 1.

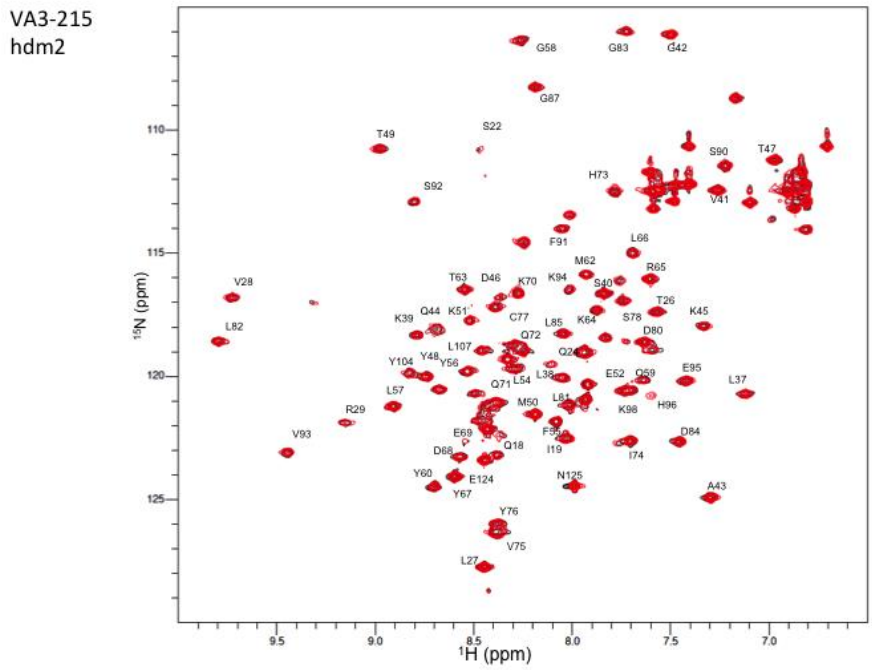

Figure S 164. ^{1}H-^{15}N HSQC of *h*DM2 in the absence and presence of Compound 3. Black is from the protein alone, with red showing the crosspeaks upon inclusion of Compound 3.

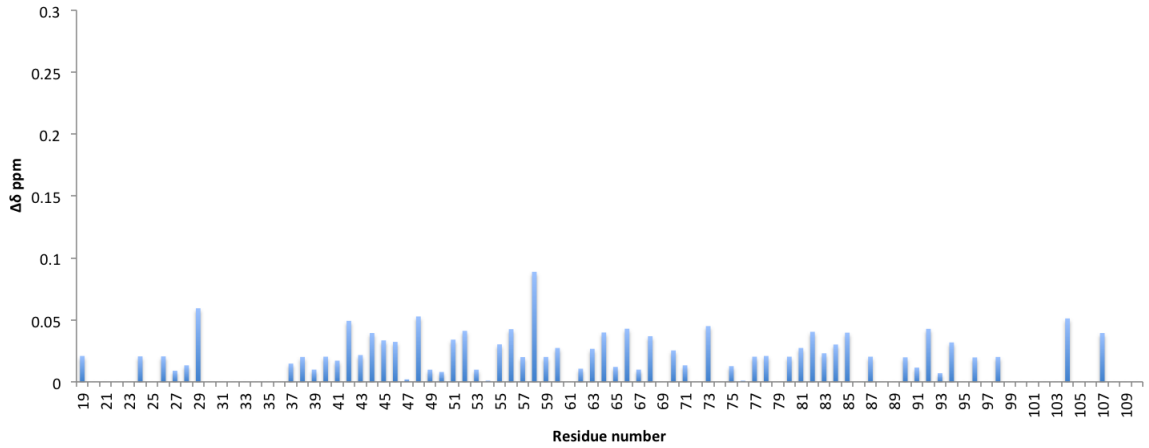

Figure S 165. Plot of chemical shifts perturbations of *h*DM2 in the presence of compound 3.

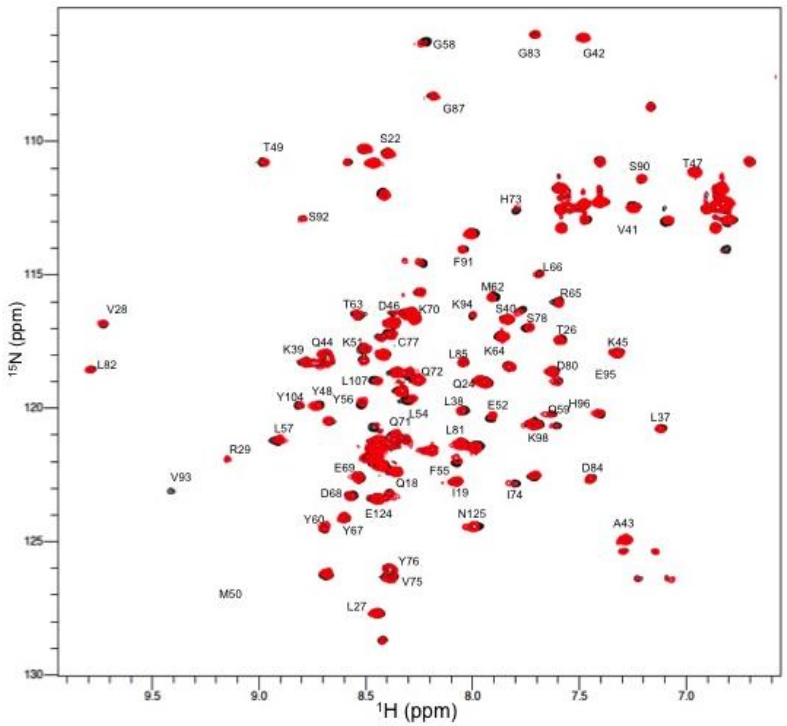

Figure S 166. ^{1}H-^{15}N HSQC of *h*DM2 in the absence and presence of Compound 15. Black is from the protein alone, with red showing the crosspeaks upon inclusion of Compound 14.

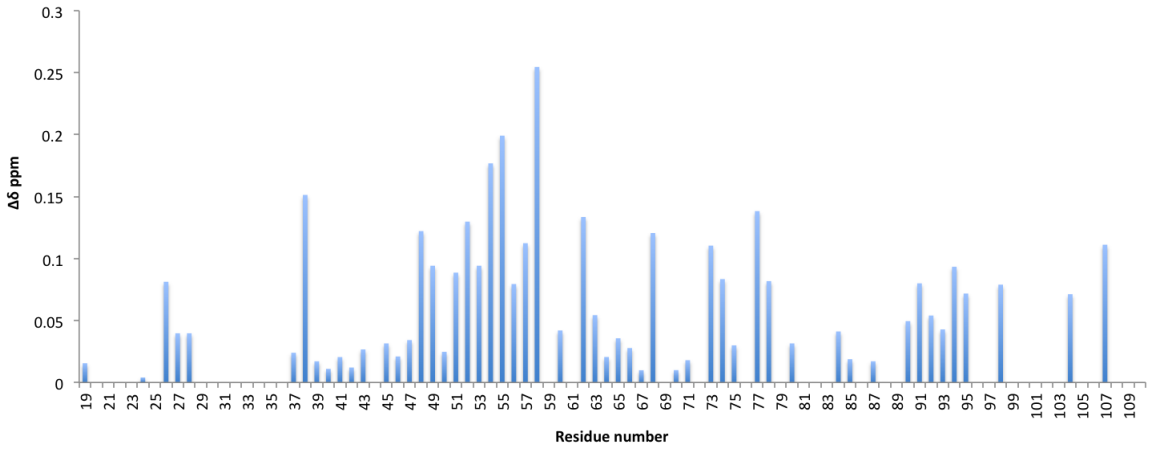

Figure S 167. Plot of chemical shifts perturbations of *h*DM2 in the presence of compound 15.

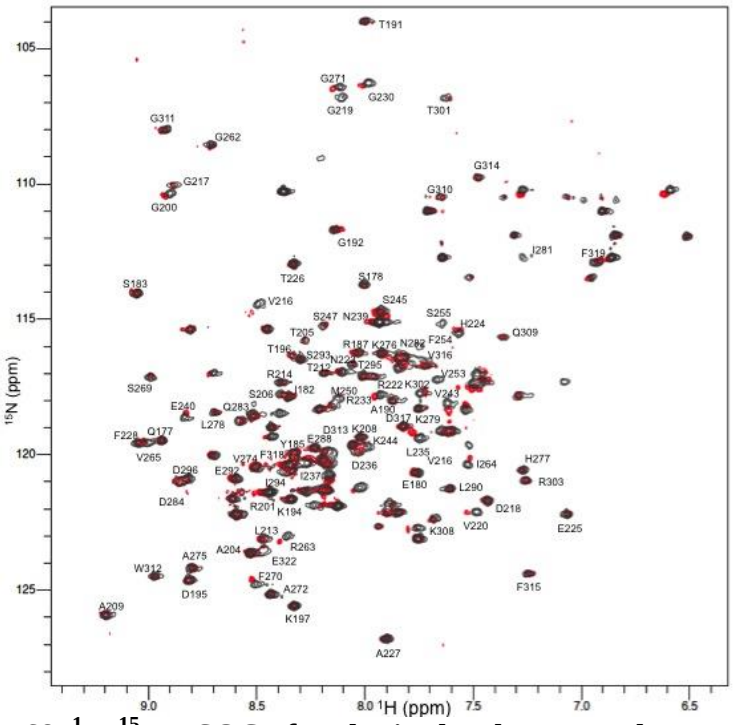

Figure S 168. ^{1}H-^{15}N HSQC of Mcl-1 in the absence and presence of Compound 1. Black is from the protein alone, with red showing the crosspeaks upon inclusion of Compound 1.

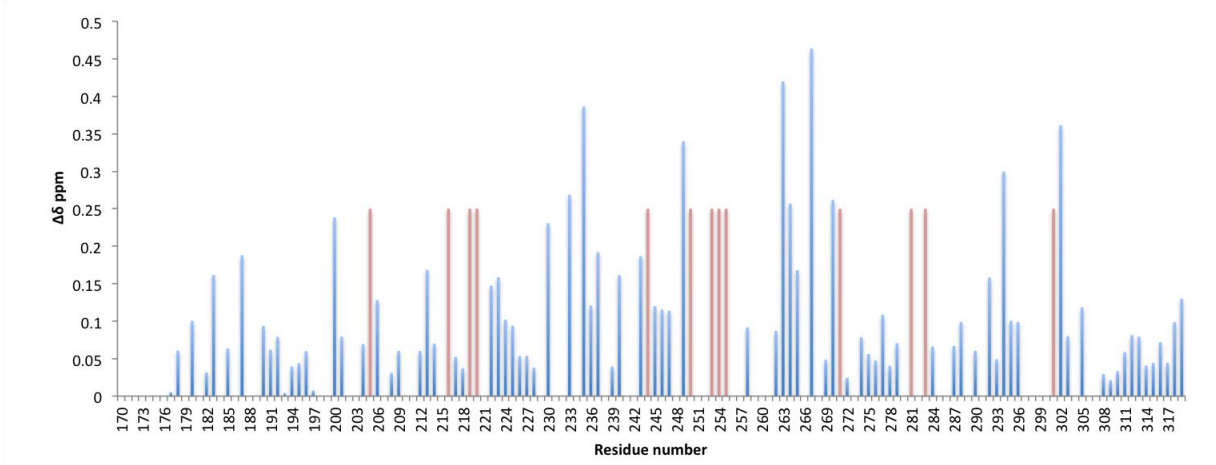

Figure S 169. Plot of chemical shifts perturbations of Mcl-1 in the presence of Compound 1. The difference in chemical shift is shown above the residue number in blue. The crosspeaks that disappear in the presence of Compound 1 are shown in red with an arbitrary value of 0.25ppm.

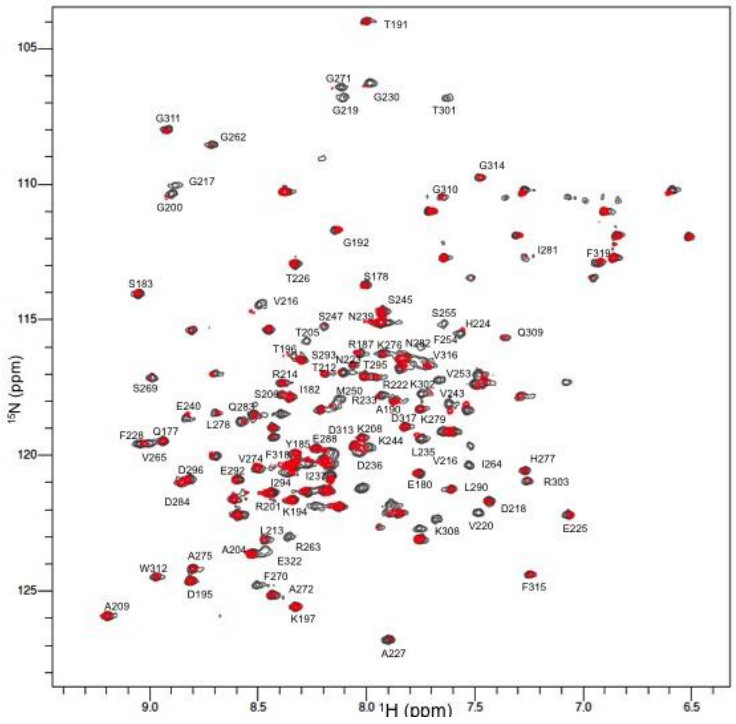

Figure S 170. ^{1}H-^{15}N HSQC of Mcl-1 in the absence and presence of Compound 15. Black is from the protein alone, with red showing the crosspeaks upon inclusion of Compound 15.

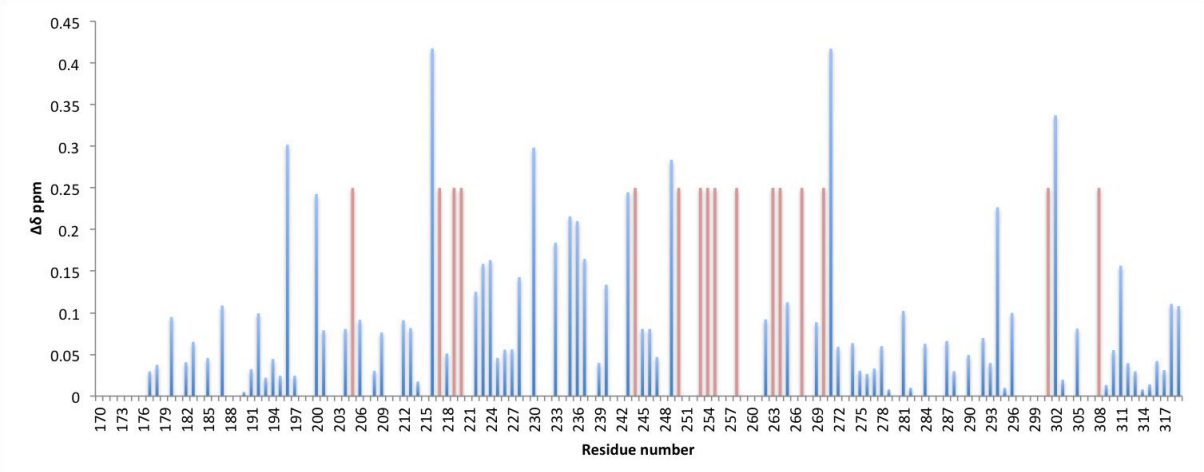

Figure S 171. Plot of chemical shifts perturbations of Mcl-1 in the presence of Compound 15. The difference in chemical shift is shown above the residue number in blue. The crosspeaks that disappear in the presence of Compound 15 are shown in red with an arbitrary value of 0.25ppm.

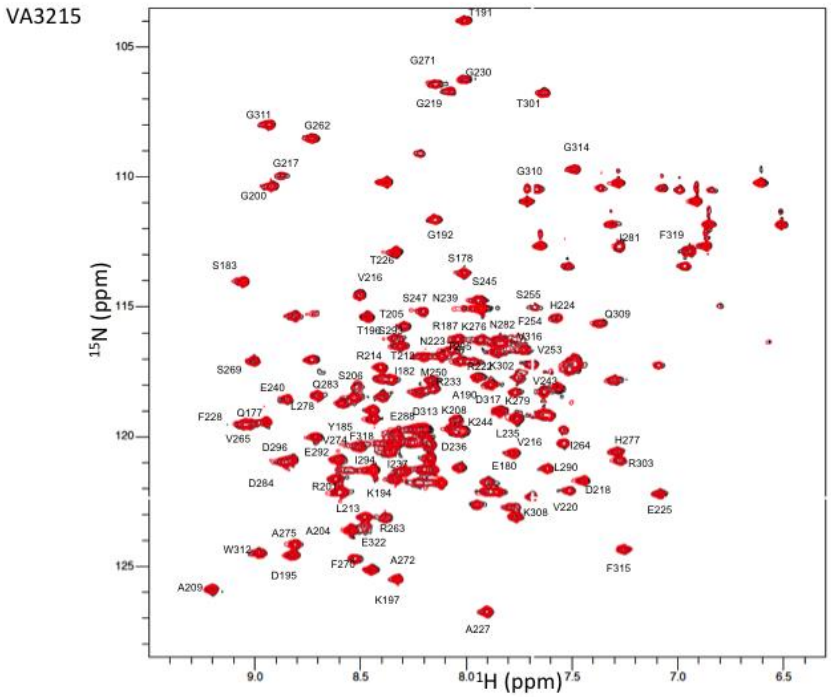

Figure S 172. ^{1}H-^{15}N HSQC of Mcl-1 in the absence and presence of Compound 3. Black is from the protein alone, with red showing the crosspeaks upon inclusion of Compound 3.

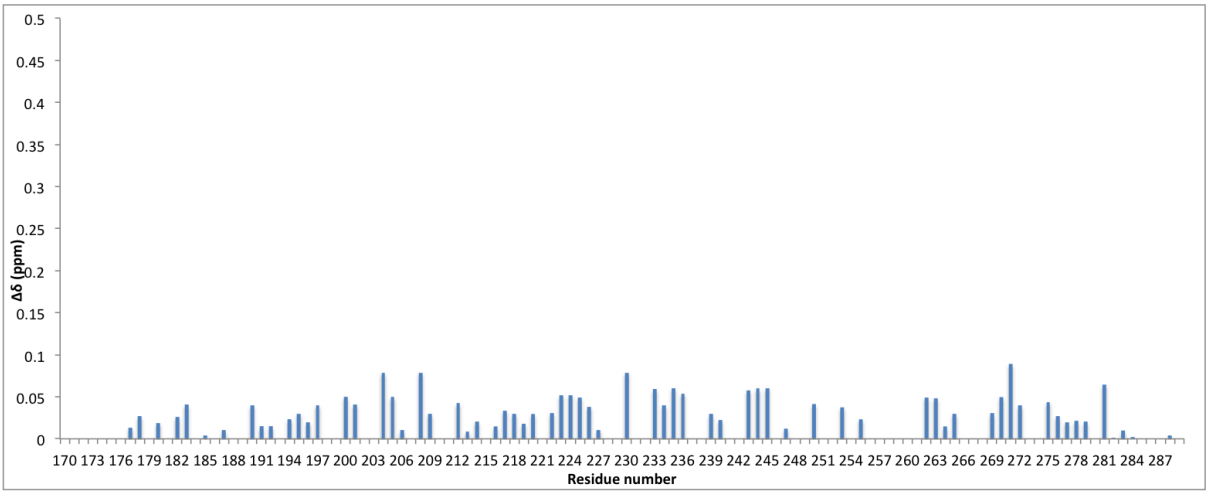

Figure S 173. Plot of chemical shifts perturbations of Mcl-1 in the presence of compound 3.

Docking Studies

A conformational search was performed on mimetics **1** and **15-17**. The structures were minimised by employing a full *Monte Carlo* search in the software Macromodel® using the MMFFs (Merk Molecular Force Fields) method. Water was chosen as implicit solvent system and free rotation around the amide bonds was allowed in order to increase the accuracy of the conformational search. The set of minimised structures within 1.5 kJ/mol from the lowest energy conformation was then docked with the crystal structure of *h*DM2 (PDB ID: 1YCR) or Mcl-1 (PDB ID: 2JM6) using the software Glide®.

Of all the poses generated from mimetic **16**, 67% assumed conformations which were binding in the *h*DM2 cleft. A representative example is shown in Figure S174.

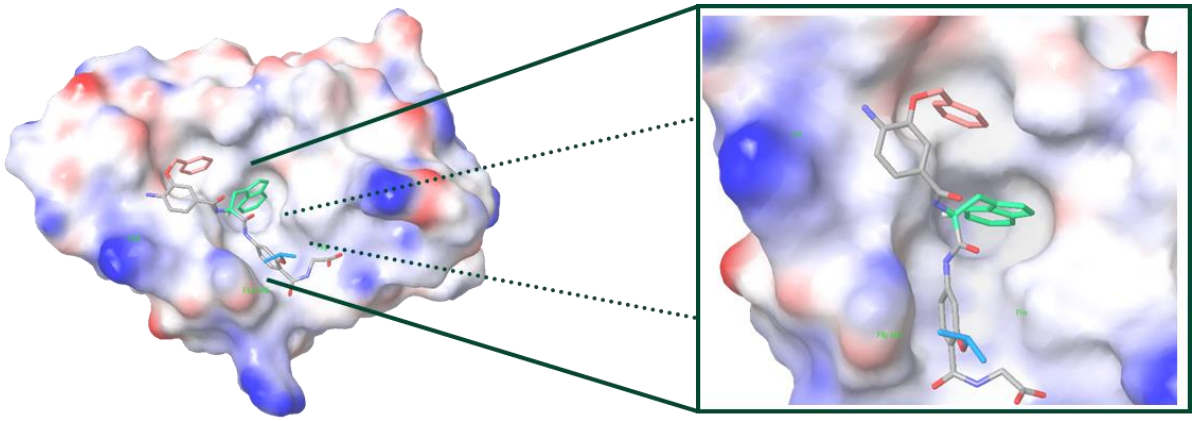

Figure S 174. Docking studies for the L-Trp hybrid mimetic 16 (PDB ID: 1YCR) with protein surface 3D representation and expansion.

Of all the poses generated from mimetic **17**, 27% assumed conformations which were binding in the *h*DM2 cleft. A representative example is shown in Figure S175.

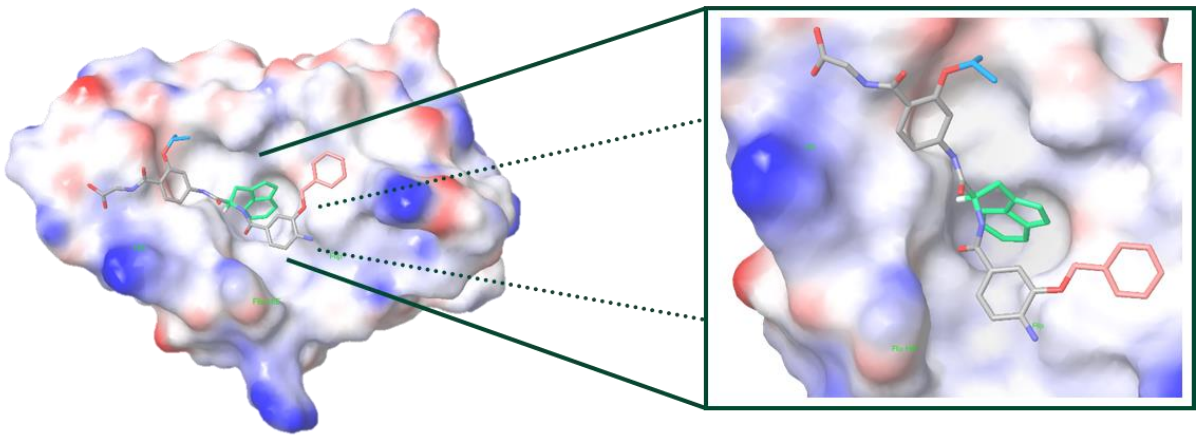

Figure S 175. Docking studies for the L-Trp hybrid mimetic 17 (PDB ID: 1YCR) with protein surface 3D representation and expansion.

Of all the poses generated from mimetic **16**, 67% assumed conformations which were binding in the Mcl-1 cleft. A representative example is shown in Figure S176.

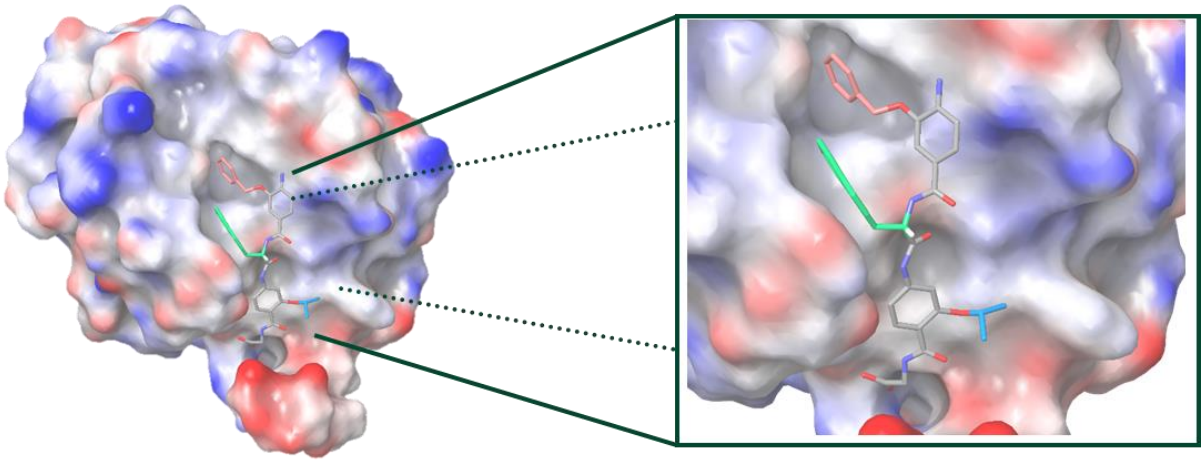

Figure S 176. Docking studies for the L-Trp hybrid mimetic 16 (PDB ID: 2JM6) with protein surface 3D representation and expansion.

Of all the poses generated from mimetic **17**, only 13% assumed conformations which were binding in the Mcl-1 cleft. A representative example is shown in Figure S177.

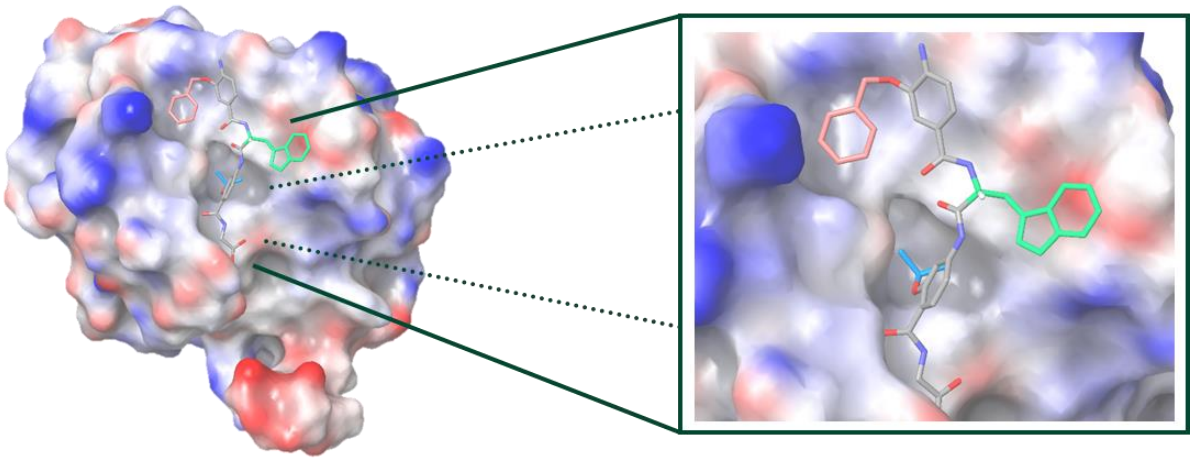

Figure S 177. Docking studies for the L-Trp hybrid mimetic 17 (PDB ID: 2JM6) with protein surface 3D representation and expansion.

Additional Modelling Studies

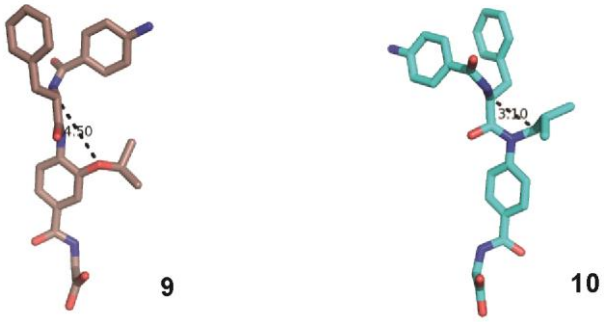

Figure S 178. Side Chain Spacing for 9 and 12.

References

1 Plante, J. *et al.* Synthesis of functionalised aromatic oligamide rods. *Org. Biomol. Chem.* **6**, 138-146 (2008).

2 Plante, J. P. *et al.* Oligobenzamide proteomimetic inhibitors of the p53-*h*DM2 protein-protein interaction. *Chem. Commun.*, 5091-5093 (2009).

3 Campbell, F., Plante, J. P., Edwards, T. A., Warriner, S. L. & Wilson, A. J. N-alkylated oligoamide α-helical proteomimetics. *Org. Biomol. Chem.* **8**, 2344-2351 (2010).

4 Azzarito, V. *et al.* 2-*O*-Alkylated Para-Benzamide α–Helix Mimetics: The Role of Scaffold Curvature. *Org. Biomol. Chem.* **10**, 6469-6472 (2012).

5 Long, K., Edwards, T. A. & Wilson, A. J. Microwave assisted solid phase synthesis of highly functionalized N-alkylated oligobenzamide α-helix mimetics. *Bioorg. Med. Chem.*, **21**, 4034-4040 (2013).

6 Murphy, N. *et al.* Solid-phase methodology for synthesis of O-alkylated aromatic oligoamide inhibitors of α-helix-mediated protein-protein interactions. *Chem. Eur. J.* **19**, 5546-5550 (2013).
7 Long, K., Edwards, T. A. & Wilson, A. J. Microwave assisted solid phase synthesis of highly functionalized N-alkylated oligobenzamide alpha-helix mimetics. *Bioorg. Med. Chem.* **21**, 4034-4040 (2013).
8 Brünger, A. T. *et al.* Crystallography & NMR System: A New Software Suite for Macromolecular Structure Determination. *Acta Crystallographica Section D* **54**, 905-921 (1998).
9 Lichtor, P. A. & Miller, S. J. Experimental Lineage and Functional Analysis of a Remotely Directed Peptide Epoxidation Catalyst. *J. Am. Chem. Soc.* **136**, 5301-5308 (2014).
10 Prabhakaran, P. *et al.* Conformational properties of O-alkylated benzamides. *Tetrahedron* **68**, 4485-4491 (2012).
11 Gellman, S. H., Dado, G. P., Liang, G. B. & Adams, B. R. Conformation-directing effects of a single intramolecular amide-amide hydrogen bond: variable-temperature NMR and IR studies on a homologous diamide series. *J. Am. Chem. Soc.* **113**, 1164-1173 (1991).
12 Campbell, F., Plante, J. P., Edwards, T. A., Warriner, S. L. & Wilson, A. J. N-alkylated oligoamide alpha-helical proteomimetics. *Org. Biomol. Chem.* **8**, 2344-2351 (2010).
13 Burslem, G. M. *et al.* Small-Molecule Proteomimetic Inhibitors of the HIF-1α–p300 Protein–Protein Interaction. *ChemBioChem* **15**, 1083-1087 (2014).
14 Yeo, D. J., Warriner, S. L. & Wilson, A. J. Monosubstituted alkenyl amino acids for peptide "stapling". *Chem. Commun.* **49**, 9131-9133 (2013).
15 Vassilev, L. T. *et al.* In Vivo Activation of the p53 Pathway by Small-Molecule Antagonists of MDM2. *Science* **303**, 844-848 (2004).
16 Liu, G. *et al.* High-Quality NMR Structure of Human Anti-Apoptotic Protein Domain Mcl-1(171-327) for Cancer Drug Design. *PLoS ONE* **9**, e96521 (2014).
17 Uhrinova, S. *et al.* Structure of Free MDM2 N-terminal Domain Reveals Conformational Adjustments that Accompany p53-binding. *J. Mol. Biol.* **350**, 587-598 (2005).